"TYCHO" STUDY GROUP

ELECTRICAL ENGINEERING DEPARTMENT

UNIVERSITY OF MINNESOTA

N66 16166

CR 69878

REPORT

of

August '65 - "TYCHO" Meeting

Contract No: NSR-24-005-047

Prepared by

UNIVERSITY OF MINNESOTA

Minneapolis, Minnesota

For

HEADQUARTERS, NATIONAL AERONAUTICS & SPACE ADMINISTRATION

Washington, D. C. 20546

PREFACE

This report is the result of the "TYCHO" Study Group meeting held in Boulder, Colorado, during August, 1965. The report is organized into sections as follows:

I. Conclusions and Recommendations

II. Aspects and Comments on Present Knowledge of the Lunar Surface

III. Summary of Research Contributions

IV. Background of the "TYCHO" Study Group

RESEARCH CONTRIBUTIONS

(A series of twelve appendices consisting of research papers written by "TYCHO" Study Group members.)

TABLE OF CONTENTS

RESEARCH CONTRIBUTIONS

SECTION I

CONCLUSIONS AND RECOMMENDATIONS

I. Conclusions and Recommendations

When the results of the study were examined by this Group, a set of recommendations became apparent. These recommendations encompassed several different points of view--all, however, within the general framework of defining the lunar surface with sufficient detail to assist the Apollo program. Some of the recommendations are for additional Earth space laboratory experiments, some for additional examination of data already on file, and several for proposed possible experiments which would further aid in describing the nature of the surface of the Moon. Several, however, are the result of a clear recognition that remote sensing of the unfamiliar terrain will not enable an accurate prediction of bearing strength to be made. This difficulty is a direct result of the fact that the interaction of electromagnetic radiation with the lunar surface does not sense those collective effects that play a role in mechanical bonding of structures.

The recommendations of the Group are as follows:

A. "TYCHO" feels it essential that a back-up experiment to the present Surveyor program be given high priority. The Surveyor vehicle represents sophisticated, complex engineering and one may reasonably expect difficulties, especially early in the program. We strongly recommend that a back-up experiment involving either a soft landing vehicle with a larger degree of tolerance or a hard landing vehicle in which nothing

other than measurements of a surface property such as density or bearing strength be attempted. The recently proposed Sandia impact probe is an example of such an experiment.

B. The landing point should be selected to minimize the danger to the astronauts from the point of view of proposed models of the lunar surface. For instance, the floor of a 50 to 100-meter wide new "crisp" crater seems to offer best possibilities as discussed further on Page 19. Infrared cooling anomalies, radar reflectivity, and optical backscatter give independent evidence of locations of high surface density. Further, all equipment and plans should be made compatible with all the models and training should take place in sand and above all in light "fluff" in vacuum.

C. Because of its importance to the Apollo program, behavior of the dust in a high vacuum and its influence on the performance of the mission equipment in such an environment should be the core of an extensive experimental program. This is particularly important because there is no doubt that there is some dust on the lunar surface since the infall of meteorites alone would pulverize any surface material.

D. All photometric studies of the lunar surface and some of the infrared and radar studies measure in effect the properties of the lunar dust layer. For this reason a wide systematic program of measurements of various properties (mechanical properties, coherency, dielectric constant and losses, thermal conductivity, light scattering and polarization) of lunar dust

substitutes under possibly realistic conditions (solar wind, churning, temperature variations, vacuum conditions, etc.) should be initiated. Preliminary experiments have already shown that many of these properties change in a drastic manner under these conditions.

E.   A laboratory verification of the model outlined in Appendix VII which shows that the backscatter intensity and the polarization can determine surface density and particle size should be attempted. If the model is verified, back-scatter during lunar eclipses versus position on the Moon should indicate fluctuations in surface density and thus porosity. This will be helpful in choosing a suitable landing site.

F.   Use of the backscatter technique at optical fre-quencies in establishing porosity and density of the top layer of the surface could be extended to greater depths by inclusion in the lunar orbiter of an active radar satellite. Through an examination of the scattering as a function of angle, greatly improved predictions of the dielectric constant and roughness of the surface could be made.

G.   Radar reflectivity at 23 cm and at 68.3 cm shows a region in which the reflectivity varies as $(\cos \phi)^{3/2}$ where ϕ is the angle between the subterrestrial point and the point of reflection. This behavior is neither simply diffuse nor specular and the variation of its magnitude with wavelengths is striking. Examination of this point should be encouraged since

it is probably the result of a particular surface structure.

H.   The infrared data indicate regions of high thermal transport (harder regions) which overlap, within limits of resolution, regions of high radar reflectivity. The experimental results of these two programs should be examined to obtain a common surface model paying particular attention to the difference in predictions based on a homogeneous or non-homogeneous surface and on a layered or a graded surface.

I.   The existence near the lunar surface of a charged layer from photoelectrons is beyond question. The possibility that this might interfer with radio communication on either packages left behind or between man and lunar excursion vehicle must be examined to insure that it presents no problem.

J.   Of considerable interest in examining the possible models for the lunar surface is a correct thermal model for the Moon's history. Much could be learned concerning the Moon's homogeneity by including in the lunar orbital program a gravity meter. This would help to answer the question whether or not there has been molten material on the Moon.

K.   The proposed thermal mechanism of lunar luminescence suggests under what conditions this effect should be observable. Systematic ground-based observations should be made to test this model and to indicate possible variations of the mineral content on the surface.

L.   Much has been said concerning laser beams to probe the contour of the lunar surface to determine its gross figure. This

experiment at the present would require an advance in laser technology and its successful conclusion would not contribute greatly to answering urgent questions about the lunar surface. Information obtained from the lunar orbiter will be far more useful. Such a program, therefore, should not be undertaken at this time.

SECTION II

ASPECTS AND COMMENTS ON PRESENT KNOWLEDGE
OF THE LUNAR SURFACE

II. Aspects and Comments on Present Knowledge of the Lunar Surface

A. Introduction

The spectrum of models proposed for the lunar surface ranges from a surface entirely covered by a dust layer of varying thickness to a surface which is completely volcanic in origin. The reasoning and conclusions made by various workers in this field are often completely contradictory. In this section an outline of conclusions drawn from observation will be presented and distinction will be made between those conclusions supported directly by evidence and those less certain which are chiefly an opinion and inference.

In considering the lunar surface it must be realized that up to the present all data available concerning the lunar surface were obtained through remote sensing. For the purpose of planning a lunar landing, it is unfortunate that the coupling of electromagnetic radiation to solids samples their dielectric and not mechanical properties. The lack of atmosphere and the presence of a flux of micrometeorites produce conditions which are sufficiently different from most laboratory experiences that conclusions drawn from analogy are highly questionable. It is, therefore, useful to examine critically the observations and the conclusions that can be made.

Historically, the optical telescope has been used to establish gross topographic features. The high resolution cameras used in the Ranger missions permit mapping of topographic contours and obtaining frequencies of occurrence of

various features down to perhaps one meter. Nevertheless, no conclusions about the physical nature of the Moon can be made without drawing on analogies with terrestrial conditions.

The measurements of scattering and polarization of reflected sunlight as a function of wavelength yield surface density and particle size. These results lead without question to a surface covered with a very fine dust, finer than is encountered in the lightest known sandy terrain.

The absolute magnitude of the thermal emission detected in the infrared region or the spectrum can be used to establish the surface temperature of the Moon. From the variation of this emission during a lunar eclipse the thermal inertia of the first centimeter can be inferred. These results suggest that the very porous low density material extends at least to about 1 cm. Detection of the emission at radio frequencies can also be used to establish a temperature. In this case the depth sampled is comparable to a wavelength which for the frequencies used is several centimeters. These results also indicate a very low density material.

The reflection of radar pulses from the Moon directly measures the dielectric constant and infers a "smoothness" and density of the surface. In this case the dielectric constant is the average over about a meter depth of material. These experiments show that the lunar surface material has a low dielectric constant which when compared to Earth rocks implies a low density. The value of porosity (i.e. fraction of voids)

thus obtained is 0.7 which is considerably higher than that
of sand. The radar reflection has been also used to infer
"smoothness." This type of analysis is possible, but unique-
ness has not been established.

In summary, the established methods of observing the
lunar surface--optical, radar, infrared, and radio emission--do
not permit drawing direct definite conclusions about the strength
of the surface. Estimates based on the assumption of a weakly
coherent micron size dust give a lower limit approximately
6 gr/cm^2 (12 lb/ft^2) and a value ten times higher for a more
strongly bonded (partially sintered) dust. For higher loads
sinking will commence.

B.   Discussion

1.   Surface Topography

The surface topography has been the source of
the most extreme conflicts in the interpretation of lunar
observations. The fundamental facts which must be understood
are the existence of large, flattish, dark lowlands or Maria;
the existence of more rugged, brighter highlands; the existence
in both these areas of vast numbers of craters extending in
size from hundreds of kilometers to meters; the morphological
features of these craters (the various shapes of crater rims
and crater bottom contours, the crater outlines and relief, the
long linear depressions in some crater interiors, the existence
of radial rays extending many diameters from some craters, etc.)
and other general patterns such as regions of differing color

in Maria and the apparent local preferred directions for linear features. On Earth, topography has been shaped by castrophic volcanims, and later by the atmospheric and hydrospheric erosion. To a lesser extent, the Earth also bears the marks of meteorite bombardment.

The origins which have been suggested for craters are a) volcanism and associated geological activity, and b) meteoric impacts (with possible secondary impact from ejecta). The only evidences of origin are the number of craters and their morphology. The number and size distribution of craters smaller than 10 kilometers is in approximate agreement with the current rate of meteoric impacts on Earth and the age of the Moon. Volcanism, on the other hand, does not provide means of predicting the number or size distribution. The scale of typical lunar craters is about ten times larger than that of known large Earth caldera.

Some craters have raised, hummocky rims, while others have softer, rounded features. This could be due to a) erosion or b) different origin for different forms of craters (e.g., meteoric impacts for raised rim craters, and secondary impacts and/or slumping for softer features). Erosion requires an erosion mechanism while slumping requires a weak sub-surface structure, (e.g., voids in lava flow).

An estimate of the minimum amount of erosion possible during the lifetime of the Moon can be made from the meteor infall rate on Earth. At least a meter depth of the surface

would have been broken into rubble by this means and the upper
few centimeters would have been pulverized by micrometeorites.
The micrometeoritic bombardment alone guarantees the presence
of at least a thin "dust" cover of very small particles.
Conservation of energy demands that most of this rubble does not
escape from the Moon. There are other erosion mechanisms for
softening lunar features, such as weathering of rock under the
influence of ultraviolet light, the solar wind bombardment and
extreme temperature cycling. The rather small relief of most
large craters is the strongest support for a major erosion
mechanism.

The Maria and many large craters have floors gen-
erally very flat, and apparently covered with a flow of some
kind of material different from the highland material. This
material could be a) the product of erosion, chiefly dust or
b) the product of volcanism, lava and/or ash flows. (Lava
surfaces produced in the absence of an atmosphere are expected
to be very different from those produced on Earth.) Color dif-
ferences in these regions have been either preserved or generated
by the surface material. An electrostatic mechanism of
levitating dust to allow erosion and dust migration has been sug-
gested but it could suspend only extremely small particles.

The existence of long, soft shouldered, linear
depressions on crater floors and their alignment with respect to
crater rims and other features has generally been taken to indicate
that such features are a natural result of subsurface structure and

movement. Such features could result from volcanism or from stress due to a changing lunar rotation speed. Slump features could be due to the withdrawal of magma, the appearance or the disappearance of ice, or the failure of weak rock (e.g., an underdense lava).

Many associations present in terrestrial caldera are present in the general features of lava craters, e.g., associated craterlets around the inner edge of a crater; crater peaks, etc. The high degree of circularity possessed by most of the lunar craters, especially the larger ones, is not typical of Earth caldera.

Bright rays often extend many crater diameters from a crater. These rays have been considered as either a) lava or ash flows, or b) the pattern of ejecta from an impact crater. Ranger photographs indicate the presence of swarms of soft-shouldered craters in these rays. Discussions based on flow patterns or projectile ballistics for particular rays are useful, but all ray effects are not necessarily of one origin.

The following description will account for all the general topographical features, including the few existing quantitative data:

> The primary source of craters is meteoric impact. Magmatic activity has also been present on the Moon; the filling of the "older" flat crater bottoms and Maria is due to lava. The linements and slump

features are due to this magmatic activity.
Erosion by bombardment rounds off all
features of the order of a few meters,
and has produced a general layer of
rubble and dust whose thickness depends
on the age of the area. For old areas,
this should be the order of a meter,
and the top of this layer is a very
finely divided material.

2. Photometry and Polarimetry

Most regions of the Moon are brightest at full
Moon, and the Moon as a whole looks uniformly bright. The back-
scatter peak is an effect of shadow. The interpretation of this
sharpness requires a material which is 90-98% empty space, and
these empty spaces must be interconnected and the material
itself must be opaque. The polarization of the reflected sun-
light from the Moon has been measured as a function of lunar
phase. It is interpreted as an effect of the finite wavelength
of light. It provides a measure of the linear dimension of the
particles of filaments of this material which turns out to be
the order of 10^{-3} cm. The color and albedo of the lunar sur-
face is too strongly influenced by the solar wind to yield
reliable conclusions about the chemical nature of the material.
While the conclusions from the photometry and polarization
studies seem secure, the measurements refer only to an optical
depth, a distance of about 10^{-2} cm.

3. Infrared and Microwave Emission Measurements

The infrared measurements determine the temperature within 10^{-2} cm of the surface. A study of the surface temperature as a function of time during varying illumination conditions provides a measure of "$k\rho c$." This parameter is connected both to the filling, decreasing as the empty space increases, and also to the degree of contact between particles, decreasing as the contact decreases. While a simple interpretation of all such results has not yet been possible, $\sqrt{k\rho c}$ of typical lunar areas is about a factor of 30 smaller than for solid rocks. From these infrared measurements one can infer $k\rho c$ appropriate to the first few centimeters of material. The evidence obtained for a second deeper and denser surface from attempting to fit cooling curves is not conclusive. A material consisting of perhaps 70% empty space, and not too well bonded (e.g. crushed basalt) would be consistent with the observed $k\rho c$.

Microwave emission measurements also yield a lunar temperature, but the effective depth of this temperature is in this case a few centimeters. There is unfortunately no a _priori_ method of determining from Earth the effective microwave depth in lunar material. While this has limited the quantitative interpretation, these data do not contradict the infrared work. Microwave emission has also been interpreted to obtain the dielectric constant (see also Para. 5).

The infrared measurements demonstrate the existence of small areas which heat and cool more slowly than

typical lunar material. These areas can be identified as small sharp craters which appear optically bright and usually have raised rims. These areas are in some sense more tightly packed, at least to a depth of the order of a centimeter. The physical aspect of such craters has sometimes been described as "looking young."

4. Celestial Mechanics Observation

The analysis of lunar dynamics has given good values for the mean lunar density and for the ratios of the three lunar moments of inertia and an approximate value for the absolute value of the moment of inertia. All these are of great interest in the geology of the Moon. Of these, the mean mass is probably the most significant at present, for it gives an indication of the elemental composition of the Moon, its radioactive heat generation, and therefore on the possibility of lunar melting. Although this has been a subject of some controversy, it now seems impossible to avoid a Moon which was partially melted and had the possibility of volcanism during its lifetime. A better knowledge of the absolute moment of inertia would give much needed additional information about the internal structure of the Moon.

5. Radar Studies

Present-day radar techniques allow a map of the radar brightness of the Moon to be constructed at a resolution capable of observing geographical lunar features. The radar brightness is measured at backscatter (transmitter-Moon-

receiver angle of zero) and return strength is related to the dielectric constant, which gives a measure of the lunar density, and to the surface roughness. The dielectric constant, as measured from the overall radar return, is consistent with a lunar surface consisting 70% of voids. The range of wavelengths over which the data have been obtained suggest that this figure is appropriate to at least the first 50 cm. (The radar effectively does not see the optical layer.) A distribution of surface slopes has been obtained. Such a distribution does not, unfortunately, give much indication of the topography. A certain percentage of "surface roughness" is deduced but whether this roughness is on the surface or indicates the presence of inhomogeneities below the surface cannot be ascertained. Polarization measurements on the lunar limbs have been interpreted as consistent with a surface dielectric constant of 1.8 but the interpretation is not unique.

The radar return from specific lunar regions shows that sharp-featured craters, especially ray craters are often bright radar reflectors. This increased brightness could be due either to an increased surface roughness or an increased density at the surface.

C. Summary

Undoubtedly the question of paramount practical importance of the present time is the nature and the mechanical strength of the lunar surface in the flat regions. There are many observations which permit an estimate of the

apparent density, particle size, dielectric constant, and even thermal conductivity of the uppermost layer of the surface but none of them lead to an unambiguous evaluation of the degree of compaction, cohesion, and differentiation with progressive depth. Without these no sensible calculation of the mechanical properties, as they effect soft landing and the mobility of astronauts, is possible. Attempts were made to by-pass these difficulties by evaluating in a semi-quantitative manner certain details of the Ranger photographs. The underlying models are, however, too arbitrary to consider the results as definite indications of the mechanical characteristics of the surface. One concludes, therefore, that at present we have no reliable information about the mechanical strength of the lunar surface in the flat regions and that it is essential to make direct measurements. Such measurements can be made using penetrometers for instance such as those most recently proposed by Sandia Corporation. The proposal is particularly attractive because it supplies information about a whole area rather than about the point of impact only. These measurements should preferably precede and at least augment the Surveyor and are absolutely necessary for a sensible design of LEM and for the safety of the astronauts.

There was and still is a considerable diversity of scientific opinion concerning the presence or absence of dust on the lunar surface. Even among those who are in favor of a dust layer, there is a great difference in the estimates of the

thickness of this layer in the flat regions. This latter question is intimately related to the problem of the amount of _erosion_ which has occurred and occurs on the Moon. Here again, the opinion ranges from a complete negation of erosion to the opposite extreme of concluding that the erosion was so great that the resulting dust layer must be up to several kilometers deep. The strongest and deciding quantitative argument in favor of erosion and of the resulting dust layer is the known influx of meteorites and micrometeorites and the experimentally investigated results of such impacts. The presence of dust finds confirmation in the photometric, radar and thermal data which do not seem to be in agreement with the assumption of highly porous "sponge-like" solids. In any case, the latter would be turned into dust by the meteoritic infall in a very short time. There is thus no doubt that erosion exists and that highlands are covered with a relatively thin layer (at least several millimeters) of rather cohesive dust. For the same reason, one is led to the conclusion that flatlands (Maria and bottoms of craters) are also covered with dust and that because of much lower slopes the layer is appreciably thicker than on the highlands. This conclusion is independent of any considerations concerning the origin and nature of the underlying material (lava, ice) in these areas. No unambiguous estimate of the dust layer on the flatlands exists although thermal observations clearly indicate that certain specific areas are rather bare. These can be identified by large thermal

inertia and they are usually associated with "crisp" bright,
"new" craters of various sizes. No convincing arguments seem
to exist against erosion and against the presence of at least
some dust. Considerations based on crater counts are weak
because of the ambiguity of the criteria used in the crater
selection for statistical methods.

Another problem about which many contradictory
statements have been made is the question whether the Moon
ever was or still is hot or molten inside. The arguments
for and against this volcanism are usually qualitative and
highly subjective. Especially those based on analogy with
terrestrial features are subject to doubt because of a dif-
ference of orders of magnitude in size and because of the
known rapid erosion on Earth. The circularity of lunar craters
or its absence, the central features in craters, the presence
or absence of a correlation between craters, their size and
other features is, at present, too qualitative to be convin-
cing one way or another. The strongest arguments in favor of
a hot Moon and of some volcanic activity are a) various numerous
cracks and faults in the lunar surface which seem not to bear
any relation to craters b) striking differences in color and
their relatively sharp boundaries within Maria and c) theoretical
calculations based on a variety of plausible assumptions concerning
the history and the radioactive composition of the Moon.
While the spectrum of evidence for and against volcanism is wide
and diversified, the weight of evidence presently available seems

to lean towards a hot Moon and towards a certain amount of restricted volcanic activity. The bottoms of many craters, especially the larger ones, are undoubtedly filled with lava although the craters themselves are meteoritic in origin.

The choice of an appropriate place to soft land on the Moon involves several considerations. Obviously, one should choose a place which is possibly safe for the astronauts rather than one which is close to some interesting features. While highlands are probably hard rock, the evidence indicates they are covered with a low porosity material (dust). In any case, their unevenness seems to involve too much of a risk for a landing site. The other two kinds of areas are the Maria and the bottoms of craters. The nature of the Maria and the depth and strength of the probably quite thick dust layer are at present too poorly known to provide a sufficient factor of safety. This conclusion could be changed of course if definite and favorable information were to be obtained from penetrometers as discussed above. Thus, at present the floors of craters seem to offer the best possibility for minimizing the dangers of a deep loose dust layer. In order to make the right choice, one should use topographical and thermal criteria. Topographical features which appear to be indicative of low erosion and thus of a relatively thin dust layer are for example "crispness" and brightness of the crater rim and a size between 50 and 100 meters. The lower size limit is suggested to facilitate a

proper landing and to provide easy access to the rim. The upper limit came from the preference for a crater which is not filled with lava which may have been pulverized to a large depth. The thermal criterion is related to the strikingly high thermal inertia of certain craters which are usually but not always of the "crisp" bright kind mentioned previously. It is almost certain that a local high thermal inertia is indicative of a thin dust layer which exposes the underlying rock and permits observing its different thermal characteristics.

SECTION III

SUMMARY OF RESEARCH CONTRIBUTIONS

III. SUMMARY OF RESEARCH CONTRIBUTIONS

Nearly all present knowledge about the Moon is based on observation of reflected or emitted electromagnetic radiation (visible, infrared and radar) from its surface. The paper by J. J. Hopfield, "Interpretation of the Brightness and Polarization Curves of the Moon,"(Appendix VII) gives a theoretical treatment of the backscattering and polarization of visible light at small phase angles. It is shown that optical data can give the density and particle size to an optical depth of lunar dust layer if the theoretical model is verified in laboratory experiments. The polarization curve at small angles is interpreted in terms of shadow effects for micron size particles rather than in terms of Mie's theory.

Present lunar data on brightness and polarization is consistent with the calculations for a porosity in the range 85 - 98%, and for particle size of about 10 microns.

Results of radar investigations are described in J. V. Evans' paper "Radar Studies of the Moon" (Appendix III). At normal incidence some 60% of the radar energy at decimeter wavelengths is reflected from the surface whose uppermost layer has an effective dielectric constant of not less than 1.8 which implies a porosity in the range 70 - 90% depending upon the nature of the material. For a two-layer model proposed to account for polarization experiments the dielectric constant of the base layer must be 4.5 - 5.0 and the material

quite compacted if not solid while the depth of the upper

layer must be greater than 23 cm. The lower boundary is

presumed to be rougher than the upper one and 20% of the

base layer is assumed to be covered with structure of the

order of the wavelength in size. Limitations of the model

are discussed.

Some of the observations described in Evans' paper

pertain to radar echoes from the lunar limb. The problems

of their theoretical interpretation are discussed in H. Suhl's

paper, "Some Considerations Concerning Radar Returns from

the Lunar Limb," (Appendix XII). Radar backscatter of small

objects on a dielectric or conducting plane is analyzed in

terms of their dependence on wavelength, polarization and

angle. The calculated λ^{-2} dependence on wavelength and

$\cos \phi$ dependence on angle for large angles is in reasonable

accord with the experimental data. The limb polarization

produced by such objects is negative and in agreement with

experiment. The predicted wavelength dependence is capable

of distinguishing this model from Hagfors' model.

"Electromagnetic and Thermal Properties of the Moon's

Surface," (Appendix VIII) are discussed by B. Lax to show

that a great deal of information can be obtained by remote

radar and infrared measurements from the ground. The evidence

indicates a layer of density of the order of 1.0 gm/cm^3 or

porosity of about .70 (or filling factor of .3) for a depth

of the order of a meter or more. According to measurements on

loose basalt powder an object of a given diameter will sink to a depth equal to this diameter in a powder of the calculated porosity under a load of 35 gr/cm^2 or 75 lbs/ft sq. There appears to be a gradient of density near the surface which is not well defined by present theory or experiments but is suggested in terms of a two-layer approximation by many investigators (see above).

Much of the present structure and nature of lunar surface is the result of impact of meteorites and micrometeorites, of solar wind and of solar electromagnetic radiation. In his paper, "Erosion on Lunar Surface by Meteor Impact," (Appendix II), R. J. Collins makes a quantitative estimate of erosion caused by the meteoritic infall. He concludes that for craters of radius less than $\sim$ 300 meters, the lunar surface is in steady state. Agreement was satisfactory between the infall rates with the proposed erosion model and the observed data.

The highest flux of all matter falling on the lunar surface is due to the micron size micrometeorites. "The Evidence for Particulate Matter in Space and its Potential Accretion Rate by Moon and the Earth" (Appendix IX) is discussed by E. P. Ney. Data on the F-Corona of the Sun, the Zodiacal light, and the direct measurements of fluxes of micro-particles on the Earth's surface, lead to lunar acquisition of interplanetary particulate matter of about 30 $\overset{\text{o}}{\text{A}}$ per year. If the figure is correct, it is necessary for the incoming particulate matter to stir up approximately 300 times its own

mass of lunar material in order to account for the lunar erosion. It seems that the input of micrometeorites to the Moon is not in itself a serious source of lunar surface acquisition. If the present flux had existed throughout 10^9 years, a total of 300 cm of density 1 material would have been acquired from the interplanetary environment.

Solar wind and micrometeoritic impacts affect the "Structure of the Lunar Dust Layer" (Appendix XI) as discussed by R. Smoluchowski. On the basis of experimental evidence, it is concluded that solar wind can sinter fine dust by producing displaced atoms which diffuse towards the surface of the grains. The micrometeoritic churning of the topmost layer of lunar dust excludes sintering through sputtering. The dust is thus probably partly cohesive (0.5 dyne per particle) which increases its mechanical strength and decreases its mobility. Its lower layers are compacted by meteoritic bombardment and a close packed density is reached probably at a depth of a meter or so. Depending upon the degree of sintering, loads of a few to a few tens gr/cm^2 will not commence to sink in the topmost dust layer.

During the lunar day, the Moon changes to a positive potential due to the photoelectric effect. This "Potential and Electric Field at the Surface of the Moon" (Appendix VI) is evaluated in a paper by H. Heffner. Assuming a photon flux (below 4000 $\overset{o}{A}$) of 2 x 10^{16} photons per cm^2 per sec, quantum efficiency 10^{-3} and 3 ev for the kinetic energy of the photo-

electrons one obtains a potential of 30 volts, a space charge layer of some 8 meters and an electric field of 1.6 volts/cm. These day time, normal incidence, values are lower for a more realistic, two orders of magnitude lower flux.

The electric field calculated in the previous paper may lead to "Levitation of Dust on the Surface of the Moon" (Appendix V) as discussed also by H. Heffner. It is shown that: a) photoelectric space charge effects are not sufficient to raise dust particles from the surface of the Moon, b) sub-micron dust particles can be suspended if they are raised to a sufficient height by micrometeorite impact, c) an appreciable fraction of these particles will be suspended as long as the angle of incidence of solar radiation is not too low, and d) under the influence of radiation pressure particles tend to migrate towards the shadow region. Charged dust particles may be a cause of much nuisance, if not danger, to an astronaut especially if he should happen to fall. Experimental tests are recommended.

Much interest and controversy has been raised by reports of excess lunar brightness. The pertinent "Mechanisms for Lunar Luminescence" (Appendix X) are discussed in a paper by E. P. Ney, N. J. Woolf, and R. J. Collins. It is shown that the visibility of luminescence on the Moon depends on the competing processes that illuminate the Moon and that provide energy for luminescence. Most favorable times for seeing luminescence are at new Moon on the far side of the Moon, and

during rare dark eclipses. The luminosity and color of these rare eclipses is explained. Direct processes for converting energy to luminescence in lunar day cannot be energized by presently known sources of particles. If storage processes occur they may give information about the dust particles at the extreme lunar surface.

The question whether the Moon was ever molten has been widely discussed. In D. L. Anderson and R. A. Phinney's paper the "Internal Temperatures of the Moon" (Appendix I) are analyzed in considerable detail and the related problem of volcanism is investigated by thermal history calculations. While the results depend on the radioactivity and age of the Moon, extensive interior melting is difficult to avoid. The chondritic Moon will start to melt at depths below about 300 km at about 1.9 billion years after formation. If the Moon has the composition of the Earth's mantle, melting will commence at about 1.6 billion years at a corresponding depth and will proceed rapidly inward. A moon with about 2/3 of the Earth's radioactivity and only 3.5×10^9 years old will not yet have melted if it started cold.

The most extensive stage of volcanism will probably follow differentiation, perhaps 2-3 billion years ago. It follows that the presence of lava and/or ash flows on the surface of the Moon is highly probable. The Moon is probably a differentiated body; but since iron is not involved in the differentiation, a heavy core is not present. It is also shown

that Mars will probably not melt and is now an undifferentiated body. This supposition is supported by the moment of inertia of Mars. It is suggested that the presently planned studies be expanded to include a lunar geodectic orbiter, a direct measurement of surface heat flow and a passive lunar seismometer. It is recommended that the feasibility of a monocycle radar pulse orbiter experiment to determine the structure of the outer several kilometers of the Moon be investigated.

In "The Case Against Volcanism" (Appendix IV) T. Gold argues that volcanism could not have been the major agency in shaping the primary features of the Moon. He suggests that ice sheets covered with dust are responsible for the flat mare and crater bottoms.

In Part II of his paper, T. Gold emphasizes the importance of high quality photography needed in future lunar exploration and the associated problems and peculiarities to be encountered in lunar photography.

SECTION IV

BACKGROUND OF THE "TYCHO" STUDY GROUP

IV. BACKGROUND OF THE "TYCHO" STUDY GROUP

A. Origin

On May 26, 1964, Mr. Homer E. Newell, Associate Administrator for Space Science and Applications, NASA, addressed a memorandum to the Deputy Administrator and to the Associate Administrator of NASA proposing that a group of approximately 20 established scientists be assembed on a part-time basis to study advanced physical problems in science as they relate to man's efforts in space exploration. This group would be free to address itself to new research areas, avenues of pursuit, and to matters of science of its own choosing. The group would consist of high caliber scientists recruited from academic and research areas primarily involved in solid state and theoretical physics. The emphasis on physics was sponsored by a need for solution of a number of physical problems encountered in the lunar program. Continuity of the group would be maintained over several years through retention of as many members as possible from year to year and through frequent sessions of several days duration in addition to an annual five to six weeks summer study session. Preliminary discussions between Mr. Newell, Mr. Willis B. Foster, Director of the Manned Space Science Division, Dr. Willard S. Boyle of Bellcomm and Dr. Robert J. Collins of the University of Minnesota in May, 1964, led to submission of a proposal by the University of Minnesota to organize and administer such a group.

The University of Minnesota's proposal was essentially consistent with the preliminary memorandum of May 26, 1964, and the discussions held at NASA headquarters. The proposal suggested expansion of the membership to include several members from other disciplines to provide cognizance of research activity and state of knowledge in related areas such as astrophysics, geology and microbiology and to include a representative from NASA headquarters for guidance on broad NASA programs and plans. Pressing lunar exploration problems would be reflected in the initial constitution of members selected for the study group who would also have demonstrated previous competence in research and scientific matters. The proposal emphasized need for orientation of members on problems under study and a general state of the art. It was planned that the location of the study groups should be removed from the usual working place of participants to avoid conflict with routine demands of their regular duties.

The University of Minnesota acts as the agency to supply fiscal responsibility and administrative organization for the study group. Administrative details are managed by an administrative officer assigned to a staff position delegated by the University of Minnesota.

The Study Group was initially called "The Manned Space Science Study Group." However, in August, 1965, in order to avoid confusion with other similarily entitled groups and organizations, the name was changed to "Tycho" Study Group

after the lunar crater "Tycho" which had figured in much of the research work conducted by the study group.

B. Members

The selection and recruitment of members to serve with the "Tycho" Study Group has been a more difficult task than anticipated. It was recognized at an early date that recruitment of well-known authorities in this area was futile because of the many demands for their services and their inability to devote extended periods of time with the group. Rather, it was decided to call upon such individuals for short presentations and special consultations as needed and when available. Dr. Gerard P. Kuiper and Dr. Eugene M. Shoemaker are examples of individuals in this category. Accordingly, it was then necessary to detect and recruit scientists who possessed significant potential for space research, but who, for a variety of reasons, had not yet achieved such widespread recognition for their work. Next, it was important to determine their motivation for this type of research activity and their availability to function with the group. The following is a list of members who have agreed to serve with the "Tycho" Study Group although several were unable to devote their full time to the summer study session in Boulder this summer:

Name	Institution	Principal Discipline and/or Area of Interest
*Allen, Frederick G.	Bellcomm, Inc.	Solid State Physics
Anderson, Don Lynn	Calif. Inst./Tech.	Geophysics
Collins, Robert J.	Univ. of Minn.	Solid State Physics
*Evans, John V.	Lin. Lab, MIT	Radar
#Gold, Thomas	Cornell Univ.	Astronomy
Heffner, Hubert	Stanford Univ.	Electrical Engineering
Hopfield, John J.	Princeton Univ.	Theoretical Physics
#Lax, Benjamin	MIT	Solid State Physics
#Ney, Edward P.	Univ. of Minn.	Astro-Physics
*Pearse, C. Arnold	Bellcomm, Inc.	Theoretical Physics
#Phinney, Robert A.	Princeton Univ.	Geophysics
Smoluchowski, Roman	Princeton Univ.	Solid State Physics
Suhl, Harry	Univ. of Calif./LJ	Theoretical Physics
#Woolf, N. J.	Princeton Univ.	Astronomy

*Participated part time and without monetary reimbursement.

#Participated part time as follows:

Gold	(one week, August 1-7)
Lax	(three weeks, August 12-31)
Ney	(two weeks, August 3-15)
Phinney	(two weeks, August 9-21)
Woolf	(three weeks, August 2-18, 26-28)

The following individuals particpated as special
consultants:

Name	Institution/Company	Principal Discipline	Date
Green, Jack	North American Aviation	Geology/ Geochemistry	8/5&6
Shoemaker, Eugene M.	U. S. Geology Service Flagstaff, Arizona	Astronomy/ Astrogeology	3/27
Shorthill, Richard W.	Boeing Aircraft Corp.	Astrophysics/ Infrared	8/2&3

Commander Trygve A. Holl, U. S. Navy (Retired) has been
retained by the University of Minnesota as Assistant Director for
the "Tycho" Study Group and has functioned as the Administrative
Officer since January 8, 1965.

C.   Meetings

A preliminary meeting was held in Washington, D. C. on December 18, 1964, to clarify the purpose of the stud' g oup, to outline a plan of action, and to evaluate individuals who might be invited to participate as members in the group. At this meeting it was decided to proceed with plans for short interim meetings in March at Kansas City, Missouri, in conjunction with the American Physical Society meeting. It was also decided to schedule the extended summer study session during the month of August at a location to be determined later. The following individuals attended this meeting although several (Wertheim and Herring) were unable to continue as members of the study group:

Collins, Robert J.	University of Minnesota
Heffner, Hubert	Stanford University
Herring, W. Conyers	Bell Telephone Laboratories
Hopfield, John J.	Princeton University
Ney, Edward P.	University of Minnesota
Suhl, Harry	University of California

The second meeting of the study group was held at Kansas City, Missouri, on Saturday, March 27, 1965, to capitalize on the presence of a number of the members who were already in Kansas City attending the March meeting of the American Physical Society earlier that week.

"THIS APPENDIX IS ALSO ISSUED AS TG-2"

APPENDIX I

INTERNAL TEMPERATURES OF THE MOON

INTERNAL TEMPERATURES OF THE MOON

R. A. Phinney and Don L. Anderson

August 1965

INTERNAL TEMPERATURES OF THE MOON

ABSTRACT

The possibility of melting in the interior of the Moon and the related problem of volcanism is investigated by thermal history calculations. Results depend on the radioactivity and age of the Moon, but extensive interior melting is difficult to avoid. A chondritic Moon will start to melt at depths below about 300 km at about 1.9 billion years after formation, assuming the age of the Moon to be 4.5×10^9 years. If the Moon has the composition of the Earth's mantle, melting will commence at about 1.6 billion years at a corresponding depth. Melting proceeds rapidly inward. An initially cold Moon with about 2/3 of the Earth's radioactivity (gram/gram) and only 3.5×10^9 years old will not yet have melted.

The most reasonable models for the Moon will predict melting early in their history. Differentiation and volcanism will accompany this melting and tend to redistribute both heat and matter. After differentiation, the near surface of the Moon heats up even more rapidly because of the increased concentration of radioactivity. The most extensive stage of volcanism will probably follow the differentiation, perhaps 2-3 billion years ago. It is concluded that the presence of lava and/or ash flows on the surface of the Moon is highly probable. The Moon is probably a differentiated body; but since iron is not involved in the differentiation, a heavy core is not present. The internal layering is probably silicic over basic, as in the Earth.

Neglected sources of heat are discussed, and it is concluded that the estimates of internal temperatures are conservative.

It is also shown that Mars will probably not melt and is now an undifferentiated body. This supposition is supported by the moment of inertia of Mars.

The thermal history calculation presented in this report represents preliminary results. It is planned to take into account the latent heats of fusion and convective transport of heat during differentiation in later calculations. This will not affect present conclusions with regard to the initiation of melting, but should give better estimates of the Moon's present heat balance.

Various lines of evidence point toward the possibility of appreciable seismicity on the Moon. Whether this poses a threat to manned missions can be determined by landing a long-lived passive seismic experiment on the Moon.

Specific first generation experiments which are suggested by the present study include a lunar geodectic orbiter, a direct measurement of surface heat flow and a passive lunar seismometer. In addition to data on composition and an age data which will be available from samples of the lunar surface, it is also recommended that the feasibility be determined of a monocycle radar pulse orbiter experiment to investigate the structure of the outer several kilometers of the Moon.

TABLE OF CONTENTS

LIST OF ILLUSTRATIONS

LIST OF TABLES

INTERNAL TEMPERATURES OF THE MOON

R. A. Phinney and Don L. Anderson

August 1965

I.   Introduction

The present hypothesis regarding the surface structure of the Moon and its relation to internal structure and processes completely bracket the possibilities. One extreme view attributes all visible surface features to phenomena external to the Moon; the other extreme attributes all these features to internal mechanisms. These positions will be referred to as the cold Moon and the hot Moon hypothesis. The surface features of the Earth represent a competition between the generation and release of internal stresses and "external" forces (wind and water erosion, meteorites, solar energy). Geologists have inferred the structure and dynamics of the upper several hundred kilometers of the Earth simply from the morphology of surface features in spite of the competition of unrelated phenomena which are continually modifying the evidence.

A.   On the Formation and Compaction of a Lunar Soil

Because of the absence of atmosphere and hydrosphere, the standard external processes of destruction and transportation with which the geologist is familiar on Earth do not operate on the Moon. Yet, clearly the surface of the Moon is undergoing erosion and at least small amounts of material transport. It is

not yet clear whether meteorites and micrometeorites supply an adequate erosional mechanism. We are attempting to explain the transformation of apparently young fresh looking features to features which are older on other counts and which have subdued relief. A fresh rock brought to the surface of the Moon from either above or below will undoubtedly no longer be in either mechanical or chemical equilibrium with its surroundings. Although it is not known what will happen to a dry rock in vacuum exposed to a high amplitude thermal cycle, it is likely to exfoliate, recrystallize, differentially evaporate and in general, disintegrate. In the process of being brought to the surface internal stresses will no longer be consistent with the absence of external stresses and mechanical disintegration will occur even in the absence of the thermal cycle. Gases from the interior, if present, will accentuate the deterioration process. It is not possible to estimate the depth of these kinds of "weathering," but there are sufficient mechanisms which will generate a lunar soil even without meteoritic impact or volcanic ash. Opposing these processes of disintegration will be processes tending to make solid rock from the disintegration fragments. Again, the common processes of cementation such as solution and deposition involving surface and ground water, do not operate near the surface of the Moon. The processes by which grains will adhere and coalesce will probably be those more familiar to the ceramic metallurgist than to the field geologist. Such sintering processes include surface and volume diffusion of material toward points of particle contact

driven by a free energy gradient, plastic or viscous flow of material at the contact points tending to bring particles closer together and increase the contact area, sputtering, and condensation of vapor at contact points. Even before these processes have a chance to operate, all being time dependent, the grains will adhere tightly as shown by Salisbury and others. The above processes are in addition to the purely mechanical compaction occuring near the surface of the Moon due to overburden pressure. This process is controlled by the stability of a loose aggregate of particles which in turn is governed by the forces between particles including strength of contact points and friction between grains, and van der Waals' forces. The particles will not become a stable aggregate until they achieve a density somewhere between open and close pack, perhaps 40% porosity. From this point on the grains will grow together by time and temperature dependent processes of diffusion even if no more load is added above. These processes will occur much more slowly than the ceramicist can tolerate because of the much lower temperatures. However, much more time is available than the ceramicist is used to.

A representative mechanism is volume or bulk diffusion, a process rate limited by the slowest diffusing ion. The area of contact between adjacent grains will grow with time as

$$r^5 = \frac{A \, R_o^2}{T} \, D \, t$$

where:

r = radius of contact

T = absolute temperature

t = time

A = constant involving interatomic distance, Boltzmann constant, surface energy

D = diffusion coefficient $D_o e^{-E^*/kT}$

R_o = original radius of particles

E^* = activation energy for diffusion

The growth of the contact area between grains due to viscous flow is

$$r^2 = \frac{AR_o t}{\eta}$$

η = viscosity $\sim \eta_o e^{+E^*/kT}$

A = constant

E^* = activation energy for viscous flow

Similar relations hold for evaporation-condensation, and surface diffusion. Temperatures on the Moon are roughly a factor of 4 or 5 less than common sintering temperatures in the laboratory, but the time scales of interest are of the order of 10^9 longer, so these processes are undoubtedly important on the Moon even at low temperatures, unless, of course, destruction mechanisms such as micrometeorite bombardment and seismicity are more important. Incidently, these latter mechanisms are probably more important in compacting loose collections of particles than in

fluffing them up. In any case, it seems difficult to maintain
an underdense collection of particles for long periods of time
or for very great depths. The conditions that retard the increase
of density with depth, namely inter-particle attractive forces
and strength at contact points, also lead to a high intrinsic
strength for the aggregate.

B. Geological Considerations

Gold's model of the surface material as consisting
of a highly underdense dust is highly attractive to physical
scientists because of the roles played by electrostatic forces
and the solar wind, and because of the peculiar photometric
properties of the surface. Certainly the photometry demands
an underdense material, but the geological relationships dis-
cussed by Kuiper and Shoemaker virtually rule out the motion of
a highly mobile thick dust layer representing material trans-
ported from the eroded highlands into the mare basins. From the
photometry, it is concluded that the surface is nearly everywhere
covered with underdense material. At the same time the distinct
albedo differences between highlands and maria (and the sharp-
ness of boundaries, especially in the flooded craters) provide
the most unequivocal evidence of a geological difference between
highlands and maria which has not been covered over by dust trans-
portation. Portions of the mare floors show up as coherent
geological units with distinct color differences between units
and sharp boundaries. The boundaries also show the kind of low
relief which is characteristic of the edge of a flow unit such

as a lava flow or rock glacier. Dust, therefore, cannot be transported in a significant quantity for distances greater than 1/2 km on the mare floors and left to build up sedimentary deposits.

The picture that emerges is not so different from that appropriate for the surface of the Earth; namely, a competition between constructive, destructive, and reconstructive mechanisms, leading to a loose surface layer grading downward to a compacted, "cemented" layer which is underlain by solid rock. The bedrock can be distinguished as one of two basic types--highland or mare; the overlying soil mantle appears to undergo negligible transportation, and develops a highly underdense surface which we will refer to by the term "dust."

C. Erosion and Transportation

The smooth surface indicated by the radar data for wavelengths in the centimeter-meter range and by the Ranger photographs requires transportation over distances of a few meters. The subdued relief of craters in the stratigraphically oldest portions of the highlands strongly suggests that up to several hundreds of meters of material has been eroded over geological time. The only direct limiting evidence we have is again the mare-highland sharp boundary, which limits the transportation to a km. or so. Of the many proposed mechanisms for breakup and transportation we can say very little; certainly no prediction of lunar geological conditions can be made on the basis of one or another theory. There is a very distinct limit to our advance knowledge of the lunar surface. It must be recognized that most

of the information about the Moon will come by sampling and observation, followed by analysis, rather than by prediction, followed by verification. It then follows that a specific experiment designed to measure bearing strength is far more relevant to Apollo than any amount of laboratory and theoretical work on Earth.

Regarding erosion, one point needs to be made. Infrared imagery shows that the soil mantle covers all but a very small fraction of the lunar surface (young craters being a possible exception). It is geologically implausible that this mantle is everywhere thick enough to give the infrared result and yet thin enough that the underlying rock is exposed to solar wind protons and micron-size micrometeorites. Since rock disintegration due to external fluxes can only be significant on exposed ridges, if erosion is regarded as taking place, most of the breakup of rock must occur by internal processes at the base of the solid mantle. It was suggested above that rocks (especially hydrated minerals) brought to the surface are sufficiently out of equilibrium with existing pressures and temperatures that internal stresses may be sufficient to disintegrate exposed surfaces. On the Earth, the disequilibrium is due primarily to the introduction of ground water, and the process is rapid in terms of geological time (e.g. $10^2 - 10^3$ years). On the Moon, the process will certainly be several orders of magnitude slower; knowledge of the numbers themselves is crucial, although the answer will probably come first from looking at the lunar surface material.

Lacking a steady transport by which the products of chemical and mechanical erosion are continuously being removed and deposited elsewhere, thus exposing fresh rock for erosion, and apparently lacking sufficient influx of particles to erode crater rims of the order of tens of meters in height, an additional mechanism seems required to level out features. Such a mechanism could be the thermal-elastic stress calculations of MacDonald (1960) or the lateral tectonic motions deduced by Fielder and Warner (1962) with the result then the Moon is probably at least as seismic as the Earth. Quite apart from possible surface evidence of faults, grabens, volcanism and distortions, the non-equilibrium shape of the Moon, thermal history calculations and large tidal forces all suggest large stresses in the interior of the Moon which may or may not relieve themselves seismically. If the Moon is sufficiently warm, these stresses can be relieved by creep or plastic flow. If the Moon is cold and brittle, active seismicity would be the preferred mode of stress energy release.

An alternate leveling mechanism would be viscous flow--the crater bottoms coming up and the walls going down. Local slumping, however, would seem to be a more efficient process leading to a similar result.

Neither seismicity nor viscosity are important leveling mechanisms on the Earth, but only because the standard mechanisms of weathering are much more rapid and efficient. Lacking these standard processes on the Moon, these slower processes may dominate.

II. A Review of the Volcanic Process; a Framework for Discussing or Rejecting Lunar Volcanism

The question of whether the Moon is, has been, or could be hot enough to produce volcanism has been considered by so many different authors, that nothing that is said here can be at all novel. Much of the discussion in the literature, however, is presented from one of two different viewpoints; 1) theoretical geophysics or 2) morphology of volcanism on the Earth. Arguments for volcanism on the Moon cannot be based solely on the latter, since any criteria for distinguishing between volcanic features and impact craters are very often ambiguous. This section is an attempt to bring together the two viewpoints and to find areas 1) where the issue is settled, 2) where more work, possible by manned expeditions, will prove decisive, and 3) where the issue could not be resolved even by extensive on-site mapping and coring.

A. Melting, Volcanism, and Outgassing

Rather than define volcanism by its surface appearance, it will be defined here to be any phenomena directly connected to the process of partial melting at depth and the related differentiation and upward transport of the melted material. It should not have to be emphasized that volcanoes are only an occasional manifestation of volcanism, but confusion of this point has been responsible for much needless controversy regarding the Moon. All igneous rocks are formed by this definition of volcanism. The process of considering all the surface phenomena of volcanism,

the geological record of deep-seated processes, and the phase equilibrium chemistry of silicates and deducing the common process of partial melting has been a major activity or geology for the last century and will not be reviewed here. While many details have not been settled, the physics and chemistry are sufficiently well understood qualitatively that they may be applied to the study of the Moon and the inner planets.

Figure 1 shows the melting curves for some of the ferro-magnesian minerals. Melting ranges are also shown for "basalt" and "pyrolite." Pyrolite is the term applied by Ringwood (1961) to his deduced upper mantle rock and satisfies the criterion that basalt magma is formed as the pyrolite is heated through its least melting temperature. Differentiation is achieved by taking a system either from complete melt to complete solid through the melting range or vice versa. The details of the process depend critically on several compositional variables and on the rate at which the bulk composition is affected by advective removal of differentiates while the process is still taking place. A great deal of laboratory work has been aimed at determining the phase equilibrium curves of rock forming systems; it has been feasible to study systems of only 2, 3 or 4 principal components so that extrapolation to actual rocks is still partly an art. In the systems which have been studied there are examples of a whole range of phenomena: binary solid solution, incongruent melting, eutectic and cotectic melting.
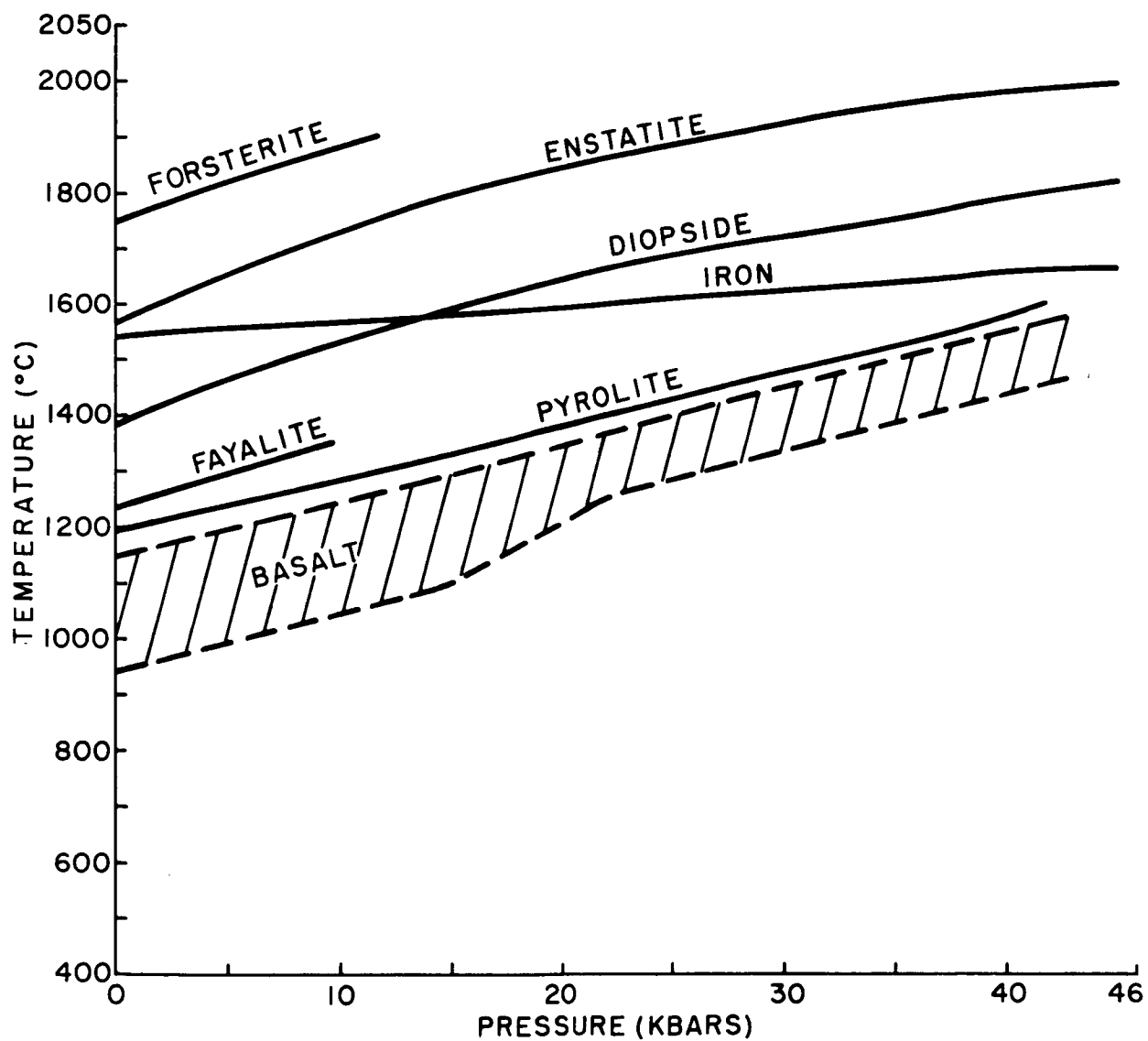
Figure 1. Melting Relations

-11-

In a general way, in a cooling magma, the denser, higher melting phases (rich in Fe, Mg, Ca) crystallize first, causing the residual liquid to become richer in the less dense, lower melting material. A completely melted pyrolite will crystallize olivine first, leaving a residual melt of basaltic composition. A completely melted basalt will crystallize pyroxenes and calcic plagioclase first, leaving a residual melt of intermediate or granitic composition. If gravitational settling of crystals proceeds faster than cooling, then the bulk composition of the remaining melt is driven toward the low melting components and an effective stratification of the final rock by density is achieved. This process is appropriate in the hypothetical cooling of an initially molten silicate planet and in the cooling of intrusive magma pockets at depths greater than a few meters. When cooling proceeds more rapidly than settling and more rapidly than the diffusion time within the crystals, then the resultant rock is macroscopically homogeneous, but microscopically differentiated in a random way due to the lack of equilibration between crystals and melt during the cooling. Extrusive basalts cool this way, the disequilibrium occasionally being such that one gets a glass. Volcanic glasses are sufficiently unstable that they devitrify within a few million years. Obviously, differentiation of an initially solid planet cannot occur this way, but must be related as we shall see to the heating of certain zones to the lowest melting point and the separation and upward migration of the liquid phase.

Evidence on the abundance of long-lived radioactive heat producing elements indicates that except for minor cooling in the outer few km. the Earth has been heating over the last 4.5 billion years. Since shear waves are observed to propagate through the mantle, it is clear that the mantle is now solid, although local partial melting is not ruled out and, in fact, is necessary to explain observed volcanism. The iron core does not transmit shear waves and is, therefore, fluid. The simplest thermal history possible under the circumstances involves an initially cold Earth warming up due to radiogenic heat sources. Volcanism provides abundant evidence that molten material has originated in the lower crust and upper mantle; one is, therefore, constrained to have only local melting which does not seriously impede the passage of shear waves. The seismic low-velocity zone in the upper mantle, from about 100 to 400 km (Gutenberg, 1959, Anderson, 1965) can adequately be explained by a high geothermal gradient and a close approach to the melting point of silicates in this region. The high attenuation of shear waves in this region (Anderson and Archambeau, 1964) is additional evidence for softening of material, and perhaps partial melting in the upper mantle. Other evidence points to this region of the Earth as the main recent source of differentiation although indirect evidence from isotopes appears to require that the lower mantle participated in differentiation in the earlier history of the Earth.

Differentiation of mantle material occurs at points where transient temperature increases or pressure release brings the system up to its least melting temperature. A minor amount of liquid phase is produced with a different bulk composition than the parent material. The production of the liquid phase uses up a great deal of heat of fusion and tends to buffer the temperature against further increase. The liquid, which for a pyrolite source has the composition of basalt, is less dense than the solid matrix and is driven upward by body forces. Usually, (by inference) it migrates upwards some distance and is intruded into shallower rocks. Occasionally the excess pressure developed at the source is sufficient to drive the magma through faults, joints and interstices to the surface, where it is observed as lava. The majority of igneous rocks are probably intrusive rather than extrusive.

On the Earth, at least, we can see the evidence of second generation differentiation by partial fusion; the source material is of the composition of basalt, and the light differentiate is the granitic material which forms the upper 20 km of the continental plates. Rubey (1951) has studied the geochemical balance of volatiles, particularly H_2O and CO_2 and has found that these must be continually brought to the surface in volcanic activity. In order of importance, the sources are hot springs (which overlay active granite intrusions) and volcanoes. The tendency of the volatiles to be found in the second generation differentiates is due to their much greater solubility in granitic

melts, but the original source zone is still the upper mantle.
A pyrolite mantle with 0.5% H_2O and differentiate for about
700 km over 4 billion years would produce enough water and
CO_2 to explain the observed quantities in the atmosphere, oceans,
and sedimentary rocks. The intimate connection of water out-
gassing and volcanism through their common history of partial
fusion is well established on the Earth. In fact, the presence
of significant ice on the Moon would imply extensive differentiation
and a "hot" Moon (Watson et al, 1961).

Phase equilibrium data appears to rule out the possibility
of significant[1] surface water on a cold Moon.

The Moon must be fairly rich in olivine, principally in the
mineral forsterite, and it can be assumed to contain about 0.5%
average water by weight. Forsterite and water coexist at
temperatures greater than about 500°C, but at lower temperatures
they react to form serpentine. Many reactions are possible,

---

[1]"Significant" is defined as ice in cold traps, forming coherent
films or bodies, as distinct from monomolecular films on grain
boundaries or distributed impurities in crystals. "Cold" is a
statement that the internal temperature is sufficiently below the
melting temperature everywhere, that partial melting cannot occur
under stress release as great as 2 kilobars or that shear
instability is not possible. The 2 kb is the release associated
with removal of 40 km of surface material as in a typical mare-
forming impact. Shear instability occurs when the thermally
activated creep rate is high enough that the frictionally
generated heat is not removed by conduction as rapidly as it is
produced.

depending on the amounts of water and silica. The following is typical:

$$\text{forsterite} + \text{water} \rightleftharpoons \text{serpentine} + \text{magnesia}$$

$$4Mg_2SiO_4 + 4H_2O \rightleftharpoons Mg_6Si_4O_{10}(OH)_8 + 2MgO$$

This means that about 8 grams of forsterite can react completely with one gram of water. To estimate the amount of forsterite in the Moon consider that

Olivine fraction for various rock types

dunite	100%
peridotite	55%
chondrite	46%
basalt	10% (variable 0-40%).

The present best estimate of the composition of a primitive un-differentiated mantle or Moon is that of peridotite mixed with 20% basalt. Being constrained to keep the density up to the vicinity of 3.34, the olivine fraction cannot go below about 35%. This means that up to 4% water will be taken up chemically by forsterite in any region where the temperature is less than $500^{\circ}C$. If the initial concentrations of the radiogenic elements of the Moon were about 1/5 the concentrations on the Earth, heating would occur in the usual way, and the central temperature would be around $700^{\circ}C$ with the 500° isotherm at half the radius. The unbound water in the center would be free to work its way outward along the pressure gradient to the 500° barrier. While the original 0.5% in the outer shell is already chemically bound, and the addition of the water from the center will cause an average

increase in the outer shell of 1/8 of 0.5%, which can be taken up in chemical reaction by the olivine without depleting the olivine supply significantly. The only way water can pass through this shell is if it is thin enough that the olivine is saturated and the excess free water can continue upward. This can only happen if the volume of the cool outer shell is 1/8 or less of the volume of the hot center. This puts the 500° isotherm at a depth of 70 km; while under all reasonable assumptions for the depths of the radiogenic elements, the approach to melting occurs at 200 km or less. It then follows that the Moon must be "hot" with conditions favoring occasional melting and the associated processes of volcanism and outgassing. It may be argued both from the geometry and lack of unmistakable recent mare-type surfaces that effusion of lava is not an important process today. It would be much more difficult to eliminate effusion of the volatiles by venting, so that any "cold" water that diffused through the serpentine would be but a small fraction of the magma-derived water. It is important to this argument that hot volatiles associated with particle melting will have their water trapped in the mantle by serpentinization.

The low pressures and low densities at the surface of the Moon would tend to favor intrusive injection of any molten lava that attempted to come to the surface just as lava commonly intrudes and underlies the weak sediments on the ocean bottoms on Earth. This again would suggest that gas emanations would be the main present-day manifestation of volcanism on the Moon.

B. On the Resemblance of Lunar Features to Terrestrial Features

1. _Maria._ There being no problem in any similarity between impact features and the flow units found to make up the mare floors, the identification of these flows would be basalt with a highly porous surface. O'Keefe, in a number of papers, has discussed the proposition that they are actually ash flows, which obtain their mobility due to mixing of fine extruded materials with hot turbulent gases. Gold, until recently, held that the mare floors were kilometer-thick basins of dust which had been transported from the highlands; he has recently suggested that the flow-like appearance of the units arises from the existence of appreciable quantities of cold-trapped ice in the interstices of the dust, which is then assumed to behave like a glacier. Such entities are observed on Earth, and are known as rock glaciers. Unfortunately for any analogy, terrestrial rock glaciers are found to originate in high mountain valleys and do not spread more than a very few km from their sources.

2. _Craters._ Shoemaker (1965) has made a strong case for the impact nature of most craters, based on comparisons of their depth-diameter ratios with terrestrial impact craters and artificially produced craters from nuclear and chemical explosions. There appears to be little question that the large rayed craters and the many smaller craters with raised rims which dot the maria are due to impact.

Regarding the numerous older craters which cover nearly all of the highlands, Green makes a stimulating, if not entirely compelling case that many of these are actually calderas, due, presumably to explosive episodes of outgassing. He makes extensive use of analogies with terrestrial volcanic features, and the juxtaposition of telescopic pictures of certain lunar features and aerial photographs of terrestrial volcanoes is most impressive. This type of evidence by itself does not prove much, because all the features involved could, by their morphology, have been produced by a hypervelocity impact, including the undoubted terrestrial volcanoes. This is because all these craters are produced by the explosive release of a great deal of energy at depths of tens to hundreds of meters. At present there is no way to distinguish the source of this explosive energy; the crater would look the same whether a meteroid or a gas pocket exploded.

The Ranger 9 photographs show rills on the floors of Alphonsus which contain small depression craters along their length; internal control is suggested. Although these are certainly not volcanoes in the usual sense, they are evidence of internal phenomena which are probably connected with the discharge of gas.

In summary it might be said that a very large percentage of craters can be plausibly discussed from an impact point of view, and a similar number as due to volcanic processes. A

discouragingly large number belong to both of these groups, and an "all or nothing" point of view about the competing theories is inappropriate.

III. A Review of Evidence on the Interior of the Moon

    A.   Internal Structure of the Earth as a Comparison

        The internal structure of the Earth is studied, in roughly the order of decreasing resolution, by:

    1.   the transmission of seismic waves,

    2.   the free oscillations of the Earth,

    3.   gravity and magnetic surveying,

    4.   geological field relationships,

    5.   electrical methods,

    6.   mass and moments of inertia,

    7.   tidal deformation,

    8.   thermal and heat flow.

No object is served in describing a program of manned lunar science involving these phenomena; this is amply covered elsewhere. At present the "probable" Moon is given by reasoning on much more limited data, specifically, the mass and moments and the geological field relationships. (The geology is less important to our present knowledge, since only the geometry is known and not the chemistry of the surface.)

    B.   First-Order Picture of the Moon

        The reasoning leading to a first-order picture is brief:

    1.   The mean density of the Moon (3.34) is so close to the mean density of the Earth's mantle in an uncompressed state, that it is irresistable to assume that the compositions of the Moon and mantle are the same. This idea can be justifiably abandoned

only if adequately sampled lunar material compels a different model. If the slight compression effect in the Moon is included, one finds that the Moon can be made out of mantle material in which the temperature depends on pressure in the same way in both objects; the entire inside of such a Moon is equivalent to the Earth's low velocity zone. Differences among models of this type are in the same speculative realm as are differences in various thermal histories which will be mentioned later.

2. The dynamic figure of the Moon as given by the differences between the moments of inertia indicates that the Moon cannot be in hydrostatic equilibrium in the same degree as is the Earth. For the Earth the actual dynamic ellipticity differs from the expected hydrostatic value by less than a percent of the ellipticity, and the nonhydrostaticity of the Earth is then a small correction to the hydrostatic figure. For the Moon, however, the triaxiality is an order of magnitude greater than the triaxiality expected on a hydrostatic tidal theory (the hydrostatic equilibrium figure of the Moon would be a triaxial ellipsoid due to the slow rotation rate and the synchronous rotation coupled with a tidal bulge). Kaula (1963) has pointed out that the stresses implied by a given term in the Moon's potential are 22 times less than the stresses implied by a corresponding term in the Earth. We, therefore, expect the Moon to depart further from an equilibrium figure than the Earth. Caputo (1965) has recently discussed this problem and has re-estimated the minimum stresses which must exist in an outer solid

shell in order to support the observed figure. Given a core with radius 3/4 the lunar radius, he finds shell stresses of the order of 20 - 30 bars. For a smaller core the stresses are correspondingly less.

This information on the figure is the basis for the statement that the Moon cannot have a liquid core or be near its melting point at any depth. If one has in mind the thermal calculations of MacDonald (1959), this attitude may be justified since his chondritic model demands a Moon which melts everywhere except in a shell of thickness less than 0.1. The stresses required would then be over 100 bars, which is believed to be greater than the "long term strength" of the Earth's mantle generally taken as a "few tens of bars." Caputo's discussion suggests that no contradictions are involved if the radius of the zero-strength core is as great as .85.

The behavior of heated solids under shear stress for long times presents certain experimental and theoretical difficulties. The existence of a "long term strength" is highly problematic, since deformation at high temperatures and low strain rate appears to proceed more or less according to an Eyring model of an activation process. The indications of stresses in the Earth and Moon may then imply that a non-equilibrium situation is involved, wherein the stresses are generated as a consequence of a tendency toward thermal convection. If the Moon's non-equilibrium shape is supported by a viscosity rather than a finite strength, a time constant for readjustment of the figure of the

Moon is about 13 times the corresponding time for the shape of the Earth. Again, this says that the Moon should depart further from an equilibrium body than the Earth. (We do not endorse the popular picture of convection cells running around in circles. The existence of a region in the Earth's crust and upper mantle which is certainly superadiabatic and the existence of unquestioned large scale vertical motions--mountain building--are strong indications that stresses due to the unstable configuration occur on the Earth. Any Moon-sized body which is internally heated by radioactive decay will be unstable with respect to convective overturn.) The lack of quantitative knowledge of the physics of such long-time processes makes it unlikely that firm statements can be made about the detailed state of stress of the lunar interior[2]. While further considerations could be discussed here, they would serve only to reinforce the non-uniqueness of this issue. Our firm knowledge is contained in the original statement that the Moon is not in hydrostatic equilibrium, which is not surprising.

---

[2]The fact that there are as many opinions on the Earth's non-hydrostaticity as there are workers in the field would suggest that it is premature to make firm statements about the Moon. One is reminded of the definition by Birch of the high-pressure state of matter.

3. Other Information

a. The present determination of the moments of inertia of the Moon is (Caputo, 1965):

$$B/Ma^2 = .58 \text{ (least .46, greatest .67)}$$

$$C/Ma^2 = .35 \text{ (least .16, greatest .54)}$$

The given values are surprising and indicate deficiencies in the theory used to compute them. A reasonable model can be made by taking .46 and .45. No concludions can be drawn from these numbers at this time. In fact, better bounds can be placed on the moments by consideration of various possible internal structures.

b. The geology of the maria makes it probable that they are composed of lava flows. The relative time relationships indicated by the stratigraphy place these within a fairly short range of geological time. With the same confidence it can be implied that the Moon was once hot enough for partial melting. This implies nothing concerning partial fusion taking place at present since extrusion of molten rock requires rather special conditions which may not have been satisfied during post-mare time.

c. If the Moon has the same composition (in major components) as the Earth's mantle (Paragraph 1), then one may propose one of two alternate working hypotheses which give an idea of the possible interior state of the Moon. Given lunar samples, these hypotheses will be improved:

1)   The temperature-pressure curve is the
same in the Moon as in the mantle. One may then "map" the
Earth into the Moon, taking account of the reduced pressure
gradient. Partial melting is then implied in the inner 1300 km
or so, and the moment of inertia becomes .42, meaning that the
density must decrease slightly with depth.

2)   The ratios of the radiogenic isotopes
are the same in the Moon as in the Earth and in the Hoyle-Burbidge
cosmogony. In additon, we take the numerical abundance the same,
with perhaps less justification. The radiogenic abundances found
in chondritic meteorites (MacDonald 1959) may be used. The heat
flow and internal temperatures resulting from these assumptions
will be discussed later in this report. These results say that
heating must have occurred to an extent that volcanism is not
likely. However, it is perhaps more justifiable to take the
maria as indicating volcanism, which implies that the initial
assumptions of this paragraph are correct within a factor of 4
or so.

Hypotheses 1) and 2) imply possibly different temperatures,
and cannot be considered simultaneously.

IV. Thermal History of the Moon

A. Introduction and Review

1. Thermal Evolution of an Initially Cold Moon Heated by Long-Lived Radioactivities

MacDonald, Lubimova, Birch, Urey, Clark, and others, in a number of recent papers have demonstrated the main features of the heat-flow balance in a non-convecting planet which is heated by the long-lived radioactive isotopes U^{235}, U^{238}, Th^{232}, and K^{40}. The major characteristics of such a thermal evolution are:

a. The importance of early heating by the relatively short-lived K^{40}.

b. The dominance of phonon conductivity with its T^{-1} behavior at temperatures below around $700^{\circ}C$ and the dominance of radiative conductivity with its T^3 behavior at higher temperatures. The radiative term tends to shorten the thermal decay time of the hot interior and reduce the thermal gradient.

c. The ratios of the radioactive isotopes one to another appear to be fairly constant for a variety of rock types, although differentiation has strongly concentrated them in granitic rocks (up to 100x). The determination of absolute abundances for primitive mantle or Moon material is a more delicate matter. MacDonald (1964) has recently determined these abundances by constraining the calculated heat flow for a variety of theoretical models to equal the observed average heat

flow on the Earth. All such models for the Earth give temperatures in the core which exceed the melting curve of iron, and temperatures in the mantle which are substantially less than the melting curve of pyrolite, except in the depth range 100-200 km, where direct evidence of volcanism and low seismic velocities indicates high temperature conditions near melting.

d. Some abundances and distributions of radio-activity give temperatures which exceed the melting curve. Since no thermal models to date have taken account of heat of fusion, they are not relevant to the actual problem. Convective transport of heat upward out of the melt zone must also be included in a realistic model. Estimation of the effective convective conductivity may require a good deal of art, and will certainly not reduce the uncertainty of the result. For the Earth, at least, models can be eliminated which take the temperature more than, say, 40° above melting, since a 400° excess is equivalent to the heat of fusion, and no widespread zones are 10% or more liquid. In the appendix we outline a computational schedule for thermal history calculations.

The best justification for working with an initially cold Earth and ignoring the initial temperature due to accretion and short-lived radioactivities is due to the essentially conservative nature of the results. The Earth comes very close to melting in the upper mantle in any case. Differences between many models can be resolved because a great deal of first-order knowledge exists about the Earth--existence and mechanism of

volcanism, seismic velocities and attenuation in the mantle, surface heat flow, and rough extent of the vertical differentiation which has brought volatiles and radioactive heat sources into the crust.

In the case of the Moon, predictions are being attempted about these very things in advance of manned expeditions. It is preferable to have in hand certain items--composition of maria and highlands, seismicity and surface heat flow-- which might give a reasonable constrained picture of the thermal evolution of the Moon. Nevertheless an attempt will be made to give an analysis and prediction, keeping in mind the discussion in Section III.

An additional source of heat in the Moon is tidal dissipation. Kaula (1963) showed that at present this effect generates 0.010 ergs/g/yr, much less than the current rate of radioactive heating. Tidal heating, however, would be comparable to radioactive heating if the Moon were only 1/3 the present distance from the Earth. The distribution of tidal heating is extremely non-uniform both radially and laterally. If tidal heating had ever been important, large thermal stresses are implied, leading to seismicity and/or convection. Kaula estimates that tidal heating would be important 10^9 years ago using the secular acceleration calculated by Munk and MacDonald (1960). He points out that the fourth-degree terms in the mass distribution of the Moon would be determined by the convective patterns and that if these terms are markedly larger than the other terms, it would be a strong indication that the Moon was once close enough to the Earth

for heating by tidal dissipation to cause convection.

The present tidal dissipation of energy of 0.01 ergs/g/yr can be compared to .0016 ergs/g/yr which is the present rate of seismicity on the Earth.

From the thermoelastic stresses being built up in a warming homogeneous chondritic Moon, MacDonald calculated that 10^{24} - ko^{25} ergs of distortional energy would be released each year. This gives .014 - .14 ergs/g/yr. Tidal forces and thermoelastic forces, therefore, give comparable energies which, if released rapidly, would give the Moon a seismicity greater than that on the Earth.

B.   Initial Temperature in an Accreting Planet

It is necessary to estimate the initial temperature in the Moon before proceeding with the evolution problem. According to modern ideas, the Earth and other planets were formed by the accretion of particles from a gas-dust protoplanetary cloud. The sources of heat which provide the "initial" temperature are several:

1.   An elastic collision of infalling matter with the surface. This tends to produce a marked temperature rise on the surface, which is counteracted by re-radiation of energy into space and by a more modest conduction of heat toward the center of the body.

2.   Adiabatic compression of the interior due to accretion of new material. If the interior is initially heterogeneous, the resulting temperatures may be far from what we consider in the

term "adiabatic gradient" since convective equilibrium is not involved (by fiat). Consequently, internal heat flows will arise, tending to minimize local thermal gradients.

   3.   Long-lived radioactivities, such as U, Th, and K^{40}, which are discussed later, can play a minor part, depending on the time required for the accretion process.

   4.   Short-lived radioactivities, with half-lives less than 10^8 years, could have produced very substantial heating, if the Moon was formed by accretion very shortly after the time of nucleogenesis. Since this time lag is so crucial, yet so unknown, we take the conservative assumption that this effect is negligible.

   The accretion process presumably begins slowly and there will be no appreciable temperature rise due to impact until the gravitational field of the growing planet becomes appreciable. From this point the gravitational energy of the incoming particles goes into heating the surfaces involved, heating the interior of the bodies by conduction, into phase changes such as vaporization and melting or formation of high pressure phases, shattering the bodies, and into outer space by radiation.

   The rate at which gravitational energy is added is:

$$\frac{dU_1}{dt} = \frac{G(r)M(r)}{r} \cdot \frac{dM}{dt} = 4 \pi \rho r G(r)M(r) \frac{dr}{dt}$$

The rate at which energy is radiated is:

$$\frac{dU_2}{dt} = 4 \pi r^2 \sigma T^4$$

The rate at which energy is used up in phase changes is:

$$\frac{dU_3}{dt} = 4 \pi r^2 \rho L \frac{dr}{dt}$$

The rate at which heat is used to heat the surface is:

$$\frac{dU^4}{dt} = 4 \pi r^2 C\rho\Delta T \frac{dr}{dt}$$

The heat balance equation, then, ignoring radioactivity and conduction is:

$$\frac{G(r)M(r)}{r} - \rho L - C_p \Delta T \frac{dr}{dt} = \sigma T^4$$

In the steady state all heat brought to the surface is radiated back into space and:

$$\frac{G(r)M(r)}{r} \frac{dr}{dt} = \sigma T^4$$

is the condition giving the equilibrium temperature.

Ter Haar (1943) estimates

$$\frac{dM}{dt} = \alpha M^2$$

$$\alpha = 2 \times 10^{-41} \text{ gm}^{-1} \text{ sec}^{-1}$$

$$T^4 = \frac{G\alpha\rho M^2}{3\sigma}$$

For the Earth the steady state surface temperature near the end of accumulation would be about 1100°K, assuming the above rate. If the Earth accumulated uniformly in 10^9 years, the surface temperature would be about 145°K; if if accumulated in 10^8 years, the surface temperature would be 250°K.

The corresponding temperatures for the Moon and Mars would be much lower. Using Ter Haar's estimate of rates, the steady state temperature of the Moon would be 110°K. If it accreted at a constant rate in 10^8 years the equilibrium temperature would be 73°K. If it accreted at the same rate as the Earth in 10^8 years, 220°K would be the surface temperature. Ter Haar's rates lead to 330°K for the surface temperature of Mars.

Similar calculations have been made by Ter Haar (1948), Hoyle (1946), and MacDonald (1959).

Ter Haar estimates the Earth's surface temperature after accretion to be between $1000^\circ$and 2000°K. A later calculation reported by Benfield (1950) is 3500°K. Hoyle gets about 2000°K for a slightly larger than Earth size planet. Lubimova (1958) reporting results of Safronov, gave a temperature increase of 200°K for a distance 0.8 R from the Earth's center for large particles impacting the surface of the Earth, and 1200°K at the same distance for small inelastically colliding particles. MacDonald gives 973°K as the surface temperature during the last stages of accretion.

Since the accretion process started slowly and ended slowly, the surface temperature rise was probably a maximum at

some intermediate stage and the resulting temperature of the fully accreted planet would have a maximum between the surface and the center. The average temperature in the body is probably roughly as given previously, i.e. probably less than $1000^{\circ}K$ for the Earth, less than $200^{\circ}K$ for the Moon, and less than $300^{\circ}K$ for Mars. Radioactive decay and self-compression during the growth process would tend to make the temperature roughly a slightly increasing function of depth.

It is assumed that the Earth and Moon accreted from a rotating dust cloud in a time short compared with the age of the Earth--10^6 to 5×10^8 years is taken as a possible range. The time of formation of the Moon may be taken either as simultaneous with the Earth or that the present Moon was formed by sweeping up several smaller protomoons at a later stage. The latter model has certain desirable features with regard to the tidal evolution of the Earth-Moon system, and may be relevant to the thermal evolution as well. The problem separates into two phases: 1) estimation of temperatures achieved during accretion, and 2) estimation of the thermal evolution of the stable Moon.

The size and age of the primordial particles is also important in determining the initial temperature of the Moon. If the Moon were formed out of chunks less than 300 km in diameter and less than 10^9 years old, then this average temperature is less than about $500^{\circ}C$ (see graph of Allan and Jacobs, 1956).

The primary source of energy in the interior of the Earth is due to the decay of radioactive elements. If the Earth

has the chondritic abundance of radioactivity and if the heat generated is balanced by the heat generated, the present surface temperature of the Earth from this source would be 33°K and the surface temperature of the Moon would be 23°K. Higher abundances, as for the Wasserburg model, would lead to slightly higher temperatures. In the above calculation, the present-day heat generation has been taken equal to 1.61 ergs/gr/yr.

Appendix A summarizes certain energies and energy rates for the Moon to demonstrate the orders of magnitude involved in certain processes.

The temperature in an accreting planet will rise due to self compression. In a reversible adiabatic process the rate is

$$dT = \frac{\alpha T}{\rho c_p} \, dP$$

$\alpha = \frac{1}{V} \left. \frac{\partial V}{\partial T} \right)_\rho$ = coefficient at thermal volume expansion

c_p = specific heat at constant pressure

ρ = density

This is probably the minimum temperature gradient that is likely to result from any model of the origin of a planet. For constants appropriate to the Earth dT/dP is a small fraction of a degree per kilometer, and a temperature at the center of the Earth of a few hundred degrees, possibly 1000°K above the surface temperature. The melting point gradient is much larger than the adiabatic gradient and this mechanism alone cannot lead

to melting.

The adiabatic temperature gradient can be written

$$\frac{dT}{dp} = \frac{dt}{dr}\frac{dr}{dp} = \frac{\alpha T}{\rho c_p}$$

$$\frac{dP}{dr} = -\rho g$$

$$\frac{dT}{dr} = \frac{\alpha g T}{c_p}$$

c_p = specific heat at constant pressure

α = coefficient of thermal expansion

g = gravity

ρ = density

p = pressure

r = radius

Everything else being equal, the temperature will increase with depth due to adiabatic compression about 1/6th as fast on the Moon because of the lower gravity. Everything considered, the starting temperature for a protomoon will be lower and more constant than the starting temperatures in a protoearth.

C. Content of Radioactive Elements

Most discussions of the thermal history of the Earth, Moon and planets assume the radioactive abundances of chondrites. The rough equality between the present-day heat production of a chondritic Earth and the observed heat flow seems to support this

assumption. In other respects chondrites also seemed to be suitable models for an undifferentiated Earth.

However, there are troublesome features. A primitive Earth of chondritic composition can account for the uranium and thorium in the crust; but only 1/6th of the potassium is required, the rest presumably remaining in the mantle. This would increase the K/U ratio of the mantle compared to the crust and this does not seem to be the case. Also the strontium isotope ratio S^{86}/S^{87} precludes the differentiation of a basalt from a chondrite (Gast 1960). Hoygle and Fowler (1964) proposed that the U content of the solar system, and presumably the Earth and Moon, differs from chondrites. From their nuclear theory of the origin of the elements they require a U and Th concentration 3 to 4 times greater than that found in chondrites. Wasserburg et al (1964) concluded that a higher U abundance for the Earth is permissible and found further that for crustal rocks K/U $\sim 10^4$, about 1/8th the chondritic ratio. They also found Th/U = 3.7 for crustal rocks. If these ratios are appropriate for the whole mantle, a uranium content of about 4 x 10^{-8} would account for the present heat loss. This is more than 3 times the uranium content required if the chondritic composition is appropriate.

Once the ratios K/U and Th/U are set it remains to assign the total U and the distribution with depth. The current uranium concentration in chondrites is about 1 x 10^{-8} g/g. The uranium and thorium content of iron meteorites is 2 to 3 orders of magnitude less. The concentrations of U, Th and K in terrestrial

rocks vary widely but roughly systematically in a magmatic differentiation series. Granites contain about 10 times as much uranium as basalts, about 100 times as much as low uranium eclotites, several hundreds of times as much peridotites and thousands of times as much as dunites. This is commonly explained on the basis of the size of the ions of U, Th and K which are too large to be retained by the high-melting silicates such as pyroxenes and olivines and are, therefore, concentrated in the low-melting fractions. Thus, most of the radioactive elements, as oxides, are concentrated toward the surface with these light melts. The present uranium content of crustal rocks implies almost complete vertical differential of the mantle.

MacDonald (1964) showed that an average U concentration in the mantle between 4 and 5 x 10^{-8} gg^{-1} with an initial temperature of 1000°C would give the observed heat flow. This serves to calibrate the Wasserburg ratios to give total abundances. As MacDonald points out, these high abundances will melt the upper mantle of the Earth unless the thermal conductivity increases substantially with depth. We will use 4.5 x 10^{-8} gg^{-1} as the U content appropriate for the Earth's mantle and will designate this the basic Wasserburg model.

In the Tables 1 and 2 we tabulate radioactive contents for various crustal and mantle rocks, for chondrites, and the new Wasserburg abundances. For comparison we list abundances used in previous calculations of the thermal history of the Moon. These are nominally chondritic abundances. Levin investigated the effect

of varying the chondritic abundances by factors of 2 and 3.

The effect of the new Wasserburg abundances will be to make the rate of heating more uniform with time since the fast decaying K^{40} is less abundant relative to chondrites.

TABLE 1

RADIOACTIVE CONTENTS

	Ratios		U Concentration	
	K/U	Th/U	$U(x10^8$ g/g)	
Chondrite	$(x\ 10^{-4})$ 8.15	4.2	1.0	
Granite	0.80	3.9	475	
Basalt	1.40	4.5	60	
Dunite	1.00	--	.1	
Ecolgite	1.22	--	4.3	
Wasserburg	1.00	3.7	4.5	
Moon A	9.0 - 3.0	4.0	100 - 3.0	Levin
Moon B	7.25	4.0	1.1	MacDonald

TABLE 2

SUMMARY OF ABUNDANCE MODELS

	Relative Abundance	% Isotope	Isotope Abundance	Q Dot	Q Dot (Earth)	Q Dot (Earth t=0)
Chondritic						
U 238	1.1×10^{-8}	99.27	1.1×10^{-8}	.94 erg/gm	1.0×10^{-8} erg/gm-sec	$2. \times 10^{-8}$
235		.72	.008	5.7	.04	4.
Th 232	4.0×10^{-8}	100.	4.0	.26	1.0	1.25
K 40	$7. \times 10^{-4}$	.012	9.0	.30	2.7	35.
					3.7	42.
Wasserburg						
U 238	4.5×10^{-8}	99.27	4.5×10^{-8}	.94	4.0	8.0
235		.72	.03	5.7	.16	16.
Th 232	$18. \times 10^{-8}$	100.	18.	.26	4.0	5.
K 40	4.5×10^{-4}	.012	5.4	.30	1.6	21.
					10.	50.

D. Thermal Conductivity

The heat generated in a planet is removed by various processes of heat transfer including phonon and radiative thermal conductivity. The phonon conductivity which dominates room temperature measurements, decreases roughly as $1/T$ while the radiative conductivity increases with temperature as T^3. Therefore, radiation transfer becomes increasingly important with depth and dominates in the interior of a sufficiently hot planet. At room temperature a wide variety of common rocks have comparable conductivities varying from 0.0177 (joules/cm sec$^{\circ}$C) for anorthosite and about 0.05 for dunite. Stoney meteorites have a conductivity of about .02 joules/cm sec$^{\circ}$C. Calculations by Lubimova show that the effective conductivity, taking into account both of the above processes, decreases with depth in the Earth down to about 100 km and then increases rapidly with depth. The effective conductivity varies by about a factor of 6 throughout the mantle at the present time.

The thermal conductivity, k, can be written:

$$k = k_1 + k_2 = \text{lattice} + \text{radiative}$$

$$k_1 = \frac{B\rho^{2/3} u^3 u^{1/3}}{T^{5/4}}$$

$$k_2 = \frac{16}{3} \frac{n^2 \sigma T^3}{E}$$

ρ = density

u = mean sound velocity

n = refractive index

σ = Stefan-Boltzmann constant

E = extinction coefficient (opacity)

MacDonald takes the first term to be a constant, independent of temperature, in his calculations. He adopts the value 0.025 joules/cm sec^{o}C, while Lubimova sets B such that this is the surface lattice conductivity.

The thermal history of the Earth and the Moon can probably be directly computed with the same equation for thermal conductivity. Calculations show that both the model Earth and model Moon have gone through a period of extensive melting and, therefore, differentiation. The formation of the iron core and the continents would be consequences of this differentiation. The mean density of the Moon indicates a defficiency in iron compared to the Earth. The differentiation process, therefore, reorganized the silicate fractions and took place at higher temperature, and presumably later in time, than the primary Earth differentiation.

Mars, however, from its ellipticity, appears to be an undifferentiated body. Its mean density is appropriate for an Earth type body in which the iron is still mixed into the mantle. This would raise the lattice thermal conductivity and dilute the radioactivity, both effects serving to lower the temperatures. The lattice conductivity of the mantle of Mars (and the undifferentiated mantle of the Earth) may be as much as 6 times the

present lattice conductivity of the Earth's mantle. This effect has not previously been considered. The net result would be to slow down the heating of a planet in the early stages. The Earth has passed through this early stage--Mars has not.

Let us assume that the Earth and Mars started as identical homogeneous bodies differing only in radius. Allan and Jacobs have shown that the temperature in such bodies can be discussed in terms of a single parameter:

$$\nu = \frac{\pi^2 k}{a^2}$$

k = thermal diffusivity

a = radius

The temperature in the two bodies will be the same if

$$k_{Mars} = \left(\frac{A^2_{Mars}}{A^2_{Earth}}\right) k\ Earth$$

$$\left(\frac{A_{Mars}}{A_{Earth}}\right)^2 \cong \left(\frac{3300}{6400}\right) \cong .27$$

that is, if the thermal diffusivity of Mars is about one-quarter that of the Earth. If the thermal diffusivities are the same for the two planets

$$\nu_{Mars} \cong 3.8\ \nu_{Earth}$$

From curves shown by Allan and Jacobs, we see that this makes the average temperature in Mars about $2000^{\circ}C$ less than the average temperature in the Earth; and it is presumably possible for an Earth-size body to partially melt and differentiate and for a Mars-size body to remain homogeneous, as observed.

If the iron is distributed as free iron in a silicate matrix, the conductivity of the mix can be 1.5 times the lattice conductivity of the iron-free silicates if the iron is distributed as separate spherical inclusions and as much as 6 times the silicate conductivity if the iron is in continuous vertical iron channels. The latter estimate leads to

$$\nu_{Mars} \cong 20 \ \nu_{Earth}$$

which leads to present-day temperature differences of as high as $8000^{\circ}C$. In fact, the calculations of Allan and Jacob indicate that such a body is presently cooling, rather than heating. The factor of 6 is extreme since the increased opacity in the radiative terms has been ignored; the iron is probably not all free and it does not exist in through-going channels. However, a thermal conductivity for Mars greater than that for the upper mantle of the Earth is probable.

If the thermal conductivity of Mars is 1-1/2 times the Earth, a lower average temperature of about $2500^{\circ}C$ is indicated.

There is another factor which tends to keep the temperature of Mars low with respect to that in the Earth. Iron meteorites and, presumably the Earth's iron core, are essentially

free of radioactivity. Now both Mars and the Earth contain about 33% iron. This iron is mixed into the mantle of Mars and dilutes the radioactivity.

If $.03 \times 10^{-6}$ g/g is appropriate for Uranium in the Earth's mantle, then $.03 \times 10^{-6}$ g/4/3 $\equiv .02 \times 10^{-6}$ g/g is appropriate for the whole of Mars.

It is difficult without detailed calculations to determine the effect on temperature of this reduced radio-activity, but a final temperature reduction of the order of several hundred degrees can be estimated.

V. Previous Studies of the Thermal History of the Moon

Levin (1962) and MacDonald (1959) studied the thermal history of the Moon using variations of chondoritic abundances and ratios. They also investigated the effect of varying the age, the opacity and the initial temperature. A brief summary of their results is given in Table 3. In all cases melting occurred for depths below 200-400 km. Latent heat removed during melting and, presumably, redistributed by convection, nullifies the results of their calculation after commencement of melting. Levin realized this difficulty and ceased his calculations after some 2.0×10^9 years when melting was complete for the interior of the Moon.

TABLE 3

PREVIOUS MOON MODELS

	R	$T_0(a)$	$T_i(o)$	$\varepsilon(cm^{-1})$	$t_m(10^9$ yrs$)$	$t_0(10^9$ yrs$)$	
I	C	$273^{\circ}K$	$\sim 550^{\circ}C$	10	~ 1.4	-5.0	Levin
II	2C	"	"	10	1.1	-5.0	"
III	2C	"	"	40	1.1	-5.0	"
IV	3C	"	"	10	1.3	-4.5	"
V	3C	"	"	10	1.3	-4.5	"
VI	C	"	"	$100cm^{-1}$	~ 2.2	-4.5	Mac-Donald
VII	C	$873^{\circ}K$	$873^{\circ}K$	$1000cm^{-1}$	~ 1.0	-4.5	"

ε = opacity

$T_0(a)$ = initial surface temperature

$T_0(a)$ = initial central temperature

t_m = times of initial melting

t_0 = origin time of Moon

C = chondritic

$T_m \sim 1473^{\circ}K$, $P = 0$

VI. Results of Calculations

A Fortran program was written to compute the thermal history of a planet given its structure, radioactive content and thermal conductivity. The results presented here were obtained at the University of Colorado and Princeton University computing centers. The method uses standard numerical finite difference initial value problem procedures. Detailed results are presented in Tables 4 through 10 which follow this section.

Moon I is a chondritic Moon with initial temperature 273°K throughout and an opacity of 100 cm^{-1} which is 4.5 x 10^{9} years old. These parameters are tabulated before each table. This Moon is similar to Moon I of MacDonald except that the temperature dependent lattice conductivity of Lubimova has been used instead of the constant value that MacDonald assumes. (Note that Mac-Donald tabulates his results in centigrate while these results are Kelvin.) The final central temperature in our model is 2098°K compared to 2053°K for MacDonald's model.

Melting starts at about 1.9 billion years after the origin time at a depth of about 300 km and proceeds rapidly inward. By 2.2 billion years the whole interior of the Moon is partially molten, and remains so up to the present. Latent heat of melting and heat transfer by differentiation will keep the interior from being total fluid. The thermal evolution of this model is shown in Figure 2.
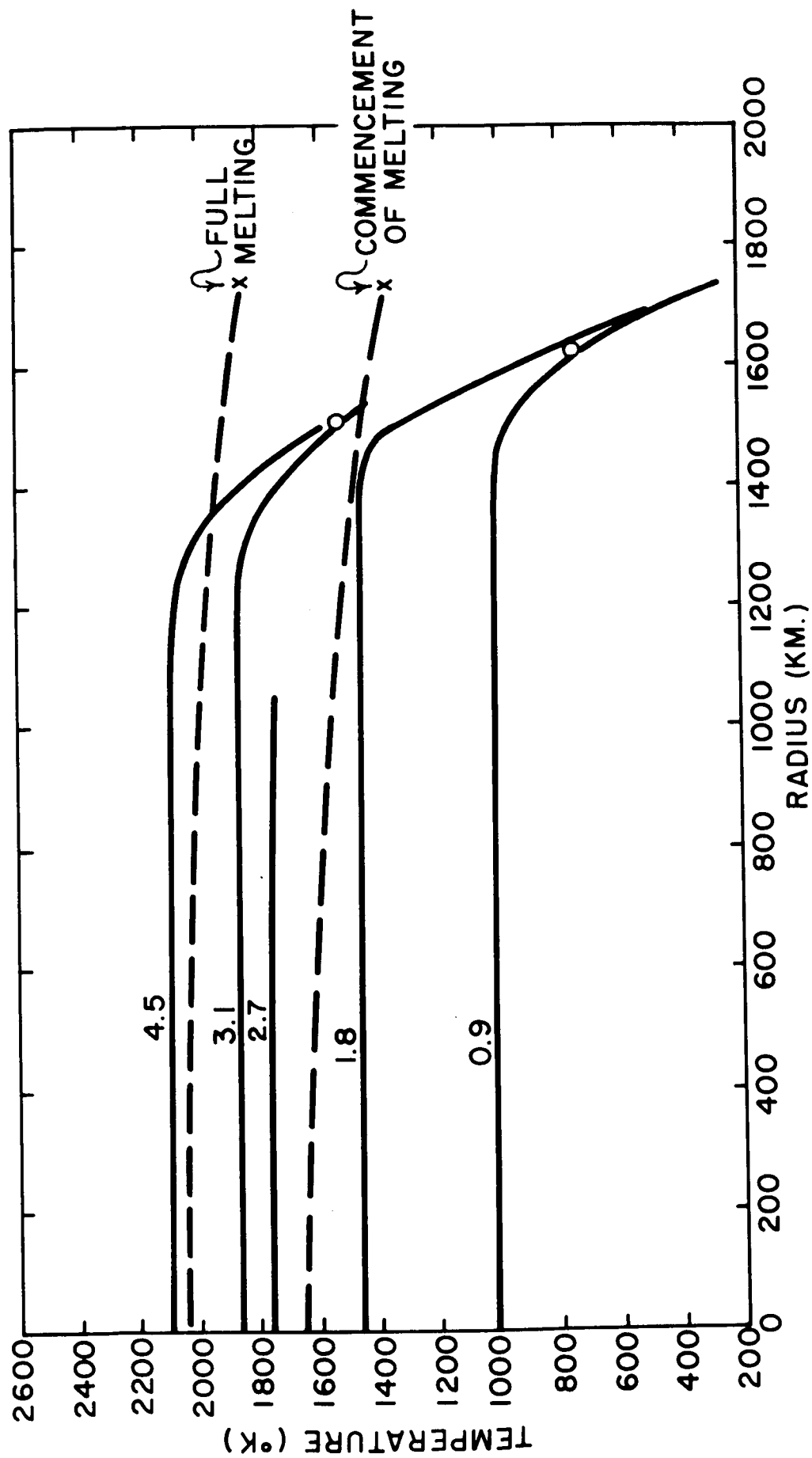
Figure 2. Chondritic Moon. $\epsilon_o = 100 \text{ cm}^{-1}$

A 4.5 billion year-old Moon with the Wasserburg abundances is shown in Figure 3. These abundances correspond to current thoughts regarding the Earth's mantle and give the observed terrestrial heat flow. Melting commences in this model at about 1.6 billion years at a depth of about 300 km. The differing opacities do not have much effect until late in the evolution of the Moon. The interior of the Moon below about 200 km is completely melted at the present time, even allowing for the latent heat of fusion. Differentiation in this model would be extreme; if the partially molten material can escape to the surface, volcanism will be well developed by 1.8 billion years and will probably continue to the present. This model has the highest internal temperatures of any calculated to date.

Temperatures can be reduced by invoking a) a later origin time for the Moon, b) radioactive abundances lower than those on Earth, or c) much higher thermal conductivities or d) heat transport by mass movement. Clearly, the large amounts of differentiation implied in these calculations will lead to heat redistribution by processes other than conduction and radiative transfer.

In Table 4 we calculate results for Moons which have been delayed by 0.5, 1.0 and 2.0 billion years. The first two have the start of melting delayed by about 0.9 and 2.5 billion years respectively. A 3.5 billion year-old Moon will have just entered a stage of extensive melting, differentiation and possible volcanism. A 2.5 billion year-old Moon will not yet have reached
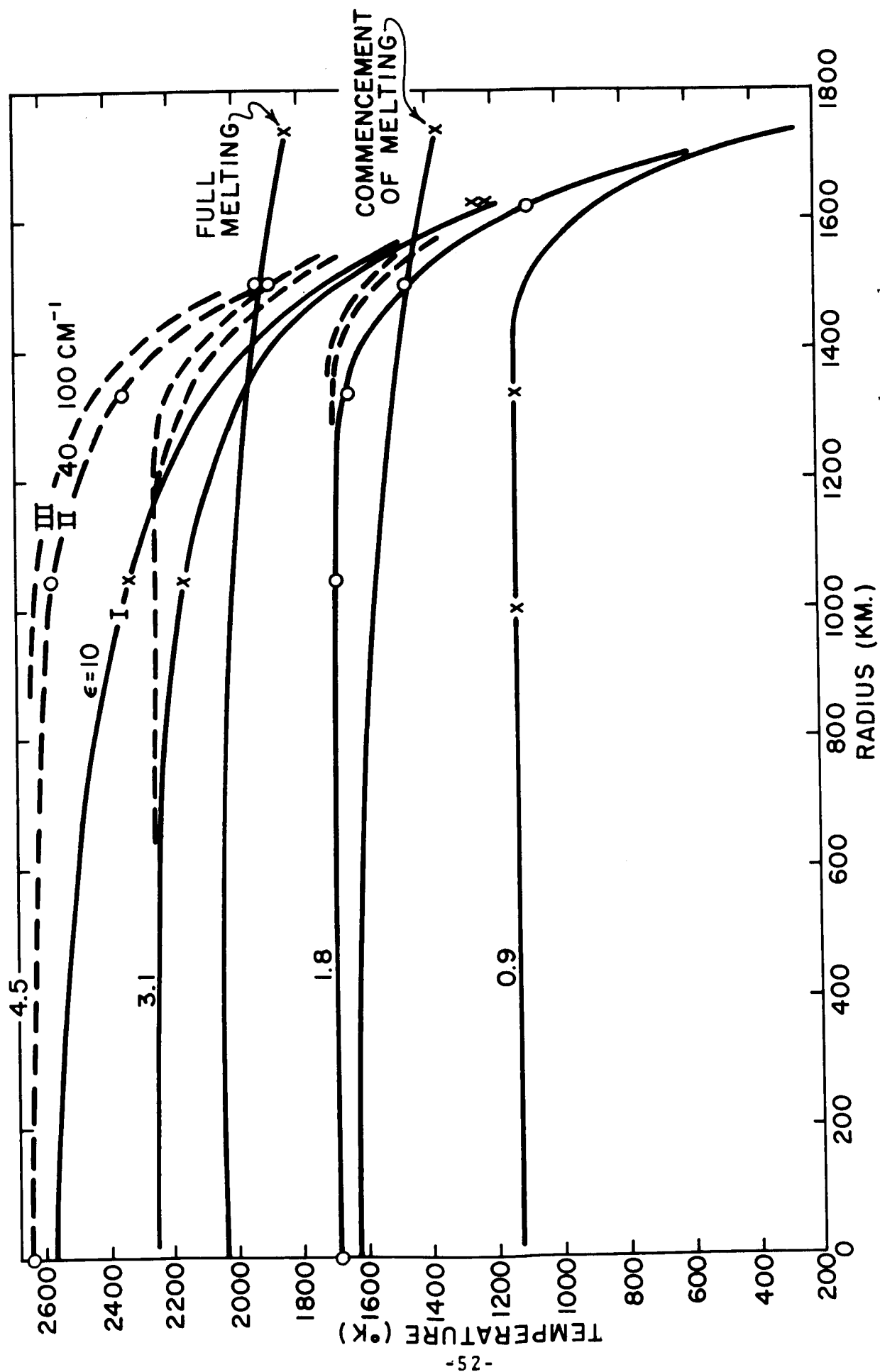
Figure 3. Wasseburg Moon I,II and III. Effect of Opacity: $\varepsilon_0 = 10\ \mathrm{cm}^{-1}$, $100\ \mathrm{cm}^{-1}$

-52-

the melting point anywhere. The ages of the Moon and the Earth, however, probably differ by less than 1 billion years.

The radioactive abundances were scaled down by a factor of 2/3 for the model designated Wasserburg VII and tabulated in Table 6. In this case melting starts at about 3.1×10^9 years and is well advanced below some 400 km. The present-day surface heat flow is 8.85 ergs/cm^2 sec as compared with 14.55 ergs/cm^2 sec for the corresponding model with Wasserburg abundances. The chondritic Moon also had about 8.84 ergs/cm^2 sec as the present-day surface heat flow. It is clear that a direct determination of the surface heat flow on the Moon will help considerably in pinning down the possible internal temperatures and the origin and history of the Moon.

Reduced abundances combined with late starting ages lead to relatively cold Moon models. A model with reduced Wasserburg abundances and delayed by 1×10^9 will not melt. This is an ad hoc way of obtaining a present-day cold Moon with all of its volcanism ahead of it. Results are tabulated in Table 6.

The previous calculations refer to models with a homogeneous distribution of radioactivity. In the course of differentiation the radioactivity gets concentrated near the surface. To investigate this effect we have designed several differentiated Moon models. By placing all of the radioactivity in the top half of the Moon, melting occurs early and shallow, and the surface heat flow is high, (see Table 7). In Wasserburg

Moon X the interior 700 km of the Moon is not molten but the remainder is except for a thin surface layer which presumably will flounder in the underlying melt.

Even with the reduced Wasserburg abundances, Moon VII D1a, a differentiated Moon, will melt at shallow depths and have a relatively high surface heat flow. Differentiated Moons were started at different times in order to estimate the rise in temperature after differentiation. These results are given in Table 9. The net effect is for the near surface temperatures to rise more rapidly after differentiation than they would have if the body had proceeded, after initiation of melting, as an undifferentiated body. The process of partial melting and differentiation is, therefore, self-accelerating, buffered mainly by the latent heat and resistence to convection.

Two thermal history calculations for Mars are presented in Table 10. The reduced Wasserburg abundances are used to allow for the mixing of low radioactivity iron into the Martian mantle to give the observed flattening. From the astronomical data Mars seems to be a homogeneous, relatively undifferentiated body. This is also borne out by the thermal calculations which keep Mars relatively cold and unmelted. The effect on opacity and lattice conductivity of mixing free iron or iron oxides into the standard silicate mantle must be investigated in more detail.

The following tables tabulate thermal results for a variety of Moon and Mars models. Specifically, the following parameters

have been varied:

1. Age (all times measured from -4.5 billion years ago) (1 billion years = 10^9 years).

2. Radioactivity

3. Opacity

4. Lattice conductivity

5. Differentiation

The results are:

1. Temperature vs time and depth

2. Heat flow at surface at last tabulated time

TABLE 4

THERMAL HISTORY CALCULATIONS

T_O = initial temperature; t_o = starting time (present time is 4.5 b.y.); H = present-day surface heat flow.

a. Cold Chondritic Moon

$T_o = 273^{\circ}K$; $t_o = 0$; $E_o = 100$ cm^{-1}; Temperatures ($^{\circ}K$); Radius (km)

time (b.y.)	Radius (km)				
	0	1000	1300	1500	1600
0.9	1005	1005	1005	986	794
1.8	1461	1461	1459	1356	900
2.2	1626				
2.7	1760				
3.1	1869	1869	1840	1548	835
RADIUS (km)		1043	1332	1506	1622
4.5	2098	2094	1985	1536	746

$H = 8.84$ ergs/cm^2 sec

b. Cold Wasserburg Moon I and (II) and (III)
(effect of opacity)

$T_o = 273^{\circ}K$; $t_o = 0$; $E_o = 10$ cm^{-1} (40 cm^{-1}); (100 cm^{-1}); Radius (km)

time (b.y.)		Radius (km)				
		0	1043	1332	1506	1622
0.9	I	1135	1135	1134	1096	889
	II		1135		1112	897
	III				1115	899
1.8	I	1698	1696	1642	1466	1092
	II		1698	1688	1544	1068
	III		1694	1696	1586	1048
3.1	I	2258	2161	1961	1671	1218
	II	2260	2252	2144	1828	1141
	III		2259	2209	1897	1055
4.5	I	2579	2335	2062	1730	1251
	II	2646	2579	2347	1930	1158
	III		2633	2476	2008	1016

$H = 22.4$ ergs/cm^2 sec (14.55 ergs/cm^2 sec)
(12.48 ergs/cm^2 sec)

TABLE 5

YOUNG COLD WASSERBURG MOON IV

T_o = 273°K; t_o = 1 b.y.; E_o = 40 cm^{-1}; Temperatures (^{o}K);
Radius (km).

time (b.y.)	Radius (km)				
	0	1043	1332	1506	1622
1.0	273	273	273	273	273
1.9	814	814	814	792	645
3.2	1356	1356	1341	1193	771
4.5	1732	1729	1657	1865	787

H = 10.13 ergs/cm^2 sec

YOUNG COLD WASSERBURG MOON V AND (VI)

T_o = 273°K; t_o = 0.5 b.y.; (2.0 b.y.); E = 40 cm^{-1}; Radius (km).

time (b.y.)	Radius (km)				
	0	1043	1332	1506	1622
1.4	947	947	947	924	747
2.3	1408	1408	1401	1291	877
2.9	647	649	646	626	522
3.1	1148	1748	1709	1483	914
4.0	2015	2009	1908	1589	923
4.23	1055	1055	1042	919	621

H = 11.97 ergs/cm^2 sec

(7.94 ergs/cm^2 sec)

TABLE 6

COLD 2/3 WASSERBURG MOON VII

$T_O = 273^O K$; $t_O = 0$ b.y.; $E = 40$ cm^{-1}; Radius (km).

time(b.y.)	Radius (km)				
	0	1043	1332	1506	1622
0.9	846	846	845	823	667
1.8	1219	1219	1213	1111	754
3.1	1592	1591	1542	1288	754
4.5	1847	1836	1708	1340	726

$H = 8.85$ ergs/km^2 sec

YOUNG COLD 2/3 WASSERBURG MOON VIII AND (IX)

$T_O = 273^O K$; $t_O = 1.0$ b.y. (2.0 b.y.); $E = 40$ cm^{-1}; Radius (km)

time(b.y.)	Radius (km)				
	0	1043	1332	1506	1622
1.9	632	632	631	611	510
(2.9)	(521)	(521)	(520)	(503)	(434)
2.8	888	888	881	799	573
4.1	1166	1165	1130	929	586
(4.2)	(791)	(791)	(777)	(681)	(495)

$H = 6.9$ ergs/cm^2 sec

$(5.4$ ergs/cm^2 sec$)$

TABLE 7

COLD DIFFERENTIATED WASSERBURG MOON X

Radioactivity in Lower Half of Moon Moved to Upper Half

$T_o = 273°K$; $t_o = 0$; $E_o = 40$ cm^{-1}; Radius (km)

time (b.y.)	0	695	811	926	1043	1448	1564	1622
				Radius (km)		Radius (km)		
0.9	274	405	740	1160	1227	1226	1148	977
1.8	218	567	1117	1665	1815	1782	1526	1183
3.1	317	879	1657	2129	2315	2147	1740	1291
4.5	371	1385	2061	2407	2555	2263	1805	1321

H = 16.8 ergs/cm^2 sec

TABLE 8

DIFFERENTIATED WASSERBURG MOON VII D1

Reduced Wasserburg Abundances
3/4 of radioactivity in bottom 1100 km.
of the Moon is put into the top 600 km.

	H (ergs/gm sec) $\times 10^8$	
	Bottom	Top
U^{238}	1.3	6.7
U^{235}	2.6	13.5
Th	0.83	4.2
K^{40}	3.5	17.8

$T_o = 273^\circ K$ $\qquad$ $t_o = 0$ $\qquad$ $\varepsilon_o = 40 \text{ cm}^{-1}$

	Radius (km)				
time (b.y.)	0	1048	1275	1506	1622
1	429	572	1035	1033	813
2	526	816	1469	1402	927
3	594	1039	1715	1554	940
4.5	668	1345	1888	1607	909

$H = 11.4 \text{ ergs/cm}^2 \text{ sec}$

TABLE 9

EFFECT OF AGE ON DIFFERENTIATED MOONS

Differentiated Wasserburg Moon VII Dl_a

$T_o = 273°K; \quad t_o = 0.5 \; b.y.; \quad \epsilon_o = 40 \; cm^{-1}$

time (b.y.)	Radius (km)				
	0	1043	1275	1506	1622
1.5	395	513	867	863	685
3.0	507	798	1354	1251	783
4.5	580	1040	1592	1366	772

$H = 9.7 \; ergs/cm^2 \; sec$

Differentiated Wasserburg Moon VII Dl_b

$T_o = 273°K; \quad t_o = 1.0 \; b.y.; \quad \epsilon_o = 40 \; cm^{-1}$

2.0	371	470	748	743	597
3.0	439	637	1051	993	673
4.5	512	843	1331	1154	684

$H = 8.6 \; ergs/cm^2 \; sec$

Differentiated Wasserburg Moon VII Dl_c

$T_o = 273°K; \quad t_o = 1.5 \; b.y.; \quad \epsilon_o = 40 \; cm^{-1}$

2.5	354	438	662	656	536
4.5	457	705	1104	977	619

$H = 7.6 \; ergs/cm^2 \; sec$

TABLE 10

COLD MARS I

Wasserburg abundances reduced by 1/3 to
allow for low-radiance core material
which has not been differentiated from
mantle.

$T_o = 100^o K$; $t_o = 0$; $E = 100$ cm^{-1}; Radius (km)

time (b.y.)	Radius (km)				
	0	2287	2855	3201	3430 Surface
1.0	722	722	722	605	$100^o K$
2.0	1113	1113	1110	715	100
3.5	1494	1494	1477	627	100
4.5	1675	1655	1637	556	100

$H = 11.6$ ergs/cm^2 sec

COLD MARS II

Lattice conductivity doubled
Reduced Wasserburg Abundances

time (b.y.)	Radius (km)				
	0	2287	2855	3201	3430
1.0	722	722	716	458	100
2.0	1113	1113	1083	455	100
3.5	1494	1494	1377	392	100
4.5	1675	1674	1465	359	100

$H = 15.9$ ergs/cm^2 sec

BIBLIOGRAPHY

Anderson, Don L. (1965)"Recent evidence concerning the Earth's mantle,"Physics and Chemistry of the Earth, Chap. 1, Vol V, p. 1-129, Pergamon Press, New York and London.

Anderson, Don L. and C. B. Archambeau (1964) "The Anelasticity of the Earth," J. Geophy. Res., 6a, 2071

Anderson, Don L. and M. N. Zoksoz, (1964), "Surface Waves in a Spherical Earth," J. Geophys. Res.

Baldwin, R. B. (1963) The Measure of the Moon, Univ. Chicago Press, 448 pp.

Fielder, G. and Warner B. (1962) "Stress Systems in the Vicinity of Lunar Craters," Planetary and Space Sci. 9, 11-17.

Gutenberg, B. (1959) Physics of the Earth's Interior, Academic Press, New York and London.

Kaula, W. M. (1963) in Advances in Space Science and Technology, ed. F. I. Ordway, III. Vol. 5, Academic Press, New York and London, 1963.

Kovach, R. and Don L. Anderson (1965) "The Interiors of the Terrestrial Planets," J. Geophys. Res.

Levin, B. J. (1962)"Thermal History of the Moon in The Moon," ed. Kopal, Z. and F. K. Mikhailov, Academic Press, London and New York.

Rubey, W. W. (1951) "Geologic History of Sea Water, "Geol. Soc. Am. Bull., 62, 1111-1147.

Watson, K., Murray, B. and Brown, H. (1961) on the "Possible Presence of Ice on the Moon," J. Geophys. Res., 66, 1598-1601.

APPENDIX

Energetics of Various Processes Involved in the Thermal Regime

of the Moon

Table 3 summarizes the energies involved in a simple model of the accretion process, and the energies involved in heating by long-lived radioactivities. The first two columns in the table give the total energy and the energy per gram for the present Moon. The next three columns show the partitioning of the energy per gram into:

1) heating to melting

$(T_{melt} = 1200^{\circ}C., C_p = 10^7$ ergs/gm),

2) partial fusion

(melting range $= 400^{\circ}C., C_{fusion} = 4 \times 10^9$

ergs/gm),

3) heating above the maximum melting temperature

$(C_p = 10^7)$.

For the sake of this survey, this crude representation of the thermal properties of pyrolite is adequate.

Gravitational energy is the total amount of energy gained by bringing the mass constituents of the Moon together at the present radius from initial dispersal at infinity. When accreting particles hit the surface of an accreting Moon, all this gained energy is in the form of kinetic energy, which must largely be dissipated in the form of heat. A small fraction

goes into adiabatic compression of the interior, and a smaller fraction yet into rotational kinetic energy. The "minimum" gravitational energy given (at half the normal value) comes from a special model of accretion in which the energy required to bring a particle from infinity to grazing circular orbit is lost by radiation, but the energy required in bringing it to the surface from orbit is retained.

If rates of accretion are assumed, the surface temperature is determined by the equilibrium between rate of kinetic energy input and black-body reradiation. The net temperature attained is considerably less than in the previous calculations, showing that only 5-25% of the available gravitational energy is retained.

To demonstrate the energies and temperatures involved in heating by long-lived radioactivity, two models for radiogenic concentrations are taken and their energy generation per billion years at various times is summarized (thus allowing for their decay). The chondritic and Wasserburg abundances are discussed elsewhere in this report. The absolute times at which melting would begin and become complete are given for these different starting times. It is seen that, in accordance with the usual thermal calculations, (MacDonald, 1959; Levin, 1962) these abundances predict a Moon which melts early in its history. However, if the Moon is assumed to come together from small planetesimals at 2 billion years after the Earth's formation, then it is problematical whether any melting at all has occurred.

TABLE 11

SUMMARY OF ENERGIES AND ENERGY RATES BY PROCESS

The Moon is assumed approximately of constant density + 3.34, radius 1.74 x 10^8, mass 7.35 x 10^{25} gm. C_p = 10^7 ergs/gm, T_{melt} = 1200° C, C_{fusion} = 4 x 10^9 ergs/cm.

	ergs	ergs/gm	ergs/gm up to melt	fusion	add.	T°C
maximum gravitational energy	1.5x10^{36}	3.0x10^{10}	1.2x10^{10}	.4x10^{10}	1.4x10^{10}	3000°
Minimum gravitational energy	.75x10^{36}	1.5x10^{10}	1.2x10^{10}	.3x10^{10}	none	1500°
equilibrium between radiation + accret. at accretion time of 10^8 yrs.	.8x10^{35}	.1x10^{10}	.1x10^{10}	none	none	100°
10^6 yrs.	2.5x10^{35}	.33x10^{10}	.33x10^{10}	none	none	330°

total energy by long-lived rad./ billion yrs	ergs/gm	begin melt	fully melt
chondritic (0)	1.0x10^{10}	1.2 by	1.6 by
(2 by)	.3x10^{10}	8 by	--
(now)	.10x10^{10}	--	--
Wasserburgite (0)	2.0x10^{10}	.5 by	.7 by
(2 by)	.7x10^{10}	4.5 by	8 by
(now)	.3x10^{10}	--	--

APPENDIX II

EROSION ON LUNAR SURFACE BY METEOR IMPACT

"THIS APPENDIX IS ALSO ISSUED AS TG-3"

EROSION OF THE LUNAR SURFACE
BY METEOR IMPACT

R. J. Collins

August 1965

EROSION OF THE LUNAR SURFACE BY METEOR IMPACT

ABSTRACT

1 6168

The bombardment of the lunar surface by meteorites will produce craters. The flux of these meteors of Earth in the range 10^8 to 10^{-14} grams has been reported by Hawkins. Correlation of this flux with the experimental effects produced by the impact of hypervelocity particles with solid surfaces allows a prediction of the impact produced crater distribution on the lunar surface. The present report shows that in small sizes (d $\lesssim$ 300 m) steady state has been reached in coverage and suggests the observed crater distribution is primarily the result of meteor infall.

Author

TABLE OF CONTENTS

LIST OF ILLUSTRATIONS

I. Introduction

With a flux similar to that observed on Earth, the lunar surface is bombarded by meteors and micrometeorites. The interaction of these incoming particles when colliding with the lunar surface will create craters in the same fashion as on Earth. The interaction transforms the kinetic energy of the particle into heat by interelastic collisions with the surface, and the effect will resemble an explosion. Since free fall velocity on the Moon is 2.8 kilometers per second which is in itself more than enough to cause vaporization of particles, any meteorite striking the lunar surface will create an explosion crater. Estimates of the impact velocity are approximatly 10 kilometers per second, and flux of such meteors is shown in Figure 1. To a good approximation the results gained in chemical explosions can give insight into size of craters formed by impacting meteors. Shoemaker has analyzed many features of the Moon in this manner. In a recent publication discrepancies between predicted and observed crater counts at small sizes were pointed out. The present reports suggest a model for erosion based on ejecta from craters formed by the impacting meteorites and shows that, based on the model, steady state has been reached for small sizes with larger craters showing only partial effects of erosion.
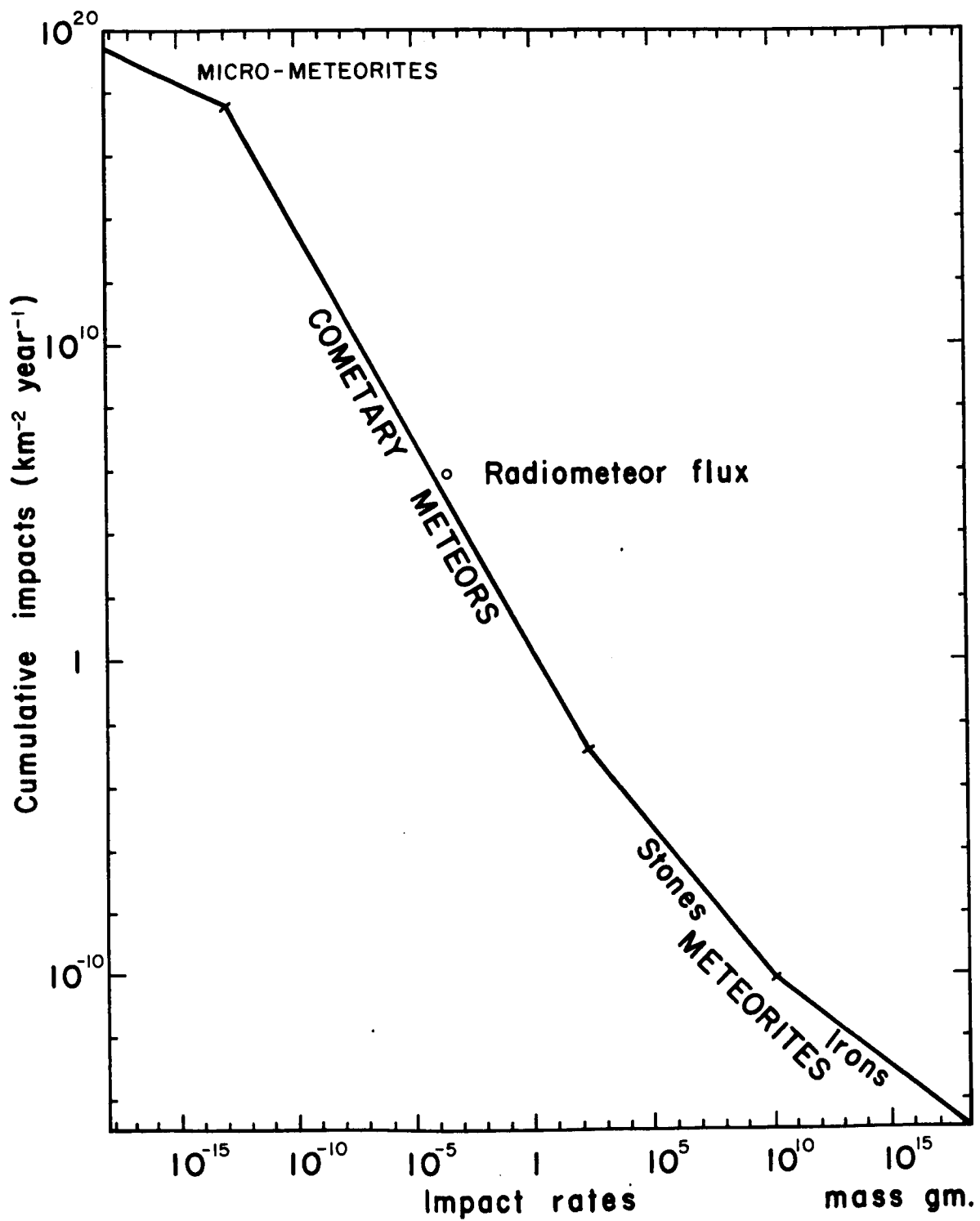
Figure 1   Flux of Extraterrestrial Objects.
From Hawkins (Reference 1).

II. Model for Steady State Distribution

A calculation of the steady state distribution requires a model for the creation and destruction of craters. The creation is assumed to relate directly to the incidence flux where the mass removed from the crater is linearly related to the energy dissipated (see Figure 2). Although this apparently ignores the effect of craters produced by larger ejecta (secondary crater of Shoemaker) since the flux of incoming particles increases rapidly with decreasing size, only a small error is introduced. The relation between the radii of the crater and the size of the incoming particle is taken from the data of Gault et. al. (Figure 2) and the assumption of spherical geometry. For craters less than kilometers across, this seems a reasonable assumption.

The model offered here for destruction of a crater is the filling with debris from other particles as shown in Figure 3. To carry out calculation on this model, a relation between the impacting particle radius and the size of the crater produced is necessary as well as a functional relation for the distribution of mass from the newly created crater. An exponential decrease with distance from the impact point will be assumed for the distribution of the ejecta. On this model a lifetime for a crater size V can be defined as:

$$\frac{\alpha}{V} \frac{dV}{dt} \equiv \frac{1}{t} = \frac{\pi r_o^2}{\frac{4}{6} \pi r_o^3} \times \frac{\text{"debris" from "b"}}{\text{unit area}} \times (\text{flux of particles at b}) \quad (1)$$
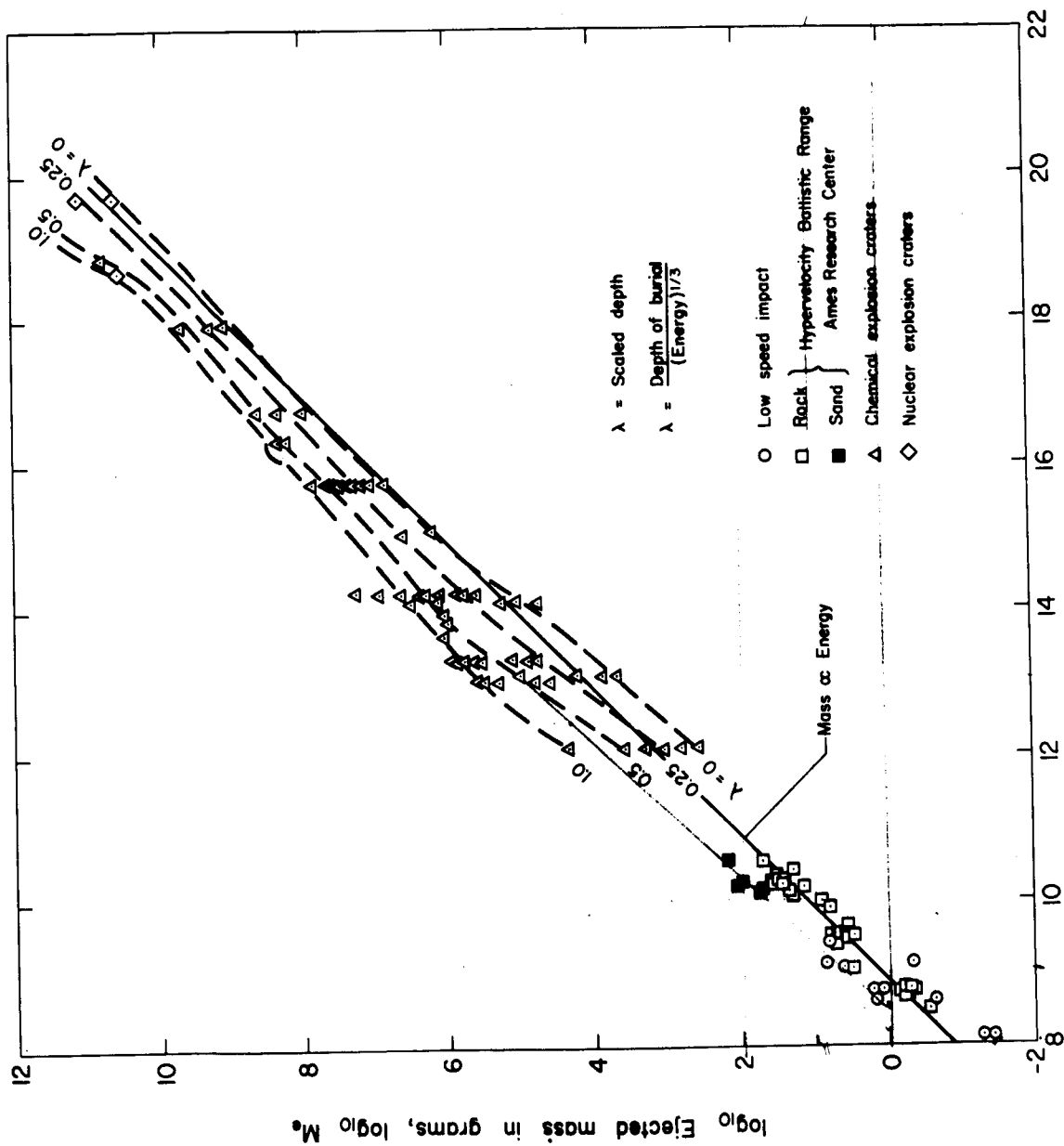
-3-

Figure 2 Relation of Ejected Mass and Energy for Hypervelocity Impact and Explosive Craters (from Gault, et. al., Reference 3).
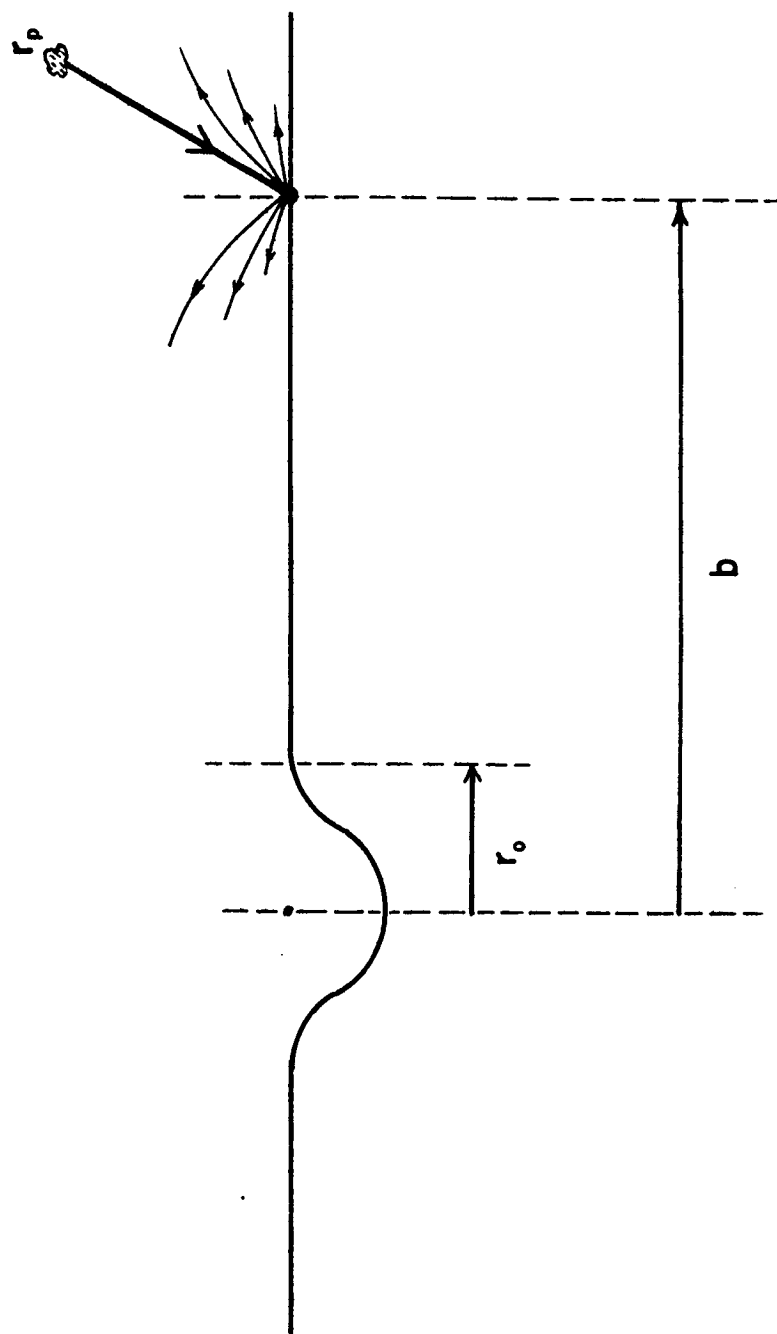
-4-

Figure 3 Erosion Model

The rate equation for the concentration of craters of size r to r + dr is:

$$\frac{dn(rt)}{dt} = F - \frac{n}{t} \qquad (2)$$

where F is the creation rate for the craters n(rt) and t is lifetime of crater of size r. It will be assumed that no material is produced for filling unless the impact occurs at radius > r_o. This model ignores the effects of direct obileration by impact of a larger crater.

Empirical relations (Figure 2) indicate

$$r_c = k \, r_p \qquad (3)$$

where for velocities of approximately 3×10^5 cm/sec k has a value of approximately 5. The exact value of k depends on density and velocity of both projectile and target. The value of k used here is 20 or that corresponding to a velocity of $\sim$ 20 km/sec if densities are equal. The exponential decay of ejecta is a reasonable assumption based on an examination of the distribution of ejecta in experiments of Gault[3]. Calculation of the "rain" of debris in terms of mass per unit area as a function of distance from the impact point is complicated by the necessity of describing the empirical infall[1] rates for meteorites in a series of three steps each with a different power law.

From the data[1] of Hawkins if an average density of 3 is assumed, the rates of meteor flux are:

(i) 10^{-4} cm $< r \leq 5$ cm (4)

$$N(r) = 1.2 \times 10^{-18} \, r^{-4.2}$$

$$= A \, r^{-4.2} \text{ particles/cm}^2 \text{ sec}$$

(ii) 5 cm $\lesssim r < 10^3$ (5)

$$N(r) = 2.1 \times 10^{-19} \, r^{-3}$$

$$= A^1 \, r^{-3} \text{ particles/cm}^2 \text{ sec.}$$

(iii) 10^3 cm $\leq r \leq 10^7$ cm (6)

$$N(r) = 4.2 \times 10^{-22} \, r^{-2.1}$$

$$= A^{1'} \, r^{-2.1} \text{ particles/cm}^2 \text{ sec.}$$

In these expressions $N(r)$ is accumulative flux of particles of size r or larger.

The volume of mass ejected from a crater formed by a particle r_p is:

$$W = \frac{M}{\rho} = \frac{4\pi}{6} (kr_p)^3 \tag{7}$$

$$= \frac{4\pi}{6} r_o^3$$

This mass is distributed on the lunar surface with a density:

$$\frac{Me^{1 - b/r_o}}{2\pi b r_o}$$

Referring to Figure 3 the "rain" in volume of material per unit area is:

$$\frac{Vol}{Area} \equiv \frac{W}{A} = \int \int \frac{dN(kx)}{dx} \, 2\pi b\,db \, \frac{4\pi}{6} \, x^3 \, \frac{e^{1-b/x}}{2\pi bx} \, dx \tag{9}$$

where the appropriate form of $N(r)$ for each range is needed to carry the integration over the allowed ranges of b and x. In the range 10^{-4} cm $< x < 5$ cm, Equation 9 becomes

$$\frac{W}{A} = \int_{r_0}^{a} db \int_{0}^{b} (Ak^{4.2} \, \frac{4.2 x 4\pi}{6}) \, \frac{e^{1-b/x}}{x^{3.2}} \, dx \tag{10}$$

The decrease in flux of these size particles is rapid enough to allow integration over $0 < x < \infty$ with introducing an error.

The region from $5 < x < 10^3$ cm gives

$$\frac{W}{A} = \int_{r_1}^{r_2} dx \int_{r_0}^{\infty} (-) A^1 k^3 \, 3 \cdot \frac{4\pi}{6} \frac{1}{x^2} \, e^{1-b/x} \, db \tag{11}$$

where r_1 and r_2 are limits of the region of validity of this power law.

For the region x > 1000 cm to prevent divergence of the integral some cut off (r_c) must be defined. This largest size can be defined in several ways. One assumption could be that size at which the ejecta would cover the entire surface several times in the life of the Moon. Another might be that size responsible for a large enough crater frequency to be statistically significant. Still another could be the largest observed crater pit size on the Moon

or still better would be that size where on Earth a reasonable statistical number have occurred. The most appropriate seems to assume a radius corresponding to a size of which a reasonable number of craters exist on the Moon. Take this to be $r_{crater} \approx 10$ km. This value implies that if the larger Mare areas were formed by impacts that virtually all craters existing at that time would have been filled at the time of impact.

Carrying out the evaluation of t (allowing fractional powers to be replaced by nearest whole number) gives:

$$\frac{1}{t} = \frac{\alpha}{r_0}\left[\frac{Ak^{4.2}\, 55}{r_0^{1.2}} + A^1 k^3\, 2.5 \int_{r_0/r_2}^{r_0/r_1} \frac{e^{-y}}{y}\, dy\right.$$

$$+ A^{11} k^{2.1}\, 18\, (r_c \rho^{-r_0/r_c} - r_2 e^{-r_0/r_2}$$

$$\left. -\left(r_0 \int_{r_0/r_2}^{r_0/r_2} \frac{e^{-y}}{y}\, dy\right)\right] \tag{12}$$

The lifetime is dominated by the filling with debris from craters near r_c. For the assumption of $r_c = 10$ km, craters of size less than approximately a few hundred meters, the crater population is in equilibrium.

The rate equation for concentration of crater of size r

$$\frac{dn(rt)}{dt} = F - \frac{n}{t}$$

is solved as:

$$n(rt) = Ft \, (1-e^{-t/t})$$

with the results shown in Figure 4. Several assumptions about relation of lifetime to filling rate (that is value of α) and cut off radii of incoming particles are possible. Results for different α shift the prediction slightly while different r_c modify region of steady state.

The slope of the curve is seen to be essentially the same as observed with the predicted crater frequency but somewhat higher than observed.
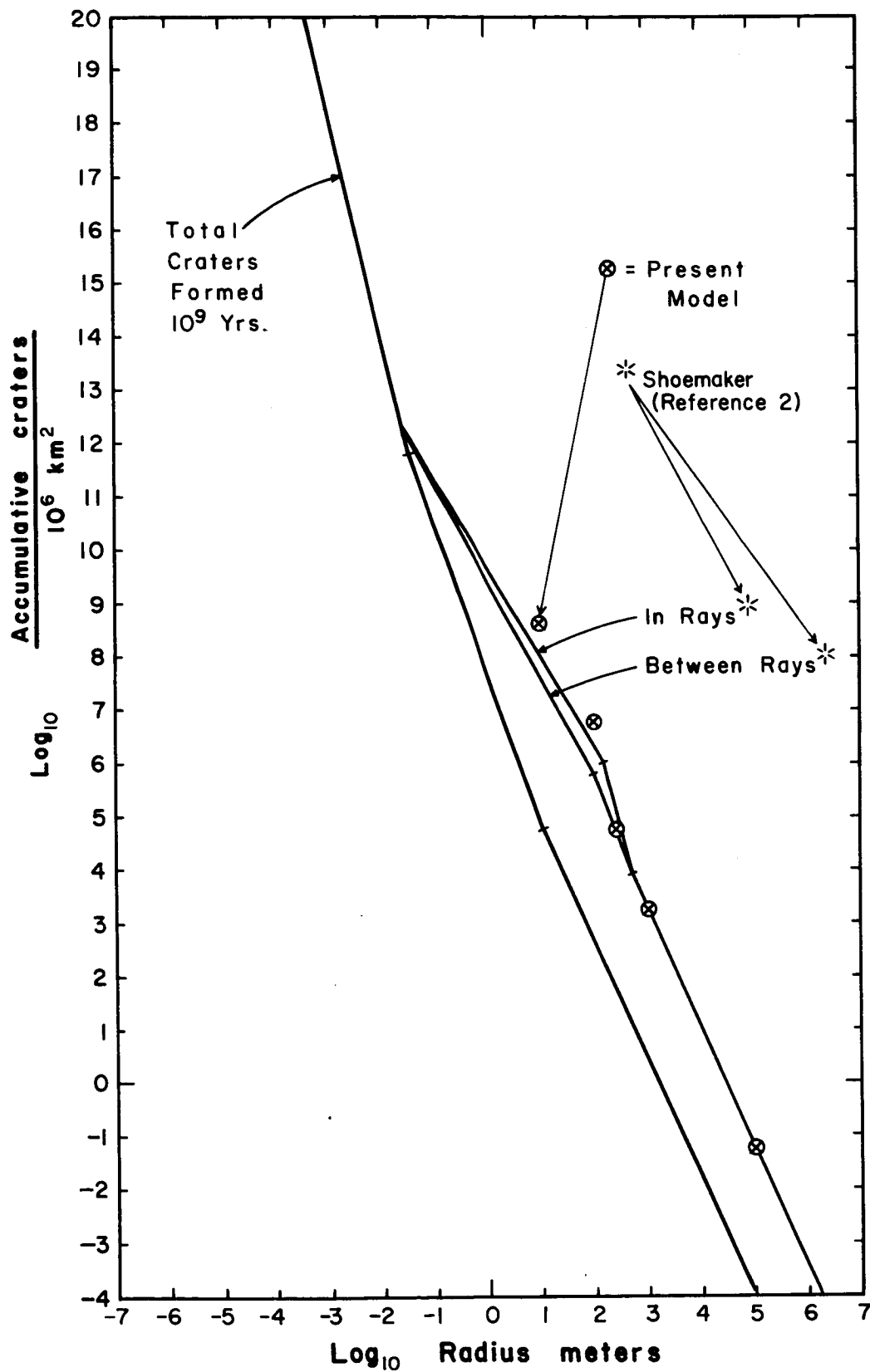
Figure 4 Crater Size Frequency Distribution on Lunar Surface

III. Conclusion

In conclusion it has been shown that the "erosion" by current meteor infall will produce an equilibrium concentration for craters of radius $\lesssim 10^2$ m. The effect of erosion will produce a change in slope consistent with observations to yield a reasonable fit to the reported observations of Ranger missions.

REFERENCES

1) G. S. Hawkins, Rev. Astronomy and Astrophysics, 1964.

2) E. M. Shoemaker, "Preliminary Analysis of the Fine
    Structure of the Lunar Surface," Ranger VII, Part II
    Experimenter's Analysis and Interpretations, JPL
    Technical Report No. 32-700, N65-22162, 10.
    February 1965.

3) D. E. Gault, E. M. Shoemaker, H. J. Moore, "Spray
    Ejected from the Lunar Surface by Meteoroid Impact,"
    NASA N63-14587, TN-D-1767, April 1963.

APPENDIX III

RADAR STUDIES OF THE MOON

"THIS APPENDIX IS ALSO ISSUED AS TG-4"

RADAR STUDIES OF THE MOON

J. V. Evans

July 1965

TABLE OF CONTENTS

RADAR STUDIES OF THE MOON

J. V. Evans

Lincoln Laboratory*
Massachusetts Institute of Technology

I. INTRODUCTION

The smallest objects on the lunar surface that are resolvable by means of large ground-based optical telescopes have dimensions of the order of 1/2 km. At the other extreme, photometric studies (Hapke and Van Horn, 1963) and polarization measurements (Dollfus, 1962) yield information about the microstructure which may at most be measured in millimeters. The success of manned exploration of the lunar surface may depend to a large extent upon the nature of the surface in the range of sizes between these two extremes. If the surface were densely covered with craters below the optical limit of resolution, or for that matter boulders of a size comparable with a landing vehicle, severe difficulties would be encountered. Until close proximity photographs were obtained, one could be guided only by radar results. These suggested that the surface is not necessarily very hostile — a result that has partly been confirmed by the Mariner pictures. The radar experiments also reveal the existence of a layer of very light material overlying most parts of the surface whose depth is not yet known. It seems that from the earth the depth of this material can only be determined by further radar studies.

A historical review of the early radar observations of the moon has been given by Evans (1962a), and here we shall present only what seems the best available experimental evidence concerning the moon's scattering behavior. For the most part, this has been obtained by measuring the distribution of the echo power as a function of range delay using short pulse transmissions. Additional measurements in which both the range and doppler resolution of the radar are exploited have shown that, though the larger part of the moon's surface is rather featureless to radar observation, the newer (rayed) craters are extraordinarily bright with respect to their surroundings. The experimental observations described here have stimulated a large number of theoretical workers to attempt to deduce from the scattering properties of the moon a physical description of its surface. There is as yet no complete understanding of the scattering behavior of a surface which contains structure of sizes both larger and smaller than the wavelength. As a result, the success with which the radar results have been interpreted remains limited. The observation that the moon is covered with a layer of light material has come from experiments in which both the range and doppler resolution of the radar are exploited and in addition the polarization of the transmitted and received signals is carefully controlled. These experiments are the most sophisticated ones so far carried out in radar astronomy. In the sections which follow we review in increasing order of complexity the experiments that have been carried out, and we discuss after each type of measurement the information that may be derived from it.

II. ECHO POWER

A. The Radar Equation for a Distributed Target

The radar equation is normally stated in a manner that is proper for the observation of "point targets", i.e., objects which when viewed from the radar subtend an angular diameter much smaller than that of the antenna beam. In this case the received echo power P_r may be stated as

$$P_r = \frac{P_t \, G \, A \, \sigma}{(4 \pi R^2)^2} \quad \text{watts} \tag{1}$$

where P_t = transmitted power (watts), G = antenna gain, A = antenna aperture (m^2), σ the cross section of the target (m^2), and R is the target's range (m). Of all the celestial objects detectable by means of radar, the moon (and perhaps the sun) are the only ones in which the target angular diameter is likely to be as large or larger than the antenna beam. The cross section σ observed during observations of the moon depends, therefore, upon the distribution of the incident power over the surface. In practice, the moon reflects preferentially from regions near the center of the disk and little loss in total reflected power will be observed until the antenna beamwidth (between half power points) is made smaller than the angular extent of the moon $(1/2^\circ)$. Thus for most forms of simple antennas this effect will not be important until the antenna diameter becomes larger than 100 λ where λ is the radio wavelength.

Radar echoes from any of the nearby objects in the solar system can, however, be resolved in range delay or in frequency. For example, it is readily possible to transmit pulses which are of insufficient length to illuminate the whole of a planet's visible hemisphere. In the case of the moon, a pulse of 11.6 m.secs is required to fully illuminate the surface, and if shorter pulses are employed,

the effective or instantaneous cross section σ will never reach its maximum

possible value (the C.W. cross section). Figure 1 shows how the peak instanta-

neous cross section falls as a function of pulse length for observations of the

moon at 68 cm wavelength. Because the largest part of the power is reflected

from the nearest regions of the lunar surface, an appreciable reduction in cross

section is not observed until pulses shorter than 1 m.sec duration are used.

Figure 1 is applicable only for wavelengths of about 50 cm, or longer, as the

scattering properties of the surface change markedly toward shorter wavelengths.

Equally, where a C.W. radar is employed, the apparent rotation of the moon may

cause the reflected signals to be appreciably doppler broadened. If the receiver

employs a narrow-band filter which does not accept all the frequency components

of the reflected signal, then again the observed cross section will be lower than

the full value.

In this review we shall use the term σ to denote the total cross section of

the moon. This could be measured with a radar employing an antenna beam of $1/2^{\circ}$

or more by determining the peak echo power observed when pulses of 11.6 m.secs

or longer are transmitted. In practice, echoes from the moon are found to fade

as a consequence of constructive and destructive interference between signals

arriving from different parts of the lunar surface. Thus, an average value for

the peak echo power (or mean square of the echo amplitude) must be obtained

from many pulses to determine σ reliably. Alternatively with a C.W. radar, many

independent determinations of the echo power are required. In some of the

earliest radar observations of the moon (e.g., DeWitt and Stodola, 1949) this

was not recognized and only the maximum value of the echo intensity was reported.

When the antenna beamwidth is comparable with the diameter of the moon, it

is possible to compute σ if the distribution of incident power over the surface

4.

FRACTION OF CROSS-SECTION Vs. PULSE LENGTH FOR THE MOON AT 68CM WAVELENGTH
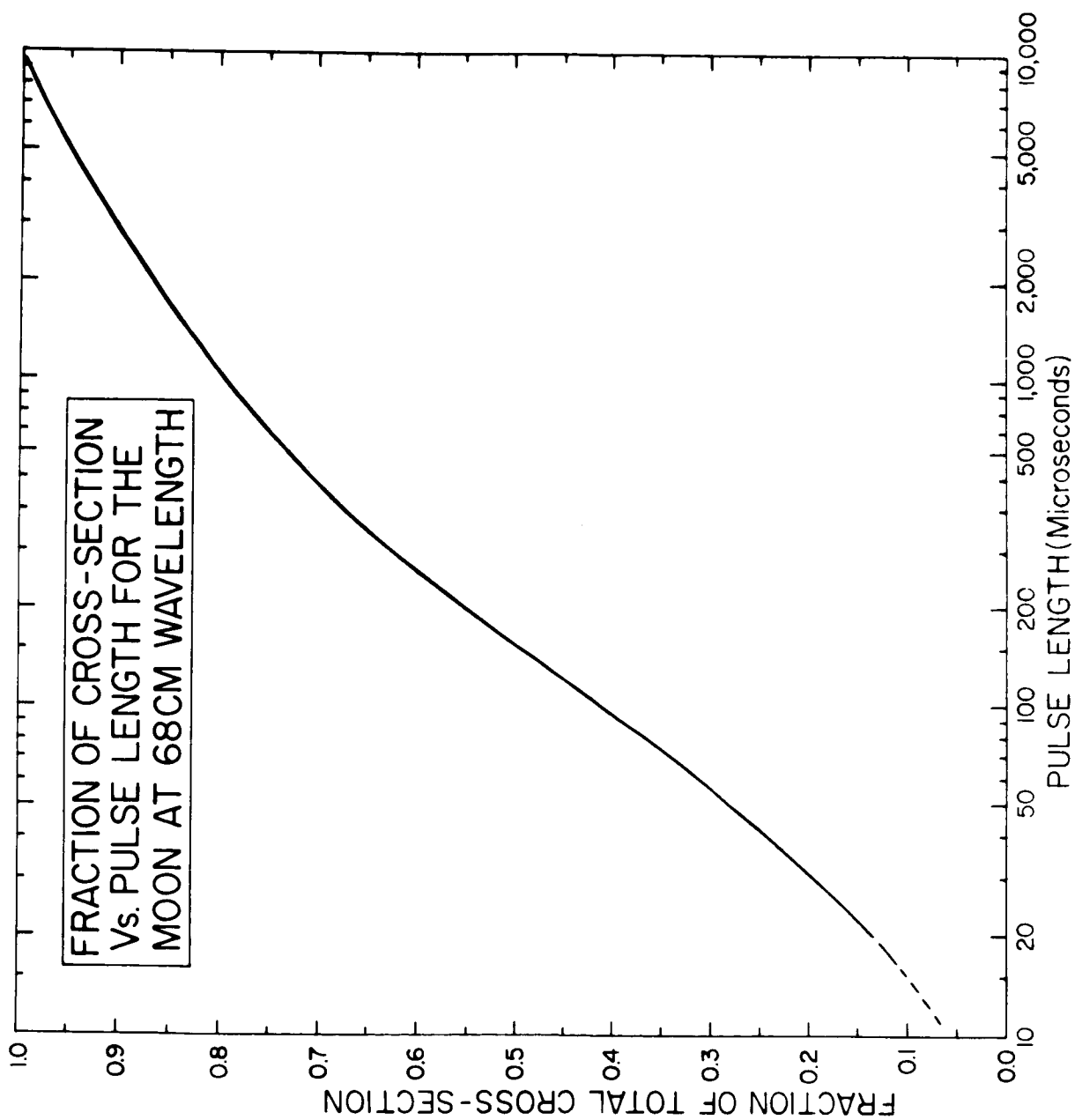
Fig. 1   The peak cross section of the moon expressed as a percentage of the total cross section σ plotted as a function of pulse length. The radar depth of the moon is 11.6 m.secs and if pulses shorter than this are employed, the echo power will fall due to the reduction in the instantaneous area illuminated by the pulse. This curve has been obtained from measurements at 68 cm.

is known (defined by the antenna pattern) and the brightness distribution observed for the lunar disk for uniform illumination is also known. Thus, if the axis of the antenna beam is directed at the center of the moon, and the antenna pattern is circularly symmetrical about this axis, the echo power is given by

$$P_r = \frac{P_t\, G_o^2\, \lambda^2\, \sigma}{64\, \pi^3\, R^4} \int_\theta A^2(\theta)\, B(\theta)\, 2\pi \sin\theta\, d\theta \tag{2}$$

in which G_o is the gain of the antenna on axis and λ is the radio wavelength. Here θ is the angle subtended at the radar between the beam axis and an annulus of width $d\theta$ on the lunar surface, $A(\theta)$ is the normalized antenna pattern (power vs. angle, $A(\theta) = 1$ for $\theta = 0°$) and $B(\theta)$ is the distribution of surface brightness that would be observed for uniform illumination. $B(\theta)$ is normalized so that the integral in Eq. (2) tends to unity for broad-beam antennas. The term $A(\theta)$ appears as a square term as the antenna weights the transmission and reception equally.

Where the antenna beam is broad but the pulse length τ is shorter than the radar depth of the moon, the echo power is given in

$$P_r = \frac{P_t\, G\, A\, \sigma}{(4\pi R^2)^2} \int_0^\tau P(t)\, dt \tag{3}$$

where $P(t)$ is the distribution of echo power with delay t (relative to the leading edge of the moon) measured with a short pulse τ' as $\tau' \to 0$ (it is sufficient for $\tau' \ll \tau$). The integral in Eq. (3) becomes unity for $\tau \gtrsim 11.6$ m.secs. The general case where the antenna beam is smaller than the diameter of the moon and short pulses are employed has been treated (Evans, 1962b) by graphically integrating areas inside contours of equal incident energy and equal range.

By repeating the observations for different positions of the antenna beam with respect to the moon's center, it was possible to recover P(t) and thence σ.

B. Range Variations

The mean range of the moon is 3.844×10^8 meters (causing an echo delay of 2.56 seconds) but due to the ellipticity of the moon's orbit, the actual range may vary over $\pm$ 8% of the mean range. As a result, the echo power will vary over a lunation by $\pm$ 30% (about $\pm$ 1 db). The accuracy achieved in most radar experiments is insufficient for this to be detected and Fricker et al (1958) appear to be the only workers who have observed this variation of echo power during the month. Even they were unable to observe the small variation (about 0.2 db) introduced by the rotation of the earth. These range changes are easily detected by measuring the echo delay time. Very accurate measurements have been made by Yaplee et al (1958, 1959, 1964) from which a mean center-to-center distance between the earth and the moon of 384,400.2 $\pm$ 1.1 km has been obtained.

The difference between the echo power expected on a given day and the mean echo power is given by

$$\Delta P_r = 40 \ [\text{Log}_{10} \ \pi - 1.756] \ \text{db} \qquad (4)$$

where π is the daily value of the equatorial horizontal parallax tabulated in the Nautical Almanac and American Ephemeris in minutes of arc.

C. Observed Values of Cross Section

Many observers have reported values of σ and some of these are presented in Table I and plotted in Fig. 2. The values have been presented as fractions of the physical cross section of the moon ($\pi a^2 = 9.49 \times 10^{12} \ \text{m}^2$), and span a range of over ten octaves (from 8.6 mm to 22 meters). The increase in cross section with increasing wavelength suggested by Fig. 2 depends largely on the three long wave measurements reported by Davis and Rohlfs (1964). These measurements

TABLE I

Values for the Radar Cross Section of the Moon as a Function
of Wavelength Reported by Various Workers

Author	Year	Wavelength (cm)	$\sigma/\pi a^2$	Estimated Error db
Lynn et al	1963	0.86	0.07	± 1.
Kobrin	1963*	3.0	0.07	±-1.
Morrow et al	1963*	3.6	0.07	± 1.5
Evans and Pettengill	1963a	3.6	0.04	± 3.
Kobrin	1963*	10.0	0.07	± 1.
Hughes	1963*	10.0	0.05	± 3.
Victor et al	1961	12.5	0.022	± 3.
Aarons	1959**	33.5	0.09	± 3.
Blevis and Chapman	1960	61.0	0.05	± 3.
Fricker et al	1960	73.0	0.074	± 1.
Leadabrand	1959**	75.0	0.10	± 3.
Trexler	1958	100.0	0.07	± 4.
Aarons	1959**	149.0	0.07	± 3.
Trexler	1958	150.0	0.08	± 4.
Webb	1959**	199.0	0.05	± 3.
Evans	1957	250.0	0.10	± 3.
Evans et al	1959	300.0	0.10	± 3.
Evans and Ingalls	1962	784.0	0.06	± 5.
Davis and Rohlfs	1964	1130.0	0.19	+ 3. - 2.
Davis and Rohlfs	1964	1560.0	0.13	+ 3. - 2.
Davis and Rohlfs	1964	1920.0	0.16	+ 3.

* Revised value -- (privately communicated to Evans and Pettengill, 1963a).
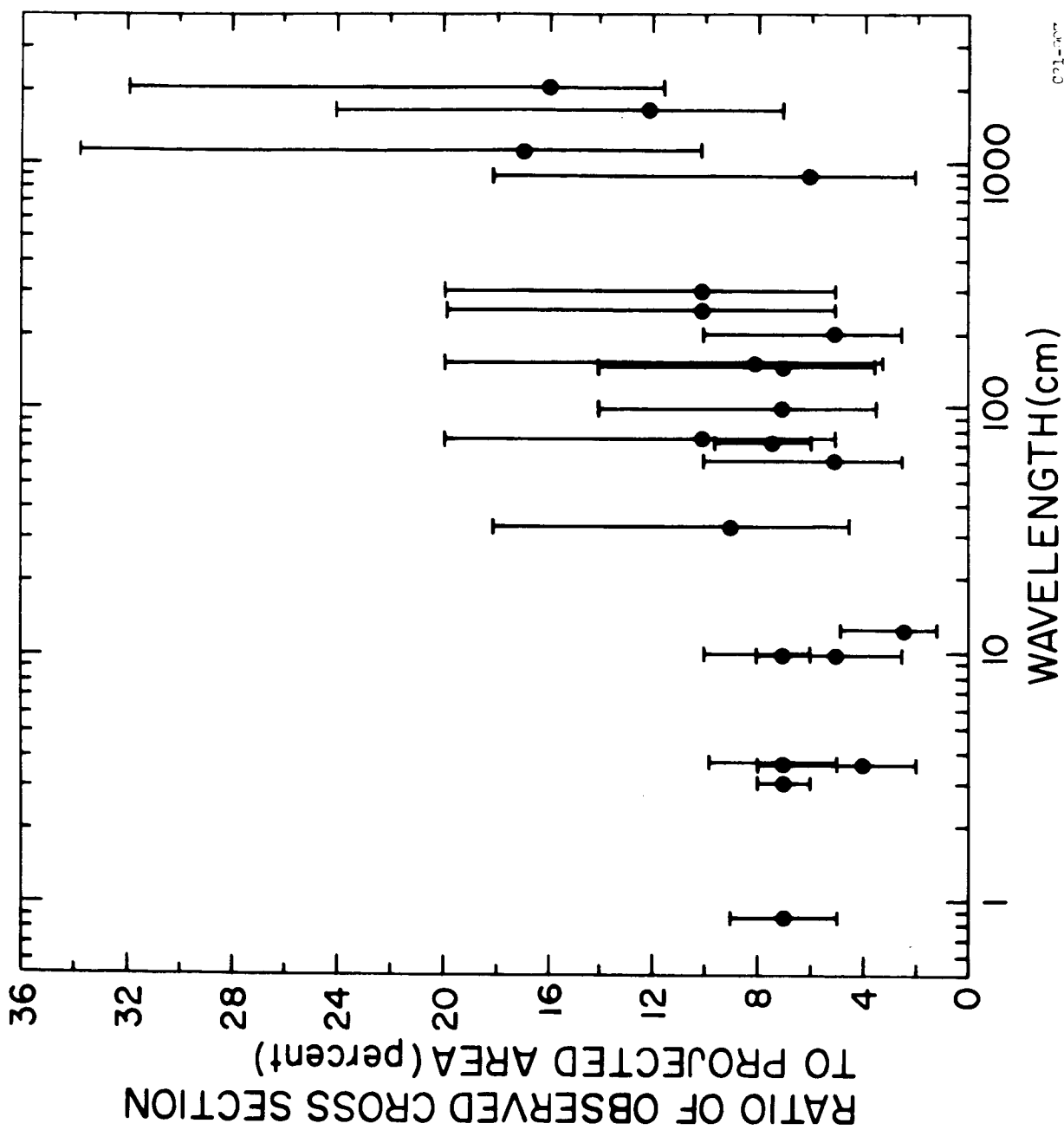
** Reported by Senior and Siegel (1959, 1960)

8.

Fig. 2   The variation of the total cross section σ as a function of the radar wavelength λ. These values are expressed as a fraction of the Moon's projected disk πa² and have been obtained from the papers listed in Table I.

may have been subject to systematic errors introduced by ionospheric effects. If these three points are ignored the remainder show no clear wavelength dependence. In part this is caused by the large error bars associated with each measurement which may conceal a marked dependence. The errors given in Table I are the reported values where these have been given, or $\pm$ 3 db where no uncertainty was published. Absolute power measurements appear to be more difficult in radar astronomy observations than radio astronomy for several reasons. In the first place, the uncertainty in the antenna performance (typically $\pm$ 1 db) enters twice. Next there is the uncertainty associated with measuring P_t; and finally, errors arise in the measurement of P_r due in part to the fading of the signals. Unless extraordinary care is taken, the uncertainty in absolute intensity is usually of the order of $\pm$ 3 db. That Fricker et al (1958) are the only observers who have reported observations of the monthly variation of P_r (which is 2 db) is indicative of the difficulties encountered. Even in the case of Fricker's results, it was not possible to determine the absolute value of P_r to better than $\pm$ 1 db. Because the moon is an extended target whose characteristics change with wavelength, it does not serve Radar Astronomers as a reference in the manner that certain radio sources (e.g., Cygnus A) are used by Radio Astronomers. Radar Astronomy would benefit by the launching of a spherical reflector into a near synchronous orbit which could become a standard test target. Any wavelength dependence in the lunar cross section would then be obtainable with greater confidence. The mean of the values listed in Table I is close to 0.07 and using this mean value, the term $\dfrac{\sigma}{(4\pi R^2)^2}$ has a value of about 1.95×10^{-25} m^{-2}. This term represents the "path loss" encountered by a signal transmitted by an antenna of unit gain and received by one of unit aperture. Expressed in this fashion, the path loss is independent of wavelength and may be taken as 247.2 db/m^2.

10.

D. Theoretical Values of the Cross Section

If the moon were a perfect sphere having a power reflection coefficient at normal incidence of ρ_o, then the cross section would be (Senior and Siegel, 1959)

$$\sigma = \rho_o \pi a^2 \quad . \tag{5}$$

it being assumed that $a \gg \lambda$. The Fresnel reflection coefficient ρ_o is related to the electrical constants of the surface by $\rho_o = |Q|^2$ where

$$Q = \frac{1 - \sqrt{\left[\frac{\mu_o}{\mu}\left(\frac{\epsilon}{\epsilon_o} + i\,\frac{s}{\omega\epsilon_o}\right)\right]}}{1 + \sqrt{\left[\frac{\mu_o}{\mu}\left(\frac{\epsilon}{\epsilon_o} + i\,\frac{s}{\omega\epsilon_o}\right)\right]}} \tag{6}$$

ϵ = permittivity, μ = permeability, and s = conductivity (the subscript o denotes free space values) and ω is the angular radiowave frequency. It can be seen that $\rho_o (= |Q|^2)$ will depend upon the wavelength, unless s, the conductivity, is zero or infinite. In the case of a perfect dielectric where $\mu \rightarrow \mu_o$ and $s \rightarrow 0$, Eq. (6) simplifies to

$$Q = \frac{1 - \sqrt{k}}{1 + \sqrt{k}} \tag{7}$$

where $k = \epsilon/\epsilon_o$ is the relative dielectric constant. Values of k for some typical rock mineral samples are given in Table II. These have been taken from many values listed in a report by Brunschwig et al (1960). The selection in Table II is somewhat arbitrary, but does indicate the wide scatter of values encountered. The basaltic specimens examined by Brunschwig et al (1960) showed the greatest range of values (from 5.5 to 26.7) and an average value for the seven samples listed is 14. For the minerals listed as forms of Andesite (5 samples) the mean

11.

TABLE II

Some Typical Terrestrial Rocks and Their Values of Dielectric Constant
(Brunschwig et al, 1960)

Mineral	Type	and	Source	Dielectric Constant k
Andesite	Vesicular Basalt		Chaffee County Colorado	6.51
Olivine Basalt Cellular			Washington	5.50
Basalt	Olivine Basalt		Jefferson County Colorado	8.89
Olivine Basalt	Basalt		Lintz Rhenish Prussia	17.4
Diabase			Mt. Tom Massachusetts	10.8
Rhyolitic Pumice	Pumice		Millard County Utah	2.29
Rhyolite			Castle Rock Colorado	4.00
Basaltic Scoria	Scoria		nr. Klamath Falls Oregon	6.08
Trachytic Tuff			nr. Cripple Creek Colorado	5.32
Quartz Sandstone	Sandstone		Columbia County Pennsylvania	4.84

was 8.8, whilst the Rhyolitic samples were lower (4.1). Silicate materials, e.g., fused quartz, are frequently suggested as making up the bulk of the lunar surface material and these have dielectric constants in the range 4 to 7.[*] Dry terrestrial sand has a dielectric constant of about half this. If the surface of the moon were solid rock having a dielectric constant k = 5 (the lowest value likely), then the reflection coefficient would be 14%. As the mean lunar cross section is only 7%, it is already evident that the surface cannot be solid rock.

If the perfect sphere discussed above is replaced by one in which the true surface departs in an irregular fashion from the mean, then the cross section is likely to change and account can be taken of this by writing

$$\sigma = g \rho_0 \pi a^2 \tag{8}$$

Here g is a directivity factor that expresses the ability of the sphere to scatter back favorably toward the source. For a smooth metal sphere ($\rho_0 = 1$) the echo power is re-radiated isotropically and the value of g is 1.0 (Norton and Omberg, 1947). As we have seen, the factor g is also unity in the case of a smooth dielectric sphere, but the scattering in this case is not isotropic and depends upon the dielectric constant k (Rea et al, 1964).

The value for g as defined by Eq. (8) for an arbitrarily rough surface is not known and only the case of a sphere with a smooth undulating surface has been examined in detail (Hagfors, 1964). In this case $g = 1 + \alpha^2$ where α^2 is half the mean square surface slope. The effect of the shallow undulations is to cause the pattern of Fresnel zones at the center of the disk to be rearranged such that parts of each zone are distributed randomly over the entire disk.

[*] An alternative argument due to Gold (1964) is to suppose that fractionation processes have not occurred in lunar rocks to the extent they have on earth. The surface rocks would then be expected to be little different from meteoritic material and have a high dielectric constant ($k \sim 20$).

13.

Provided that the antenna beam is broad enough to illuminate the whole surface, a small increase in mean cross section will be observed when this hypothetical ideally smooth sphere is replaced by one with an undulating surface.
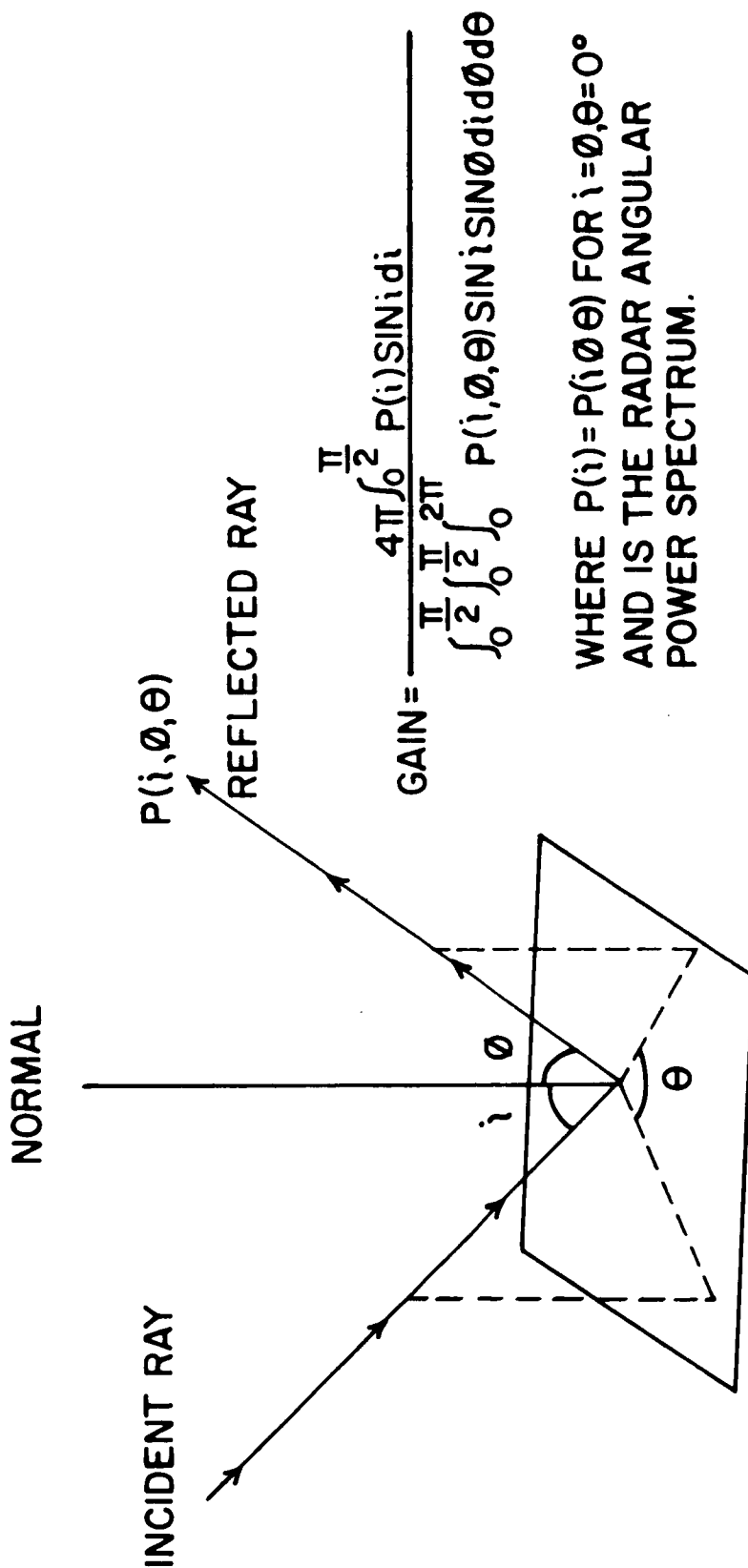
An alternate and widely adopted approach to obtaining the scattering cross section is to consider the scattering properties of the target as specified by a function σ_o (i ϕ θ) which defines the reflected intensity per unit surface area per steradian. This function is obtained by exploring the power reflected from an elemental area of surface illuminated at an angle of incidence i, and observed at an angle of reflection ϕ; the planes containing these two rays and the surface normal are at an angle θ as shown in Fig. 3. Provided there is no coherence between returns from different surface elements the gain G_m of the moon in the direction of backscattering is given by (Evans and Pettengill, 1963b)

$$G_m = \frac{4\pi \int_0^{\pi/2} \sigma_o (i) \sin i \, di}{\int_0^{\pi/2} \int_0^{\pi/2} \int_0^{2\pi} \sigma_o(i \, \phi \, \theta) \sin i \sin \phi \, d\theta \, d\phi \, di} \tag{9}$$

where $\sigma(i)$ is the particular case in which i = ϕ, θ = 0. From earth-based observations alone only $\sigma_o(i)$ can be determined and hence G_m as defined by Eq. (9) cannot be obtained. If, however, G_m were known either from theory or observation, the cross section for the whole sphere could be written as

$$\sigma = G_m \, \bar{\rho} \cdot \pi a^2 \tag{10}$$

Here $\bar{\rho}$ is the albedo averaged over the hemisphere, and this is usually different from the reflection coefficient at normal incidence ρ_o. This distinction has not always been recognized and the literature contains several instances where ρ_o has

14.

NORMAL

INCIDENT RAY

REFLECTED RAY

$P(i,\emptyset,\theta)$

$\emptyset$

i

θ

$$\text{GAIN} = \frac{4\pi \int_0^{\frac{\pi}{2}} P(i)\text{SIN}i\,di}{\int_0^{\frac{\pi}{2}} \int_0^{\frac{\pi}{2}} \int_0^{2\pi} P(i,\emptyset,\theta)\text{SIN}i\,\text{SIN}\theta\,di\,d\emptyset\,d\theta}$$

WHERE $P(i)=P(i\emptyset\theta)$ FOR $i=\emptyset,\theta=0°$
AND IS THE RADAR ANGULAR
POWER SPECTRUM.

THE SURFACE PHOTOMETRIC FUNCTION P(iØθ)

C314-212

Fig. 3   The geometry required for studying the complete scattering characteristics
of an irregular surface in order to obtain a value for the gain of the whole
moon over an isotropic scatterer.

15

been equated with $\bar{\rho}$ without proper explanation. If this is done, the directivity factor g is automatically made the same as G_m. Rea et al (1964) have pointed out that these approximations are certainly not valid for the case of a smooth dielectric sphere.

III. ECHO POWER VS. DELAY

   A. Relation to the Angle of Incidence

   With modern radar equipment, echoes from the moon may readily be

resolved either in delay or in frequency. The libration of the moon causes the

lunar disk to appear to be rotating to a terrestrial observer with a radial

velocity usually in the range 10^{-6} to 10^{-7} radian/sec. This gives rise to

doppler broadening of the signals so that the echo power at a given frequency offset

is proportional to the reflectivity of a particular strip on the moon's disk

that is parallel to the apparent axis of rotation as shown in Fig. 4 (Browne

et al 1956). Thus the determination of the echo power spectrum $\bar{P}(f)$ yields the

brightness distribution over the moon's disk. Such measurements have been made

by a number of workers (Evans 1957, Evans and Ingalls 1962, Daniels 1963a).

The best measurements of this kind have been performed using phase coherent

radar systems, such as the Millstone Hill radar which was employed by Pettengill

and Henry (1962a) to obtain the results shown in Fig. 5. The limb-to-limb

doppler broadening introduced by the moon is typically 2 cps for a radar frequency

of 100 Mc/s, and hence it is difficult to achieve good resolution by this tech-

nique. In Fig. 5, for example, the frequency resolution of the radar is 1/40th

of the total echo spectrum.

   Much better resolution can be obtained by resolving the echoes with

respect to delay. For example, pulse lengths of 12 μsec and shorter have been

used to study the scattering behavior of the moon (whose full radar depth is

11.6 m.sec.). A short pulse illuminates at any instant an annulus on the surface

as shown in Fig. 4. The amount of actual area illuminated by the pulse is given

by $\pi a\, c\, \tau$ (where c = the velocity of light and τ is the pulse length) and is
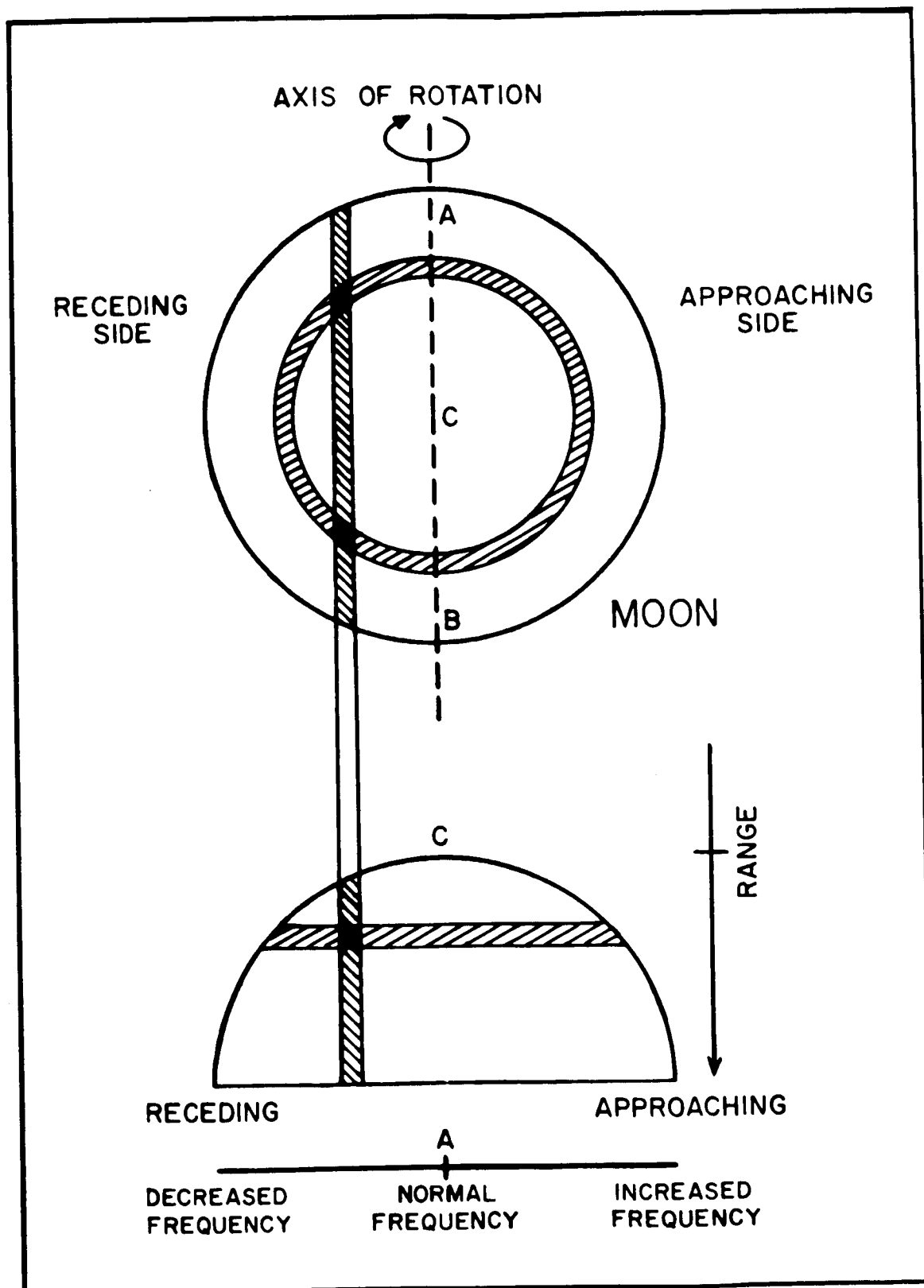
Fig. 4   The contours of constant delay τ and constant doppler shift f are shown for a hypothetical pair of values. The shaded regions indicate the two areas having the same frequency and range coordinates.
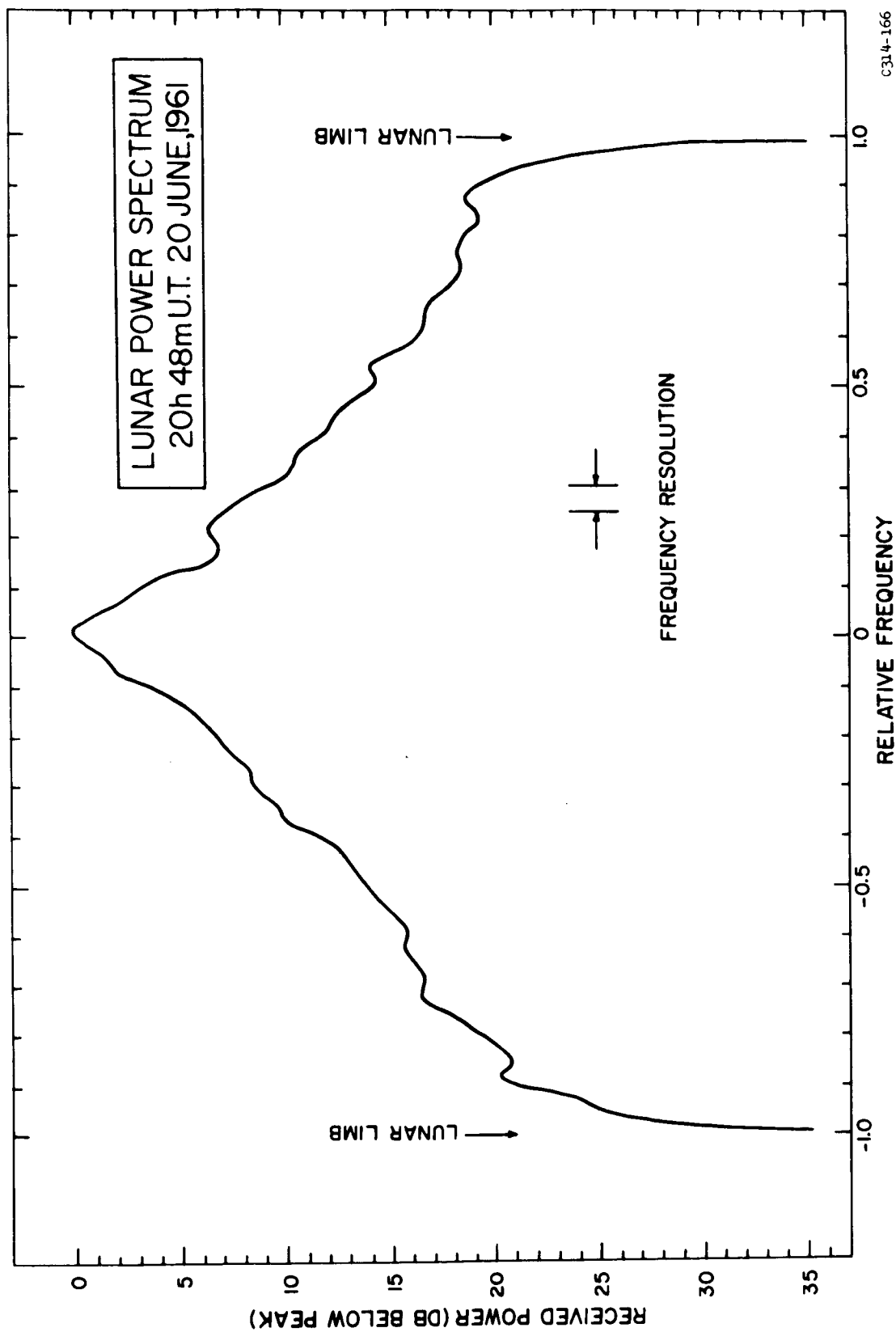
Fig. 5   The power spectrum $\overline{P}(f)$ of moon echoes obtained by Fourier analyzing a chain of coherent pulses by means of a fast digital computer. These observations were made at 68 cm wavelength and show the brightness distribution across the lunar disk.

19

$\sigma(i \not\phi \theta)$ used in Eq. (9), i.e., norm~lized to unit a~t~l~ surface a~

follows that for a uniformly bright surface we have from Eq. (12)

$$\bar{P}(\not\phi) \propto \cos \not\phi \qquad \text{(Lommel-Seeliger)} \qquad (13)$$

and for Lambert's law

$$\bar{P}(\not\phi) \propto \cos^2 \not\phi \qquad \text{(Lambert)} \qquad (14)$$

In all likelihood, the surface of the moon may be regarded as statistically uniform from annulus to annulus. It follows that by exploring the distribution of echo power with delay $\bar{P}(t)$, one can see if the angular power spectrum can be represented by simple laws such as Eq. (13) or (14). That is, if the surface is statistically uniform, then the plot $\bar{P}(\not\phi)$ obtained is simply the angular scattering law $\tau_o(\not\phi)$ defined previously. To make it clear that an assumption is involved here, we shall use the symbol $\bar{P}(\not\phi)$ to denote the angular dependence obtained from short pulse measurements. In the limit, where very short pulses (i.e., as $\tau \to 0$) are used to observe a statistically uniform sphere $P(\not\phi) \to \sigma_o (\not\phi)$.

20.

INCIDENT AND REFLECTED RAY

a = RADIUS OF THE MOON
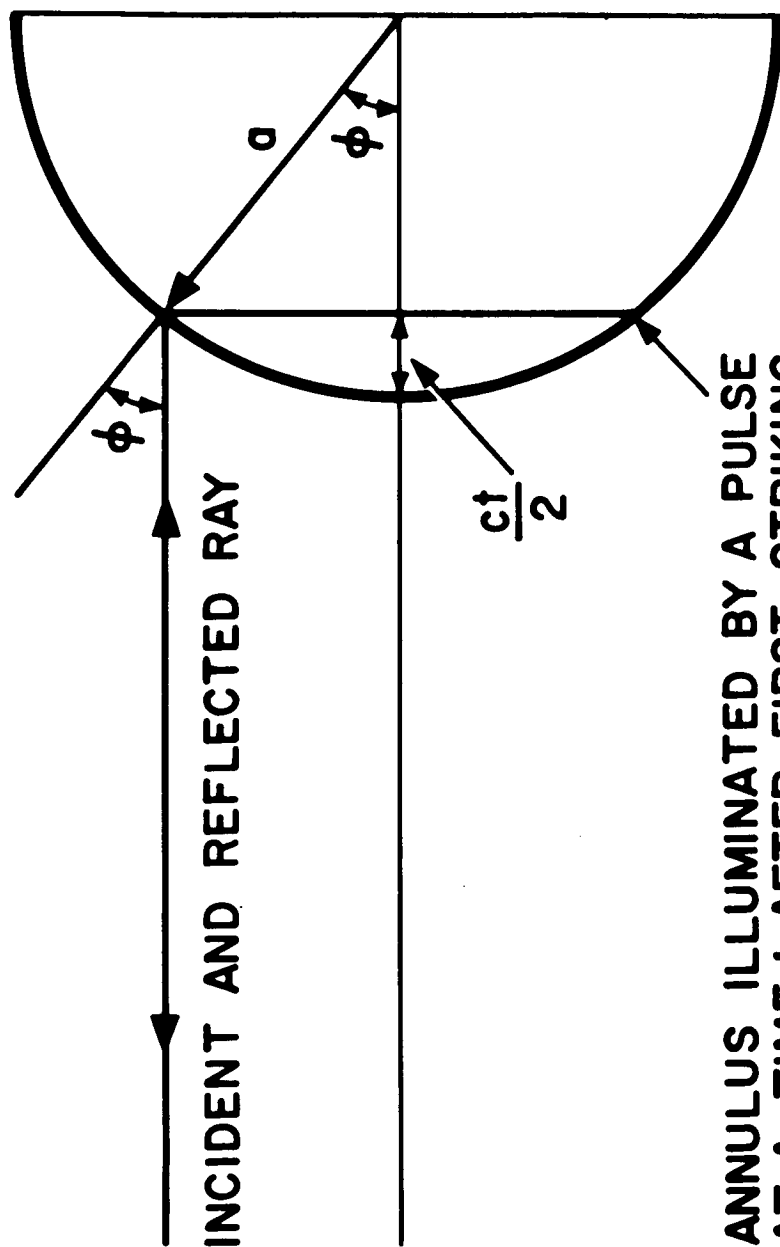
c = VELOCITY OF LIGHT

ANNULUS ILLUMINATED BY A PULSE
AT A TIME t AFTER FIRST STRIKING
THE SURFACE.

$\frac{ct}{2}$

C31-502

Fig. 6 The relation between the range delay t and the angle of incidence and reflec-
tion ϕ of the radio waves.

B. Short Pulse Observations

Kerr and Shain (1951) were the first to attempt short pulse observations of the moon in order to see if the pulses were lengthened by the distribution of the scattering centers in depth. They reported that 1 m.sec. pulses were lengthened in support of their conclusion (obtained from echo spectrum measurements) that the moon was approximately a uniformly bright reflector. Evans (1957) using 2 m.sec. pulses reached the reverse conclusion in support of his observation (also from echo spectrum measurements) that the moon was in fact a limb dark scatterer. Immediately on publication of these later results, the work performed several years previously at the Naval Research Laboratory was released (Trexler, 1958). Trexler employed a radar operating at 198 Mc/s with pulse length of 12 μsecs and Fig. 7 illustrates the range display observed in this work. Some 50% of the echo power was returned within the first 50 μsec of the pulse. The exponential tail of the echo appeared to extend some 500 microsec beyond the leading edge of the echo, but this appeared to be a function of signal-to-noise ratio. Yaplee et al (1958), later Hey and Hughes (1959) reported similar behavior at a wavelength of 10 cm, when 2 and 5 μsec pulses were used, respectively.

The difficulty involved in these observations is to obtain good range resolution together with adequate signal-to-noise ratio. To achieve good range resolution, one is obliged to use short pulses which (a) causes the peak echo power to fall due to a reduction in the illuminated surface area (Fig. 1), and (b) requires the receiver bandwidth b to be adjusted to match the pulse length τ according to

$$b \approx \frac{1}{\tau} \tag{15}$$

and hence makes the receiver admit more noise power as the pulse is shortened. Thus the signal-to-noise ratio falls rapidly as the pulse length is reduced and
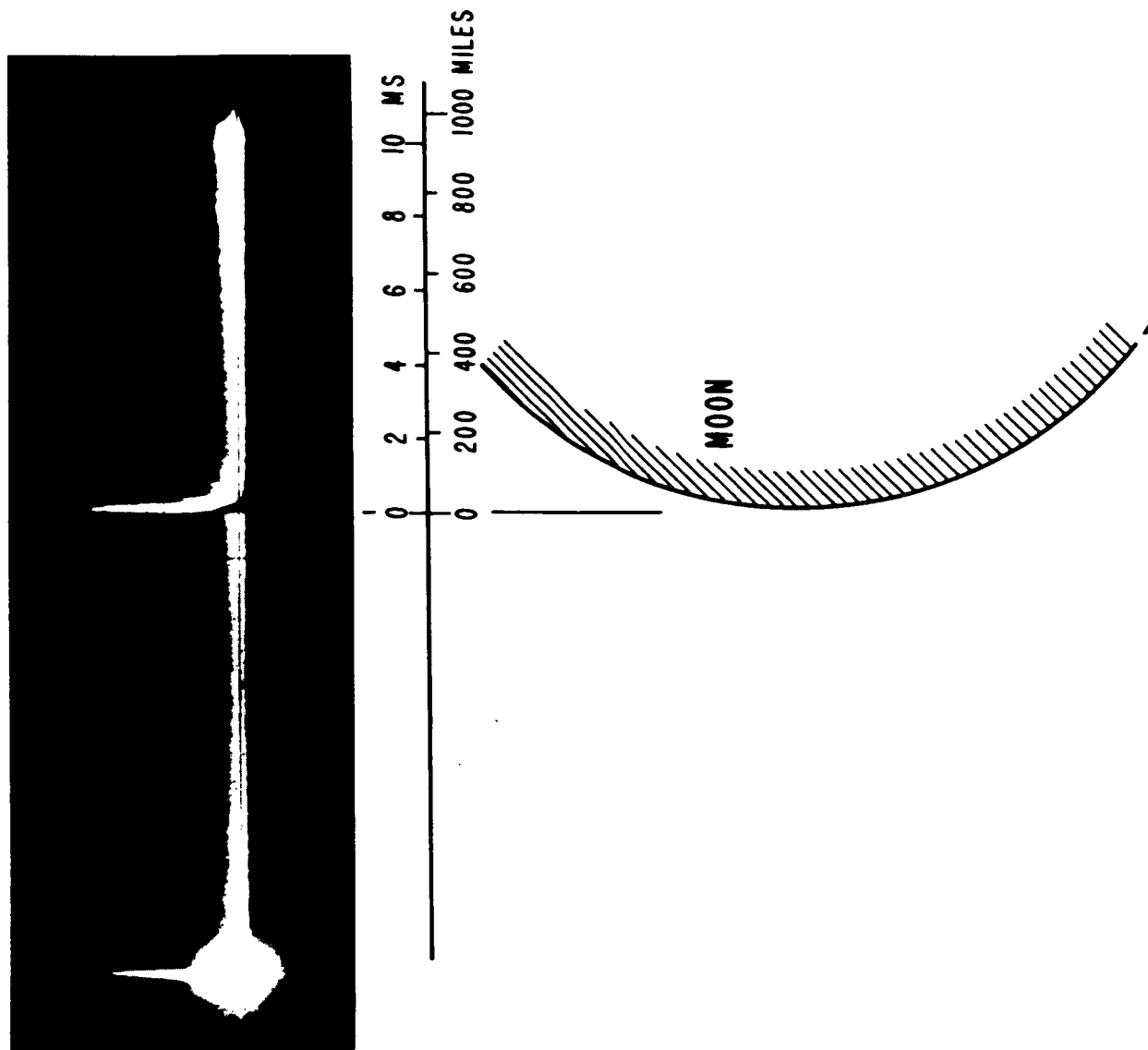
22.

Fig. 7   Moon echoes observed by Trexler (1958) compared to scale with curvature of the moon (modified from a sketch in the TRE which had the moon radius 2000 miles). (Courtesy of the editors of Proc. IEEE)

even at the present time short pulse observations have been made only at a limited number of wavelengths, though the total cross section has been measured at many. The observations of Trexler, Yaplee et al, and Hey and Hughes indicated that echoes come only from a portion of the surface near the center of the disk. This proved to be a consequence of the limited sensitivity of their equipment. Pettengill (1960) and Leadabrand et al (1960) showed that echoes could be measured all the way out to the limbs with a sufficiently powerful radar system.

The first truly quantitative measurements of echo power vs. delay from the leading edge to the limb were performed by Pettengill (1960), Pettengill and Henry (1962a) at a wavelength of 68 cm using 65 μsec pulses. They employed a digital computer to average the echo intensity at range intervals of 250 μsecs. Meanwhile, Hughes (1961) made observations at a wavelength of 10 cm using 5 μsec pulses and averaging the echo power by means of a single channel analog integrator with a resolution of 20 μsec. Hughes was unable to obtain echoes beyond 1 m.sec. delay measured from the leading edge, but in the region 0-1 msec obtained results in good agreement with Pettengill and Henry (1962a). Accordingly, he concluded that the radio wave scattering properties of the moon were independent of the radio wavelength λ. However, in reaching this conclusion, he ignored the fact that the resolution in the two sets of measurements was considerably different.

A search for a wavelength dependence in the scattering was undertaken by Evans (1962b,c). A forty-eight channel integrator was constructed and first employed with a 30 μsec pulse radar operating at 3.6 cm. For reception, the resolution in delay was 20 μsec. Later the measurements were repeated at 68 cm wavelength with the same pulse length and resolution in delay. The two sets of measurements are compared in Fig. 8. A clear change in $\bar{P}(t)$ is evident. At the shorter wavelength, the leading edge echo is not so prominent as at 68 cm.
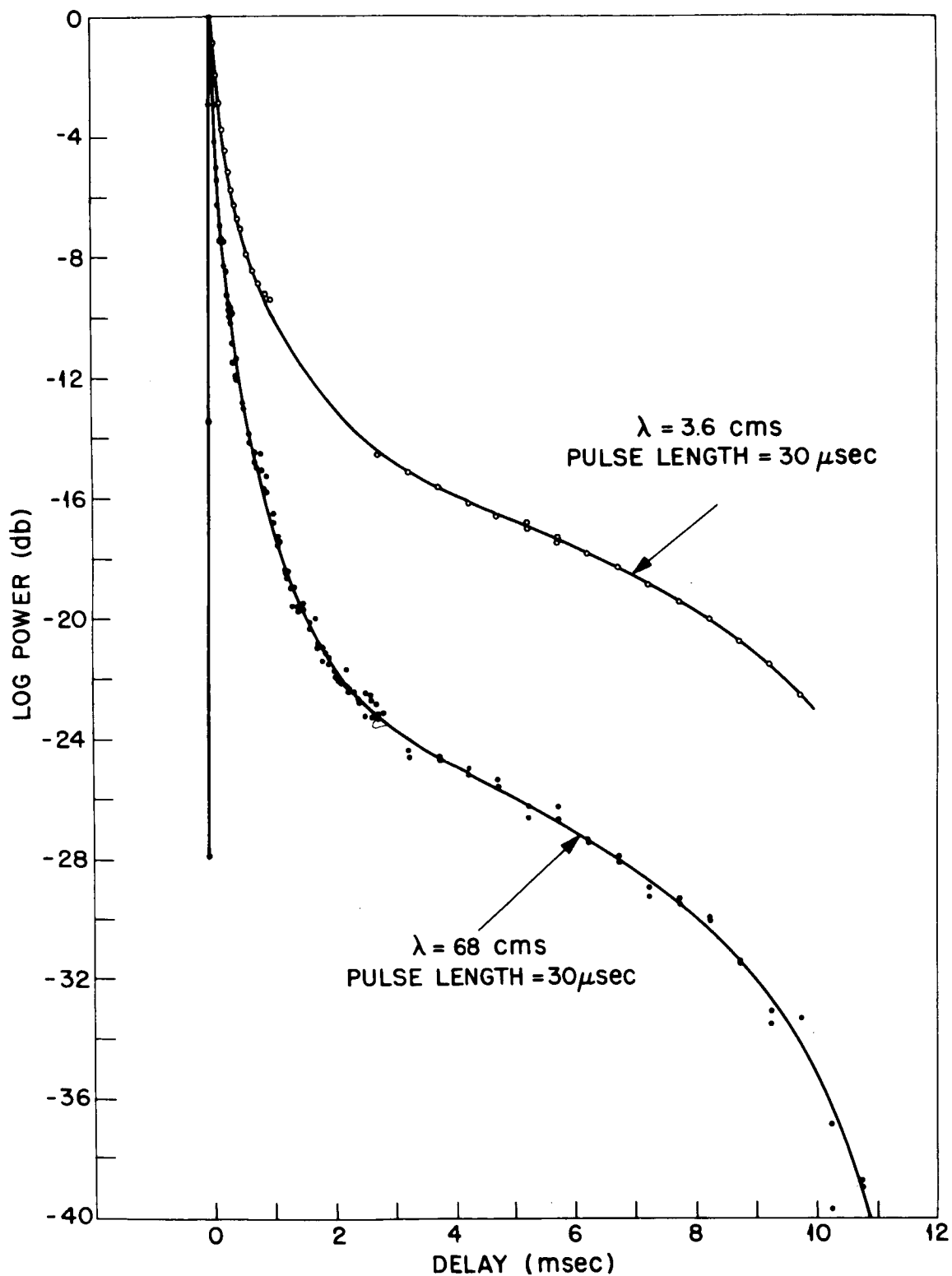
Fig. 8 The average echo power reflected by the moon $\bar{P}(t)$ as a function of delay measured with respect to the point closest to the radar. The 68 cm results were obtained using the same methods of averaging as were employed to obtain the 3.6 cm results. The curves have been normalized at zero delay.

More recent observations at a wavelength of 23 cm with the same range resolution (Evans and Hagfors, 1965) confirm the behavior shown in Fig. 8.

The measurements at 68 cm were later repeated with 12 μsec pulses and 10 μsec resolution in delay to achieve an over-all resolution comparable to that of Hughes (1961). A comparison of these 68 and 10 cm results is given in Fig. 9. Once more a clear dependence on wavelength is evident.

At longer wavelengths (λ = 7.84 m) Evans and Ingalls (1962) found that the echo power spectrum was indistinguishable from that observed at λ = 68 cm. However, Faraday fading of the echoes (Browne et al, 1956) and possibly iono-spheric scintillation may have introduced error. Davis and Rohlfs (1964) have employed a 250 μsec pulse radar at 11.3 m wavelength to obtain the scattering behavior over the first 4 m.sec of delay. Despite the long pulse used, they found (Fig. 10) that the wavelength dependence shown in Fig. 8 is continued in the meterwave region. Because ionospheric scintillation effects cannot intro-duce systematic errors in short pulse determinations of the scattering behavior, this seems to be the only reliable technique at these long wavelengths.

At shorter wavelengths, Lynn et al (1963) have determined the scattering behavior at 8.6 mm. These observations were remarkable in that a transmitter power of only 12 watts was employed and that resolution of different range delays was achieved solely by means of the angular resolution afforded by the antenna beam (4.3 min arc). Thus the antenna was directed at different distances from the center of the lunar disk to determine the brightness distribution. This achieves poor range resolution at the limbs as equal projected areas are illuminated as distinct from the equal surface area illuminated by short pulse radars. To correct the observations at the limb for the amount of the antenna pattern projected onto the sky which provided no illumination of the moon,
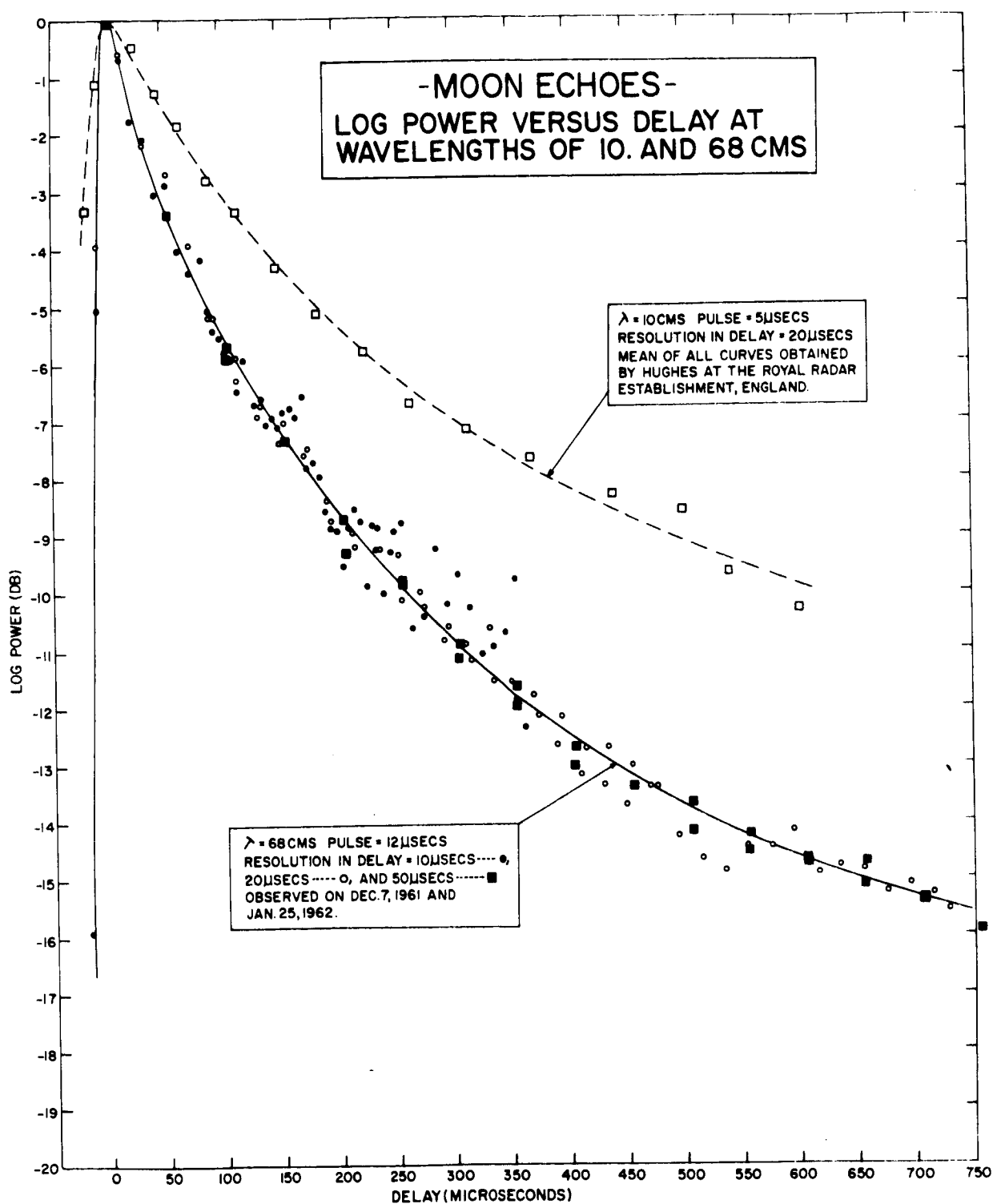
Fig. 9 High resolution measurements of $\bar{P}(t)$ at 68 cm wavelength and at 10 cm wavelength (Hughes, 1961). As in Fig. 8, a clear wavelength dependence can be observed. The curves have been normalized at zero delay.
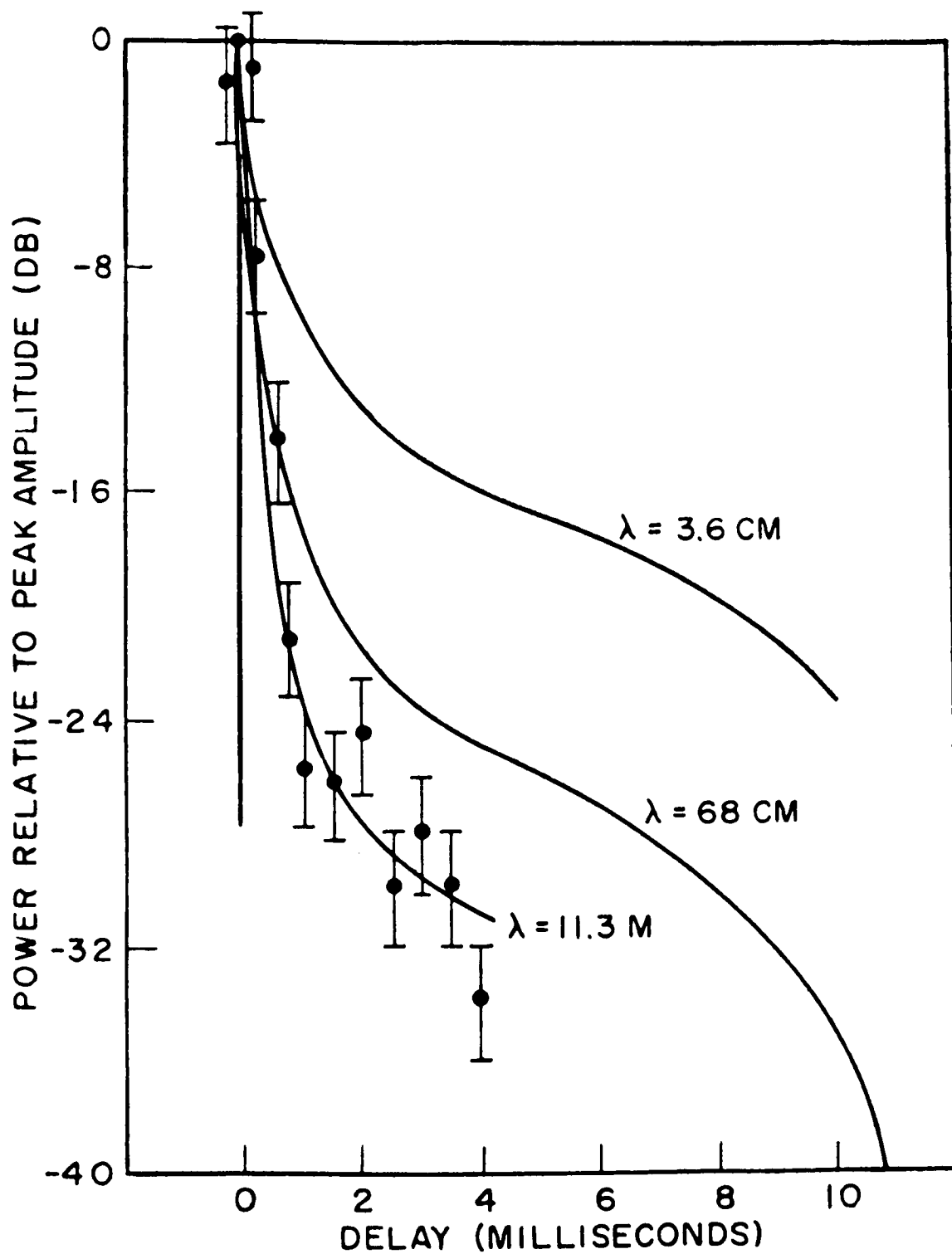
Fig. 10   The results obtained by Davis and Rohlfs (1964) at 11.3 m wavelength using 250 μsec pulses are shown here with the results presented in Fig. 8 for comparison.

28

Lynn et al (1963) assumed that the moon behaved as a uniformly bright reflector (Lommel-Seeliger Law). Their results when put in the same form as those of Evans and Pettengill (1963c) are shown in Fig. 11. The wavelength dependence of the scattering of electromagnetic waves by the moon in the wavelength range 1 meter to that of light is very evident. At 8 mm only a small highlight appears at the center. The brightness there exceeds that of other regions by only a factor of two. At 3.6 cm this ratio is of the order of 25 and at 68 cm, 150. Lynn et al (1963) also reported that there were no differences between the brightness of the maria and the highlands larger than ($\pm$ 2 db) -- the accuracy of their observations. It would seem that the rough structure responsible for diffuse scattering at 8.6 mm is to be found overlying highlands and maria equally. It is tempting to conclude that the microrelief responsible for the moon's photometric properties also controls the scattering at 8.6 mm, perhaps by extending in depth to several millimeters.

We may summarize these results as follows. At a radio wavelength of 1 meter, the moon scatters predominantly from those regions at the center of the visible disk which are nearly normal to the line of sight. This suggests a rather smooth surface. However, as the wavelength is reduced, more and more power is returned from other regions showing that as the scale of the exploring wave is reduced, the surface is found to appear increasingly rough. At 1-cm wavelength the disk appears to be almost uniformly bright, indicating that the surface is now essentially covered with structure having dimensions comparable with the wavelength.

C. Orthogonal Polarization Observations

Browne et al (1956) observed that the nulls introduced by the Faraday fading were quite deep and that the amount of depolarized power was about 10%. This was later confirmed by Blevis and Chapman (1960). Senior and Siegel (1960)
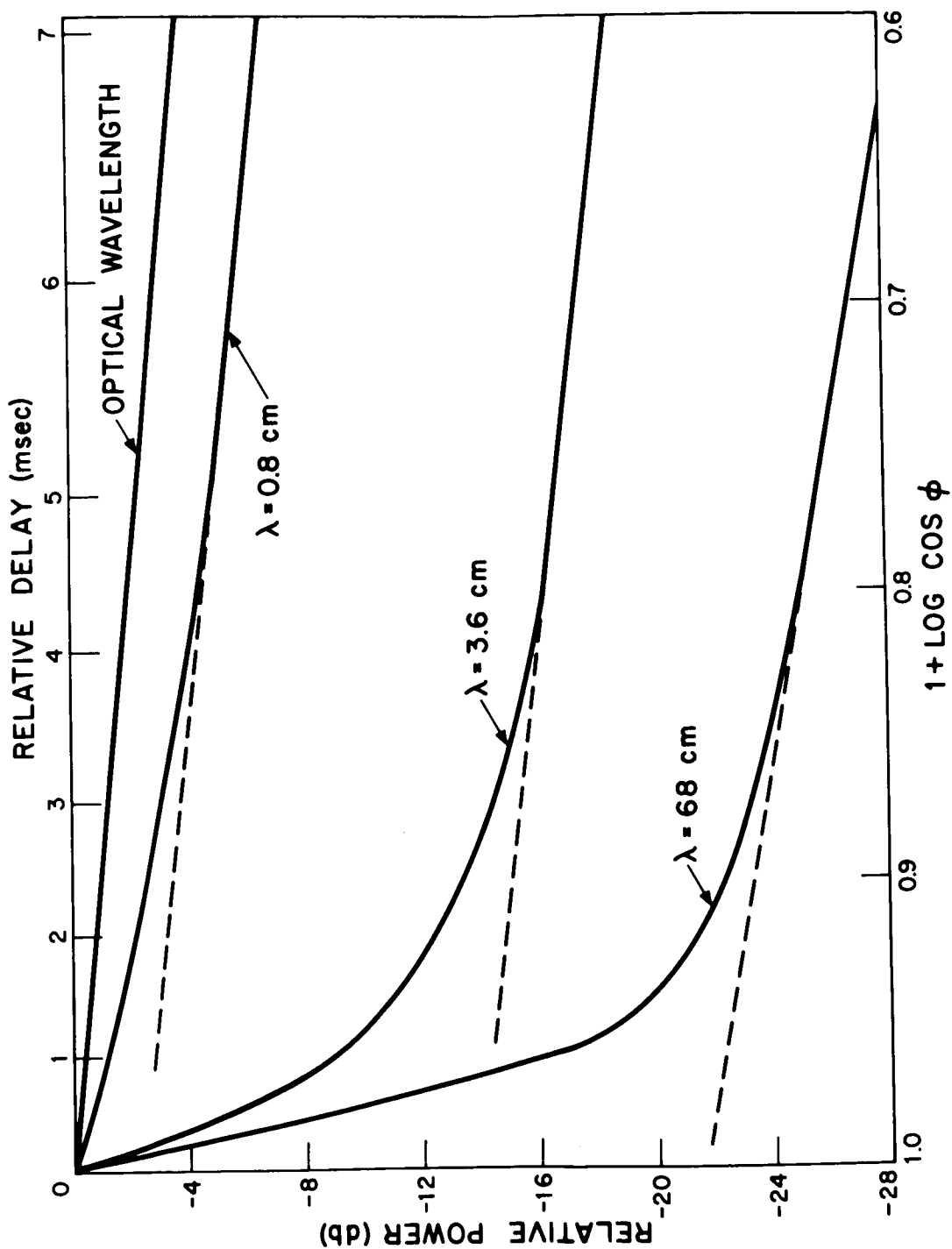
29.

Fig. 11   The distribution of echo power as a function of $1 + \cos \phi$ at 8.6 mm wavelength (Lynn et al, 1963). The 3.6 cm and 68 cm results have been included for comparison.

were the first to argue that this result alone demonstrates that the reflection occurs from largely smooth surfaces. In order to study the depolarizing ability of the lunar surface, it is desirable to overcome the Faraday fading, and this is most easily accomplished by using circularly polarized waves and receiving the circular component having the same sense as that transmitted. This experiment has been performed at 68 cm wavelengths by Pettengill and Henry (1962a) using 400 μsec pulses, and later by Evans (1962c) using 200 μsec pulses. As may be seen in Fig. 12, the depolarized component of the power obeys the law $\bar{P}(\phi) \propto \cos \phi$ indicating that these signals are scattered equally from all parts of the projected disk. The percentage polarization can be expressed in the form

$$\text{Polarization} = \frac{\bar{P}(t) - \bar{D}(t)}{\bar{P}(t) + \bar{D}(t)} \times 100\% \qquad (16)$$

where $\bar{P}(t)$ is the average polarized or expected return and $\bar{D}(t)$ the depolarized component. The percentage polarization has been plotted in Fig. 13 for both the 400 and 200 μsec pulse observations. It appears that the percentage polarization falls linearly out to a delay of 3 m.secs where it has a value of 60%. Beyond this value of delay the depolarization falls less rapidly, and the ratio of the amount of power in the two components $\bar{P}(t)/\bar{D}(t)$ is approximately constant at 3:1.

Two mechanisms which could give rise to depolarization are (a) multiple reflections at the surface in which one or more reflections occur near the Brewster angle, and (b) the excitation of surface elements which are comparable in size to the wavelength and re-radiate as dipoles. Probably both mechanisms contribute to some extent, but (a) seems incapable of converting one quarter of the incident power into the depolarized component. On the other hand, just this difference would be expected if the scattering were produced by a random collection of dipoles,[*] i.e., suggesting (b) as the principal mechanism.

31.

[*]This result has been derived in connection with the Project West Ford dipoles. See C. L. Mack and B. Reiffen, "RF Characteristics of Thin Dipoles," Proc. IEEE 52, 533-542 (1964).
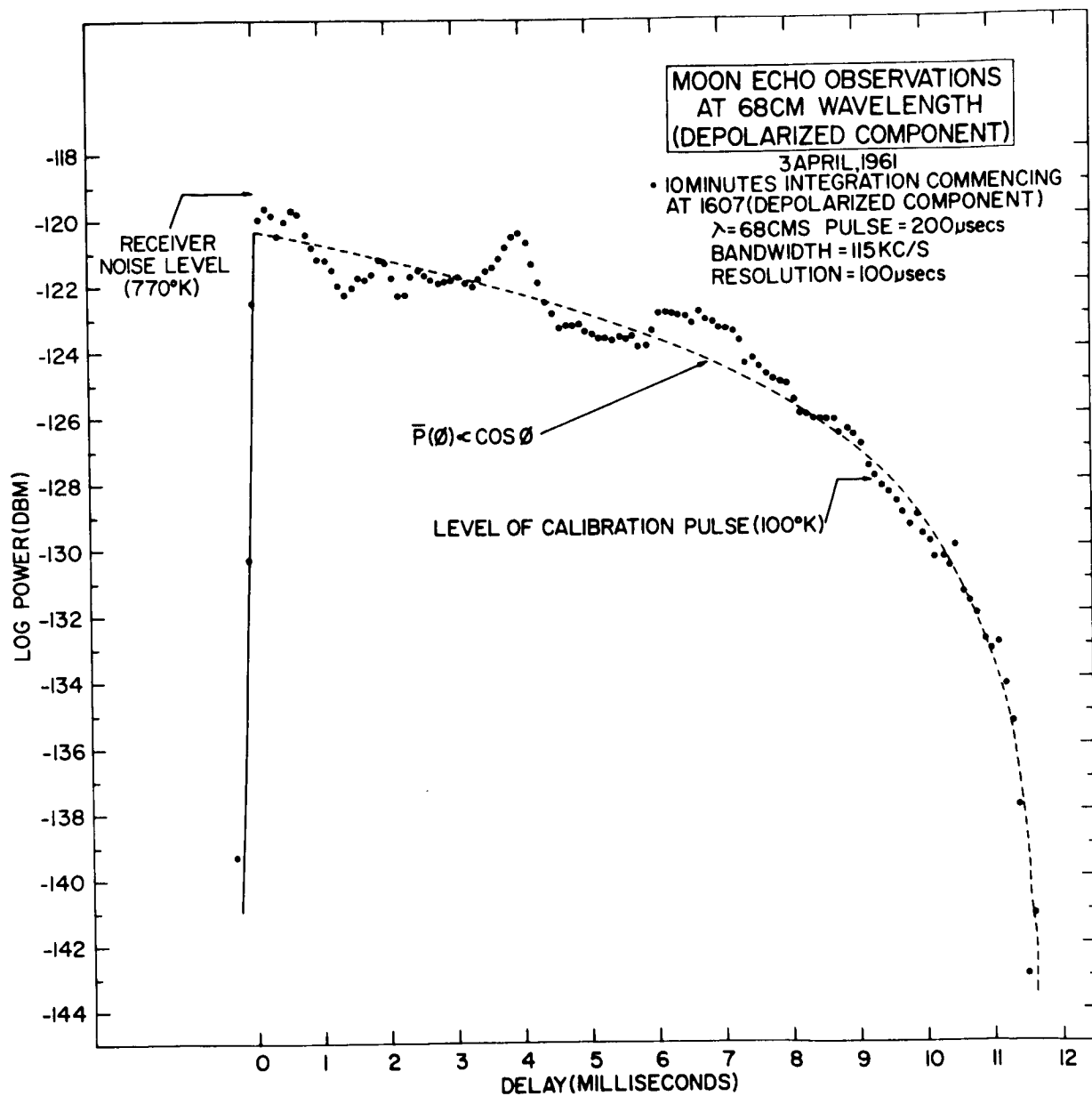
Fig. 12   The average echo intensity vs. range delay $\overline{D}(t)$ for the depolarized compo-
nent of the signals (Evans and Pettengill, 1963c). The dotted curve indi-
cates the expected behavior for a uniformly bright moon. The departures
from the smooth curve are thought to represent the existence of departures
from statistical uniformity of the surface features over the moon's disk.
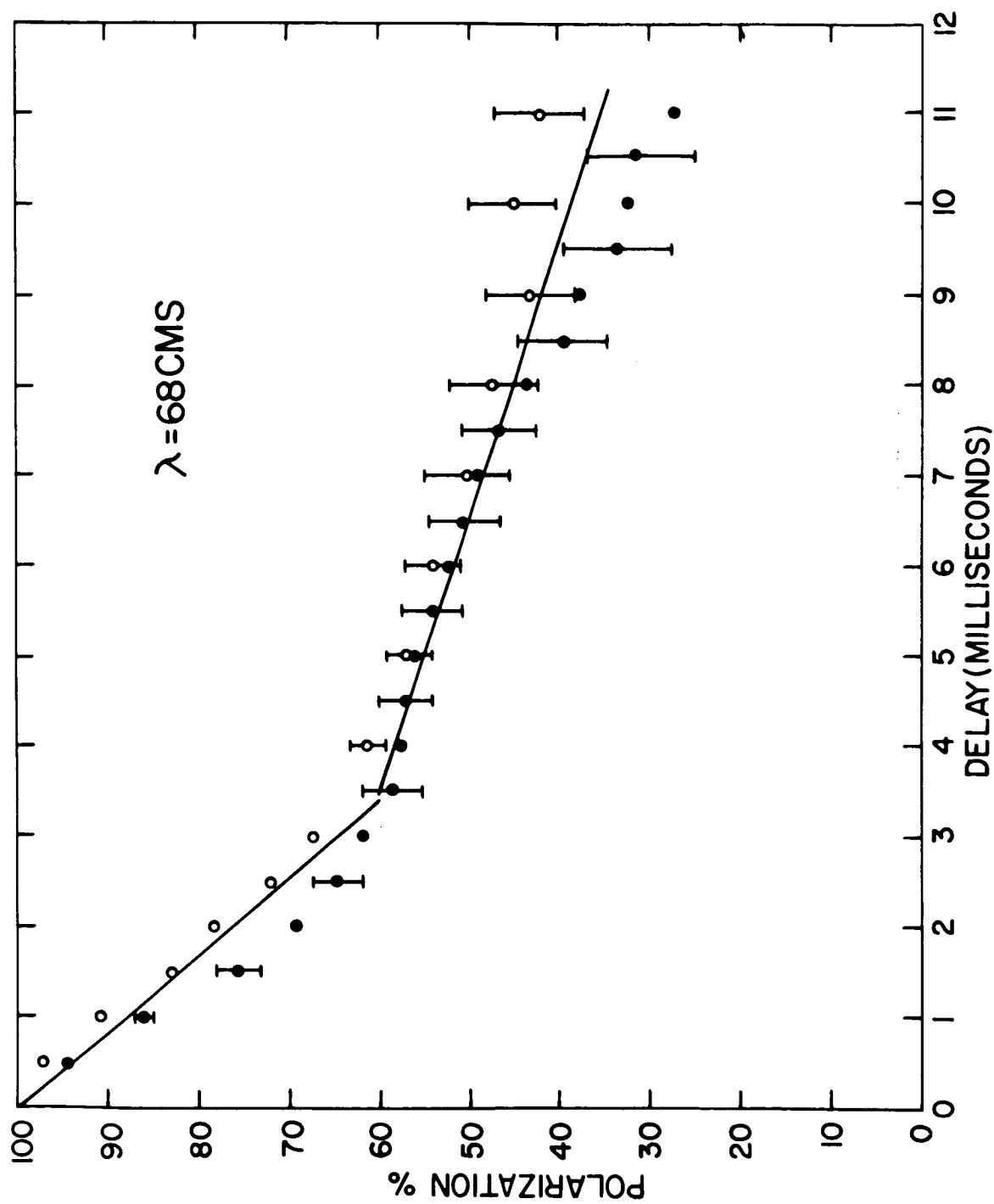These might be expected to be more easily seen in the depolarized than
polarized component.

Fig. 13 The percentage polarization of moon echoes as a function of range delay observed at 68 cm wavelength (Evans and Pettengill, 1963c). These values were computed from the results shown in Fig. 12 by means of the expression 16. The earlier values obtained by Pettengill and Henry (1962a) are also shown.

It seems that further polarization studies might be most profitable. They are capable of showing the presence or absence of a dust layer on the surface through which the radar signals may be propagated. The experiments which would need to be carried out have been considered by Hagfors (privately communicated).

IV. THE ANGULAR SCATTERING LAWS

Evans and Pettengill (1963c) have explored a number of empirical laws by which to represent the angular power spectra $\bar{P}(\phi)$ of the signals. In this section we briefly review this work. The most obvious way to proceed is to plot the logarithm of the power against log cos ϕ to see if simple laws of the form

$$\bar{P}(\phi) \propto \cos^m \phi \qquad\qquad m = \text{constant} \qquad\qquad (17)$$

can be made to fit the results. The experimental uncertainties in the measurements made to date are least in those for 68 cm wavelength. As we have seen, the depolarized component $\bar{D}(t)$ observed at this wavelength (Fig. 12) is fairly well represented by this type of law where $m = 1$, i.e., indicating that the surface is uniformly bright (Sec. III-A). The polarized or expected component $\bar{P}(t)$ observed at 68 cm is shown in Fig. 14. It can be seen that over the region $80^\circ < \phi < 90^\circ$ the same law is found to hold; namely,

$$\bar{P}(\phi) \propto \cos \phi \qquad\qquad (13)$$

but for $45^\circ < \phi < 80^\circ$ it is found that

$$\bar{P}(\phi) \propto \cos^{3/2} \phi \qquad\qquad (18)$$

This law lies midway between Lommel-Seeliger (13) and Lambert (14). The behavior shown in Fig. 14 has also been found for echoes obtained at a wavelength of 23 cm (Evans and Hagfors, 1965). At wavelengths longer than 68 cm, the behavior of this tail region of the echo has not yet been reported.

At shorter wavelengths, e.g., $\lambda = 3.6$ cm, the measurements are somewhat less reliable due to the difficulties involved (Evans and Pettengill, 1963c) but indicate that for $60^\circ < \phi < 90^\circ$ the Lommel-Seeliger law, Eq. (13) holds. That is, the limb region appears uniformly bright (Fig. 15). The same behavior is inferred at a wavelength of 8.6 mm (see Fig. 11) though the poor resolution of the limb region obtained in these measurements makes it difficult to be certain that this is so.
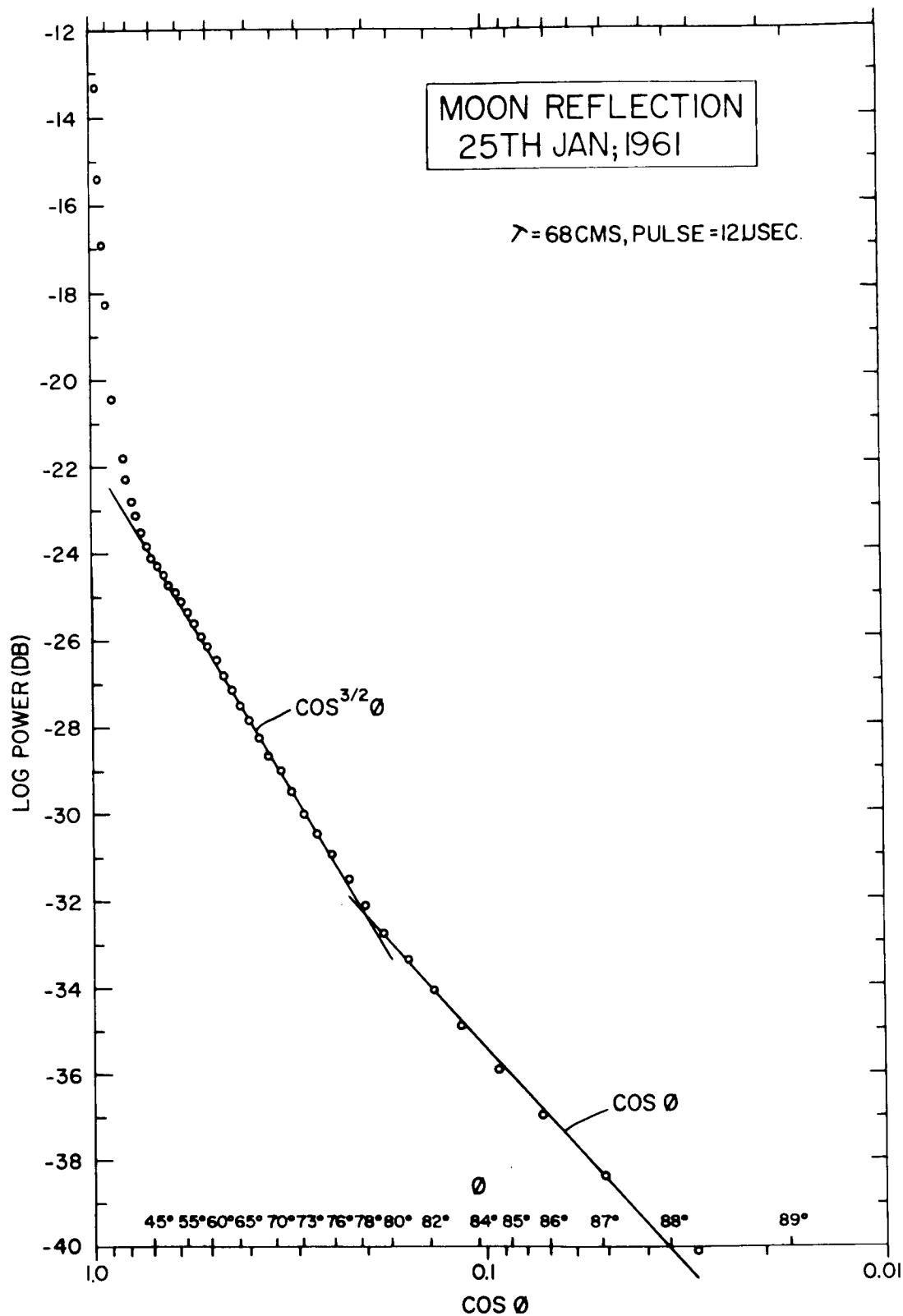
Fig. 14   The average echo power $\overline{P}(\phi)$ plotted as a function of Log cos ϕ for observations at 68 cm wavelength with 12 μsec pulses.
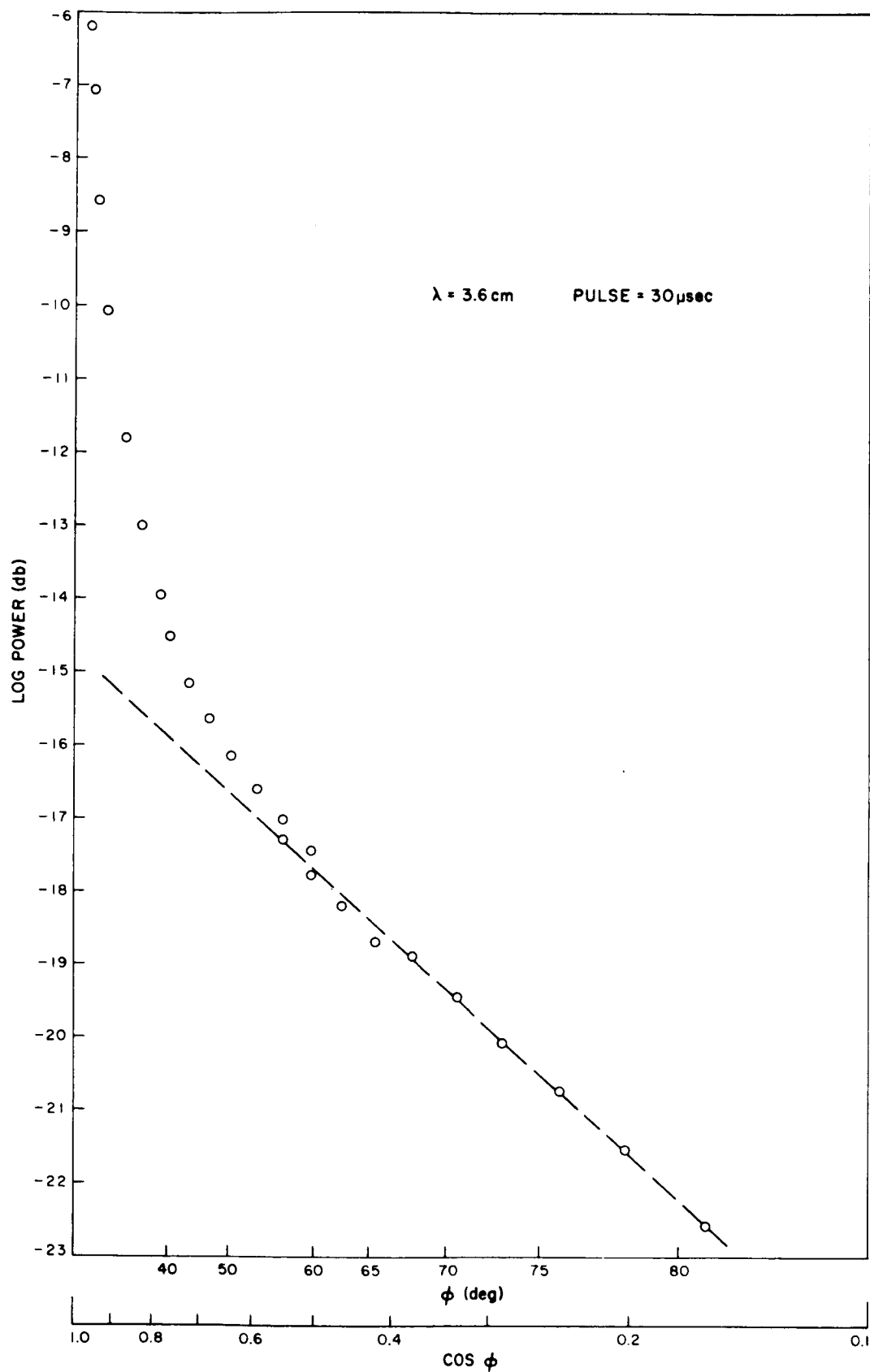
36

Fig. 15   The average power $\overline{P}(\phi)$ plotted as a function of Log cos ϕ for observations at 3.6 cm wavelength with 30 μsec pulses.

The Lambert law might be expected to hold where the surface is covered with irregularities of comparable size to the wavelength. The Lommel-Seeliger law could be expected to hold where the elements of the surface are largely smooth but arranged with a wide range of slopes. Thus near the limbs one sees elements normal to the line-of-sight and these screen from view regions which would not reflect favorably. The $\cos^{3/2} \phi$ dependence observed at 68 cm and 23 cm has not been satisfactorily explained at the present time. Evans and Pettengill (1963c) supposed that it might represent a combination of Lommel-Seeliger and Lambert scattering. They termed this component of the echo power "diffuse" to distinguish it from that observed for $\phi < 45°$ where the angular dependence is steep.

When the diffuse components of the echo power obeying the $\cos^{3/2} \phi$ or $\cos \phi$ laws have been subtracted from the total, the remainder represents the power attributable to the central portions of the lunar surface. The marked dependence of this component upon the angle of incidence and reflection ϕ caused Evans (1957, 1962a), Pettengill (1960), Pettengill and Henry (1962a) to describe it as a "specular" component. This term has given rise to some confusion, and as it was not intended to convey that the moon is perfectly smooth, we shall here use the term "quasi-specular".

The observations of the orthogonal component $\bar{D}(t)$ unfortunately have only been conducted at a wavelength of 68 cm at the present time. They do, however, strengthen the case for treating the polarized return as the superposition of two components, as approximately one third of the "diffuse" echo power is observed when the depolarized component is examined. This seems to support the view that the "diffuse" component is due to scattering from components of the surface structure which are small-scale elements of a whole distribution of structure sizes (Evans and Pettengill, 1963c; Fung and Moore, 1964). It seems probable

that this structure can be identified with the numerous small craters that are found on the surface of the moon and whose number increases rapidly with diminishing size.

The quasi-specular component at 68 cm wavelength was observed by Pettengill and Henry (1962a) to obey a law of the form

$$\bar{P}(\phi) \propto \exp\ (-10.5\ \sin\ \phi) \tag{19}$$

and a similar dependence was obtained by Hughes (1961). However, Evans and Pettengill (1963c) showed that the law observed for the quasi-specular component at 68 cm changes with pulse length as

65 μsec pulses $\qquad \bar{P}(\phi) \propto \exp\ (-10.5\ \sin\ \phi) \qquad 7.5^{\circ} < \phi < 60^{\circ}$ (19)

30 μsec pulses $\qquad \bar{P}(\phi) \propto \exp\ (-12.5\ \sin\ \phi) \qquad 5^{\circ} < \phi < 12^{\circ}$ (20)

12 μsec pulses $\qquad \bar{P}(\phi) \propto \exp\ (-15.3\ \sin\ \phi) \qquad 3^{\circ} < \phi < 9^{\circ}$ (21)

As the pulse is shortened, the exponent increases and the range of angles over which the law holds decreases. Thus, Evans and Pettengill (1963c) concluded that a law of this form had no general validity, and instead proposed a law of the form

$$\bar{P}(\phi) \propto \frac{1}{1 + b\ \phi^2} \tag{22}$$

where b is a constant. However, a recomputation of the power in the quasi-specular component (shown in Fig. 16) indicates that this law also is a poor fit. A good fit to the experimental results can be obtained from a theoretical treatment of the scattering from a rough surface as described in the next section. As yet, no very simple empirical law has been found which by adjusting only one parameter can be made to fit the quasi-specular component at all wavelengths.

39.
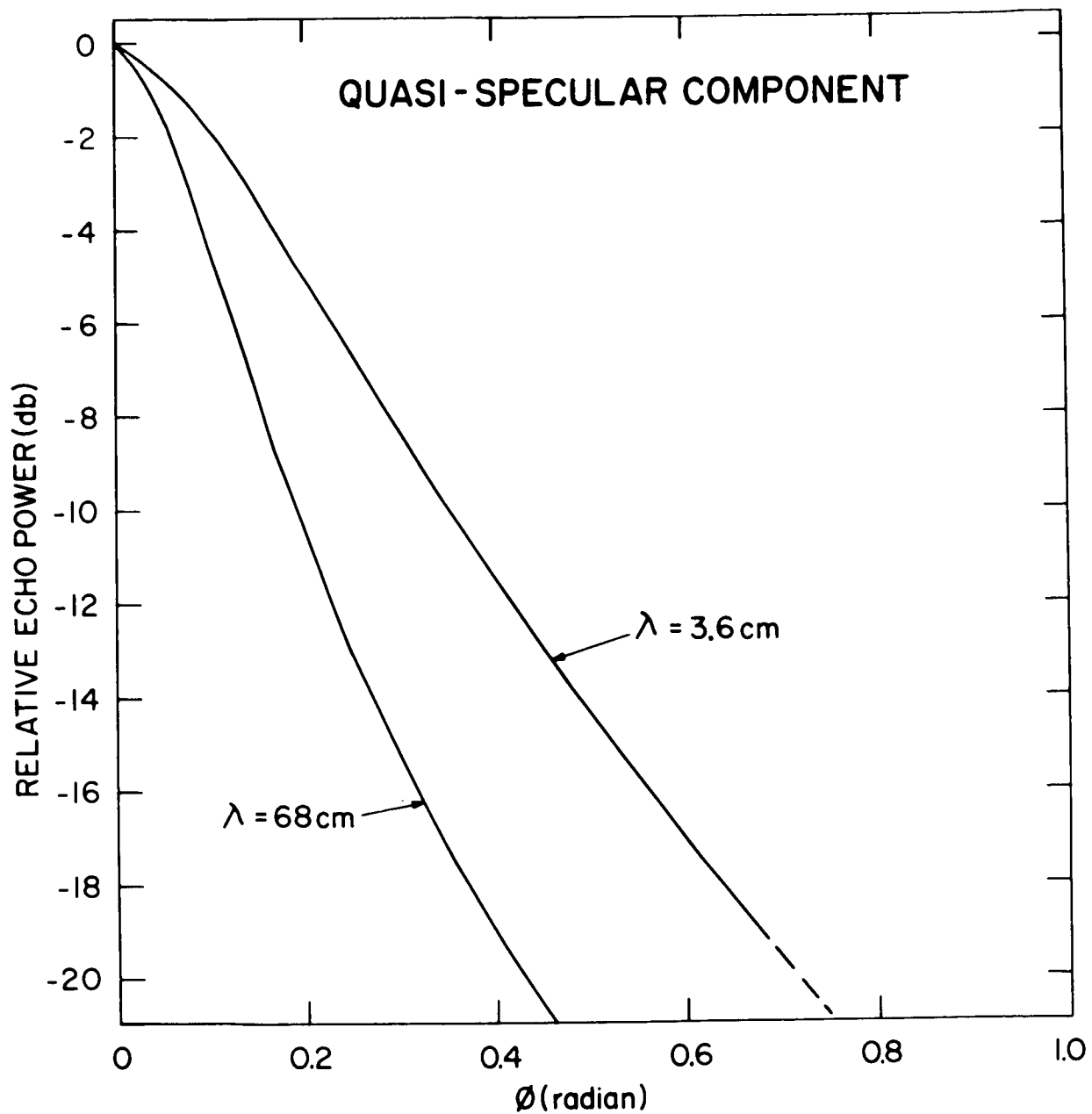
Fig. 16   The quasi-specular component of lunar echoes at 3.6 and 68 cm wavelength. These curves were obtained from the results shown in Figs. 14 and 15 after subtracting the component of power which conforms to the straight lines in those plots. The quasi-specular component is believed to be attributable to the reflections from the large scale smooth undulating parts of the surface.

V. THE SCATTERING BEHAVIOR OF AN IRREGULAR SURFACE

We have seen from the results presented in the two previous sections that the way in which the moon scatters radio waves is distinctly different from the manner in which it reflects light. For wavelengths of 1 meter or longer, the moon appears to be a very limb dark reflector whereas optically it is almost uniformly bright (Markov, 1948). One may conclude, therefore, that on a scale of one meter the moon is much smoother than on a scale of a few microns. The extent to which it is possible to deduce the statistical properties of the lunar surface from these results can only be reviewed briefly here.

The simplest type of theory is one involving geometric optics and has been adopted by a number of authors (Brown, 1960; Muhleman, 1964; Rea et al, 1964). This has the virtue of avoiding a difficulty encountered in the other treatments; namely, that the reflection coefficient will be a function of the angle of incidence and reflection. This difficulty has caused several authors to treat the moon as an irregular <u>perfectly</u> <u>conducting</u> sphere -- which is clearly not the case. In the geometric optics approach only surfaces normal to the line-of-sight scatter back favorably, and their reflection coefficient is simply the Fresnel reflection coefficient for normal incidence ρ_o. This approach can be outlined as follows. We pass a vertical plane through the surface and examine the distribution of the slopes in this plane. If the probability of finding an elemental length dS (measured along the mean surface and not the actual surface) associated with a slope in the range ϕ to $\phi + d\phi$ between the actual surface and the mean is $f(\phi)\, d\phi$ then the angular power spectrum $\overline{P}(\phi)\, d\phi$ is given in

$$\overline{P}(\phi)\, d\phi \propto \frac{f(\phi)\, d\phi\, dS}{\cos \phi} \tag{23}$$

41.

It follows that the distribution of surface slopes $f(\phi)\,d\phi$ and the mean slope $\bar{\phi}$ can be obtained directly from the radar measurements of the angular power spectrum $P(\phi)$ (Sec. VI). One would expect a law of the form (23) to describe only the scattering from the large smooth elements of the surface which give rise to the quasi-specular component of the echo (Fig. 16). This follows because a geometric optics treatment is applicable only to the extent that the surface can be regarded as gently undulating, and makes no allowance for small scale structure (which would cause diffraction) and shadowing effects. It is clear from the wavelength dependence of the scattering (Sec. III) that the moon's surface does have a considerable amount of structure with dimensions comparable to the wavelength, and it follows that this must become increasingly important as $\phi \to 90°$.

Other workers have chosen to treat the surface as being <u>perfectly conducting, smooth</u> and undulating and causing no shadowing. The requirement that the surface be smooth is here intended to mean that it contain no structural components having horizontal and vertical dimensions comparable with the wavelength, since the boundary conditions are established locally by means of Fresnel's reflection formulae. It is next commonly assumed (e.g., Hargreaves, 1959; Daniels, 1961; Hagfors, 1961; and Winter, 1962) that the departure of the true surface from the mean follows a gaussian probability distribution. That is, the chance of finding a given point to be at a height h above the mean surface is proportional to $\exp\left[-\frac{1}{2}(h/h_0)^2\right]$ where h_0 is the rms height variation. Other forms of height distribution (Bramley, 1962) have been used but the theory should not be very sensitive to this function provided $h_0 \gg \lambda$, (Hargreaves, 1959; Daniels, 1961, 1962). This follows because the phase variation in the reflected wave-front will be many times 2π radians when $h_0 \gg \lambda$ and it becomes impossible to determine h_0 from the observations. Having described the vertical behavior of the surface,

42.

it remains only to describe its horizontal structure. This is done by means of an autocorrelation function $\rho(d)$ where

$$\rho(d) = \frac{\overline{h(x)\ h(x+d)}}{(h_o^2)} \tag{24}$$

in which $h(x)$ is the height of the surface at a point x and $h(x+d)$ at a distance d away. The case where $\rho(d)$ is another gaussian function

$$\rho(d) \propto \exp\left[-\frac{1}{2}\left(\frac{d}{d_o}\right)^2\right] \tag{25}$$

in which d_o is the horizontal scale size, has been treated by Hargreaves (1959) and Hagfors (1961). If the surface be considered plane and extending in one direction only, then each point on the surface introduces a phase change in the reflected wave of $(4\pi h/\lambda)\cos\phi$ radians. These phase fluctuations are said to be shallow if the rms phase fluctuation $\Omega = (4\pi h_o/\lambda)\cos\phi$ is less than 1 radian, and in this case the autocorrelation function describing the variation of radio phase with distance d over the surface will be the same as $\rho(d)$. If, on the other hand, $h_o \gg \lambda$, the rms phase fluctuation Ω becomes greater than 1 radian and the correlation distance in the reflected phase front will fall from d_o to d_o/Ω (since 0, 2π, 4π, ... radians are indistinguishable). At a large distance from the surface, the initial phase variations become modified due to the overlapping of many rays and amplitude fluctuations appear. An rms phase fluctuation $\Omega/\sqrt{2}$ is then observed (Bowhill, 1957).

The angular power spectrum $\sigma(\phi)$ is given by the Fourier transform of the autocorrelation function describing the reflected phase front immediately after reflection, and can be written

$$\sigma(\phi) \propto \exp\left[-\frac{1}{2}(\phi/\phi_o)^2\right] \tag{26}$$

43.

where $\phi_o = \lambda/2\pi d_o$ for $h_o \ll \lambda$ and $\phi_o = h_o/d_o$ when $\lambda \ll h_o$. It follows that where the wavelength is much larger than the vertical extent of the height fluctuations, the value of ϕ_o yields directly the horizontal scale of the structure. When $\Omega \geq$ 1 radian ϕ_o yields only the ratio h_o/d_o. Since h_o/d_o is the mean surface gradient, this means that only the rms surface slope can be determined, but not the actual horizontal or vertical scale sizes. If observations could be made as the wavelength was increased eventually (when $\lambda > h_o$) it would be possible to determine d_o. However, in the case of the moon this would require low frequency radio waves which could not propagate through the earth's ionosphere. Daniels (1961, 1962) has discussed at length this limitation in radar observations and shown that one cannot obtain information on the rms height fluctuation when this is many times the wavelength in size. It is also clear that small scale height fluctuations $\leq \lambda/8$ will introduce only small phase changes in the reflected phase front and will be unimportant. Thus radar observations may be regarded as being sensitive to structure in the range $\lambda/8$ to about one hundred or so wavelengths. Only by repeating the observations over a wide range of wavelengths can the true nature of the surface be determined.

Other forms than gaussian for the autocorrelation function $\rho(d)$ have been explored. These include exponential

$$\rho(d) \propto \exp(-d/d') \qquad (27)$$

(Daniels, 1961; Hayre and Moore, 1961; Hughes, 1962a, 1962b) which closely approximates many terrestrial surfaces. Fung and Moore, (1964) and Beckmann, (1964a, 1964b) have employed a sum of such terms.

When allowance is made for the curvature of the moon's surface, and the physically most plausible series of approximations for the terms in the expression for the reflected field (Huygen's integral) are made, the following results are obtained (Hagfors, 1964).

44.

Gaussian $\quad \rho(d) \propto \exp\left[-\frac{1}{2}\left(\frac{d}{d_o}\right)^2\right]$ $\qquad\qquad$ (25)

$$\sigma(\phi) \propto \frac{\exp\left[-\phi^2/2\phi_o^2\right]}{\cos^4 \phi} \qquad\qquad (28)$$

where $\phi_o = h_o/d_o$

Exponential $\quad \rho(d) \propto \exp(-d/d')$ $\qquad\qquad$ (27)

$$\sigma(\phi) \propto \left\{\frac{1}{\cos^4 \phi + C \sin^2 \phi}\right\}^{3/2} \qquad\qquad (29)$$
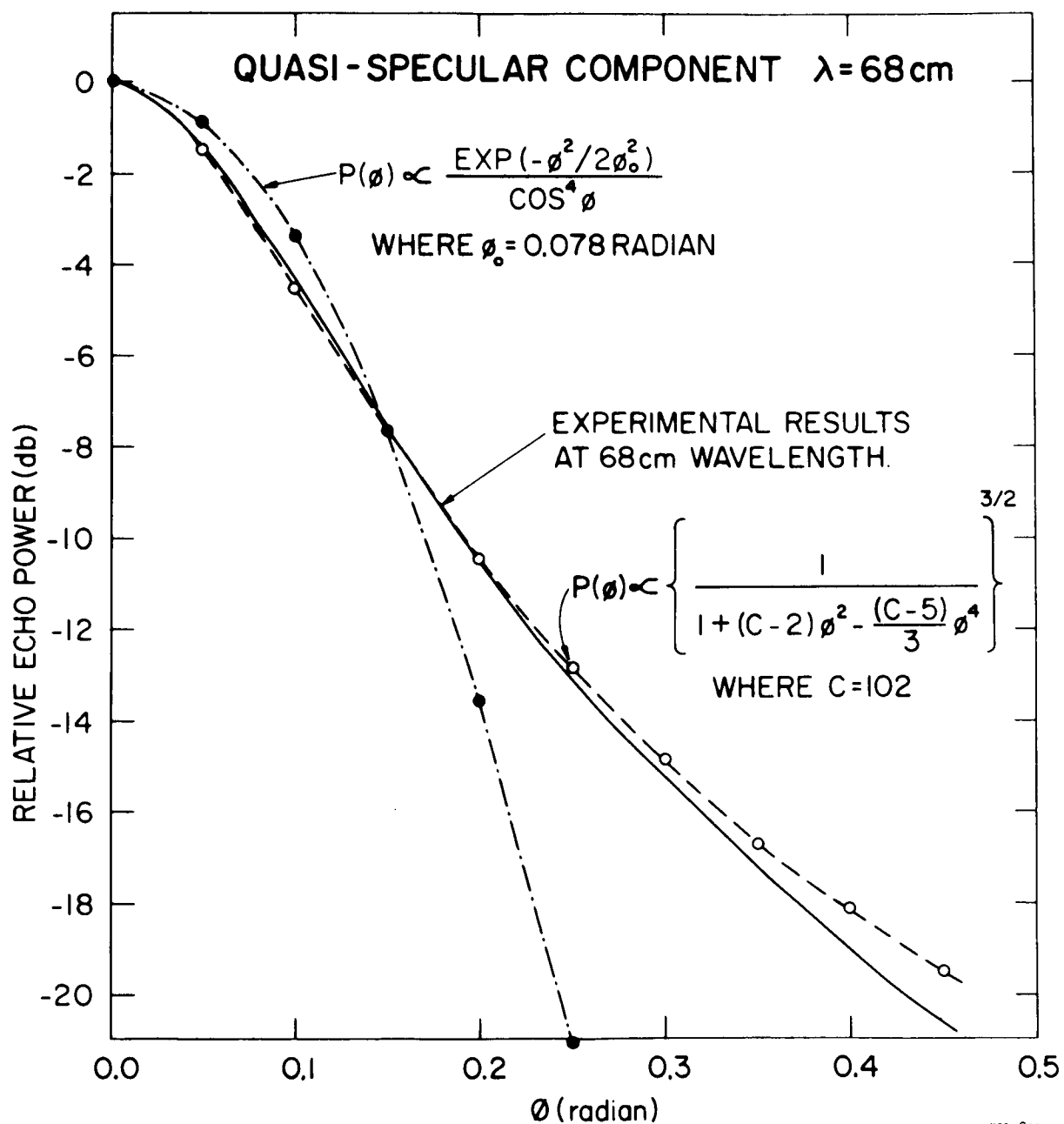
where $C = \left[d'\lambda/4\pi h_o^2\right]^2$

Hagfors (1965) has shown that if the statistics of the surface slopes are made the same, then the geometrics optics approach outlined earlier can be made to yield precisely these same results. Hence, the two approaches are equivalent.

If one re-expresses Eq. (29) for the case where ϕ is small, a simpler expression can be obtained,

$$\sigma(\phi) \propto \left\{\frac{1}{1 + (C-2)\,\phi^2 - \frac{(C-5)}{3}\,\phi^4}\right\}^{3/2} \qquad\qquad (30)$$

The experimental results for the quasi-specular component observed at 68 and 3.6 cm wavelength are compared with the closest fitting curves corresponding to the laws expressed in (28) and (30) in Figs. 17 and 18. At both wavelengths the exponential result (Eq. 30) provides a much better fit to the measurements than the gaussian model for the surface autocorrelation function.

In the exponential model the constant C (Eq. 30) contains the wavelength λ Thus we would expect C to vary as λ^2, yet this does not appear to occur. We must

QUASI-SPECULAR COMPONENT $\lambda = 68\,cm$

$$P(\phi) \propto \frac{EXP(-\phi^2/2\phi_0^2)}{COS^4\phi}$$

WHERE $\phi_0 = 0.078$ RADIAN

EXPERIMENTAL RESULTS AT 68cm WAVELENGTH.

$$P(\phi) \propto \left\{ \frac{1}{1+(C-2)\phi^2 - \frac{(C-5)}{3}\phi^4} \right\}^{3/2}$$

WHERE $C = 102$

RELATIVE ECHO POWER (db)

ϕ (radian)

C31-821

Fig. 17   The values obtained for the echo intensity at 68 cm using 12 μsec pulses (after the cos ϕ and cos$^{3/2}$ ϕ components shown in Fig. 14 have been removed) compared with the theoretical laws for the angular dependence of the reflected power.

46
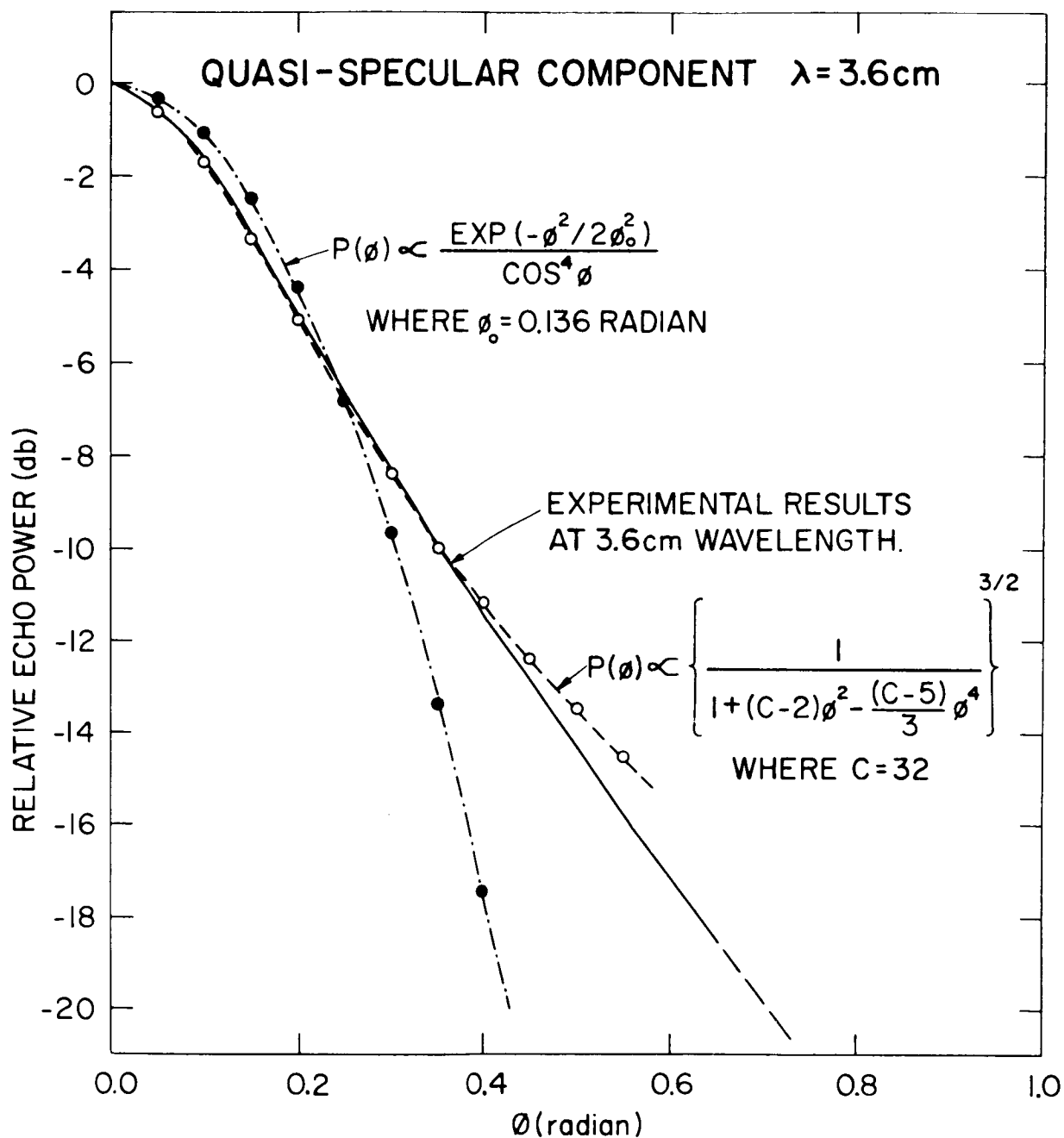
Fig. 18   The values obtained for the echo intensity at 3.6 cm (after the cos ϕ component shown in Fig. 15 has been removed) compared with the best fitting curves for the theoretical laws predicted for a surface having a lateral correlation of surface heights that is a Gaussian or exponential.

conclude that though the model employing the exponential autocorrelation function to describe surface roughness appears to provide a better fit at both wavelengths, it is not characterized by the same value of d'. Presumably the change in wavelength makes the reflection properties of the surface dependent on a different range of structure sizes. Some authors (Muhleman, 1964; Fung and Moore, 1964; and Beckmann, 1964a, 1964b) have not distinguished between the diffuse and quasi-specular scattering, and have attempted to fit their theoretical results to the whole curve for $\overline{P}(\phi)$. In some cases they have been surprisingly successful and have argued that this demonstrates that the distinction between the two regimes is artificial. Unfortunately, each author has commenced by assuming that the surface is locally smooth and no theory has properly attempted to account for small scale structure, diffraction, and shadowing effects. These must be important as $\phi \rightarrow 90^{\circ}$ and it seems a doubtful procedure to conclude that the theory is adequate, simply because it can be made to match the results by emprically adjusting two or more constants.

At the present time, experimental approaches are being employed in some laboratories to gain a better knowledge of the relation between the statistical properties of a surface and its scattering behavior. In this work a surface is modeled (usually in sand) over a large area of floor space and the scattering properties explored at mm wavelengths.

On a somewhat larger scale observations of the scattering behavior of the earth's surface conducted using airborne radar equipment can assist in interpreting the lunar echoes. We note that these airborne studies indicate that marked "quasi-specular" behavior is encountered only over deserts or moderately calm sea (Grant and Yaplee, 1957; Edison et al, 1959).

48.

VI. SURFACE SLOPES

From the 68 cm results presented in Section III, different workers have derived values for the average surface slope in the range 5° and 15°. In part this wide scatter of values reflects differing interpretations of the results. For example, Muhleman (1964) has averaged over the whole $\bar{P}(\phi)$ curve whereas Evans and Pettengill (1963c), Rea et al (1964), and Daniels (1963b) have attempted to subtract out the diffuse component of the echo power before computing the slope. Differences also have arisen because most authors weight the values for the slope by the amount of area projected on to the mean surface associated with that slope; yet others, e.g., Rea et al (1964) weight by the actual amount of area at each slope. The first method is in effect a value for the slope that would be deduced by repeatedly dropping down on to the moon, and the second after walking over the surface and measuring the slopes.

Table III lists some of the values for the rms or average slope of the lunar surface that have appeared in the literature. They refer to measurements made in the wavelength range 3 m to 10 cm and hence are roughly comparable. It seems that with the possible exception of the results published by Rea et al (1964), none of the values in Table III are close to the value that would be encountered by a landing vehicle. This follows because most authors have computed the average of the slopes encountered when passing a vertical plane through the surface. Thus, in the geometric optics approach, the mean slope $\bar{\phi}$ has been taken as

$$
\bar{\phi} = \frac{\int_\phi \phi f(\phi)\, d\phi}{\int_\phi f(\phi)\, d\phi} = \frac{\int_\phi \phi\, \bar{P}(\phi) \cos\phi\, d\phi}{\int_\phi \bar{P}(\phi) \cos\phi\, d\phi}
\tag{31}
$$

which follows directly from Eq. (23). However, the slope encountered in any plane cut through the surface is not necessarily the steepest gradient for that facet,

TABLE III

Values for the rms or average slope of the undulating part of the lunar surface derived by different authors from radar reflection measurements in the wavelength range 3 m to 10 cm.

Author	Meter Wave Values for the Average Slope	Wavelength	Comments
Hargreaves (1959)	6°	2.5 m	rms value obtained by "Gaussian" fit to data published by Evans (1957).
Hagfors (1961)	4°	3 m	rms value obtained by "Gaussian" fit to the data published by Evans et al (1959).
	3°	68 cm	rms value obtained by "Gaussian" fit to the data published by Hey and Hughes (1959).
Daniels (1961)	$8\text{-}12^{\circ}$	68 cm	average value obtained by "Exponential" fit to data published by Pettengill (1960).
Daniels (1963a)	14°	70 cm	average value obtained by "Exponential fit to data privately communicated by J. V. Evans.
Daniels (1963b)	6.5°	70 cm	average value after correcting results of Daniels (1963a) for the diffuse component.
Hey and Hughes (1959)	3°	10 cm	rms value obtained by "Gaussian" fit to own data.
Evans and Pettengill (1963c)	4.5°	68 cm	rms value obtained by "Gaussian" fit to own data.
	5°	68 cm	average value obtained by "Exponential" fit to own data.
Muhleman (1964)	8°	68 cm	rms value obtained by "Gaussian" fit to results of Pettengill (1960). Includes diffuse component.
	7°	68 cm	average value obtained by "Exponential" fit to results of Pettengill (1960).
Rea et al (1964)	11°	68 cm	average value obtained for results of Evans and Pettengill (1963c) when diffuse power subtracted.*
	15°	68 cm	rms value obtained for results of Evans and Pettengill (1963c) when diffuse power subtracted.*

*Here the slope has been defined somewhat differently -- see the text.

and to obtain the true mean slope encountered by a landing vehicle, one must pass the vertical plane through the surface at all possible azimuth angles. That is, the most meaningful value for $\bar{\phi}$ is given in

$$\bar{\phi} = \frac{\int_{\phi} \phi f(\phi) \sin\phi \, d\phi}{\int_{\phi} f(\phi) \sin\phi \, d\phi} = \frac{\int_{\phi} \phi \, \bar{P}(\phi) \cos\phi \sin\phi \, d\phi}{\int_{\phi} \bar{P}(\phi) \cos\phi \sin\phi \, d\phi} \tag{32}$$

As stated earlier, it is our view that the function $\bar{P}(\phi)$ employed in Eq. (23) should not be the whole curve but one corrected for the presence of the diffuse component (e.g., the curves shown in Fig. 16).

Essentially the same difficulty in defining what is meant by the mean slope has arisen when an autocorrelation function has been used to describe the surface. Thus in the Gaussian case the ratio h_o/d_o is the rms slope only when the distribution is examined in a single vertical plane, and when all such planes are averaged, the rms slope is found to be $\sqrt{2}h_o/d_o$ (Hagfors, 1965). In the case of the exponential autocorrelation function, the relation between the constant C which appears in Eq. (30) and the mean slope has been shown by Hagfors (1965) to be

$$\overline{\tan \phi} \approx \frac{1}{2\sqrt{C}} \cdot \frac{C-4}{C-\sqrt{C}-2} \cdot \log_e 4 \, C \tag{33}$$

Eq. (33) holds only for large values of C (>100) and Hagfors (1965) concurs with the view of Rea et al (1964) that to characterize the slopes by a single number is almost certainly misleading. The most meaningful statement is a curve of $\bar{P}(\phi) \cos\phi$ which may be taken as the probability distribution encountered in a single plane. The results for $\bar{P}(\phi)$ shown in Fig. 16 have been employed in Eq. (32) to yield values for the mean slope $\bar{\phi}$ by numerical integration. The results are

at λ = 68 cm $\bar{\phi}$ = 10.2° and $\bar{\phi}$ = 14.3° at λ = 3.6 cm. These values are probably

overestimates since the behavior of $\bar{P}(\phi)$ for $\phi < 2.5°$ has not properly been

explored due to the finite width of the pulse. The mean slope is evidently a

function of wavelength, and this reflects the fact that each wavelength acts as

a filter and is sensitive only to a given range of structure sizes. It seems

probable that the slope obtained by the procedure outlined here will be determined

principally by elements of the surface of the order of 10 λ across. Thus the

average slope observed at 68 cm (10.2°) seems the appropriate value to employ,

for example, for the design of a lunar landing craft.

VII. COHERENT PULSE RADAR OBSERVATIONS

When a radar system is so designed that the transmitter and receiver frequencies are determined by very stable oscillators (preferably the same one), it becomes possible to derive spectral information from the phase of the signal. This is achieved by replacing the normal rectifier at the output of the receiver by two phase detectors which mix the incoming signals at a radial frequency near ω radians/sec with sin ωt and cos ωt, respectively. The outputs of these two detectors are the sine and cosine components of the signal.

For CW radar observations, the amplitude of the sine and cosine components of the signal can be determined at intervals by means of two sampling voltmeters. The sampling may be thought of as resembling the lines ruled on a spectrum grating. The longer the train of samples (number of lines), the greater will be the resolution obtained. Thus, if samples are taken over a period of 10 seconds, a spectral resolution of 1/10 cps can be achieved. The spacing of the samples $(1/f_s)$ determines the spacing of the "orders" in the spectrum. Thus, if no orders are to overlap, it is required that $f_s \geq f_{max}$ where f_{max} is the frequency difference between the lowest and highest frequency components in the signal. The power spectrum $\overline{P}(f)$ in Fig. 5 shows the doppler broadening of radar signals at 440 Mc/s determined by this technique.

For pulse observations it becomes possible to obtain simultaneously range and frequency resolution by phase coherent observations. This technique was first exploited by Pettengill (1960) and Pettengill and Henry (1962b). When pulse observations are made, the sample frequency f_s automatically becomes the same as the pulse repetition frequency. Thus the pulse repetition frequency must be made higher than the spectral width of the signals. As the radar wave frequency is increased, this eventually will lead to a situation where the interpulse period T

53

becomes shorter than the radar depth of the target. In the case of the moon, the interpulse period T must be greater than 11.6 milliseconds. The doppler width of the spectrum for a wave frequency of 100 Mc/s is rarely larger than 2 cps so that difficulties are not usually encountered at frequencies of less than 5,000 Mc/s, provided that the gross doppler shift is properly compensated.

Figure 4 shows that when doppler and range resolution are combined, it is possible to isolate localized regions of the lunar surface. If the antenna beam-width is large with respect to the moon, there will always be two such regions for given range and doppler coordinates (except along the apparent equator). In the earliest work reported by Pettengill (1960) a doppler resolution of 1/10th of a cycle was achieved from observations lasting 10 seconds, and as such, each cell in the range doppler grid was effectively sampled only once. That is, the rms scatter in intensity was equal to the mean. By repeating the observations and superimposing 20 images, Pettengill and Henry (1962b) were able to reduce the rms fluctuation (to a factor of 2/9 the mean power). These workers also made measurements on the orthogonal component of the signal D(T), (Fig. 12) where the dynamic range encountered is much less. During the course of one afternoon's observations, Pettengill and Henry (1962b) observed a strong echo in both the expected and orthogonal component of the signals at a delay of about 2.85 m.secs (Fig. 19) which had an intensity of about 7-8 times the mean at that range. They were able to resolve the ambiguity in the position of this scatterer by observing its change in doppler frequency with respect to the center with time (as a consequence of the projection of the moon's axis of libration changing with time). The discrete scatterer proved to be the crater Tycho.

In many respects Tycho is well placed to be detected in observations such as these. It is at a range where the "quasi-specular" component contributes little to the echo, and is not near the edge of the spectrum where the resolution becomes
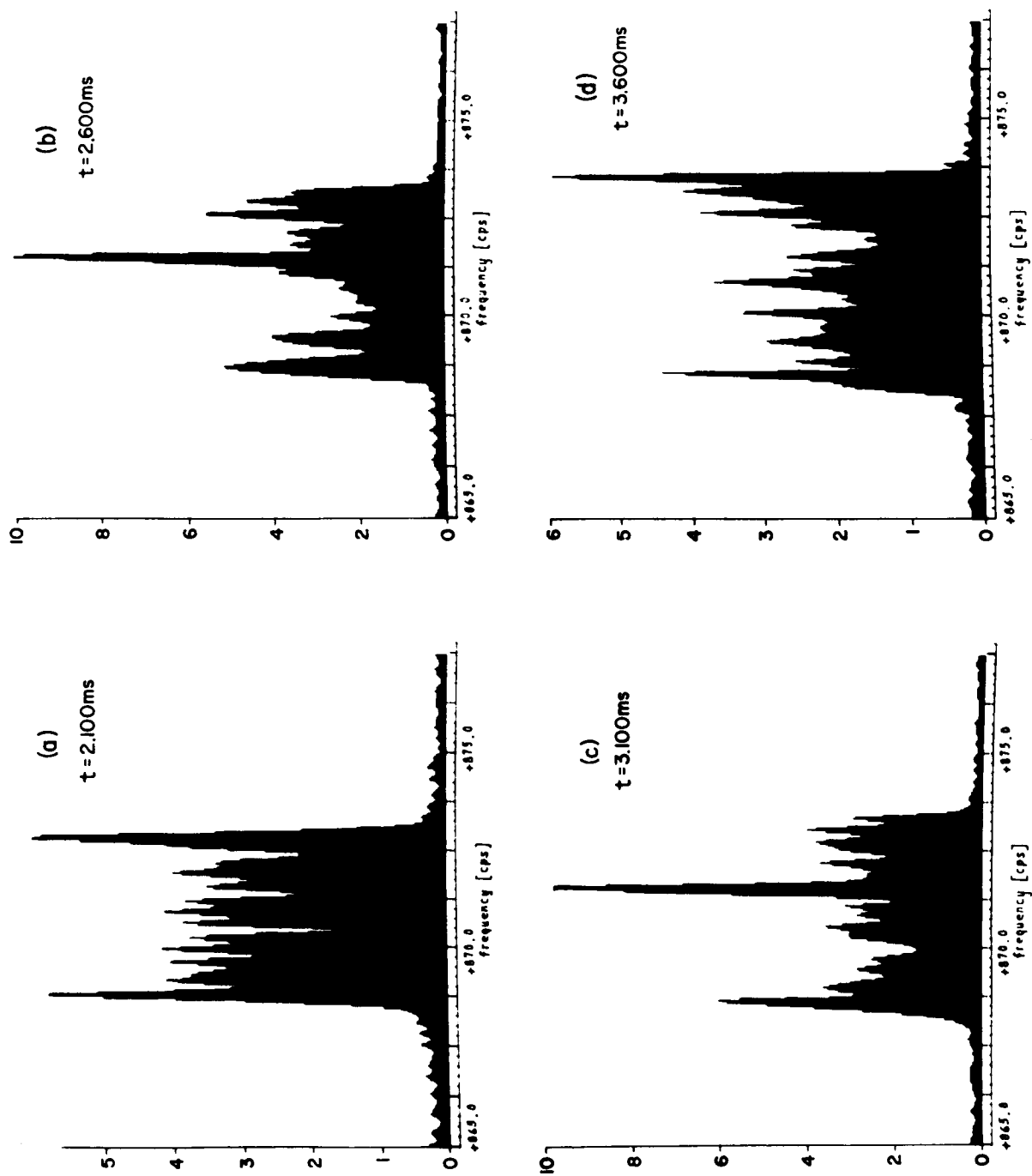
Fig. 19 Lunar echo power spectra at 4 intervals of range, taken 19 h 00 m 19 s UT, June 20, 1961. The central peaks in (b) and (c) correspond to the position of the crater Tycho. Peaks at the extremes of the spectra result from the large common area of the intersecting range and doppler contours (Fig. 4) and probably do not represent individual surface features.

55

poor due to the increased area in each cell (Fig. 19). If Tycho were nearer the center of the moon, it is doubtful if the range resolution afforded by the 0.5 m.sec pulses employed by Pettengill and Henry (1962a) would have been adequate to resolve it. These considerations partly account for why only Tycho was identified as an anomalous scatterer in this early work.

In view of the fact that the cells in Pettengill and Henry's "map" were of comparable size to the area occupied by Tycho, it is probable that the crater is actually about ten times a better reflector than an equal area in its environs. This remarkable result is made all the more remarkable by the fact that it is equally bright with respect to its surroundings for the polarized and depolarized signals. This latter observation precludes any explanation based upon large flat facets normal to the line-of-sight in the vicinity of Tycho, since these would not be expected to depolarize.

If the surface material in the vicinity of Tycho were solid rock, exposed perhaps because there have been no subsequent impacts which could have covered it with rubble, or because any natural erosion processes have not been operating for a comparable length of time as elsewhere on the surface, then part of the anomaly can be accounted for by the increased reflection coefficient. It also seems reasonable to believe that the extreme roughness associated with fracturing (brecciation) caused by the original meteoric impact is still preserved and visible to the radar. (A thin layer of material overlying the rock could account for the optical behavior without influencing the radar scattering). Thus the enhanced reflectivity may be explained as a combination of denser and rougher material in and around the crater as compared to the older unperturbed surroundings. Since only ~ 8% of the surface is thought to be rough (Sec. VII) at this frequency, a ten-fold increase in reflectivity can just be obtained by assuming a localized

56

region which is nearly a perfect Lambert scatterer. If, in addition, it is assumed that the surface reflection coefficient is higher (due to the increased density), then proportionally less roughness need be involved.

Shorthill et al (1962) have observed that virtually all the rayed craters have anomalous thermal properties at infrared. During eclipses or the waning cycle of the moon, they cool less rapidly than their surroundings. The reverse is true during the waxing phase. This behavior can be attributed to the absence in these recent craters of an appreciable dust layer which overlies most of the remainder of the surface. The extent to which this effect is observed seems to bear a direct relation with the estimated age of the craters concerned (Tycho being the most conspicuous example). It is tempting to suppose that these same craters are also anomalous radar reflectors. Work presently underway to test this hypothesis, at the Arecibo Ionospheric Observatory, has shown that most of the rayed craters are indeed anomalously bright scatterers (Pettengill, privately communicated). In this work unambiguous maps of regions of the lunar surface are obtained by using a pencil beam which discriminates against one of the pair of cells having the same range and doppler coordinates.

The extraordinary reflectivity of these objects compared to their surroundings supports the view advanced earlier that most of the surface must be relatively smooth and covered to a very considerable depth (perhaps meters) with material that is broken and porous and no more dense than sand.

Combined coherent pulse and polarization experiments have recently been undertaken by T. Hagfors (privately communicated). Hagfors was struck by the extreme smoothness of the lunar surface as observed in the Mariner photographs. Whilst a gently undulating and largely smooth surface has been predicted from the radar observations alone, we have also seen that a small fraction of the surface is required to be covered with objects having radii of curvature comparable to the wavelength. Few such objects can be found lying on the regions of surface observed by the three Mariner spacecraft. Hagfors suggested therefore that these objects lie beneath the surface, and hence the diffuse tail of the echoes (i.e., for delays t $\geqslant$ 3 m. sec) arises from reflections that have penetrated an upper surface layer. If this were the case and the layer depth is irregular but everywhere greater than the wavelength one would expect the echo intensity to depend upon the angle between the incident electric field and the normal to the surface, i.e., one might expect Brewster angle effects. That is the component of the incident electric field that lies closest to the Brewster angle will couple into the surface best, and hence will be stronger than any other. In order to test this hypothesis Hagfors made observations using the 23 cm wavelength Millstone Hill radar. The whole moon was illuminated with a circularly polarized wave. This may be thought of as two orthogonal linearly polarized waves spaced $\lambda/4$ apart. The two orthogonal circularly polarized components obtained on reception were combined in such a way that two orthogonal linear components were recovered. This was accomplished using two hybrid couplers and two variable length sections of transmission line. The orientation of these two orthogonal linear components could be controlled at will and this was

58

continuously adjusted to align one with the projection of the moon's libration axis into the plane of the antenna (computed in advance). We now have a situation in which the radar is tracking the moon (in azimuth and elevation), adjustments are continuously being made to the receiver to compensate for the gross doppler shift of the echo (to an accuracy of better than 0.1 cps) and the sampling of the signals is accomplished in such a manner that the continuously changing position of the echo on the timebase is also compensated. In addition adjustments are made at short intervals to maintain one of the linear modes recovered at the receiver aligned with the libration axis. Finally a large computer is employed for spectral analysis of the returns. In practice two separate receivers were employed to amplify the two linear components, and the two sine and two cosine signals that resulted were sampled simultaneously every 160 μsec. Pulses of 200 μsec length were transmitted. Spectra were obtained by processing over a range of $\pm$ 16' cps with a resolution of 2 cps for both linear components at several delays with respect to the leading edge of the echoes. The two spectra obtained at each delay were normalized to include the same area in order to remove any differences in the receiver gains, or non-circularity of the incident wave. This is justified since the circular symmetry of the illuminated annulus makes it almost certain that the total power reflected at a given delay should be independent of the incident polarization.

The component of the signal aligned with the libration axis (component A) will be incident on the surface closer to the Brewster angle at the center of the spectrum (i.e., near zero relative doppler shift) than the orthogonal component (B). Thus at the center we might expect A > B if the hypothesis

of an irregular layer deeper than the wavelength is in fact correct. On the other hand at the wings of the spectrum the reverse should be true, i.e., B > A. This behavior is indeed observed as may be seen in Fig. 20. The extreme frequencies are marked L and points at 0.707 times this value (which ought to appear equally strong) are marked C. As can be seen in Fig. 20 the echo curves do cross at the points marked C. A total of 25 minutes data has been analyzed and included in Fig. 20, so that the statistical uncertainty is only $\pm$ 2%, i.e., much less than the systematic effects due to the different polarizations.

One interesting feature in Fig. 20 is the sharp peak at 4.48 msec range plot at a frequency offset of +4 cps. Here the intensity of the two components is nearly equal indicating the absence of any layer (compare the ratio at -4 cps at the same range). At the time of observation the predicted range-doppler coordinates of Tycho were 4.30 msec and + 2 cps, and thus it seems plausible to ascribe the anomalous peak to the Tycho region. Apparently Tycho is not covered by a deep layer of light material, though one much thinner than the wavelength (23 cm) might go undetected.

FREQUENCY SPECTRA, MOON, 18 JUN.1965
0340 - 0435 EST

λ = 23 cm, PULSE LENGTH 200μsec, FREQ. BOX 2 cps

L = MAXIMUM FREQUENCY, C = CROSSOVER POINT

—X— E-FIELD ALIGNED WITH LIBRATION AXIS
—O— E-FIELD NORMAL TO LIBRATION AXIS

θ = 35° ± .8°
RANGE = 2.08 ms

θ = 52° ± .7°
RANGE = 4.48 ms

θ = 66° ± .5°
RANGE = 6.88 ms

θ = 77.5° ± .5°
RANGE = 9.28 ms

DOPPLER FREQUENCY, cps
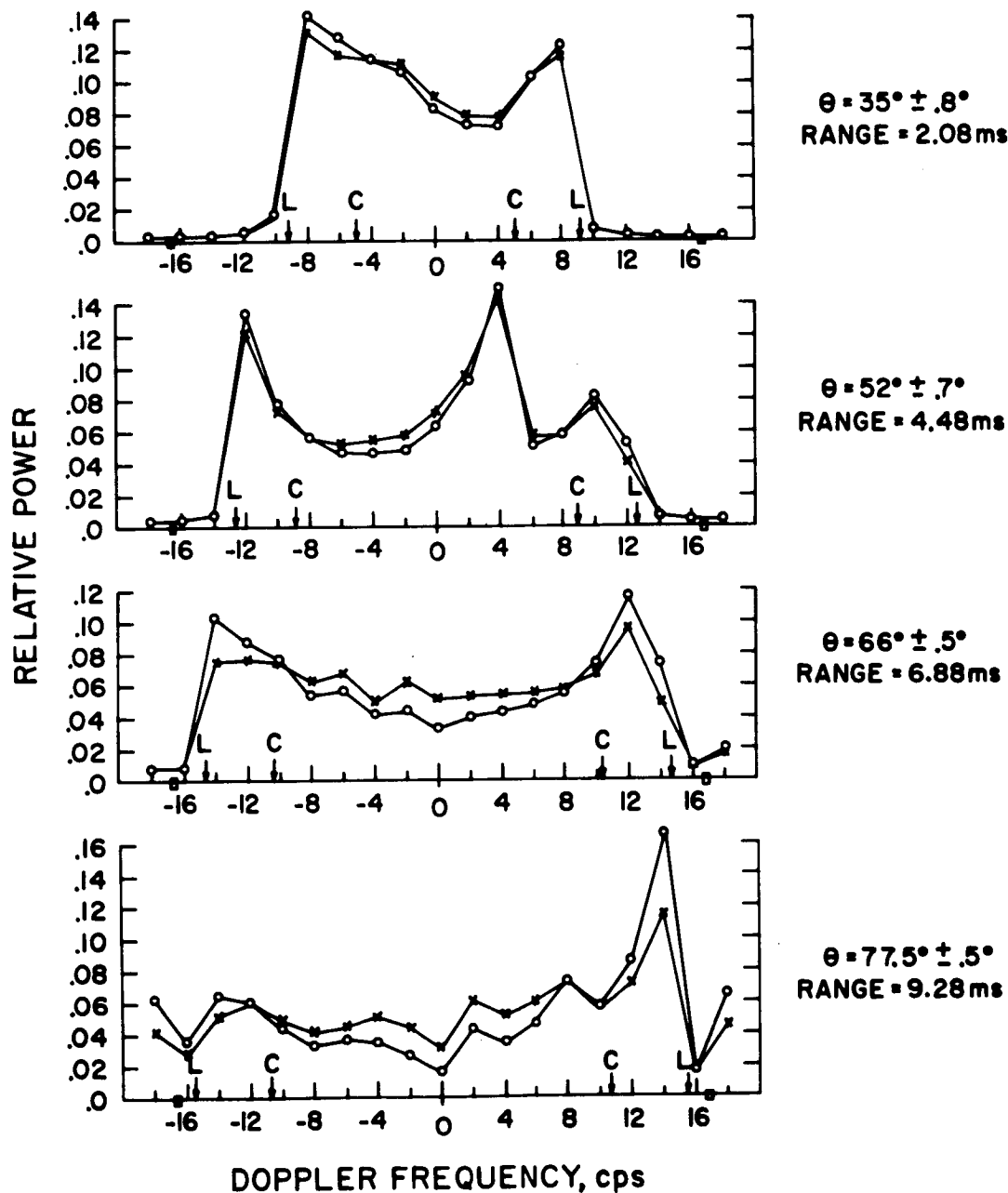
Fig. 20   Spectra obtained at four ranges during the course of the polarization experiments conducted by T. Hagfors which are described in the text. The dependence of the echo intensity on the orientation of the incident electric field provides evidence for reflections from within the upper layer of the lunar surface.

61

VIII. THE DIELECTRIC CONSTANT k

In Section II we introduced two generalized radar equations for an irregular sphere,

$$\sigma = g \rho_0 \pi a^2 \tag{8}$$

and

$$\sigma = G_m \bar{\rho} \pi a^2 \tag{10}$$

We have seen from the foregoing results that the moon appears to scatter in part as a smooth undulating sphere and in part as a collection of small scale, almost isotropic, scatterers. At 68 cm wavelength the ratio of the powers due to these two parts is 4:1. In attempting to derive a value for the dielectric constant k, Evans and Pettengill (1963c) supposed that a fraction X of the actual surface area could be associated with the diffuse component, and further that these scatterers obeyed the Lambert Law (Eq. 14) for which the gain $G_m = 8/3$ (Grieg et al, 1948). The remainder of the surface they took to be smooth and undulating and assumed it to have a directivity factor $g \rightarrow 1.0$. Hagfors (1964) has since shown that $g = 1 + \alpha^2$ for the smooth part of the surface where $\alpha = h_0/d_0$ for a gaussian surface (Eq. 25) and hence is related to the rms slope (Sec. VI). Since $\alpha \sim 0.1$ at $\lambda = 68$ cm, it follows that $g \rightarrow 1.0$ and the assumption $g = 1.0$ made by Evans and Pettengill (1963c) is not a bad one. The total cross section σ was thus obtained as the sum of two parts, the smoother being obtained from Eq. (8) and the rough from Eq. (10).

$$\sigma = \left[(1 - X) \rho_0 + \frac{8}{3} X \bar{\rho} \right] \pi a^2 \tag{34}$$

With no real justification, Evans and Pettengill (1963c) equated $\bar{\rho}$ to ρ_0, since otherwise Eq. (34) cannot be solved. The error introduced into the value for the dielectric constant k is likely to be small because the second term in Eq. (34)

has a value of only 1/4 of the first. However, the value for X (which is found to be 8%) might be somewhat in error. At all events the cross section was then written

$$\sigma = \left[(1 - X) + \frac{8}{3} X \right] \rho_o \pi a^2 = .074 \pi a^2 \tag{35}$$

From this ρ_o was found to be .065, and this lead to a dielectric constant k = 2.79. Evans and Hagfors (1964) applied these arguments to the observations conducted at 3.6 cm and 8.6 mm to obtain the results shown in Table IV.

We have remarked that provided the amount of power in the diffuse component remains small, this series of approximations probably does not introduce serious error in the value for k, although the percentage area of the surface X that is rough may be in error. When the largest part of the power appears in the diffuse component (e.g., at 0.86 cm) it is doubtful that Eq. (35) has much validity. Hence, little significance should be attached to the apparent wavelength dependence in k shown in Table IV. If the wavelength dependence could be shown to be real, it might result either as a consequence of a finite conductivity $\underline{s}$ in the medium (Eq. 6), or the surface may be inhomogeneous and have density variations with depth.

A somewhat more rigorous approach to the problem of dealing with the smooth and rough portions of the surface has been published by Rea et al (1964). In this approach the moon is assumed to be covered with equal sized flat facets having a distribution of slopes $f(\phi)$. The cross section can then be computed and the directivity g is found to be simply the ratio of the actual area to the projected area (i.e., $2\pi \int_o^{\pi/2} f(\phi) \sin \phi \, d\phi$). In order to obtain $f(\phi)$, Rea et al (1964) subtracted from the observed echo power function $\bar{P}(\phi)$ the power in the orthogonal component $\bar{D}(\phi)$. In this way they sought to remove the influence of the small scale roughness in determining $f(\phi)$. Since it is not clear what

TABLE IV

Values for the reflection coefficient at normal incidence ρ_0 and dielectric constant k deduced by Evans and Hagfors (1964)

	Power in the Diffuse Component	X	ρ_0	k
68 cm	20%	8%	.065	2.79
3.6 cm	30%	14%	.060	2.72
0.86 cm	85%	68%	.035	2.13

fraction of the incident energy one might expect to appear in the depolarized component, several possibilities were tried, namely:

Case 1 $\qquad$ $f(\phi) \propto \overline{P}(\phi)$

Case 2 $\qquad$ $f(\phi) \propto \overline{P}(\phi) - \overline{D}(\phi)$

Case 3 $\qquad$ $f(\phi) \propto \overline{P}(\phi) - 2\overline{D}(\phi)$

Case 4 $\qquad$ $f(\phi) \propto \overline{P}(\phi) - 3\overline{D}(\phi)$

If we assume that at the limb only small scale elements contribute to the scattering, then we might expect Case 4 to be closest the truth. This follows from the results of Sec. III which showed that the ratio of $\overline{P}(\phi)$ to $\overline{D}(\phi)$ at the limb is approximately 3:1. Rea et al (1964) concluded that the actual case lay between 3 and 4 by a similar process of reasoning. The fraction of the total power remaining for Case 4 was found to be 0.85, and the directivity factor g determined by graphical integration was 1.11. By assuming a total cross-section ... coefficient ... was found to be .057 leading to a dielectric constant k = 2.6.

In view of the recent experiments carried out by Hagfors and described in the previous section it is evident that any value for the dielectric constant derived from the strength of the echo power near normal incidence must represent some composite average, since reflections apparently come both from the top of and within the surface.

In order to test the hypothesis of a penetration mechanism through a tenuous top layer on the lunar surface somewhat further, Hagfors has obtained the ratio of the power in the two orthogonal linearly polarized components as a function of the angle of incidence on the mean lunar surface. This information was most

readily derived from the spectra shown in Fig. 20 near zero frequency. The

same information could, in principle, be derived from the maximum frequency

regions also, but in these latter regions the angles between the planes of

polarization and the plane of incidence changes much more rapidly with changes

in frequency offset than they do near zero frequency, and for this reason the

ratios were only computed on the basis of information derived from the power

spectra near zero frequency offset.

It was next assumed that for all the delays examined and plotted in Fig. 20,

the echo is wholly the result of reflections from within the surface. This

assumption is reasonable in view of the large angles of incidence to which

these delays correspond. It seems that it would be extremely unlikely to

encounter flat regions of the surface normal to the incident wave. The

possibility of small scale structure lying on the surface and contributing to

the echo remains, however. The Mariner pictures indicate that few elements of

the surface have radii of curvature comparable to 23 cm, but this cannot be

regarded as an absolute guide. A second assumption was next made, namely

that the scattering mechanism within the surface converts little of the incident

power into an orthogonal mode. This too seems reasonable on the basis of the

results presented in Sec. IIIc which showed that circularly polarized waves

are returned in the expected sense more strongly than the depolarized sense

even in the diffuse part of the echo. A third and final assumption was that

the reflection process inside the layer is independent of the polarization angle.

This will be true if the signals are backscattered from an irregular layer. The

relative strength of the two components then depends only upon the square of

their respective transmission coefficients (since the wave passes through the

66

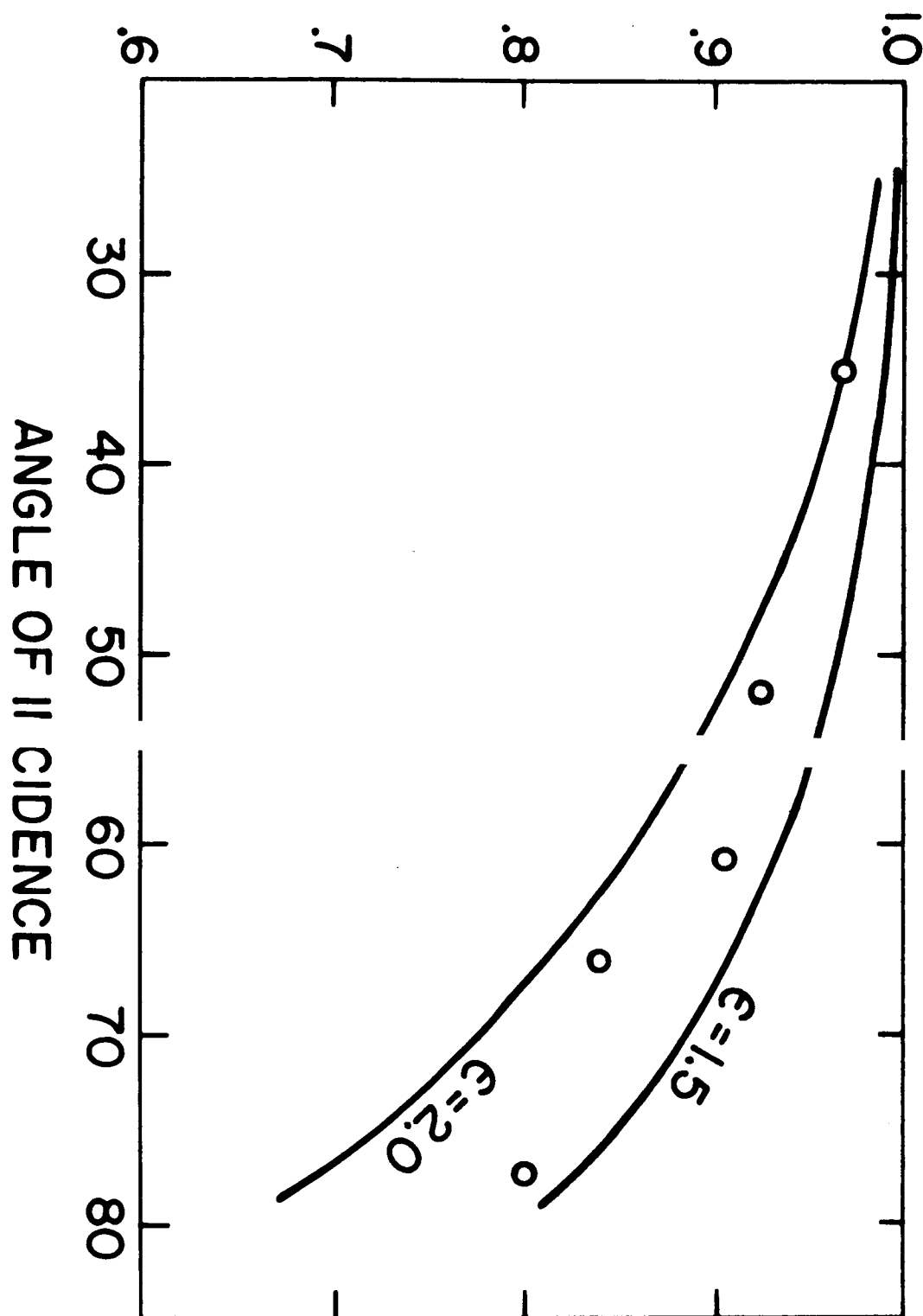# RATIO OF TRANSMISSION COEFFICIENTS

Fig. 21   The ratio of the square root of the echo powers observed for the two linear components whose spectra are plotted in Fig. 20. If all the power is scattered from within the surface at large angles of delay, and further if there is no spill-over from one linear component into the other, then this is the ratio of the transmission coefficients into the surface. The experimental values suggest that the upper layer has a dielectric constant of 1.7 - 1.8.

67

boundary twice). In Fig. 21 the square root of the ratios derived from the ratio of the backscattering coefficients is plotted against the mean angle of incidence. In the same diagram is shown the ratio of the corresponding transmission coefficients for dielectric constants of 1.5 and 2.0. As might be seen it is very tempting to ascribe to the top layer a dielectric constant of about 1.7 - 1.8. It is interesting and it might be quite significant that this value corresponds very closely to the ones derived from radiometric observations of the polarization of the thermal emission from the lunar surface (Soboleva [1962], Heiles and Drake [1963]) and other values inferred from passive observations (Troitsky 1962, Salomonovich and Losevsky 1962, Kotikov and Troitsky 1962). All these values were found to lie in the range 1.5 to 2.0, and hence disagreed with the radar value (2.6 - 2.8) derived earlier in this section.

It is evident that if at these delays substantial amounts of power are reflected without penetrating the surface, or that if substantial amounts are converted into orthogonal modes, then the points in Fig. 21 will be higher than they should be. Similarly if parts of the surface are not covered by a layer of material the points will be raised. Thus a value for the dielectric constant of the layer of 1.7 - 1.8 can be taken as a definite lower limit.

Let us suppose then that the lunar surface consists of two layers. The upper one is irregular in depth, largely smooth, and has a dielectric constant of 1.8. The lower one is somewhat denser and more irregular. Possibly also there may be irregularities in density within the upper layer which contribute to the backscattered power. The radiometric determinations of the dielectric constant based on the polarization of the thermal emission can be brought into line with this naive two layer model. Calculations show that near grazing

68

angles of incidence the polarization of the emission will practically entirely be determined by the top layer. It therefore appears that a two-layer model of the lunar surface of the type suggested provides a rather self-consistent explanation of several different types of observations made of the moon by radio waves. The simple two-layer model suggested could be refined by introducing a gradual change in the dielectric constant with depth but as yet it does not appear that the experimental data warrant such a refinement.

If a two layer model of the surface is accepted as a working model, what are the other properties that can be derived? In order to reconcile the observed reflection coefficient at normal incidence (6%) with that expected for a homogeneous layer having a dielectric constant k = 1.8 (i.e., 3%) it is necessary to have a base layer with a dielectric constant ϵ = 4.5 – 5. As to the depth of the layer one can only say that is must be irregular and greater than 23 cm (i.e. the wavelength employed in these observations). If the depth is less than say 5 meters, one would be able to account for the increase in cross-section observed by Davies and Rohlfs (1964) (see Table I), since a thin layer would be unimportant at such wavelengths. However as noted earlier these long wave measurements are extremely difficult to perform reliably and perhaps not too much importance should be attached to this possible upper limit.

In view of the fact that at normal incidence some 60% of the echo power is reflected from within the surface, we are obliged to ask, what if any, is the meaning of the distributions and rms values of the surface slopes obtained in Sections V and VI? The answer is that these cannot apply to the uppermost layer, but to some hypothetical surface lying within that layer. For a two layer model this hypothetical surface would roughly lie midway between the two

69

boundaries and have characteristics roughly comparable to the sum of the two layers. It follows that since the hypothetical surface is largely smooth and undulating neither boundary can be particularly rough. In our present interpretation we have ascribed the small scale roughness entirely to the base layer, but this may be improper. A variety of models can be invented which would match the results. For example, the base layer could be equally as smooth as the top, and irregularities in the density of the upper layer (e.g., boulders) might be responsible for the diffuse component.

IX.   THE PACKING FACTOR OF THE LUNAR MATERIAL

Some constraints can be placed on the packing factor W_o which describes the fraction of the volume occupied by the material. If W_o is small, then it seems that an expression developed by Twersky (1962) which relates the observed dielectric constant k_{obs} to that of the material in bulk should apply. If the surface is assumed to consist of grains of pure dielectric material whose size is small compared with the wavelength, and which are well separated so that they can act as independent dipoles, the observed dielectric constant will be

$$k_{obs} = 1 + \frac{3E}{1 - E} \quad \text{where } E = \frac{W_o(k-1)}{k + 2} \tag{36}$$

in which k is the dielectric constant of the material in bulk. Where W_o is large and the surface can more properly be modeled as a continuous dielectric with small well separated cavities embedded in it (which now act as the scatterers), then a formula developed by Odelevskii and Levin (see Krotikov and Troitsky, 1962) should apply

$$k_{obs} = k \left\{ 1 - \frac{3(1-W_o)}{\frac{2k+1}{k-1} + (1-W_o)} \right\} \tag{37}$$

The two formulae can be shown to be equivalent by regarding the holes in the second model as vacuum spheres suspended in a dielectric and using (36) to recover (37).

If we assume that the lower layer is largely silicate material then the value for the dielectric constant that has been derived $\epsilon = 4.5 - 5.0$ indicates that this material must be more or less solid. If in addition we assume that the upper layer consists of the same material, but broken and more porous, then from (36) we conclude $W_o = 45\%$ and from (37) $W_o = 30\%$. As it is not clear which of these values is the better one to take, we have plotted in Fig. 22 the variation of the observed dielectric constant k_{obs} ..... $_o$ .... and (37) together with some experimental points reported by Brunschevig et al (1960) for sand. It appears from this comparison that (37) provides a much closer fit to the experimental results. It is evident from Fig. 22 that the value observed for the upper layer $k_{obs} = 1.8$ would be consistent with a light sand having a packing factor of 0.3. Since quartz has a rather low value of k (see Table II), this may perhaps be taken as an upper limit to the value of W_o. A lower limit can be obtained by putting $k = 20$ whence $W_o = 0.10$ is obtained. It is of course not possible to say anything on the basis of the radar results concerning the bearing strength of such a light material. This must depend considerably on the physical structure of the material, and presumably the rock froth envisaged by G. P. Kuiper and others would have a greater strength than the dust layer conceived by T. Gold.
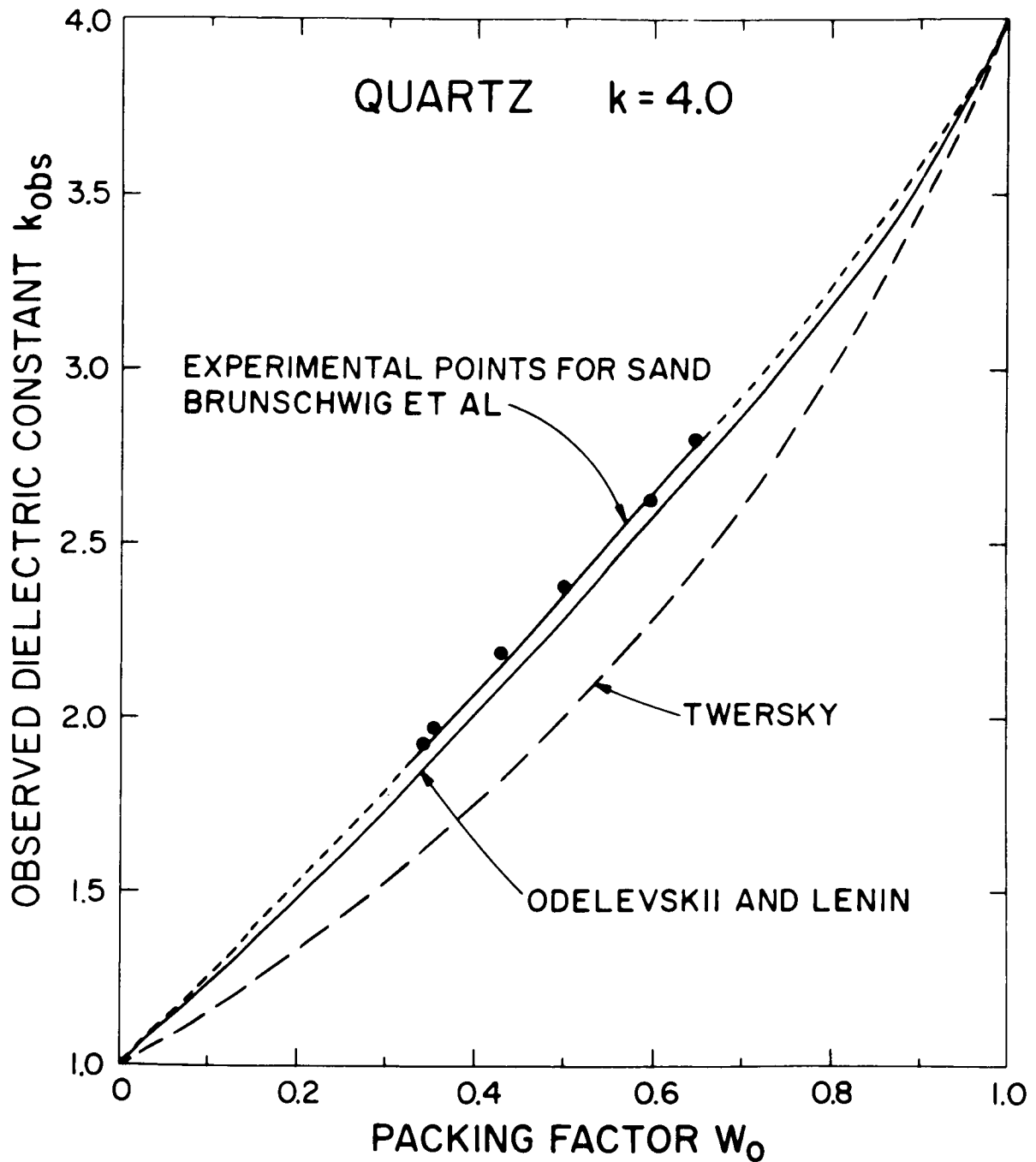
Fig. 22 The variation of the observed dielectric constant k_{obs} with the packing factor W_0 of a material having a bulk value of dielectric constant $k = 4$. The packing factor W_0 is defined as the ratio of the density of the actual broken material to the material in bulk. The results obtained from two theoretical formulas (36) and (37) are here compared with experimental results reported by Brunschwig et al (1960) for sand.

X.   SUMMARY

The results described in this report were obtained principally using radar systems operating at decimeter wavelengths. It appears that at normal incidence some 60% of the echo energy is reflected from within the surface, presumably at points where the density increases rapidly with depth. The uppermost layer of this surface has a dielectric constant of not less than 1.8, which implies that it has a porosity in the range 70 - 90% depending upon the nature of the material.

If it is assumed that there is only a single reflecting layer within the surface (two layer model) the dielectric constant of the base layer must be 4.5 - 5.0 and the material there quite compacted if not actually solid. The depth of the upper layer must be greater than about 23 cm, and irregular, but beyond this little more can be said at present.

The two boundaries appear to be characterized by smooth surfaces with rms slopes of the order of 1 in 10. The lower boundary is presumed to be rougher than the upper one. In order to account for the fact that 20% of the power lies in the diffuse component at 68 cm wavelength we require that a comparable fraction of the base layer be covered with structure of the order of the wavelength in size.

A two layer model of the surface as envisaged here is in all probability a mere approximation. It seems likely that the density will increase continuously with depth since a material with a porosity of 10-30% could perhaps hardly support its own weight to any considerable depth. If this is the case then the reflection from within the material will be a function of how rapidly the density changes in a depth of one wavelength. Thus the shortest wavelengths

73

may be reflected almost entirely from the uppermost interface, and longer wavelengths will be increasingly reflected from within the material. It seems that by exploiting further the technique of range doppler mapping with controlled polarization at a number of wavelengths, the properties of this layer can be explored further. There seems no other ground-based technique for making such studies.

REFERENCES

Beckmann, P., "Scattering by Composite Rough Surfaces", Dept. of Elec. Engr., Univ. of Colorado. Report No. 4 (1964a).

Beckmann, P., "Radar Backscatter from the Surface of the Moon", Dept. of Elec. Engr., Univ. of Colorado, Report No. 5 (1964b).

Blevis, B. C. and J. H. Chapman, "Characteristics of 488 Megacycles Per Second Radio Signals Reflected from the Moon", J. Res. NBS, 64D, 331-334 (1960).

Bowhill, S. A., "Ionospheric Irregularities Causing Random Fading of Very Low Frequencies", J. Atmos. Terr. Phys., 11, 91-101 (1957).

Bramley, E. N., "A Note on the Theory of Moon Echoes", Proc. Phys. Soc., 80, 1128-1132 (1962).

Brown, W. E., "A Lunar and Planetary Echo Theory", J. Geophys. Res., 65, 3087-3095 (1960).

Browne, I. C., J. V. Evans, J. K. Hargreaves and W. A. S. Murray, "Radio Echoes from the Moon", Proc. Phys. Soc., B69, 901-920 (1956).

Brunschwig, M., W. E. Fensler, E. Knott, A. Olte, K. M. Siegel, T. J. Ahrens, J. R. Dunn, F. B. Gerhard, Jr., S. Katz and J. L. Rosenholtz, "Estimation of the Physical Constants of the Lunar Surface", Univ. of Mich. Report 3544-1-F (1960).

Daniels, F. B., "A Theory of Radar Reflection from the Moon and Planets", J. Geophys. Res., 66, 1781-1788 (1961).

Daniels, F. B., "Author's Comments on the Preceding Discussion", J. Geophys. Res., 67, 895 (1962).

Daniels, F. B., "Radar Determination of the Root Mean Square Slope of the Lunar Surface", J. Geophys. Res., 68, 449-453 (1963a).

Daniels, F. B., "Radar Determination of Lunar Slopes: Correction for the Diffuse Component", J. Geophys. Res., 68, 2864-2865 (1963b).

Davis, J. R. and D. C. Rohlfs, "Lunar Radio-Reflection Properties at Decameter Wavelengths", J. Geophys. Res., 69, 3257-3262 (1964).

DeWitt, J. H., Jr., and E. K. Stodola, "Detection of Radio Signals Reflected from the Moon", Proc. IRE, 37, 229-242 (1949).

Dollfus, A., "The Polarization of Moonlight", in Physics and Astronomy of the Moon, (ed. Z. Kopal), Chapter 5, Academic Press, London (1962).

Edison, A. R., R. K. Moore, and B. D. Warner, "Radar Return at Near-Vertical Incidence -- Summary Report", Univ. of New Mexico Tech. Rept. EE-24 (1959).

Evans, J. V., "The Scattering of Radiowaves by the Moon", Proc. Phys. Soc., B70, 1105-1112 (1957).

Evans, J. V., "Radio Echo Studies of the Moon", in Physics and Astronomy of the Moon, (Ed. Z. Kopal), Chapter 12, Academic Press, London (1962a).

Evans, J. V., "Radio Echo Observations of the Moon at 3.6 cm Wavelength", MIT Lincoln Lab Tech. Rept. 256, ASTIA No. DDC 274669 (1962b).

Evans, J. V., "Radio Echo Observations of the Moon at 68 cm Wavelength", MIT Lincoln Lab Tech. Rept. 272, ASTIA No. DDC 291102 (1962c).

Evans, J. V., S. Evans and J. H. Thomson, "The Rapid Fading of Moon Echoes at 100 Mc/s", Paris Symposium on Radio Astronomy, (Ed. R. N. Bracewell), p. 8, Stanford Univ. Press, Stanford (1959).

Evans, J. V. and T. Hagfors, "On the Interpretation of Radar Reflections from the Moon", Icarus, 3, 151-160 (1964).

Evans, J. V. and T. Hagfors, "The Scattering of the Moon at 23 cm Wavelength", in preparation (1965).

Evans, J. V. and R. P. Ingalls, "Radio Echo Studies of the Moon at 7.84 meter Wavelength", MIT Lincoln Lab Tech. Rept. 288, ASTIA No. DDC 294008 (1962).

Evans, J. V. and G. H. Pettengill, "The Radar Cross Section of the Moon", J. Geophys. Res., 68, 5098-5099 (1963a).

Evans, J. V. and G. H. Pettengill, "The Scattering Properties of the Lunar Surface at Radio Wavelengths", in The Moon, Meteorites and Comets -- The Solar System, Vol. 4, (Ed. G. P. Kuiper and B. M. Middlehurst), Chapter 5, Univ. of Chicago Press, Chicago (1963b).

Evans, J. V. and G. H. Pettengill, "The Scattering Behavior of the Moon at Wavelengths of 3.6, 68 and 784 Centimeters", J. Geophys. Res., 68, 423-447 (1963c).

Fricker, S. J., R. P. Ingalls, W. C. Mason, M. L. Stone and D. W. Swift, "Characteristics of Moon Reflected UHF Signals", MIT Lincoln Lab Tech. Rept. 187, ASTIA No. DDC 204519 (1958).

Fricker, S. J., R. P. Ingalls, W. C. Mason, M. L. Stone and D. W. Swift, "Computation and Measurement of the Fading Rate of Moon-Reflected UHF Signals", J. Res. NBS, 64D, 455-465 (1960).

Fung, A. K. and R. K. Moore, "Effects of Structure Size on Moon and Earth Radar Returns at Various Angles", J. Geophys. Res., 69, 1075-1081 (1964).

Gold, T., Presented to the MIT Compass Seminar, Cambridge, Mass. (January 1964).

Grant, C. R. and B. S. Yaplee, "Backscattering from Water and Land at Centimeter and Millimeter Wavelengths", Proc. IRE, 45, 976-982 (1957).

Grieg, D. D., S. Metzger and R. Waer, "Considerations of Moon-Relay Communication", Proc. IRE, 36, 652-663 (1948).

Hagfors, T., "Some Properties of Radio Waves Reflected from the Moon and Their Relation to the Lunar Surface", J. Geophys. Res., 66, 777-785 (1961).

Hagfors, T., "Backscattering from an Undulating Surface with Applications to Radar Returns from the Moon", J. Geophys. Res., 69, 3779-3784 (1964).

Hagfors, T., "The Relationship of the Geometric Optics and the Autocorrelation Approaches to the Analysis of Lunar and Planetary Radar Echoes", presented at the International URSI Meeting on Planetary Surfaces and Atmospheres, Arecibo, Puerto Rico (1965).

Hapke, B. W. and H. Van Horn, "Photometric Studies of Complex Surfaces with Applications to the Moon", J. Geophys. Res., 68, 4545-4570 (1963).

Hargreaves, J. K., "Radio Observations of the Lunar Surface", Proc. Phys. Soc., B73, 536-537 (1959).

Hayre, H. S. and R. K. Moore, "Theoretical Scattering Coefficient for Near Vertical Incidence from Contour Maps", J. Res. NBS, 65D, 427-432 (1961).

Heiles, C. E. and F. D. Drake, "The Polarization and Intensity of Thermal Radiation from a Planetary Surface", Icarus, 2, 281-292 (1963).

Hey, J. S. and V. A. Hughes, "Radar Observations of the Moon at 10 cm Wavelength", in Paris Symposium on Radio Astronomy, (Ed. R. N. Bracewell), p. 13, Stanford Univ. Press, Stanford (1959).

Hughes, V. A., "Radio Wave Scattering from the Lunar Surface", Proc. Phys. Soc., 78, 988-997 (1961).

Hughes, V. A., "Diffraction Theory Applied to Radio Wave Scattering from the Lunar Surface", Proc. Phys. Soc., 80, 1117-1127 (1962a).

Hughes. V. A., "Discussion of Paper by Daniels 'A Theory of Radar Reflections from the Moon and Planets'", J. Geophys. Res., 67, 892-894 (1962b).

Kerr, F. J. and C. A. Shain, "Moon Echoes and Transmission Through the Ionosphere", Proc. IRE, 39, 230-242 (1951).

Krotikov, V. D. and V. S. Troitsky, "The Emissivity of the Moon at Centimeter Wavelengths", Astron. J. USSR, 39, 1089-1093 (1962).

Leadabrand, R. L., R. B. Dyce, A. Fredriksen, R. I. Presnell and R. C. Barthle, "Evidence that the Moon is a Rough Scatterer at Radio Frequencies", J. Geophys. Res., 65, 3071-3078 (1960).

Lynn, V. L., M. D. Sohigian and E. A. Crocker, "Radar Observations of the Moon at 8.6 mm Wavelength", MIT Lincoln Lab Tech. Rept. 331, ASTIA No. DDC 426207 (1963). See also, J. Geophys. Res., 69, 781-783 (1964).

Markov, A. V., "Brightness Distribution over the Lunar Disk at Full Moon", Astron. J. USSR, 25, 172-179 (1948).

Muhleman, D. O., "Radar Scattering from Venus and the Moon", Astron. J., 69, 34-41 (1964).

Norton, K. A. and A. C. Omberg, "The Maximum Range of a Radar Set", Proc. IRE, 35, 4-24 (1947).

Norton, K. A. and A. C. Omberg, "Errata", Astron. J., 63, 42 (1958).

Pettengill, G. H., "Measurements of Lunar Reflectivity Using the Millstone Radar", Proc. IRE, 48, 933-934 (1960).

Pettengill, G. H. and J. C. Henry, "Radio Measurements of the Lunar Surface", in The Moon, IAU Symposium 14 (Ed. Z. Kopal and Z. K. Mikhailov), p. 519, Academic Press, London (1962a).

Pettengill, G. H. and J. C. Henry, "Enhancement of Radar Reflectivity Associated with the Lunar Crater Tycho", J. Geophys. Res., 67, 4881-4885 (1962b).

Pettit, E., "Planetary Temperature Measurements", in Planets and Satellites: The Solar System, Vol. III (Ed. G. P. Kuiper and B. M. Middlehurst), Chapter 10, Univ. of Chicago Press, Chicago (1961).

Rea, D. G., N. Hetherington and R. Mifflin, "The Analysis of Radar Echoes from the Moon", J. Geophys. Res., 69, 5217-5223 (1964).

Salomonovich, A. E., and B. Y. Losovsky, "Radio Brightness Distribution of the Lunar Disk at 0.8 cm", Astron. J. USSR, 39, 1074-1082 (1962).

Senior, T. B. A. and K. M. Siegel, "Radar Reflection Characteristics of the Moon", in Paris Symposium on Radio Astronomy, (Ed. R. N. Bracewell), p. 29, Stanford Univ. Press, Stanford (1959).

Senior, T. B. A. and K. M. Siegel, "A Theory of Radar Scattering by the Moon", J. Res. NBS, 64D, 217-228 (1960).

Shorthill, R. W., "Measurements of Lunar Temperature Variations During an Eclipse and Throughout a Lunation", Boeing Report D.1. 82-0196 (1962).

Soboleva, N. S., "Measurement of the Polarization of Lunar Radio Emission on a Wavelength of 3.2 cm", Astron. J. USSR, 39, 1124-1126 (1962).

Trexler, J. H., "Lunar Radio Echoes", Proc. IRE, 46, 286-292 (1958).

Troitsky, V. S., "Radio Emission of the Moon, Its Physical State and the Nature of Its Surface", in The Moon, IAU Symposium 14, (Ed. Z. Kopal and Z. K. Mikhailov), p. 475, Academic Press, London (1962).

Twersky, V., "On Scattering of Waves by Random Distributions, II. Two Space Scatterer Formalism", J. Math. Phys., 3, 724-734 (1962).

Victor, W. K., R. Stevens and S. W. Golomb, "Radar Exploration of Venus", Jet Propulsion Lab Tech. Rept. 32-132 (1961).

Winter, D. F., "A Theory of Radar Reflections from a Rough Moon", J. Res. NBS, 66D, 215-226 (1962).

Yaplee, B. S., R H. Bruton, K. J. Craig and N. G. Roman, "Radar Echoes from the Moon at a Wavelength of 10 cm", Proc. IRE, 46, 293-297 (1958).

Yaplee, B. S., N. G. Roman, K. J. Craig and T. F. Scanlon, "A Lunar Radar Study at 10 cm Wavelength", Paris Symposium on Radio Astronomy, (Ed. R. N. Bracewell), p. 19, Stanford Univ. Press, Stanford (1959).

Yaplee, B. S., S. H. Knowles, A. Shapiro, K. J. Craig and D. Brouwer, "The Mean Distance to the Moon as Determined by Radar", Naval Research Lab Rept. 6134, (1964).

APPENDIX IV

THE CASE AGAINST VOLCANISM

PHOTOGRAPHY ON THE MOON'S SURFACE

"THIS APPENDIX IS ALSO ISSUED AS TG-5"

I. THE CASE AGAINST VOLCANISM

II. A RECOMMENDATION FOR PHOTOGRAPHY
ON THE MOON'S SURFACE

T. Gold

August, 1965

TABLE OF CONTENTS

PART I. THE CASE AGAINST VOLCANISM

PART II. A RECOMMENDATION FOR

PHOTOGRAPHY ON THE MOON'S SURFACE

PART I

THE CASE AGAINST VOLCANISM

T. Gold

August, 1965

I. Introduction

Has volcanism been a major agency in shaping the fea-
tures of the Moon? Are the flat plains hugh lava beds? Are
a significant proportion of craters of volcanic origin?

At the present time there appears to be no active
volcanoes on the Moon that would compare with any one of hun-
dreds of terrestrial volcanoes. Outbursts such as occur
commonly on the Earth in many volcanic regions would be plainly
visible if they occurred on the Moon, both for effects con-
nected with the gas that escapes, the small particles that are
thrown up and make reflecting clouds, and the heat of lava
flows. The discussion of the gas that may have escaped in the
crater Alphonsus as seen by Kozyrev indicates that the quantities
involved may be tens of kilograms. These are very tiny amounts
compared with gases that constantly escape from very many ter-
restrial volcanoes. The amounts of gas coming out of a
volcanic erruption is reckoned in millions of tons. The ash
clouds thrown up would, in a lunar vacuum and lunar gravity,
be thrown up to a great height by the gases escaping at the
speed of sound and the scattered light of such phenomena could

hardly be missed. There appears to be no active volcano on the Moon now of a level of activity such as occurs in hundreds of places on the Earth. If volcanism and lava flows were once common on a scale much greater than on the Earth, it must by now have ceased or been reduced to a scale of activity much below that of Earth.

The stability of the lunar ground is remarkable by comparison with the Earth. Craters are seen of a great variety of ages as judged by the manner in which they overlap with each other. It is clear that even the oldest of them have not suffered any significant horizontal deformations. The old craters appear to have lost a large proportion of their initial height and many crater rims can clearly be seen that are only a few per cent as high as those of a new looking crater of the same diameter. Many old craters have an interior floor which is quite flat, clearly unlike the newer looking ones, having clearly been filled up with some substance. Yet, despite these great changes that they seem to have suffered, the outline of even the oldest craters appears to be remarkably accurately circular. In contrast, on the Earth much horizontal deformation of the structure has taken place and this is true especially in volcanic regions. Horizontal deformations on the Earth are reckoned in hundreds of kilometers, while on the Moon two or three kilometers seem to be the most that can be seen. The dense packing that the highland regions show of overlapping

craters would be an excellent ground in which to see any horizontal displacements. We thus have to conclude that the lunar ground has shown a much higher stability against horizontal displacements than the Earth. Yet, if one wanted to attribute all the flat mare ground to lava flows, one would have to think of it as several kilometers deep in most areas and one would therefore have required a very liquid substance to have come up in most areas; and one would be concerned with the displaced volume of perhaps 10 million cubic kilometers. Is it conceivable that a ground that contained so much highly liquid lava close underneath the surface and had displaced such large volumes from one place to another would have remained motionless?

In the first place, if the ground is hot enough over most areas at a sufficiently shallow depth, would the mountains not have slumped? Would the shape of the Moon not have adjusted itself much more closely to the hydrostatic equilibrium for its present orbit? Yet we know that the triaxial shape of the Moon is not only incompatible with an equilibrium shape at its present position, but also incompatible with that at any previous orbit the Moon might have possessed. The Moon appears to have a triaxial shape of random values of the moments of inertia limited only by being no further from equilibrium than the compressive strength of rock would allow. It does not appear to have adjusted itself more closely to an equilibrium shape.

Secondly, if such large volumes of lava have been dis-
tributed very unevenly on the surface of the Moon, how could
the adjacent ground which was not flooded have escaped major
horizontal deformations everywhere? What has happened to the
pockets of lava that were emptied? Their large volume is
implied and the movement of overlying solid stuff to fill them
would have made very major deformations.

Many craters in the highlands show a very similar sur-
face in their flat interior filling as the maria. One would
have to suppose that in each case lava welled up from a local
supply area just underneath and that despite the availability
of lava in so many places close to the surface no significant
horizontal movements of all the highland ground were ever
caused. This, of course, is in great contrast to the events
on the Earth where much horizontal deformation was always
associated with magmatic processes.

If all the maria were made by lava, it would imply much
larger and more fluid lava outpourings than have occurred on
the Earth. Would we not be entitled to expect to see a whole
range of clearly defined volcanic structures? A small number
of tiny objects that look like volcanoes hardly seems adequate.
Should there not be hugh volcanic mountain ranges? Should
there not be some big distances of lava flows with a gradient
of a few degrees leading to high mountainous terrain with con-
centrations of volcanic features in them? The flat maria sur-
face to be produced by lava would have had to have been supplied
by very many small supply points and never by a few major ones.

-4-

Those would have given rise to large inclined regions. A mean gradient of even only one degree over big distances on maria surfaces would easily be seen as a result of the deformation of the terminator.

The complete absence of any volcanism at the present time would imply that such lava sheets if they existed are thoroughly cold by now. The maria would thus consist of solid sheets of rock some kilometers thick. Yet, it is characteristic of maria surface that it shows wrinkles, ridges and rills which suggest that not only have many small horizontal deformations taken place there, but that they have taken place in comparatively recent times as judged by the erosion rates which seem to be implied by the observations of small craters. The maria ground appears to be particularly unstable to small horizontal deformations and yet the neighboring highland ground is left undisturbed. A thick solid sheet of rock could hardly be expected to show such behavior. If it is distorted as a result of underlying deformations, one might expect that those would equally influence the neighboring ground. The rock sheets would be mechanically as strong as the neighboring ground and deformations would therefore not tend to cease at the edge of maria as is commonly observed.

I am not discussing here some arguments that have been advanced against the majority of craters being meteoritic in origin, for I regard this discussion as settled.

II. Arguments for the Presence of Ice Under the Moon's Surface

The mean density of the Moon is slightly less than the un-compressed density of the Earth would be. If from this fact one were to speculate on the mode of origin and the resulting chemical composition of the Moon, one would judge that it had formed at a lower temperature and from pieces which contained a larger proportion of the more volatile light elements. Water would be among the constituents that would be favored. Thus, if one were to make a judgment of the degree of hydration of the sub-surface rocks of the Moon, one might judge that it would be more hydrous than the rocks of the Earth. The heating in the interior of the Earth has resulted in some water being driven out which has managed to reach the surface and supply the mean amount of 3-kilometer depth averaged over the Earth. The Moon's internal heat may be a great deal less than that of the Earth, but the intrinsic hydration may be more. The amount of water that would be driven up cannot be calculated but it would have significant effects even if it were as little as an average depth of 100 meters rather than the 3 kilometers on the Earth.

On the Moon such internal water could not easily reach the surface. It is incorrect to think that because the Moon is in a vacuum any internal supply of water would have led to rapid evaporation and escape. The reason is that the surface temperature of the Moon, below the diurnally varying layer, is well below the freezing point of water. Any internal water

percolating upwards would thus freeze in any cracks through which it might move, as soon as in the internal temperature gradient it reaches the freezing point, and there it would block all passages of escape and would accumulate. This is likely to be at a depth where the overburden is sufficient to prevent any rapid evaporation by diffusion through the ground even though the exterior is in a perfect vacuum. For most materials a depth of 100 meters would be sufficient to reduce the diffusion rate to such a low value that the amount of water lost in all of geologic time would be insignificant.

Water in the ground is always at such a pressure that it would come to the surface since it is lighter than rock. The freezing layer in the Moon would prevent such an escape unless it occurred through sufficiently large holes or cracks so that it could rush out fast enough not to freeze during its passage. A large impact or a large crack would thus lead to the temporary escape of some water, but the cracks and holes would soon recover the normal temperature structure and the escape of water would be halted. Thus, the self-sealing properties of a ground well below freezing point would tend to bottle up ice and water below the ground. The ice in turn would also assist in bottling up other volatiles and gases that might come up from the Moon's interior. Furthermore, any crack in that ice will become a supply line for water and gases to come up.

If the maria were filled with rubble and dust, the initial floors might be the chief sites for such underground glaciation. The same would be true of the interiors of the initially sufficiently deep craters. If such glaciation had occurred, it would account for the comparative mobility of mare ground despite the firmness of surrounding highlands. Ice is very plastic and over geologic times would flow flat in any basin. If on the other hand a basin had either a further supply of water from underneath or a significant rate of evaporation of ice through the overlay, the equilibrium of the ice sheet could be disturbed and a slow plastic flow could take place. The overburden of debris might then show the ridges and crevices that result from this slight movement and yet such movements of ice would never be associated with forces large enough to cause horizontal deformations of the surrounding terrain. Even the fast flowing glaciers on the Earth do not move the neighboring mountains.

Gases accumulating under the ice sheet would come out almost explosively in any new crack. They would no doubt then cause surface features and perhaps surface discoloration on the top of the overlying effects.

Some craters appear to have a flat floor at a much higher level than the surrounding plain. If a liquid filled them, this liquid must be of lower density than the rock or otherwise the structural strength of the Moon would be grossly inadequate to maintain the hydrostatic difference.

For water and ice this would be no problem since it is three times lighter than the rock. Water could be supplied through cracks at all levels. How much accumulated in any one place would merely depend on the rate of supply that was available there.

All this implies that it would be well worth investigating whether the small quantities of water vapor are escaping from the Moon that might correspond to the slight evaporation from the top of the underlying ice. Comparatively recent craters would obviously be the places through which such evaporation would be fastest. It is possible that such craters of sufficient depth to penetrate the initial ice sheet, would have developed structures in their interior that resulted from the initial rush of water into the vacuum. Structures in recent craters that are more than 100 meters deep might be of such origin. Also, the slumping of the walls of large craters may be related to the fact that a significant proportion of the thrown up material was ice which, when it was brought to the surface, quickly evaporated, causing the remaining rubble to collapse. The characteristic difference between young mare and highland craters might be due to this. Copernicus and Tycho are both uneroded and of similar diameter and yet have rims of very different heights, with Copernicus, the mare crater, being much lower and showing more signs of collapse. It is also possible to think that some of the central features in large craters are directly

due to the psuedo-volcanic activity of escaping water.

There are numerous convex structures on the Moon's surface, both inside craters and around the edges of maria, which have strong similarity with terrestrial pingos. Pingos are perma-frost ice lenses in the ground which heave up the overlying material. The Moon, whose temperature regime is in the perma-frost domain, might well be expected to have some such structures wherever an underground supply of water reached fairly close to the surface.

III. The Depth of the Dust Layer

Radiometric and radar evidence is clear about there being a layer of at least a few meters thickness in which the density is much less than that of any solid rock and which covers most of the ground. This knowledge combined with the knowledge that the old craters have lost a large part of their initial height, suggests that an erosion mechanism is active which, while removing material from the high ground, keeps almost all the ground covered with an underdense debris. At any one time the surface of this debris layer when optically investigated appears to be in the form of a fine powder. It is hard to envision any erosion and transportation mechanism that would maintain the surface in that condition while transporting most of the material in a form other than a fine powder.

If most of the eroded material that is missing on the highlands was indeed transported away as dust, then the dust deposits in some places must be very deep.

Radar evidence makes clear that over all but the youngest craters there is a radio-absorbing overlay some meters in thickness. This applies to craters of a widely varying range of ages, excluding only the very youngest. It seems unlikely that the process that covered the initially undoubtedly solid crater wall material has everywhere accumulated to just the same thickness, despite the fact that

the process must have been going on for very much longer in some places than in others. Since a minimum radar effective thickness is required almost everywhere, it must be expected that on the older structures this thickness of loose over-burden is much greater than the minimum amount over the older structures.

The Ranger pictures show with high definition many young looking craters in the depth range of 10 meters. Had there been an abrupt discontinuity in the structure of the ground within this depth, the craters' shape would have revealed it. If there was only a gradual compaction with depth, no particular discontinuity could be seen. In fact, these craters show no discontinuity.

Gault has given convincing evidence that secondary craters would not as commonly be accurately circular if the material were substantially cohesive. It would thus appear that the material is not substantially cohesive over a depth of some meters. The shape of the dimple craters suggests an underground collapse or cavity with a draining of a noncohesive material from above.

PART II

A RECOMMENDATION FOR
PHOTOGRAPHY ON THE MOON'S SURFACE

T. Gold

August, 1965

The astronauts on the Moon are likely to see a great
variety of phenomena and structures which have never been
seen on Earth. The mode of packing of surface materials, the
fine structure of its packing, electrostatic effects on
dust grains, structures connected with vacuum processes
of erosion or the escape of volatiles--all these are features
that will look completely unfamiliar and that may contain
an important clue as to the surface processes that have
taken place on the Moon. It is extremely important to have
high quality and expert photography available at the
earliest time so that a subsequent investigation can lead
to sound conclusions. This is vital not only for the
scientific understanding of the Moon's surface but very likely
also for the avoidance of many hazards which the Moon's sur-
face will present.

Photography on the Moon's surface is by no means an easy
matter. Lighting conditions in the sunlight are unusually
harsh and with the low albedo of the ground and the absence
of a diffused light from the sky, the difference in brightness

between illuminated and shadowed areas will often be too great for both to be adequately visible on the same exposure. Several other novel complications also arise and the whole subject of photography on the Moon's surface ought to receive an intensive study.

The astronauts should have photography as an essential part of their training under the supervision of expert professional photographers. Furthermore, they ought to be guided by scientists familiar with the optical properties of the Moon's surface and much experimentation in simulated surroundings should be made. The entire photographic endeavor including the design of the equipment, the training and eventual direction of the astronauts for the lunar photographic work should be treated by NASA as a major program and it ought to be under the guidance of one or a committee of senior scientists close to the field of lunar optics and photography.

The design of a camera must be treated as a major problem. Design of good cameras that are convenient to use and are extremely reliable has been a very lengthy and expensive business even when the very large commercial sums of money were available and the commercial pressure for an early success was great. Each type of camera has required several rounds of progressive perfection before it became convenient and reliable. Since the requirements for a Moon camera are sufficiently different from present-day commercial cameras, one

has to anticipate a lengthy period of development with much testing and experimentation of intermediate models before a successful model can be devised. The program has to be put into high gear now and even then it would seem that the time is already too short for complete confidence that a really successful new camera can be devised.

The particular requirements for the camera are that it must work in a vacuum, that it must be capable of storing substantial amounts of film, that film reloading must be quick, easy and secure, that all its controls must be accessible to a man in space suit gloves, and that it must be exceedingly reliable in operation. More particular requirements that we might place on it might be as follows: It should be a stereo camera taking simultaneously two pictures when the stereo button is pressed, but capable of taking individual frames when no stereo is required. It should be capable of taking in quick succession two or three different exposures around the value indicated by the exposure meter so that a well defined picture both of the illuminated and the shadowed ground results. If necessary, such pictures could be subsequently superimposed to show the light and dark ground in the same frame.

It will be desirable for the same camera to be capable of taking very high definition pictures of small objects, perhaps up to a 1 to 1 object to image ratio. High definition color film will be desirable. On the other hand, the far focus must

clearly go to infinity, necessitating probably some interchange of lenses. There should be a positive indication at each exposure of light having actually reached the vicinity of the film. There should also be a positive indication of the successful transportation of the film between exposures since one could not take the risk of either a malfunction of the shutter or of the film sprocket mechanism destroying the success of the entire photographic work unbeknown to the astronaut at the time.

The view finder of such a camera will necessitate new design since it clearly would be advantageous, especially for close-up photography, to have a through-the-lens viewing system but nevertheless to have the eye more than four inches away from the (exit) pupil of the view finder.

Many hand-made versions of Mark I of such a camera should be made at the earliest opportunity. They should be used by the astronauts and by photographic experts in the ordinary surroundings as well as in vacuum chambers and simulated lunar surface surroundings for a few months and in close consultation with the designers. A set of Mark II cameras should be then built and again thoroughly tested. The process must be continued until all requirements are met, including a reasonable size and weight.

If the modern 35-mm reflex cameras did not exist and one were to require the design of a camera having all these features, i.e. the reflex action, the coupled iris, the view finder, the

quick film transport action, the built-in light meter with output visible in the view finder, one would almost certainly in the first round be led to a camera weighing several times as much as those that now exist. It is also certain that the first round of such a design would be far less reliable and convenient than the highly evolved objects we now have. One has to contemplate a similar evolution and also contemplates therefore a clumsy set of first new designs compared with that which can be ultimately achieved. A major part of the scientific value of the Appollo mission will depend upon this work having been done to perfection.

Really good photography on the Moon's surface would be a major factor also in the interest and participation that the general public will feel in this great exploration venture.

BIBLIOGRAPHY

Kozyrev, N. A., 1962, Physical Observations of the Lunar Surfaces. In "Physics and Astronomy of the Moon" (Z. Kopal, Ed.) Academic Press, New York, 361-384.

Gault, D.; W. Quade; V. Oberbeck; 1965. Interpreting Ranger Photographs from Impact Cratering Studies; paper presented at the Conference on the Nature of the Lunar Surface, Goddard Space Flight Center, Greenbelt, Maryland, April.

APPENDIX V

LEVITATION OF DUST ON THE SURFACE OF THE MOON

"THIS APPENDIX IS ALSO ISSUED AS TG-6"

LEVITATION OF DUST ON THE SURFACE
OF THE MOON

H. Heffner

August 1965

LEVITATION OF DUST ON THE SURFACE OF THE MOON

ABSTRACT

\16171

It is shown that a) photoelectric space charge effects are not sufficient to raise dust particles from the surface of the Moon, b) submicron dust particles can be suspended if they are raised to a sufficient height by micrometeorite impact, c) an appreciable fraction of these particles will be suspended as long as the angle to incidence of solar radiation is not too low, and d) under the influence of radiation pressure particles tend to migrate towards the shadow region.

Charged dust particles may be a cause of much nuisance, if not danger, to an astronaut especially if he should happen to fall. Experimental tests are recommended.

Author

TABLE OF CONTENTS

LIST OF TABLES

LEVITATION OF DUST ON THE SURFACE OF THE MOON

H. Heffner

August 1965

I. Introduction

The evidence from photometric and polarization studies of the
Moon, together with the relative flatness of its surface, have prompted
several authors to propose the existence of a dust layer on the Moon.
Estimates of its thickness vary from millimeters to kilometers.
Gold has proposed that the erosion of the Moon has produced a thick
layer of dust which has filled lunar craters so that they now appear
to be shallow and flat-bottomed. Originally, Gold proposed that
unbonded dust grains are charged by both the solar wind and the photo-
electric effect to be lifted up and levitated for a time in the
photoelectric space charge field. Subsequently, he modified this
model to consider only those grains which are in flight following
a micrometeorite impact and which are then prevented by the space
charge from immediately falling down.

P. D. Grannis[Ref. 1] has analyzed the mechanisms proposed by
Gold and under optimistic assumptions still finds that hopping of
dust grains is too small an effect to account for the transport of
enough material to fill craters. On the otherhand, Grannis' cal-
culations did seem to indicate that the gliding of positively
charged dust grains levitated in the photoelectric space charge
field could account for a fluidization and a mass transportation of
dust.

Grannis, however, did not estimate in a realistic way the fraction of dust particles having a sufficient charge to be levitated and, moreover, assumed an electrostatic field at the Moon's surface of some 20 volts per centimeter, a value which even under most favorable assumptions is more than a factor of ten too large. We shall attempt to include more realistic estimates of particle charge distributions and surface field to explore the efficiency of the dust levitation mechanism.

II. The Model

During the lunar day, the solar photon flux liberates photo-electrons from the surface of the Moon which create a space charge layer much the same as that produced near the cathode of a space charge limited vacuum tube. The characteristics of this space charge layer have been estimated in a previous section under two assumptions concerning the photoelectric flux, a) an optimistic estimate (e.g. a probable overestimate) and b) a perhaps more realistic estimate. These characteristics are shown on the following page on Table 1.

The surface of the Moon is also being bombarded by the solar wind composed of equal fluxes of protons and electrons. At the orbit of the Moon the density of protons and electrons is about $10/cm^3$ and the solar wind flux is approximately $10^9/cm^2$ sec.

There are then several mechanisms whereby dust particles may be charged. They may be charged positively by:

a) the emission of a photoelectron

b) the capture of a solar wind proton

c) the secondary emission of an electron due to the primary impact of a proton or an electron.

They may be charged negatively by:

a) the capture of a photoelectric space charge electron

b) the capture of a solar wind electron.

Because the photoelectric process produces an emitted flux of photoelectrons which is two to four orders of magnitude larger

TABLE 1 CHARACTERISTICS OF LUNAR PHOTOELECTRIC SPACE CHARGE LAYER

Characteristics	Photoelectron Flux a) $N_\nu\eta = 2 \times 10^{13}\dfrac{\text{electrons}}{\text{cm}^2\,\text{sec}}$	Photoelectron Flux b) $N_\nu\eta = 2 \times 10^{11}\dfrac{\text{electrons}}{\text{cm}^2\,\text{sec}}$
Potential of the Moon	32 volts	18 volts
Electric Field at the Surface	1.6 volts/cm	0.16 volts/cm
Thickness of Space Charge Layer	790 cm	770 cm
Plasma Frequency at Surface	4.4 mc	0.4 mc

than the solar wind flux, only processes a), e.g. emission and absorption of photoelectrons, are important in the particle charging processes.

The mechanism of dust levitation and transport then involves the chance charging of a dust grain sufficiently positive so that its electrostatic repulsion from the positively charged surface of the Moon can overcome the downward force due to gravity and to radiation pressure. If the charge lifetime on the particle is sufficiently long, it will "float" above the surface and seek its balance position in the decreasing electric field above the surface. Again, if the lifetime is sufficiently long, it may glide along the electric field or gravitational gradients or may be pushed along by the horizontal component of radiation pressure. As the distance from the Moon's surface increases, the space charge density decreases. As a result, the rate for electron capture decreases with height. Thus, those particles which are sufficiently positively charged to rise from the surface will tend to acquire more positive charge. This process will not continue indefinitely; however, for as the particle increases its positive charge, its cross section for electron capture increases and its efficiency of photoemission decreases. At some point equilibrium is reached and, except for statistical fluctuations, no further net charge is accumulated.

III. Statistics of Charged Particles

The charging of an isolated dust particle is composed of two independent Poisson processes; one representing the random acquisition of positive charge through photoelectron emission at an average rate R_p, and the other the random acquisition of negative charges at an average rate of R_n. These rates are given by:

$$R_p = \eta N_\nu \, \sigma_p$$

$$R_n = (1/e) \, I \, (x) \, \sigma_n$$

where

ηN_ν =	photoelectron flux
$I \, (x)$ =	total electron current at position x
σ_p =	photoelectron escape cross section
σ_n =	electron capture cross section

From elementary considerations of Coulomb scattering, the cross section for electron capture for a spherical particle of radius r charged with z charges (z may be either positive or negative) is:

$$\sigma_n = \pi r^2 \left(1 + \frac{z \, e^2}{2 \pi \, \epsilon_o m \, v_o^2 r} \right)$$

where v is the velocity of the incoming electrons. So long as the second factor in the parenthesis is less than unity, we may

adapt this expression to apply to a particle immersed in a thermal distribution of electrons by replacing mv^2 by its thermal average, 6 kT to obtain

$$\sigma_n = \pi r^2 \left(1 + \frac{Ze^2}{12\pi \, \epsilon_o \, kTr} \right)$$

In general then,

$$\sigma_n = \pi r^2 (1 + \alpha z)$$

For an electron temperature such that $\frac{kT}{e} = 3$ volts, and a particle of 5 microns diameter

$$\alpha = 6.4 \times 10^{-5}$$

Again. if αz is less than unity, the photoelectron emission cross section can be taken as

$$\sigma_p = \pi r^2 (1 - \alpha z)$$

The average rate of negative charging for a particle with charge z is then

$$R_n(z) = (1/e) \, I \, (x) \, \pi r^2 (1 + \alpha z)$$

and of positive charging is

$$R_p(z) = \eta N_\nu \, \pi r^2 (1 - \alpha z)$$

At the surface of the Moon the rate of positive and negative charging must be equal, that is

$$(I/e) \, I \, (0) \, \pi r^2 = \eta N_\nu \, \pi r^2 = R$$

Although the mean charge of the surface particles is zero, there is a statistical distribution which allows deviations. Let us determine the probability distribution of charge in the steady state.

If we identify the probability that at time t the particle has a charge z by the symbol $P_z(t)$, then $P_z(t)$ obeys a differential difference equation[Ref. 2].

$$\frac{dP_z(t)}{dt} = -\left(R_p(z) + R_n(z)\right) P_z(t) + R_p(z-1) P_{z-1}(t) + R_n(z+1) P_{z+1}(t)$$

Since we are interested in the steady state, we set

$$\frac{dP_z(t)}{dt} = 0$$

and obtain

$$R_n(z+2) \, \Delta^2 P_z + \left(2R_n(z+2) - R_p(z+1) - R_n(Z+1)\right) \Delta P_z$$
$$+ \left(R_n(z+2) - R_n(z+1) + R_p(z) - R_p(z+1)\right) P_z = 0$$

For reasonably large z, we may convert this to a differential equation for the probability distribution of charge for a surface particle,

$$(1+2\alpha+2\alpha z) \frac{d^2 P_z}{dz^2} + 2\alpha z \frac{dP_z}{dz} + 2\alpha \, P_z = 0$$

Since we have demanded $\alpha z \ll 1$, we may approximate this equation by:

$$\frac{d^2 P_z}{dz^2} + 2\alpha z \frac{dP_z}{dz} + 2\alpha \, P_z = 0$$

The solution to this equation which has zero slope at $z = 0$ is:

$$P(z) = Ke^{-2\alpha z^2}$$

Thus the steady state distribution of charge is a normal distribution with root mean square deviation, $(4\alpha)^{-1/2}$. For the five-micron particle under the conditions we have chosen, this amounts to 62 charges. For the number of charges z several times $(4\alpha)^{-1/2}$ the value of $P(z)$ is so small that the deviation from a normal distribution at large αz resulting from the omitted term in the differential equation is of little significance. Thus, we can determine the value of the constant K by demanding the integral of P_z be unity. Hence,

$$P_z = \sqrt{\frac{2\alpha}{\pi}}\, e^{-2\alpha x^2}$$

For a particle with a charge z, the differential charging rate tending to return it to equilibrium is $2\alpha R$. Thus, the particle will tend to reduce its charge to zero as

$$z(t) = ze^{-2Rt}$$

and we may define a charge lifetime for particles on the surface as

$$T = (2\alpha R)^{-1}$$

For 5-micron particles, assuming $\eta N_{\nu} = 2 \times 10^{13}/cm^2$ sec, we find

$$T = 80 \text{ seconds}$$

IV. Levitation of Dust Particles

There are several forces acting on a charged particle at the Moon's surface. There is a levitation force F = zeE acting on a positively charged particle in the photoelectron space charge field, and in opposition, the gravitational attraction, radiation pressure, and the attractive force due to molecular bonding of the particles. The force due to radiation pressure is some two orders of magnitude less than the gravitational force for micron size particles. It may thus be neglected except as a mechanism for translational motion at low angles of solar illumination once a particle has been levitated. Estimates of bonding for micron size particles vary from 0.04 dynes to 1.0 dyne depending upon whether the bonding is of a van der Waals or covalent type. Even if the lower figure is taken, more than 10^{10} charges would be required to liberate a particle in a field of 1.6 volts/cm. Even if two adjacent 5-micron dust grains were each charged, it would require some 10^5 charges on each before the coulomb repulsion would amount to 0.04 dynes. This number of charges is more than 1000 standard deviations away from the mean so that the probability of having a particle with 10^5 charges is essentially zero.

Even if one assumes the dust particles on the surface are free from bonding forces, the charge required to balance the gravitational force and maintain levitation is:

$$z = \frac{Mg}{eE} = 1.2 \times 10^4$$

for a 5-micron particle of density 3 gm/cm^3 in a field of 1.6 v/cm. The probability of a particle acquiring even this charge is completely negligible. From these considerations we find the chance of liberating a surface particle or balancing the force of gravity for levitation near the surface is essentially zero.

Well above the surface where dust particles may be thrown up by micrometeorite impact, the situation is quite different, for the photoelectron current and, hence, the negative charging rate decreases with height. A particle or radius r, a height x above the surface intercepts from below a current $\pi r^2 I_o \exp(-eV/kT)$ emitted from the Moon and an equal current above returning to the Moon. Thus, its rate of negative charging is (neglecting its cross section change with charge)

$$R_n = \frac{2\pi r^2}{e} I_o \exp(-eV/kT)$$

$$= \frac{2\pi r^2 I_o}{(1+\beta x^2)}$$

$$= \frac{2\eta_1 N_\nu}{(1+\beta x)^2}$$

where

$$\beta = m^{1/4} (eI_o)^{1/2}/(kT)^{3/4} \epsilon_o^{1/2}$$

For the values chosen previously, e.g. 5-micron particle,
$nN_\nu = 2 \times 10^{13}$ and $\frac{kT}{e} = 3$ volts,

$$R_n(z=0) = \frac{7.8 \times 10^6}{(1+0.54x)^2} \text{ charges/sec}$$

$$R_p(z=0) = nN_\nu \ \pi r^2 = 3.9 \times 10^6 \text{ charges/sec}$$

where x is measured in centimeters. Thus, if a particle rises about a centimeter above the surface of the Moon, it will see a net positive charging rate.

The particle will then acquire positive charge until its cross sections for capture and emission have been changed enough to bring the positive and negative charging rates into equality. If this equilibrium value of positive charge is sufficiently great, the upward force due to the electrostatic field will balance the downward force of gravity and the particles will be suspended.

The amount of charge necessary for suspension increases with height since the field falls off as

$$E(x) = \frac{E(o)}{1+\beta x}$$

Let us obtain a rough estimate of whether the conditions for suspension can be met. We need a better estimate of the photoelectron emission cross section for large particle charge. If the particle is charged with z positive charges, it has a potential $ze/4\pi\epsilon_o r$. Only photoelectrons with normal energies

greater than $ze^2/4\pi\epsilon_0 r$ can escape. Assuming a Maxwellian distribution of velocities, the emission rate is then reduced by

$$\left(1 - \text{erf } (ze/4\pi\epsilon_0 kTr)^{1/2}\right) = \left(1 - \text{erf } (3\alpha z)^{1/2}\right)$$

The rate of positive charging is then

$$R_p = \eta N_\nu \pi r^2 \left(1 - \text{erf } (3\alpha z)^{1/2}\right)$$

The rate for negative charging is

$$R_n = \eta N_\nu \pi r^2 \, 2(1 + \alpha z)/(1 + \beta x)^2$$

The steady state charge at a given height x is then determined by equating these charging rates,

$$\left(1 - \text{erf } (3\alpha z)^{1/2}\right) = 2(1 + \alpha z)/(1 + \beta x)^2$$

At height x, however, the particle must have a charge:

$$z = \frac{Mg}{eE(0)} \, (1 + \beta x)$$

in order to be suspended. If a simultaneous solution to these last two equations yielding a positive x exists, the particle will be able to float. One finds that no solution exists for 5-micron particles of density 3 gm/cm^3 under the conditions chosen, e.g. $E(0) = 1.6$ v/cm. There is a solution for one micron particles, however, showing that they will float at a distance of about 37 cm from the surface. Thus, for the rather extreme solar flux conditions chosen such that $\eta N_\nu = 2 \times 10^{13} \, \dfrac{\text{photoelectron}}{\text{cm}^2 \text{ sec}}$ there is a levitation "cut-off" for particles having a diameter above a value somewhere between 1 and 5 microns. Under a somewhat more realistic

solar flux assumption (ηN_ν = 2 x 10^{11} photoelectrons/cm^2 sec) only particles with a diameter less than about 1/2 micron will be suspended.

All of the foregoing assumes each particle has the same mean photoelectric efficiency η. Certainly some dust particles are made of material having a relatively low work function and hence a higher rate of photoelectric charging than the mean surface material of the Moon. Particles of such material larger than the cut-off values quoted above will be capable of suspension.

We thus come to the conclusion that if by micrometeoritic impact micron size particles can be lifted above 30 to 40 centimeters and remain sufficiently long (0.1 to 1 second) above that height, they will acquire sufficient charge to remain suspended. R. Smoluchowski has calculated that micron particle ejecta from micrometeoritic impact have mean flight times of 10 seconds. For purely ballistic trajectories, these particles would reach a height of 80 meters and spend most of their 10 seconds above the 30 to 40 cm level. Thus, it would seem that a large fraction of the particles with diameters below about one micron which are ejected by micrometeorite impact will be suspended if the impact area is in the vicinity where the sun's radiation is normally incident.

V.   Conclusion

We have shown that:

1)   The photoelectric space charge effects are not sufficient to raise dust particles from the surface of the Moon.

2)   Dust particles under about a micron diameter can be suspended if they are raised to a sufficient height. Moreover, the maximum size for suspension of the particle is relatively insensitive to assumptions of solar flux and electron temperature.

3)   An appreciable fraction of the micron particles ejected by micrometeorite impact will be suspended so long as the angle of incidence of the Sun's radiation is not too low.

We may make several inferences from the above results.

First, the dust which is suspended will migrate toward the shadow region of the Moon due to the horizontal component of radiation pressure. As the particle drifts farther away from the region of vertical incidence of solar radiation, the photoelectric field strength decreases and the particle sinks closer to the surface. Eventually, the solar flux is too small to allow suspension and at this point the particle drops to the surface. The smaller particles can drift farther toward the shadow zone before they are no longer capable of being suspended. Further calculations need to be made to determine whether a sufficient amount of dust can be transported by this mechanism to account for the filling of craters and the visible erosion by this means.

Although particles of one micron diameter are one hundred times smaller than those of powdered cement, they might, as Gold has pointed out, still be a nuisance if not a danger to an astronaut on the lunar surface. During daylight, the astronaut's suit will charge positively due to the photoelectric effect. Thus, he will tend to repel particles which are suspended for they too are charged positively. If, however, he should happen to fall to the lunar surface, he will encounter a layer of particles approximately half of which are negatively charged. Thus his suit, face plate, electrical connectors, etc. will be covered by a layer of dust clinging electrostatically. In addition, even the act of walking may throw up enough negatively charged dust to coat the surface of his suit. Any attempt to wipe away the dust coating will only serve to increase the electrostatic charge and will be largely ineffective.

Electrostatic attraction of dust in conditions like this is not particularly amenable to calculation. It would seem wise to carry out a few experimental observations of the effect by having an astronaut walk over a highly illuminated dust layer under vacuum conditions.

REFERENCES

1) P. D. Grannis, "Electrostatic Erosion Mechanisms on the Moon," *J. of Geoph. Res.*, 66, 4293-4299 (1961)

2) William Feller, *An Introduction to Probability Theory and Its Applications*, Vol. 1, 2nd ed. John Wiley and Sons, New York (1957), p. 407.

APPENDIX VI

THE POTENTIAL AND ELECTRIC FIELD AT THE
SURFACE OF THE MOON

"THIS APPENDIX IS ALSO ISSUED AS TG-7"

THE POTENTIAL AND ELECTRIC FIELD

AT THE SURFACE OF THE MOON

H. Heffner

August 1965

THE POTENTIAL AND ELECTRIC FIELD AT THE SURFACE OF THE MOON

ABSTRACT

\65172

During the lunar day, the surface of the Moon charges to a positive potential due to the photoelectric emission of electrons from its surface. Using the assumptions for solar photon flux below 4000 $\overset{o}{A}$ $N_\nu = 2 \times 10^{16}$ $\dfrac{\text{photons}}{\text{cm}^2 \text{ sec}}$ for quantum efficiency ($\eta = 10^{-3}$) and for the temperature of the photoelectrons $\dfrac{kT_p}{e} = 3$ volts   employed here, we find the potential of the Moon to be approximately 30 volts when the Sun's radiation has normal incidence. The Moon is surrounded by a space charge layer extending outward some 8 meters. The electric field at the Moon's surface, again under conditions of normal incidence of solar radiation, is approximately 1.6 volts/cm. Somewhat more realistic values for the photoelectron flux ($\eta N_\nu = 2 \times 10^{11}$), two orders of magnitude less than the value first assumed, yield a surface field of 0.16 volts/cm, a potential of 18 volts and virtually the same value for the extent of the space charge layer.   Author

TABLE OF CONTENTS

LIST OF TABLES

-iii-

THE POTENTIAL AND ELECTRIC FIELD AT THE SURFACE OF THE MOON

H. Heffner

August 1965

I. The Physical Nature of the Charging Process

During the lunar day, sunlight of sufficiently short wave-length striking the lunar surface will liberate photoelectrons which will tend to charge the Moon positively. Since escape velocity is equivalent to an electron energy of some 16 micro-volts, it is clear that gravitational effects are of no importance in retaining the photoelectrons. Moreover, since the high energy tail of the Sun's black body radiation extends indefinitely, no matter to what potential the Moon rises, some electrons will still escape, further increasing the potential. Thus another source must be found to provide a compensating electron current to the Moon to exactly balance the lost photoelectric current. The potential of the Moon is determined by how positively it must charge in order to bring the photoelectric current into equality with the incoming current.

The source of the incoming compensating current is the solar wind. The solar wind is composed of grossly equal numbers of protons and electrons. From measurements on Explorer X[Ref. 1] the average proton intensity is $10^{8.5}$ cm^{-2} sec^{-1}. The average velocity of the protons is $10^{7.5}$ cm sec^{-1} giving a proton density of the order of 10 cm^{-3}. The electrons have the same density and a thermal

velocity of approximately 10^8 cm sec^{-1}. Since in order to keep a charge balance at the Sun the electron drift velocity must equal that of the protons, it is seen that the electron drift velocity is approximately equal to the electron thermal velocity. The Debye length

$$\left(\frac{kT_e}{4\pi Ne^2}\right)^{1/2}$$

in the solar wind at the Moon's distance is 10^2 to 10^3 cm. The Debye length represents the distance over which potential fluctuations are screened.

We shall later calculate the compensating solar wind electron current by assuming that the Moon's electric field is confined to a region extending outward from the Moon's surface a distance d. This distance will be equal either to the Debye length of the solar wind or to the distance of the photoelectric current space charge minimum, whichever is shorter. It will turn out that this latter distance to the space charge minimum is the shorter and hence is the appropriate length. Any electrons which diffuse across a hemispherical shell a distance d away from the Moon's surface are captured. This model in effect ignores the drift motion of the electrons which carries a current to the Moon--just cancelled by the equal proton drift current.

The electric field at the surface of the sunlit Moon is determined by the distribution of charge nearby. In effect, the Moon is a large space charged limited diode operating with a negative

anode potential. Fortunately the surface's electric field and the Moon's potential are relatively insensitive to exact values of the Moon's physical parameters.

II. Calculation of the Potential of the Moon

Let us first estimate the flux of photoelectrons ejected from the surface of the Moon. Only radiation which has a photon energy greater than the work function of the lunar material will be effective in producing photoelectrons. If the flux of these solar photons is N_ν photons/cm^2 sec and the photoelectric quantum efficiency is η, then the number of photoelectrons emitted per cm^2 per second is ηN_ν and the photoelectric current emitted is

$$I_o = e \eta N_\nu$$

We shall later take N_ν as the solar flux below 4000 Å (above 3 ev) which is estimated to be

$$N_\nu = 2 \times 10^{16} \frac{photons}{cm^2 \ sec}$$

and the photoelectric quantum efficiency to be

$$\eta = 10^{-3}$$

giving an emitted photoelectric current density of

$$I_o = 3.2 \times 10^{-6} \ amp/cm^2$$

These values probably give an overestimate of the photoelectron current. We use them in order to get a maximum estimate of the surface conditions produced by the photoelectric effect. A more reasonable estimate of the photoelectric current might be one or even two orders of magnitude lower. We shall also characterize the emitted photoelectric current as having a Maxwell-Boltzmann velocity

-4-

distribution appropriate to a temperature T_p. Because of the broad spectrum of solar radiation, the velocity distribution will be very broad. We shall take the effective temperature such that

$$\frac{kT_p}{e} = 3 \text{ ev}$$

It is perhaps worthwhile to note that other processes of electron production such as secondary emission or electron ejection due to the impact of protons from the solar wind are several orders of magnitude less effective than is the photoelectric effect.

Now, given that the emitted photocurrent has a Boltzmann distribution, if the Moon is charged to a potential V, the current escaping I_e is given simply by

$$I_e/I_0 = \exp -(eV_m/kT_p)$$

or

$$V_m = \frac{kT_p}{e} \ln \left(\frac{I_0}{I_e}\right) = \frac{kT_p}{e} \ln \left(\frac{e \eta N_\nu}{I_e}\right)$$

The current escaping is just balanced by the current flowing in from the solar wind. We estimate that value as mentioned before by determining the number of solar wind electrons which cross a unit area of a shell a short distance away from the surface of the Moon. Assuming the solar wind electrons are in thermal equilibrium at a temperature T_e and have a density ρ_e, the number of electrons crossing a unit area in a unit time is

$$1/4 \, \rho_e \, \bar{v} = \left(\frac{kT_e}{2\pi m}\right)^{1/2} \rho_e$$

where $\bar{v}$ is the mean thermal electron velocity.

Thus the current is

$$I_e = 1/4 \; e \; \rho_e \; \bar{v}$$

and the Moon's potential is

$$V_m = \frac{kT_p}{e} \ln \left(\frac{4 \eta N_\nu}{\rho_e \bar{v}} \right) = \frac{kT_p}{e} \ln \left(\sqrt{\frac{2\pi m}{kT_e}} \; \frac{\eta N_\nu}{\rho_e} \right)$$

We see that the potential is not very sensitive to the ratio of emitted to escaping current, but is sensitive to the temperature of the photoelectrons. This result is reasonable since it is only those electrons in the high energy tail which constitute the escaping current.

Using the assumed values of

$$N_\nu = 2 \times 10^{16} \; \frac{\text{photons}}{\text{cm}^2 \text{ sec}} \qquad \rho_e = 20 \text{ electrons/cm}^3$$

$$\eta = 10^{-3} \qquad \bar{v} = 10^8 \text{ cm/sec}$$

$$\frac{kT_p}{e} = 3 \text{ ev}$$

we find $V_m = 32$ volts.

III. Calculation of the Electric Field

Once the photoelectric emission current I_o and the escaping current I_e are known, the field at the surface of the Moon can be determined from Langmuir's[Ref. 2] analysis of the space charge limited parallel plane diode. Assuming a Maxwellian velocity distribution, the current per unit area composed of electrons with velocities between u_1 and $u_1 + du_1$ is

$$dI = I_o (mu_1/kT_p) \exp (-mu_1^2/2kT_e) du_1$$

The charge density a distance X away from the Moon's surface is

$$\rho(x) = \int_{(2eV_o/m)^{1/2}}^{\infty} (1/u) \ dI + 2 \int_{(2eV/m)^{1/2}}^{(2eV_o/m)^{1/2}} (1/u) \ dI$$

where V is the potential at x, and u is the corresponding electron velocity,

$$u^2 = u_1^2 + 2 \ eV/m$$

and V_o and x_o are the potential and distance of the potential minimum. We can integrate Poisson's equation,

$$\frac{d^2V}{dx^2} = -\frac{\rho(x)}{\varepsilon_o}$$

between the limits (x,V) and (x_o, V_o) to get

$$\left(\frac{d^2V}{dx}\right)^2 - \frac{dV}{dx}\Bigg|_{x=x_o} = \frac{2}{\varepsilon_o} \int_{V_m}^{V} \rho(x)\, dV$$

At x_o the position of the potential minimum $\frac{dV}{dx} = 0$. Langmuir introduced dimensionless variables η' and ξ in order to carry out the integration obtaining

$$\frac{d\eta'}{d\xi} = (eL/kT_p)\,\frac{dV}{dx} = \left(\exp(\eta') - 1 + \exp(\eta')\,\mathrm{erf}(\eta')^{1/2} - 2(\eta'/\pi)^{1/2}\right)^{1/2}$$

where

$$\eta' = e(V + V_o)/kT_p$$

$$\xi = (x - x_o)/L$$

$$L = (2kT_p)^{3/4}\,\varepsilon_o^{1/2}/(2\pi m)^{1/4}\,eI_a$$

and,

$$I_o = I_a \exp(eV_o/kT_p)$$

At the surface of the Moon (the cathode)

$$\eta'_c = \frac{eV_o}{kT_p} = \ln\frac{I_a}{I_o}, \qquad -\xi_c = \frac{x_o}{L}$$

and at the "anode"

$$\eta'_a = \frac{e(V_M + V_o)}{kT_p} = \frac{eV_M}{kT_p} + \eta'_c, \qquad \xi_a = \frac{x_a - x_o}{L} = \frac{x_a}{L} + \xi_c$$

Taking the previously estimated values for

$$I_o = 3.2 \times 10^{-6} \text{ amp/cm}^2$$

$$I_e = 8 \times 10^{-11} \text{ amp/cm}^2$$

and assuming for the moment that the distance to the potential minimum x_o is smaller than the Debye length so that $I_e = I_a$ and $V_o = V_M$, we find

$$\eta'_c = \ln 4 \times 10^4 = 10.6$$

and[3]

$$\xi_c = -2.547$$

this latter figure with an assumed photoelectron temperature of $\frac{kT_p}{e} = 3$ ev gives a distance to the potential minimum of $x_o = 790$ cm.

Since the Debye length of the solar wind is several times this length, the potential minimum distance rather than the Debye length determines the region over which the field exists.

Returning to the expression $\frac{d\eta'}{d\xi}$, we can determine the electric field strength

$$-E = \frac{dV}{dx} = \left(\frac{kT_p}{e}\right)^{1/4} \left(\frac{I_a}{2\xi_o}\right)^{1/2} \left(\frac{\pi m}{e}\right)^{1/4} \left[e^{\eta'}\left(1+\text{erf } \eta'^{-1/2}\right) -1 -2\left(\frac{\eta'}{\pi}\right)^{1/2}\right]^{1/2}$$

Since the ratio of emitted to escaping photoelectric current is large, the value of η at the cathode plane is large. Under these conditions, only the exponential term in the square brackets is important and erf $(\eta^{1/2}) \approx 1$. Thus, assuming only that a small fraction of the emitted photoelectric current escapes,

we find for the field at the surface of the Moon

$$E(o) = - \left(\frac{\pi m k}{\varepsilon_o^2}\right)^{1/4} T_p^{1/4} (nN_\nu)^{1/2} = 2.7 \times 10^{-8} T_p^{1/4} (nN_\nu)^{1/2}$$

Taking again the assumed values of

$$N_\nu = 2 \times 10^{16} \frac{photons}{cm^2 \, sec}$$

$$n = 10^{-3}$$

$$\frac{kT_p}{e} = 3 \, ev$$

we obtain

$$E = -1.6 \, v/cm$$

So long as the escaping current is small compared to the emitted current, the potential near the surface (within 150 cm in this case) can be expressed as

$$-V = \frac{2kT_p}{e} \ln \left[1 + \frac{(m\pi)^{1/4}}{(kT_p)^{3/4}} \left(\frac{eI_o}{\varepsilon_o}\right)^{1/2} x \right]$$

and the field as

$$E(x) = \frac{E(o)}{\left[1 + \frac{(m)^{1/4}}{(kT_p)^{3/4}} \left(\frac{eI_o}{\varepsilon_o}\right)^{1/2} x \right]}$$

For the values chosen above

$$-V = 6 \ln \left[1 + 0.54x \right] \text{ volts}$$

$$E(x) = \frac{1.6}{\left[1 + 0.54x \right]} \text{ volts/cm}$$

where x is the height above the surface measured in centimeters. The charge density is given by

$$-\rho = \epsilon_o \frac{d^2 V}{dx^2} = \epsilon_o \frac{kT_p}{eL^2} \frac{d^2 \eta'}{d\xi^2} = \epsilon_o \frac{kT_p}{eL^2} \, 1/2 \, e\eta' \left[1 + \text{erf} \sqrt{\eta'} \right]$$

For the majority of the space charge cloud η' is sufficiently large that erf $\sqrt{\eta'}$ may be approximated by unity. Under these conditions, one finds

$$-\rho(x) = \frac{1/2 \left(\frac{(m\pi)}{(kT)} \right) I_o}{\left[1 + \frac{(m\pi)^{1/4}}{(kT)^{3/4}} \left(\frac{eI_o}{\epsilon_o} \right)^{1/2} \right]^2}$$

or, the plasma frequency is

$$\omega_p = \frac{\left[1/2 \left(\frac{\pi}{mkT} \right)^{1/2} \frac{eI_o}{\epsilon_o} \right]^{1/2}}{\left[1 + \frac{(m\pi)^{1/4}}{(kT)^{3/4}} \left(\frac{eI_o}{\epsilon_o} \right)^{1/2} x \right]}$$

For the conditions assumed

$$\frac{\omega_p}{2\pi} = f_p = 4.4 \times 10^6/(1 + 0.54 \text{ x})$$

where x is again the height above the surface measured in centimeters.

It is instructive to see how the space charge conditions change when the assumption of photoelectric current is reduced by two orders of magnitude below the admittedly high value previously assumed. If one takes the product of photoelectric quantum efficiency, η, and the solar flux in an appropriate spectral region, N_ν, to be

$$\eta N_\nu = 2 \times 10^{11} \frac{\text{photoelectrons}}{\text{cm}^2 \quad \text{sec}}$$

rather than the previous value of 2×10^{13}, but keeping the photoelectron temperature the same, then the space charge characteristics are those shown in the accompanying table.

TABLE 1 Space Charge Characteristics Near the Moon's Surface for Two Assumed Values of Photoelectron Flux. (The temperature of the photoelectrons is assumed to be such that $\frac{kT_p}{e} = 3$ in each case.)

	$\eta N_\nu = 2 \times 10^{13} \dfrac{\text{Photoelectrons}}{\text{cm}^2 \text{ sec}}$	$\eta N_\nu = 2 \times 10^{11} \dfrac{\text{Photoelectrons}}{\text{cm}^2 \text{ sec}}$
Moon's potential	32 volts	18 volts
Electric field at surface	1.6 volts/cm	0.16 volts/cm
Distance over which space charge extends (distance of minimum)	790 cm	770 cm
Plasma frequency at surface	4.4×10^6 cps	4.4×10^5 cps

IV. Summary

During the lunar day, the surface of the Moon charges to a positive potential due to the photoelectric emission of electrons from its surface. Using the assumptions for solar photon flux below 4000 $\overset{\text{o}}{\text{A}}$

$$N_\nu = 2 \times 10^{16} \frac{\text{photons}}{\text{cm}^2 \text{ sec}}$$

for quantum efficiency ($\eta = 10^{-3}$) and for the temperature of the photoelectrons ($\frac{kT_p}{e} = 3$ volts) employed here, we find the potential of the Moon to be approximatly 30 volts when the Sun's radiation has normal incidence. The Moon is surrounded by a space charge layer extending outward some 8 meters. The electric field at the Moon's surface, again under conditions of normal incidence of solar radiation, is approximately 1.6 volts/cm. Somewhat more realistic values for the photoelectron flux ($\eta N_\nu = 2 \times 10^{11}$), two orders of magnitude less than the value first assumed, yield a surface field of 0.16 volts/cm, a potential of 18 volts and virtually the same value for the extent of the space charge layer.

REFERENCES

1) Biermann, L. and Lust, Rh., "Comets: Structure and Dynamics
    of Tails," in The Moon, Meteorites and Comets, ed. by
    B. M. Middlehurst and G. P. Kuiper, Univ. of Chicago Press (1963).

2) Langmuir, I., Phys. Rev. 21, (1923) 419.

3) Kleynen, P. H. J. A., Philips Res. Rep., 1, (1946), 81,
    Tabulation of the Langmuir Equation.

APPENDIX VII

INTERPRETATION OF THE BRIGHTNESS AND POLARIZATION
CURVES OF THE MOON

"THIS APPENDIX IS ALSO ISSUED AS TG-8"

INTERPRETATION OF THE BRIGHTNESS AND POLARIZATION CURVES OF THE MOON

J. J. Hopfield

August 1965

INTERPRETATION OF THE BRIGHTNESS AND POLARIZATION
CURVES OF THE MOON

ABSTRACT

16 17 3

Theoretical models of the polarization of Moonlight and the lunar brightness at small phase angles are given. From lunar data, theoretical models, and laboratory experiments on simulated lunar surfaces, it should be possible to obtain the density and typical particle size of an optical depth of the lunar dust layer.

Author

TABLE OF CONTENTS

LIST OF ILLUSTRATIONS

INTERPRETATION OF THE BRIGHTNESS AND POLARIZATION
CURVES OF THE MOON

J. J. Hopfield

August 1965

I. Introduction

The brightness and polarization of the Moon as a function of lunar space angle θ (Earth-Moon-Sun) have long been studied as a source of physical and chemical information about the lunar surface. Good surveys of the literature are available[1, 2 & 3]. Typical brightness and polarization curves are shown in Figure 1 and 2.

There are two particularly important features shown in these figures. One is the fact that there is no sign of a smooth turnover in the brightness curve at small phase angle; the data suggests the existence of a cusp. Careful recent observations on particular lunar features by van Diggelen[4] near lunar eclipse have shown that this rapid rise is even more accentuated in the 1° – 2° region (Figure 3). The second striking feature is the rapid rise of negative polarization for small phase angles. (Negative polarization is the sense opposite to that introduced by reflection from a dielectric surface.) The data again suggest a cusp at the origin.

The dependence of the brightness of the lunar surface on phase angle, latitude, and longitude near 0° phase angle is generally agreed to be an effect of shadow. The qualitative arguments for this are summarized in Appendix A. In what follows we will show in a simple fashion why the brightness cusp is a consequence of shadow, and a relation between this cusp and the packing factor will be derived.
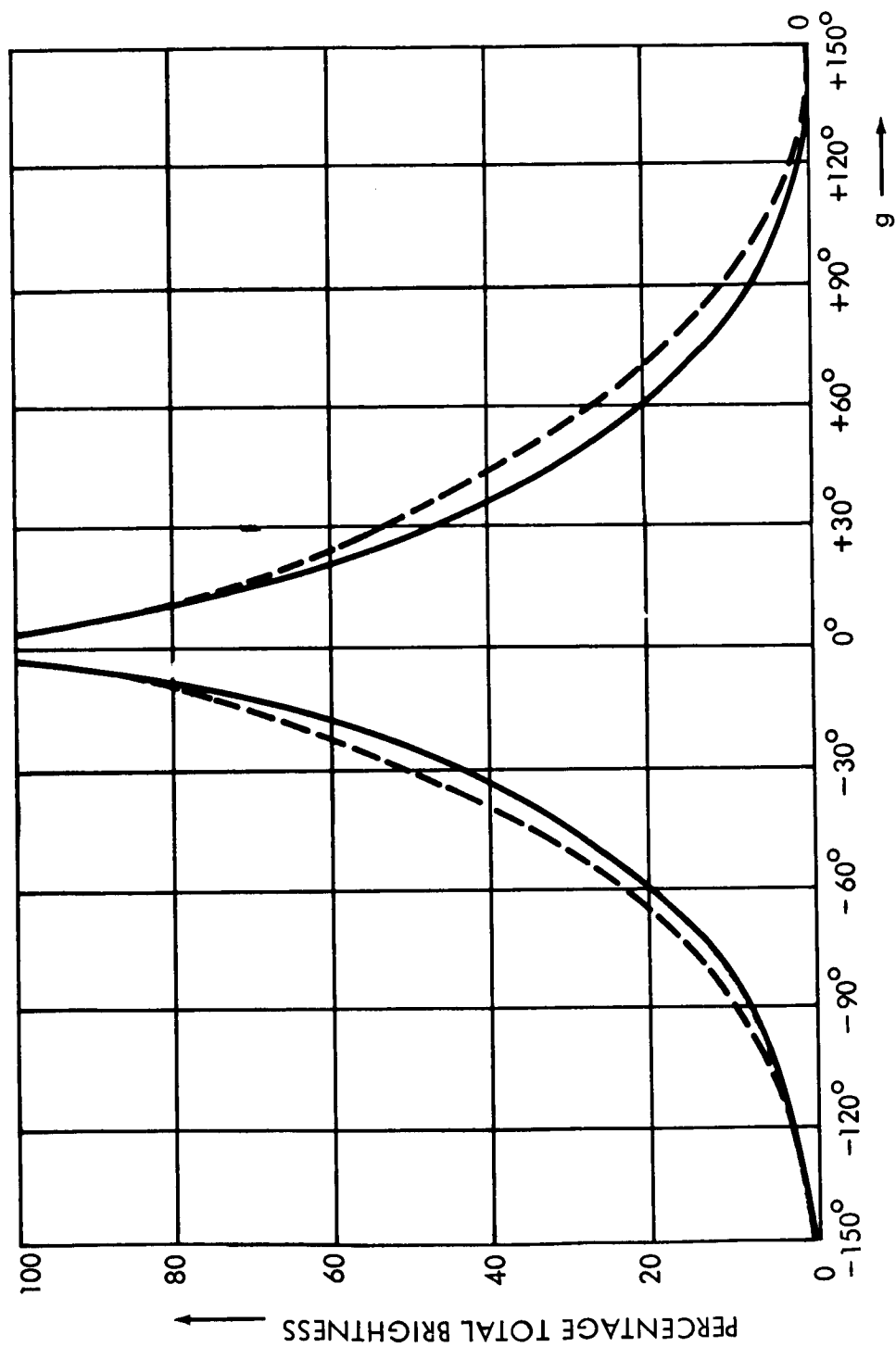
FIGURE 1   THE TOTAL BRIGHTNESS OF THE MOON AS A FUNCTION OF THE
PHASE ANGLE, g.   AFTER ROUGIER (Full Line) AND RUSSELL
(Dashed Line). (Courtesy of C. A. Pearse)
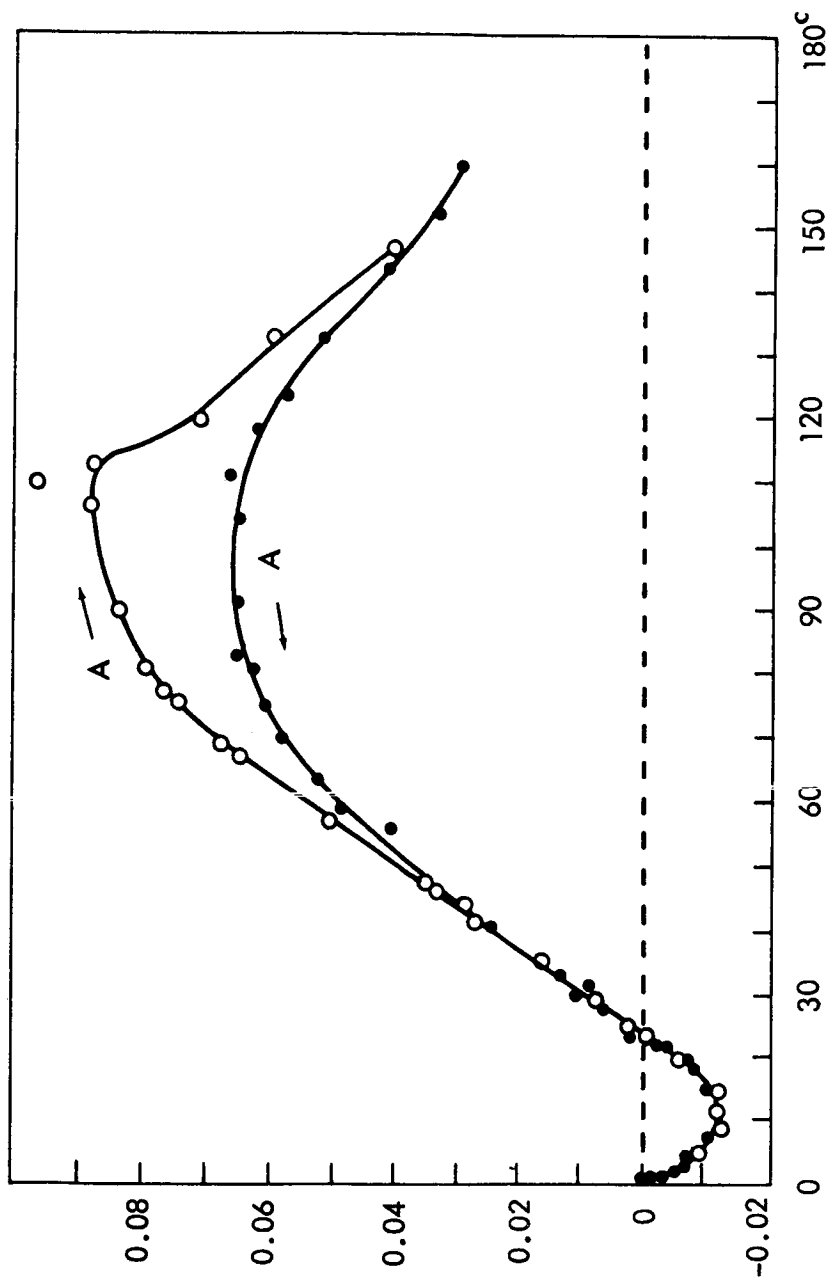
Figure 2 POLARIZATION OF THE MOON (After Lyot , 1929)

(Courtesy of C. A. Pearse)
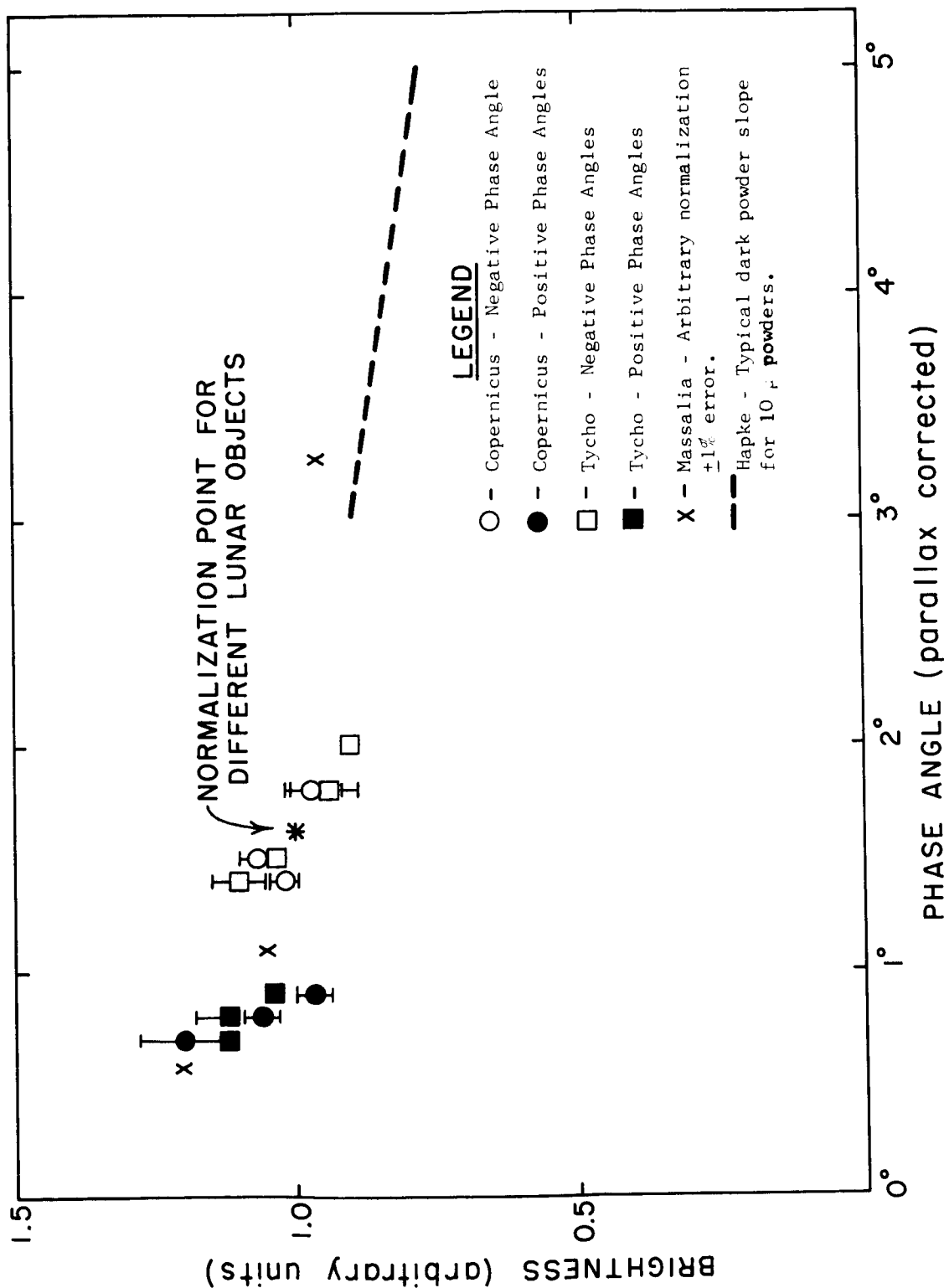
FIGURE 2. The brightness of two lunar craters for small phase angles (after van Diggelen). There appears to be an asymmetry between positive and negative phase angles due to the fact that the craters are not at zero longitude. Typical fractional slopes here are the order of 0.2 degree^{-1}, while in Figure 1 the maximum fractional slope is about 0.04 degree^{-1}.

The physical origin of the rapid onset of negative polarization will also be shown to be a consequence of shadow. The conclusions which can be drawn from present lunar data are discussed, and suggestions for further Earth based experiments given.

II. Shadow and the Lunation Cusp

Consider an opaque, diffusely scattering object located a distance "t" above a plane which diffusely scatters light. Let "d" be a linear dimension of the object. The object and plane are illuminated from above, and observed at a direction Θ with respect to the normal. For $\Theta = 0$, the object and the screen are both illuminated, and the shadow of the object is invisible. For small Θ, an area Θ td of shadow is visible, so that total light returned drops at a rate proportional to Θ . If this shadow is to represent a typical piece of grainy surface, t is the absorption length in the surface layer. The entire surface is covered with such objects. The net surface will have a brightness versus Θ given by
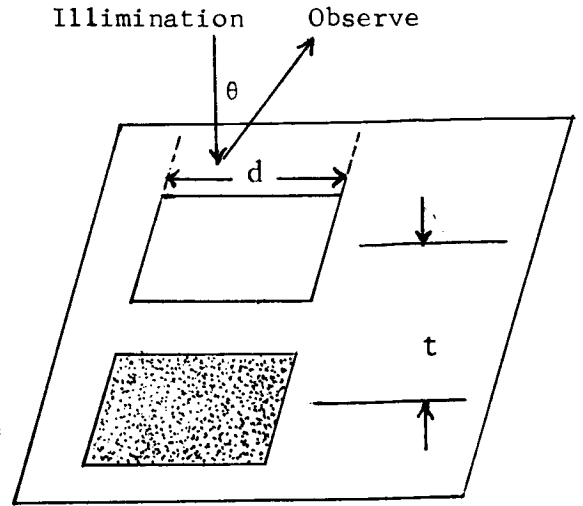
$$B(\Theta) = 1 - \left| \Theta \right| \frac{t}{d} \tag{1}$$

This results in a cusp at $\Theta = 0$ for small Θ.

For opaque particles of dimension d, located at random, having a number density such that the fraction of volume filled is ρ , the absorption length is given by

$$t = d/\rho \tag{2}$$

so the brightness then is

$$B(\Theta) = 1 - \left| \Theta \right| /\rho \tag{3}$$

and directly determines the fraction of volume filled.

Typical small irregular opaque particles have scattering properties which depend weakly on direction, but behave as Θ^2 for small Θ (when averaged over all particle orientations). Unless these particles themselves are underdense and show

-6-

shadow effects, the coefficient of a θ^2 term will be of the order of 1. It is therefore possible to obtain ρ by examination of the backscatter cusp without knowing any details of the particle scattering properties. Use of the $0^\circ - 2^\circ$ points of Figure 4 would yield, from Eq. (3), a ρ in the range 0.05 - 0.15. To obtain a more precise interpretation of the backscatter cusp, it is necessary to construct a model of the covering of the surface with particles. For any particular model, one can obtain the coefficient of the $|\theta|/\rho$ term in Eq. (3), a coefficient which is of the order of one but is model dependent. It is also necessary to estimate to how large angles Eq. (3) holds, and calculate correction terms if possible to extend it to at least $5^\circ - 10^\circ$. Theoretical models are discussed in Appendix B.

SMALL ANGLE BACKSCATTER

UM

HAPKE

BRIGHTNESS

1.00

0.75

0.50

θ/ρ (RADIANS)

0   1   2   3   4
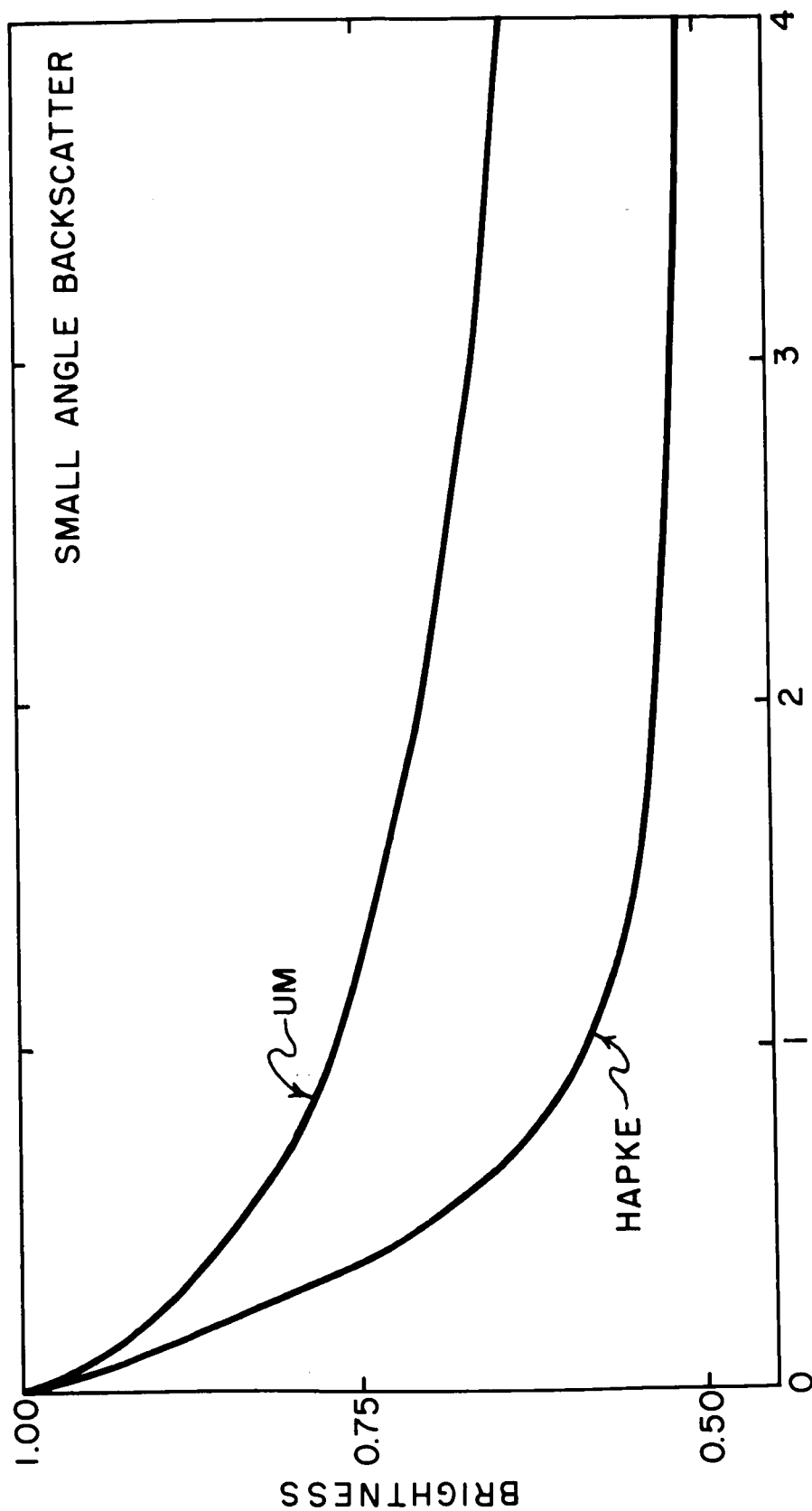
FIGURE .. Backscatter laws for small angle versus angle according to Hapke and the uncorrelated model. For small angles and small angles of incidence, the results are functions of θ ρ only.

-8-

III. Shadow and the Negative Polarization

Let us draw the shadow region of the
object illuminated from above in more detail,
admitting that t and d are not infinite com-
pared to the wavelength of light. The shadow
line is now not arbitrarily sharp, but instead,
some diffraction occurs. For an opaque dielectric or metallic obstacle, the
light diffracted into the region of geometric shadow is partially polarized[Ref. 6 & 7],
its polarization being perpendicular to the shadow edge is shown in the sketch.
The following paragraphs sketch the theory of negative polarization. Details are
given in Appendix C.
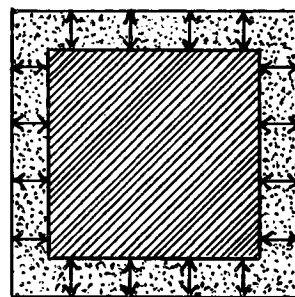
The width of the diffraction region is of the order of $\sqrt{\lambda\ t/2}$, where λ is
the wavelength of the light and t is the distance between the object causing the
shadow and its shadow (see sketch on Page 6). The mean brightness in this
region is 1/8 of the unshadowed brightness.

The behavior of the polarization with the diffraction angle θ in the shadow
region is not simple, but an overall average $P \cong 2.5\ (\theta)$ is about right for the
edge region.

The physical origin of the negative polarization is now easy to see. The
shadow area which becomes exposed to view for small phase angles contains some
diffracted light, and this light is polarized with its E - vector lying in the
plane of incidence (negatively polarized). If t is an absorption length and d is
a typical particle size, this negative polarization saturates at a value

$$P \cong 0.3\left(\frac{\lambda}{d}\right) f \tag{4}$$

where f is a depolarizing factor described in Appendix C. Possible values of f

range from 0.5 to 1.0, and the value for the Moon should be very near 0.67. The maximum negative polarization observed of 0.012 could be produced using Eq. (4) by particle sizes d of about 10 microns. The polarization should attain its half-value at the diffraction angle

$$\phi = 0.7 \sqrt{\lambda/t}$$

A more detailed description of the derivation of Eq. (4) is contained in Appendix C.

While there can be no direct experiments which show this to be the polarization mechanism responsible for the negative lunar polarization, several qualitative results indicate that this is indeed the mechanism of polarization in laboratory experiments on simulated lunar surfaces. Dollfus[Ref. 3] has found that dark powders which produce a negative polarization at small angles do not produce this negative polarization when investigated a grain at a time. His and previous investigations have also shown that powders made from small, opaque particles generally show the negative polarization. All these results are simple consequences of a theory based on shadow.

If a variety of particle sizes are present, the polarization measurement weights the small particles heavily. Thus, if ten parts by weight of 100 μ particles are mixed with one part by weight of 10 μ particles, the resultant polarizaton would be that characteristic of 20 μ particles.

IV. Discussion

The small angle brightness and polarization properties of the Moon are qualitatively explicable in terms of a simple theory of the effect of shadow and diffraction in an underdense system whose particles are many wavelengths in size. That these functions could be experimentally reproduced in such a system was shown by Hapke[8], following the work of Lyot and others. The question which we shall attempt to answer here is how unambiguously to compare lunar observations, theory, and experiments on simulated lunar surface.

Brightness measurements and comparisons over large ranges of phase angles necessarily involve an understanding of the angular dependence of the scattered intensity and polarization of the light scattered by a single particle. The scrambling of single particle properties, the effects of microscopic shadowing, and the effect of microscopic structure (for example, roughness on a one centimeter scale) preclude any unambiguous comparisons for large angles. This point is well illustrated by the theoretical attempt of Hapke[5] to fit the photometric data of the Moon at all angles*. His fit, generally quite good at angles of 10° and greater, fails badly at the small angles shown in Figure 4. His value of a parameter g of ~ 0.5 corresponds to a density of about 0.5 (see Appendix B), while the experimental points at small angles require a filling factor more like 0.1 (g of ~ 0.1). At large angles Dollfus[3] has found that the positive polarization of powders in the laboratory is not strongly sensitive to particle size, while the small angle negative polarization increases with decreasing size. These are but two examples of the problem of large angle interpretations.

---

*The theoretical curves in this reference are badly drawn. Each should have a large slope discontinuity at the origin instead of the smooth rounded peaks indicated.

The qualitative theory of small angle brightness and polarization phenomena suggests that unambiguous interpretation of lunar small angles data can be made by comparison to laboratory experiments on appropriate powder specimens. The laboratory experiments ideally would be similar to those already performed by Hapke[Ref. 8] on dark powders. The scant information available in this angle range is not in fact inconsistent with lunar data (Figure 4). It is, however, the 0° - 5°, and especially the 0° - 2° range which should be emphasized. Additional parameters essential to the interpretation beyond the brightness and polarization curves are the sample surface density (or optical depth) mean particle size, and the depolarizing factor for the sample at normal incidence. At present no such complete laboratory experiment has been done.

The theoretical situation on brightness versus phase angle for small phase angles is relatively simple. The problem in interpreting the experiments is to know whether the small angle limit has been reached, or whether the ambiguities of theory at larger angles are present. Presuming (and this is sheer presumption) the small angle regime has been reached, a filling factor ρ of ~ 0.1 would be the best estimate. If the uncorrelated model is more appropriate and this presumption were not true, the present data could be interpreted as a ρ as low as 0.02. The theoretical situation on the polarization is not as clear, for the diffraction problem needs to be considered in detail. Here an error of a factor of 5 in the particle size is not impossible. Further theoretical work can improve both these estimates.

There are certain limits which must apply if the theory is qualitatively correct. First, the requirement of "geometrical shadow" leads to a limit

$$\lambda \lesssim 2 \rho d$$

Second, the fact that the backscatter peak does not show strong diffraction limitation at 2° while the polarization is rapidly rising in this region puts limits on the typical diffraction effects. One finds

$$t \gtrsim 100 \quad \lambda$$

The quoted values do obey these limits.

The comparison between lunar data and either theory or laboratory experiments is at present severely limited by the large error limits on the lunar brightness data for small phase angles. It seems both possible and strongly desirable to lower van Diggelen's error limits by a factor of 5.

Measurements by Gehrels[Ref. 9] on the asteroid Massalia are also of interest in attempting to understand the brightness curve of the Moon. In this case the quoted accuracy of the data is $\pm 1\%$. Apparently Massalia, like lunar features, also has an abrupt rise in its brightness for very small phase angles. This data is also shown in Figure 4.

The optical data itself is insensitive to the form of the particles. Linear particles as in steel wool or more complicated interconnected structures could yield similar backscatter and polarization results at similar densities and diameters of "particles."

While firmer numbers must await further experimental and theoretical investigations, certain limits seem clear. The lunar surface material cannot have a filling factor appreciably greater than 0.1 and quite possibly less. Typical particles are opaque and have linear dimensions of the order of 10 microns. This as a suggestion is scarcely original. The present state of theoretical understanding of the optical data now seems to <u>require</u> such a "fairy castle" surface though it need not be more than about .01 cm thick to cause the observed optical effects.

REFERENCES

1) C. A. Pearse, "Photometry and Polarimetry of the Moon and Their Relationship to the Physical Properties of the Lunar Surface," Bellcomm Report dated August 23, 1963.

2) V. G. Fessenkov, "Photometry of the Moon," in Physics and Astronomy of the Moon, editor Z. Kopal, Academic Press, New York (1962).

3) A. Dollfus, "Polarization of Moonlight," Physics and Astronomy of the Moon, editor Z. Kopal, Academic Press, New York (1962).

4) J. van Diggelen, "Planet" Space Sci. 13, 271 (1965).

5) B. Hapke, Journal of Geophysical Research C8, 4571, (1963).

6) Born and Wolf, Principles of Optics, pp. 562-575 Pergamon Press, London (1962).

7) F. Jentzsch, Ann. der Physik 84, 292 (1927-28).

8) B. Hapke, Annals of the New York Academy of Sciences 123, Art. 2., 711 (1965).

9) T. Gehrels, Astrophys. j. 123, 331 (1956).

APPENDIX A   GENERAL CONSIDERATIONS ON BRIGHTNESS VERSUS PHASE ANGLE

The surface of the Moon has an albedo for an average region of about 0.08.
This number is of the same order as that to be expected for a wrinkled dielectric
surface made up of minerals having an index of refraction around 1.7 - 1.8.
If multiple scattering were important, the albedo would be much larger.

A simple distribution of slopes on a dielectric lunar surface would not give
a backscatter peak. Nor, would it give a uniformly bright (neither limb-bright
nor limb-dark) Moon. There are, however, two understood mechanisms by which
backscatter peaks can occur. One is due to the backscatter peak of transport
spheres (or of corner cube reflectors), familiar in beaded movie screens. The
other is due to the shadow, and the fact that shadow is not visible when viewed
from the source of illumination.

The strong backscatter peak of transparent spheres disappears in opaque spheres,
or in transparent irregular objects. The albedo of the Moon demands covering
particles (if any) which are opaque or very nearly so. Since a theory of shadow
as the origin of the backscatter peak is immediately consistent with the correct
albedo and does not demand specific regularly shaped objects, it has been the
basis of most recent attempts at understanding the brightness curve of the lunar
surface. It seems much more likely that the Moon is covered by irregularly
shaped particles than by sufficiently regular spheres.

Both the transparent sphere and the shadow calculations of backscatter
recognize the necessity of involving relationships between two different parts
of the lunar surface. In the case of the spheres, this effect is an amplitude
interference effect of physical optics between light scattered from different

areas of a spherical surface. In the case of shadow, the effect is an intensity effect of geometrical optics between light scattered from a surface and light not scattered from its shadow. Whereas the scattering from spheres demands surfaces which are regular on the scale of a wavelength to preserve phase in the interference effect, the shadow effect does not.

APPENDIX B   THEORETICAL BRIGHTNESS MODELS AT SMALL ANGLES FOR AN UNDERDENSE

SURFACE

We will treat a model of the lunar surface consisting of independent

scatters distributed below a plane called the "lunar surface." Only scattering

near normal incidence will be treated, larger angles

being conceptually no more difficult but

computationally messy. An object located a

distance x below the surface contributes to

the brightness of the Moon if the incoming

and outgoing paths are not blocked. Let the

volume of each (opaque) scatter be d^3 and the

number density of the scatterers be n per cc.

The absorption coefficient is then nd^2, and

the absorption length, expressed in terms of the fractional density ρ , is d/ρ.
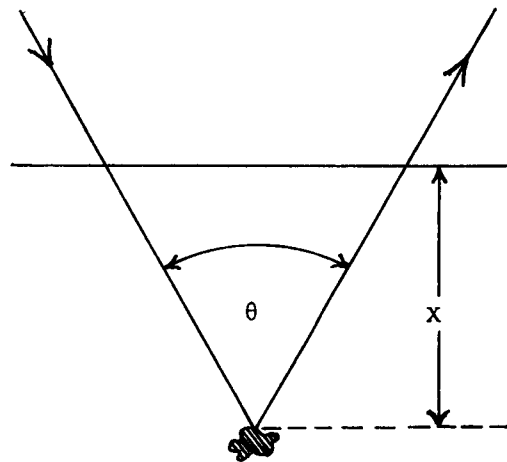
The intensity scattered $B(\theta)$ as a function of θ , is proportional to

$$B(\theta) \propto \int_0^\infty ndx \, W(x,\theta)$$

where $W(x,\theta)$ is the probability that neither the incoming path nor the outgoing

path is blocked by an object. When $\theta = 0$, the incoming and outgoing paths

are the same, the probability of a straight line path of length x not being

blocked is simply $e^{-x/d}$ for this medium. For $\theta \neq 0$, two models will be dis-

cussed. One model, the uncorrelated model is new; the other is a corrected

statement of a model treated by Hapke[Ref. 5].

In the uncorrelated model the particles of the surface materials are regarded

as being distributed at random. The probability that the incoming and outgoing

-17-

paths are both not blocked can then be calculated as follows. Draw cylinders of cross section d^2 around the incoming and outgoing rays. The path is clear if the volume of these cylinders contains no particles. Let V be the total volume of these cylinders, counting the common volume of intersection only once. The probability that this volume is empty is then

$$W(x,\theta) = e^{-nV}$$

For $\theta = 0$,

$$W(x,\theta) = e^{-x\rho/d}$$

For $\theta >> \rho$ but $\theta << 1$

$$W(x,\theta) = e^{-2x\,\rho/d}$$

Thus, the backscatter peak will be a factor of 2 in intensity. For general θ, a numerical calculation is necessary to obtain the form of the brightness $B(\theta)$ and this is shown in Figure 4. For $\theta << \rho$, the brightness can be analytically calculated to be

$$B(\theta) = 1 - |\theta|/\rho$$

That this small angle form is valid only at very small angles (for the uncorrelated model) $\theta \simeq 1/20 \, \rho$ can be seen from Figure 4. The effect of finite lunar longitude at very small phase angles on the backscatter cusp is to increase the steepness on one side and decrease the steepness on the other so that the average of the two is the same as zero longitude.

Hapke's model is similar up to the point of attempting to construct a model for $W(x,\theta)$. Hapke argues that, looking toward the surface from a typical scattering center, one sees an open space whose linear dimension is y, and thus an open cylinder cross section of area y^2 and length x exists. If the return

light stays within this cylinder, it is unattenuated. If the return light does not stay entirely within this cylinder, Hapke assumes its attenuation would be as great as that for any random single path of length x. These suppositions lead to the form of the backscatter law which is shown in Figure 4. For small θ, this law gives

$$1 - \frac{3|\theta|}{4\rho}$$

but the range over which a linear approximation is valid is much larger than for the uncorrelated model.

The identification of y in Hapke's model is necessary for a comparison with other models or with experiment. Hapke misidentifies this parameter as being the particle separation. It is clear, however, that if one looks toward the surface from an absorption length below the surface, one observes a projected surface on which approximately half the area is covered by objects of linear size d. The separation between these objects on the projected surface is also of the order of d, not of the order of the actual particle separation. The best interpretation of Hapke's model parameter g is simply ρ. Even this interpretation is unfortunately not certain within about a factor of 2, as y is not given a mathematical definition in Hapke's model. (The densities of lunar material derived in Hapke's paper are based on this erroneous interpretation of y and should be discounted.)

Both models suffer from the fact that their characterization of the correlation between particles of the surface material is poor. A better model of the surface could improve this point. The Hapke model does not in fact define a surface structure which would give the calculated scattering properties.

The uncorrelated model surface is well defined, but incapable of supporting its particles mechanically.

Further calculations on correlated structures should be made. The detailed experimental investigation of any surface which shows small angle backscatter would clearly be of assistance in assessing the need to construct a correlated model and the range of the $1 - |\theta|/\rho$ approximation.

An attempt to account for the diffraction produced polarization only to first

order will be made. Single diffraction only

will be treated. Thus, an area must be either

illuminated by the direct beam or visible

in a rectilinear path to contribute to the

brightness.

Consider an edge of length d illuminated from

above and casting a shadow on a diffuse screen

at distance x below the edge. Let the diffuse

screen be viewed at an angle θ with respect to

the illuminating direction as shown in the sketch.
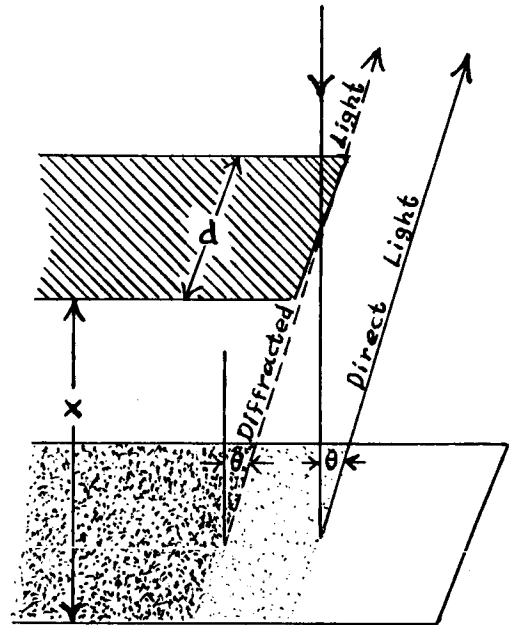
Exact expressions for the polarization of light near the edge of the

geometric shadow are available for ideal geometries and a diffraction edge

consisting of a perfectly conducting plane of negligible thickness. While

these expressions are not precisely of quantitative applicability to the

present problem of diffraction around an irregular opaque dielectric obstacle,

the essential physics of the situation is preserved. The two essentials are

first, that an opaque diffracting edge exists, and second, that the edge be

made of a material with a large (complex) electric

susceptibility at optical frequencies, so that the

boundary conditions suppress electric fields

tangent to the surface E_t in the sketch com-

pared to the component E_n. Indeed, experiments

performed by Jentzsch [Ref. 7] on steel knife edges at optical frequencies (at
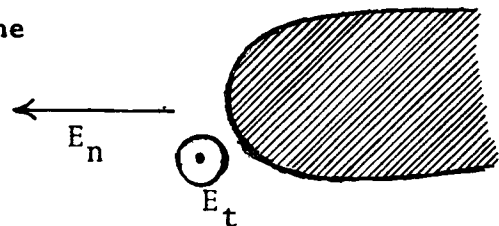
these frequencies steel is a very poor metal) still give agreement with the idealized calculation within about a factor of 3. We will in fact use the empirical result of Jentzsch, that the fractional polarization

$$P \equiv \frac{P_1 - P_2}{P_1 + P_2}$$

behaves as $P = 2.5\,\theta$, where θ is the diffraction angle in radians.

The illumination in the shadow region can be in good approximation obtained from the Cornu spiral. If an average is made over a diffraction angle

$$\theta = \sqrt{\frac{\lambda}{2x}}$$

the diffraction region is lit at about 1/8 intensity of the nonshadow region. These crude approximations will be used to calculate the expected polarization.

Each edge which polarizes (two per square) is associated with an unpolarized return from a surface of area $d(d/2)$. If t is the absorption length, the distribution of edge-to-screen distances will be an exponential with t as the absorption length. The net polarization of the return is then

$$P = \frac{5}{8}\,\frac{1}{d}\left\{\theta^2\left[1 - 3^{-1/2\,\lambda/\theta^2\,t}\left(\frac{\lambda}{2\theta^2 t}+1\right)\right]+\frac{\lambda}{2t}\,e^{-\lambda/\theta^2 t}\right\}$$

For small θ, $P \simeq (5/8)\theta^2(t/d)$ $\theta^2 \ll \dfrac{\lambda}{2t}$

For large θ, $P \simeq 0.3\,\dfrac{\lambda}{d}$ $\theta^2 \gg \dfrac{\lambda}{2t}$

This polarization would be received if the screen on which the shadow falls did not depolarize the light. In fact, the lunar surface does depolarize initially polarized light to about 1/3 of the initial polarization. The opposite edge from that shown in sketch on previous page is an edge in which there is a

region of screen fully illuminated by the incident light but not visible to the observer except via diffraction. Exactly the same considerations apply to this edge as to the one just treated, except that no depolarizing factor occurs in this case. The net depolarizing factor (f of Eq. (4) in the main text) is the average of these two values, or 2/3.

The calculation as done here does not reproduce the linear rise of negative polarization seen experimentally for small phase angles. Indeed, one of the mysteries of present lunar data is that there is as yet no evidence of the diffraction turn-over in the sharpness of either the backscatter or the polarization peak. Present data suggests that this diffraction angle is at or below 2°. If this is the case, the form of the rise of the observed polarization peak will be due to density fluctuations, an occurrence not allowed for in the present theory. The saturation value would be unaltered by such fluctuations.

APPENDIX VIII

ELECTROMAGNETIC AND THERMAL PROPERTIES OF THE MOON'S SURFACE

"THIS APPENDIX IS ALSO ISSUED AS TG-9"

ELECTROMAGNETIC AND THERMAL
PROPERTIES OF THE MOON'S SURFACE

B. Lax

August 1965

ELECTROMAGNETIC AND THERMAL PROPERTIES OF THE MOON'S SURFACE

ABSTRACT

1 6 1 7 4

Radar reflection has provided an estimate of the dielectric constant k of the Moon's surface to depths of meters. The value of k = 2.6 corresponds to a porosity of $\sim$ 70% and a density $\rho \approx 1.0$ gm/cm^3. Thermal measurements at infrared of the lunation and eclipses yield values of the thermal inertia $(K\rho C)^{-1/2} \approx 750$. Since C = 0.2 cal/cm sec deg, the thermal conductivity is estimated to be $K \approx 8.5 \times 10^{-6}$ cal/cm sec deg C. From radiometric measurements at microwave and millimeter frequencies the ratio of the thermal and electrical conductivities are determined. This yields an electrical conductivity $\sigma \approx 4.3 \times 10^{-5}$ mho-cm^{-1} corresponding to a loss tangent of $\sigma/\omega^t \approx 3 \times 10^{-3}$. The most important of all these results is that an estimate of the bearing strength can be made from the density and the thermal inertia when correlated with laboratory measurements of porous and powdered rocks of many varieties. If the estimate is made conservatively to correspond to powdered rock, then the bearing strength is approximately 75 lbs/sq ft. It is recommended that more extensive experimental and theoretical studies of combined radar, radiometric, infrared and supporting laboratory experiments be conducted to verify the present estimates and to reduce the limits of uncertainty of the relevant thermal and electromagnetic parameters.

Author

TABLE OF CONTENTS

LIST OF ILLUSTRATIONS

ELECTROMAGNETIC AND THERMAL PROPERTIES OF THE MOON'S SURFACE

B. Lax

August 1965

I. Introduction

Sufficient information exists within the published literature regarding the optical, radar, radiometric and infrared measurements of the Moon's surface to provide an intelligent guess of the physical strength and constitution of the surface to depths of several meters. An important ingredient in making these estimates is the pertinent data supplied by laboratory measurements of the electromagnetic, thermal, and physical properties of terrestrial material in various composition and physical states. There are limits of uncertainty in the quantitative estimates of some of the parameters which will only be removed when actual tests of the Moon's surface material is made by future space projects in conjunction with Surveyor and Apollo. Nevertheless the ground-based experiments and those space borne in the near future will provide complementary information that will enhance our knowledge of the Moon's surface and permit a greater selection of suitable sites for landing of instruments, and subsequently, manned vehicles on the Moon.

The radar data provides us with the best estimate of the actual dielectric constant of the Moon. If we can identify the material on the Moon with those on Earth, we can then predict within

certain limits the packing fraction or porosity of the Moon's surface to an average depth of a meter or more depending on the wavelength. We can also bracket the mean density of the porous material. From infrared data of the cooling during lunation and eclipse, it is possible to estimate quantitatively the thermal parameter of inertia cooling. This quantity can then be correlated with the density giving upper and lower bounds to the probable nature of the constitution of the material as correlated with a fair number of similar measurements on laboratory specimens of a wide variety. From radiometric measurements of temperature variation of the lunar surface at microwave and millimeter frequencies, information is obtained about the thermal and electrical conductivities of the Moon's material near the surface. The estimate of the thermal inertia parameter does provide a rough index of the bearing strength when correlated with probable density from the radar data. The remainder of this paper is devoted to a discussion and review of the situation followed up by recommendation for further investigations for the future.

II. Radar Measurements

The measurement of the electromagnetic properties of the Moon's surface from ground-based instruments is a useful and relatively convenient approach to deducing the physical nature of the upper layer of the Moon. Optical reflection, radiometric and infrared emission and radar reflection constitute some techniques examined to date. The optical investigations provide information essentially about the immediate surface to depths of the order of microns, whereas the infrared radio and radar offer possibilities to probe deeper into the surface layer, the latter to depths of a meter or more, depending on the nature of the surface itself and the wavelength. The experimental and theoretical work carried out to date indicates that quantitative raw data with reasonable reliability can be obtained from the measurements. The difficulty in the problem lies in the detailed interpretation and evaluation of the numbers. These are critical in establishing some sensible model of the physical nature of the Moon's surface layer in both the highlands and maria.

Radar data, which at this stage appears to be the most reliable means for determining the average or statistical dielectric constant of the surface layer, yields a value[1] of about 2.6 - 2.8. This is in disagreement with those deduced from radiometric measurements of temperature[2] and polarization[3] which yield 1.5 - 2.0. In spite of this disagreement, the conclusion drawn from either result is that the surface layer is porous or "dust-like." However, the

packing fraction may vary from about 0.1 to 0.5 from the low to the high limit of the estimates of the dielectric constant if we assume material of dielectric constant k_i of about 7 in solid form as appropriate from laboratory studies and other indirect evidence. A larger value of k_i will further reduce the density estimate of the porous material. In order to estimate the porosity, a simple formula is quite adequate at this stage where only rough estimates can be made; namely,

$$k_{eff} = 1 + (k_i - 1) W_o \qquad (1)$$

where K_{eff} is the deduced or effective dielectric constant evaluated from the reflection coefficient R, and W_o is the packing fraction.

$$k_{eff} = \frac{1 - \sqrt{R}}{1 + \sqrt{R}} \qquad (2)$$

The above formula of Eq. (1) can be obtained by simple logical argument, but actually has been evaluated theoretically from a homogeneous layer of structure in which the dimensions of the layers are small compared to the wavelength. The next higher order of expansion takes into account the dimensional effects which serve to reduce the dielectric constant. The above expression serves our purposes as well as the more elaborate treatments of scattering from aggregates by spheres or spherical holes in a porous solid as indicated in Figure 1. This shows experimental points of observed dielectric constant of powdered quartz of varying density and is compared with theoretical curves including that of Eq. (1).
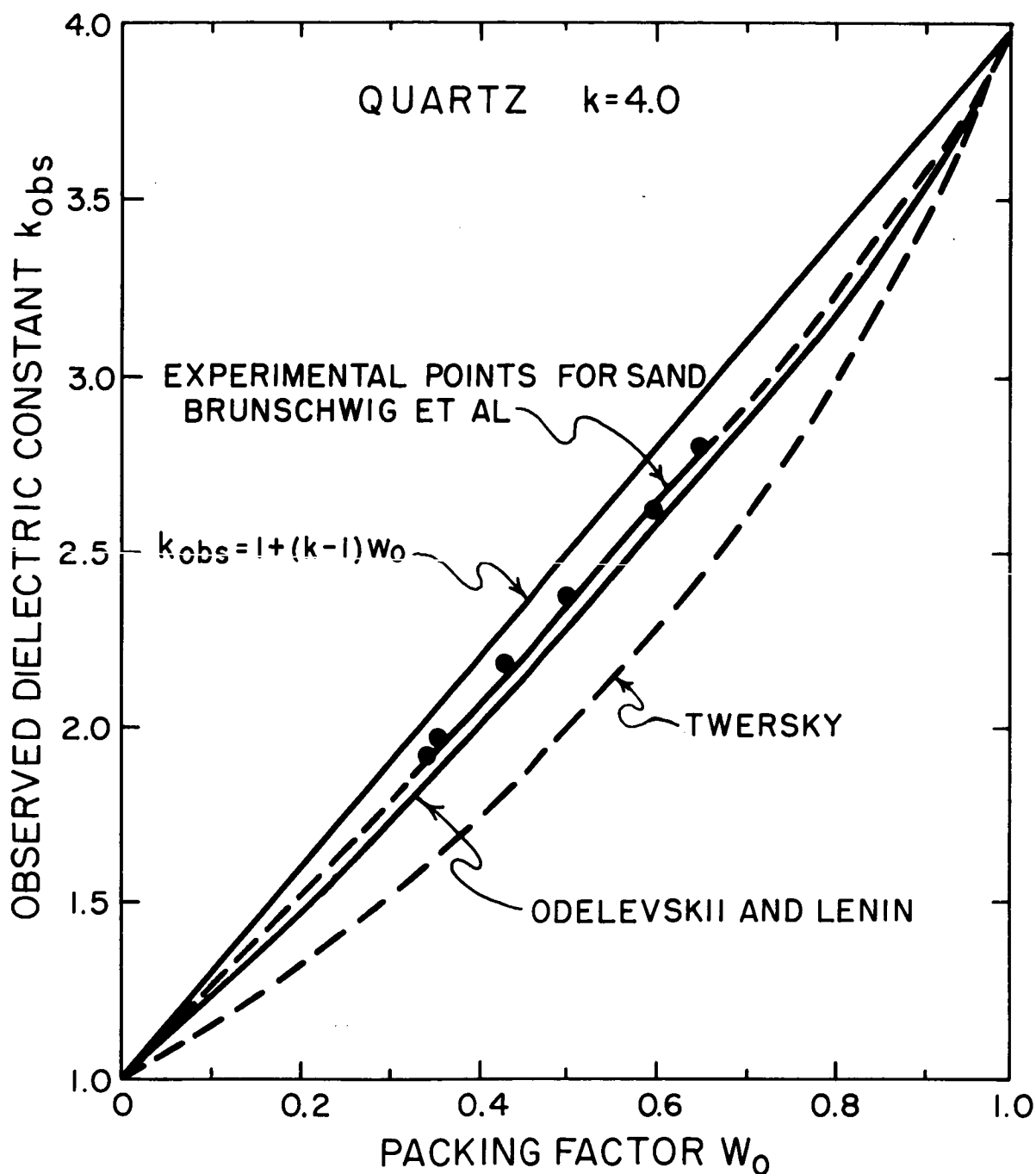
Figure 1 Variation of dielectric constant of powdered quartz as function of density. Dots are experimental data from Tensler, et al, Ref. 6. Theoretical curves reproduced from Evans, Ref. 1. The straight line is the theory of equivalent porous layered structure.

III. Radiometric and Infrared Measurements

There have been two kinds of radiometric measurements made at microwave and millimeter wavelengths on the surface of the Moon. The earliest and most extensive measurements have been those which have measured the temperature variations of the Moon's surface with lunation and the phase lag associated with it[4]. The other measurement has been to study the polarization of the thermally emitted radiation[3]. This measures the dielectric constant directly as in the radar case. The measurement of the temperature variation on the other hand relates the electromagnetic properties to the thermal properties[2]. However, in order to deduce the former it is necessary to know the thermal parameters of the Moon's surface. The usual scheme is to take this data from other sources such as the lunation or eclipse temperature decay experiments at infrared[5]. The radiometer experiments give the ratio of the penetration depth of the electromagnetic wave to the thermal wave[2]. These are given respectively in terms of the electromagnetic and thermal parameters as follows:

$$\delta_e = \frac{1}{\sigma} \sqrt{\frac{\varepsilon}{\mu}} \tag{3}$$

where δ_e is the penetration depth for microwaves and ε the effective permitivity, μ the permeability (assumed to be that of free space) and σ the conductivity of the porous medium. The above formula holds when the medium has a low loss tangent, an assumption which is quite reasonable for a good dielectric such as one would

expect for terrestrial material[6]. The thermal depth δ_t is given by

$$\delta_t = \sqrt{\frac{2K}{\rho c \omega}} \qquad (4)$$

where K is the effective thermal heat conductivity, ρ the density, c the thermal capacity of the porous surface material on the Moon, and ω the frequency of lunation. The experiment provides information about the ratio of the thermal and microwave penetration[2]. This establishes a relation between the thermal conductivity and the electrical conductivity. One of these has to be independently determined to evaluate the other. The procedure that is indicated is as follows. From the thermal data of lunation or eclipse a value of the thermal parameter

$$\gamma = (K\rho c)^{-1/2} \qquad (5)$$

is obtained. For most materials measured in the laboratory the accepted value of the heat conductivity is c = 0.2 cal/cm sec deg. The value of $\gamma \cong 750$ is estimated as a good one in light of most recent fitting of theoretical curves to the cooling data of the Moon[7]. The difficult task is to estimate the value of the density. In principle this can be deduced from the radar data. If we take the value of the real dielectric to be about 7 corresponding to a mean of earthly rocks and other material (slightly higher than quartz), then from Eq. (1) the filling factor we obtain is $W_0 \cong 0.3$ which corresponds to a density ρ = 1.0 gm/cm^3. The value of K one then obtains from Eq. (5), K $\cong$ 8.5 x 10^{-6} cal/cm sec deg c, is a very reasonable number consistent with terrestrial

material of granulated structure[7],[8]. Now that K is known, it is also possible to estimate the value of the electrical conductivity as follows: From radiometric measurements[2] it is deduced that the ratio of the penetration parameters $\alpha = \delta_e / \delta_t$

$$\alpha / \lambda \approx 2.0 \text{ cm}^{-1} \text{ or } \delta_e \approx 2\lambda \, \delta_t \qquad (6)$$

But now, δ_t can be calculated from Eq. (4) since all the parameters are already estimated. The value obtained for 10 cm radiation is $\delta_e \approx 116$ cm, indicating that the microwaves of this wavelength penetrate to the order of a meter or more. Since the wavelengths that have been utilized vary from 11 meters for radar to 4 mm for the radiometers, the corresponding electromagnetic penetration is estimated to be 130 meters to 4.6 cm respectively. The assumption is that the conductivity is wavelength dependent or that the dielectric loss ε'' is frequency independent. This is borne out by experiments[6]. Then from Eq. (3) we can evaluate $\sigma = 4.3 \times 10^{-5} \text{ mho}^{-\text{cm}^{-1}}$. This yields for the loss tangent $\varepsilon'' / \varepsilon = \sigma / \omega \varepsilon \approx 3 \times 10^{-3}$. This is fairly low as compared with fragmentized material of terrestrial material[6] suggesting very small particle sizes of the order of 1 - 25 microns if compared to material found on Earth[8].

IV. Bearing Strength

The density and thermal inertia quantities determined from the radar and infrared data can be used to estimate the probable value of the bearing strength of the Moon's upper layer to depths of about a meter if these values are identified with equivalent terrestrial material. These values of density ρ = 1 gm/cm^3, thermal constant K and thermal inertia coefficient $\gamma = (K\rho c)^{-1/2}$ = 750 from ground measurements correspond to a porous or powdered material. This is deduced from the graph of Fig. 2 obtained from experimental data in the laboratory[8] for fragmented or pulverized material of 1 - 25 micron size. The graph also shows porous material which is foam-like sintered material whose thermal interior is lower than that of powdered material. Jaffe[9] has measured the load under which a penetrameter of a given diameter will sink into loose basalt powder to a depth equal to its diameter. The graph of Fig. 3 shows the plot of bearing strength as a function of density for powdered material as a function of density. When this is extrapolated to lower values to that corresponding to the porosity measured for lunar dust, the bearing strength is 35 g/cm^2 or 75 lbs/sq ft.
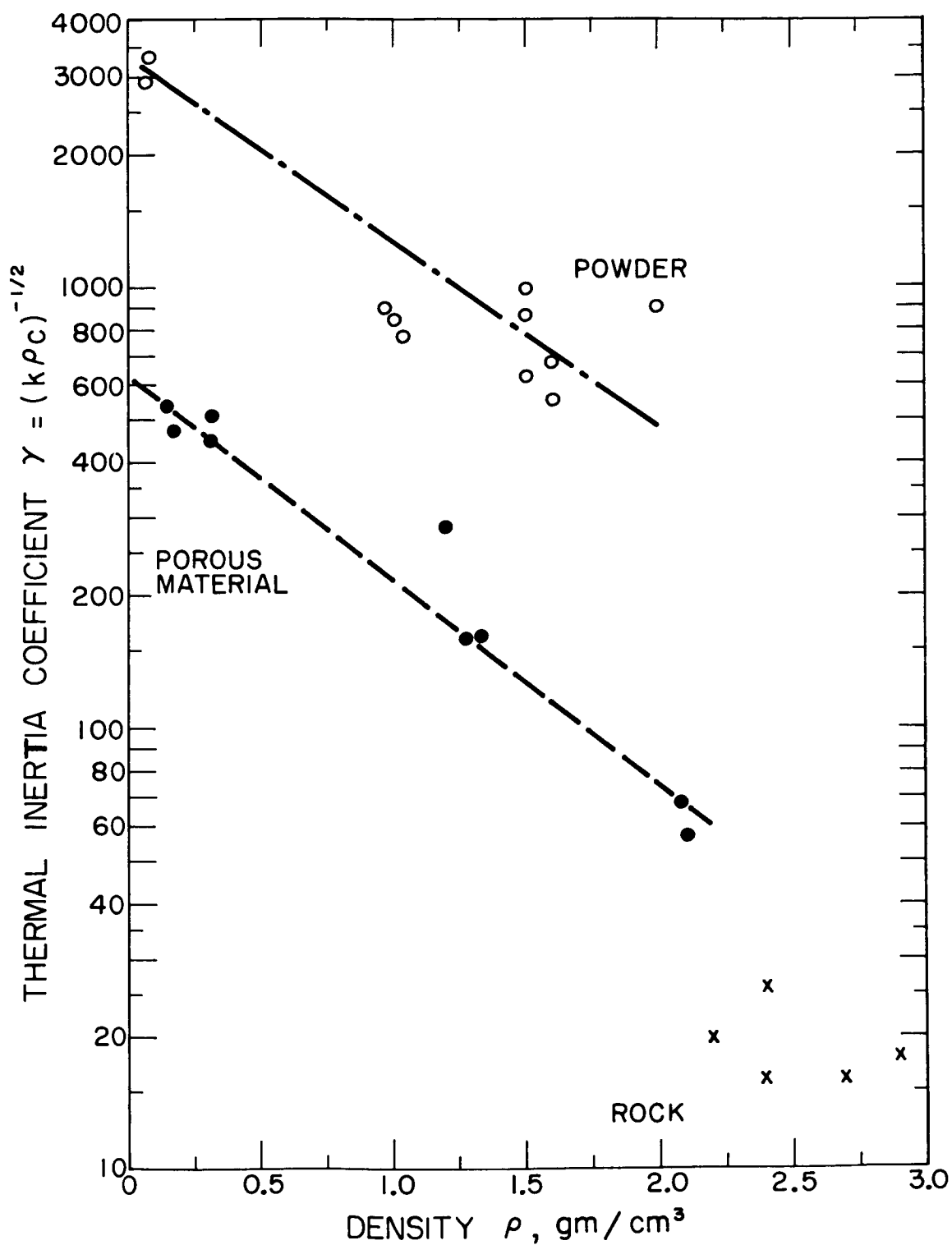
Figure 2 Experimental data of the variation of thermal inertia coefficient $\gamma = (K\rho c)^{-1/2}$ as a function of density for two classes of material (1) pulverized powdered rock and (2) sintered porous material. Data obtained from Glaser, et al, Ref. 8.
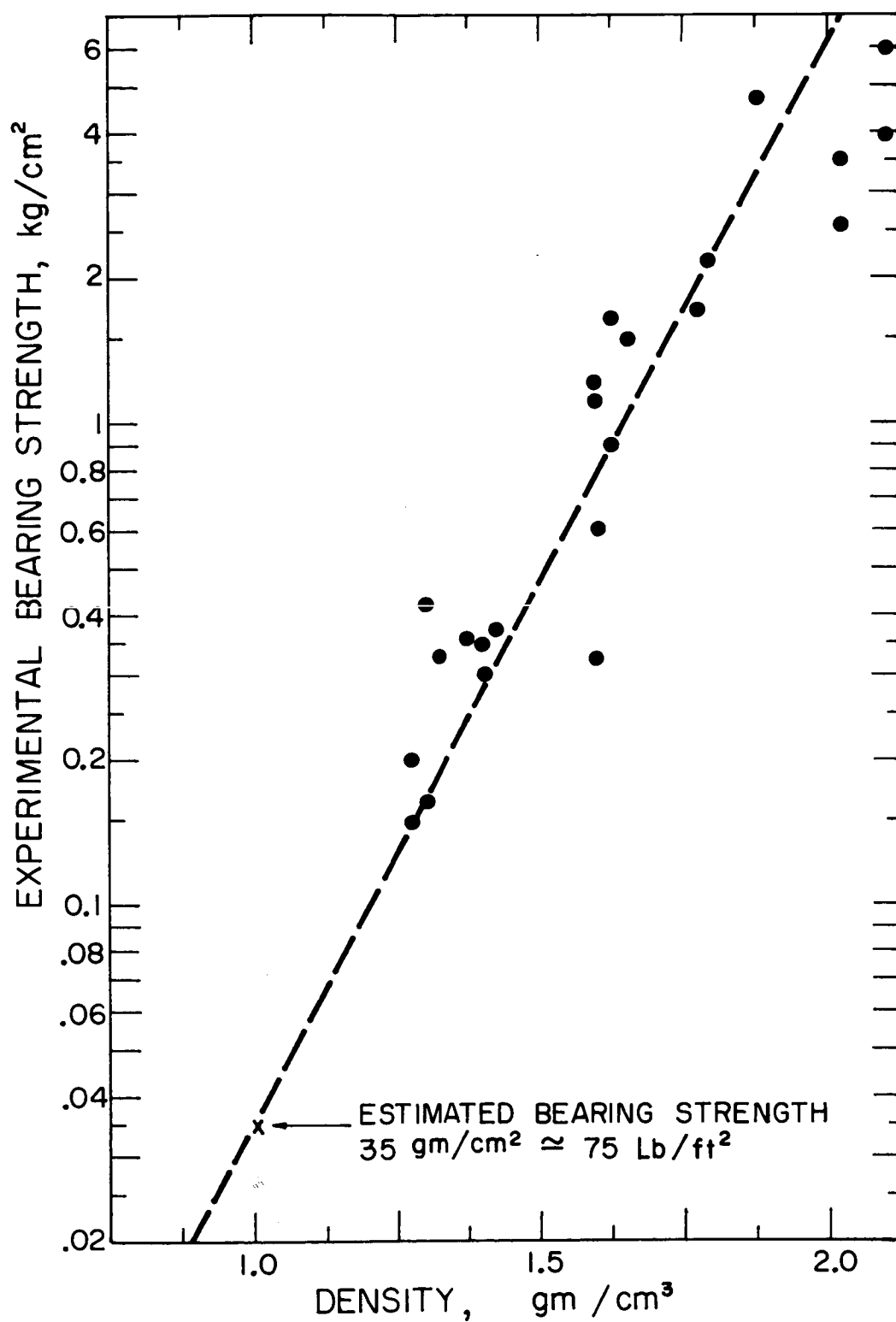
Figure 3 Experimental measurements of bearing strength of powdered material as a function of density extrapolated to probable value of surface layer of Moon. Data is that obtained by Jaffe, Ref. 9.

V. Conclusions

The estimates made in this paper based on the review of the data in the literature is still speculative. Almost all of the estimates of the parameters quoted are based on a homogeneous model of the Moon's surface. Consequently, the values quoted represent a statistical average of the quantities desired. An assumption of the homogeneous model does not appear to be realistic if one considers the evidence of radar measurements, the difference in porosity deduced from optical data at the immediate surface, radiometric data and radar data. However, in effect these three experiments sample the Moon's surface layer to different depths. The optical data which may penetrate to about a millimeter estimates a porosity of 90% per $\rho = 0.25$ gr/cm^3. The radiometry estimates 80% or $\rho = 0.5$ gr/cm^3, whereas the radar measurements give 40 - 50% porosity per $\rho = 1.0 - 1.25$ gm/cm^3 depending on assumed dielectric constant of 5 to 7 as representative. These results indicate that perhaps the density varies with depth and that the parameters be re-evaluated with this in mind.

This paper indicates that a great deal of information can be obtained by remote measurements from the ground. A case has been made for semi-quantitative evaluation of electromagnetic and thermal parameters of the Moon's surface from these and complementary laboratory data. The evidence indicates a porous or powdered layer of density of the order of 1.0 gm/cm^3 or porosity of about .70 or filling factor of .3 for a depth of the order of a meter or more.

According to measurements on loose basalt powder, an object of
a given diameter will sink to a depth equal to this diameter in a
powder of the calculated porosity under a load of 35 gm/cm^2 or
75 lbs/ft sq.   There appears to be a gradient of density near the
surface which is not well defined by present theory or experiments,
but is suggested in terms of a two-layer approximation by many
investigators.

The radar data should be further explored in frequency at
both longer and shorter wavelength. Dielectric parameters should
be evaluated for small regions by the doppler-range technique. The
evaluation of parameters given above for the Moon as a whole should
then be repeated for regions of varying properties. Hot spots,
highlands and lowlands or Marias should be distinguished if possible.
Polarization data both by radiometry and radar should be extended
to all frequencies available particularly at shorter wavelengths with
present facilities. These should be analyzed for indication of
scattering center below and above surface in terms of the diffuse
component of the signal. A variation of density factor of 0.1 to
0.5 as estimated by various workers from radar and radiometric data
is much too large and this important number should be established
within reasonable limits of error. In addition, it is desirable
to obtain estimates of the depth of the porous layers, variations in
density, both horizontally and vertically and to distinguish between
properties of different topologies. The radar data provides some
indication as to surface roughness or equivalent information about
inhomogeneties of structure below the surface layers. The statistical

nature of the radar data can be localized to smaller and selected regions of the Moon's surface when the range-doppler information can be assigned to grids of the order of 2-kilometer dimensions. This is achievable by the Haystack antenna at X-band. Radar reflection which includes polarization data and frequency variation, hopefully into the millimeter region, will begin to distinguish between structure within the surface layer itself. A theoretical model of two layers is being suggested as a first approach for explaining the observed polarization effects. Perhaps a more sophisticated model of stratified media may be called for eventually. In any event, either model would suggest that the dielectric constant evaluated from a homogeneous model would have to be corrected.

In essence the present review suggests that more extensive measurements by radar, infrared, radiometry combined with more refined and sophisticated analysis, both supplemented by related experiments on terrestrial material in the laboratory will bring substantial dividends for a modest investment of effort in terms of human and existing physical resources.

REFERENCES

1) J. V. Evans and G. H. Pettengill, "The Scattering Properties of the Lunar Surface at Radio Wavelengths;" The Moon, Meteorites and Comets; The Solar System, Vol. IV, (Ed. B. M. Middlehurst and G. P. Kuiper) Ch. 5; The University of Chicago Press (1963).

J. V. Evans, "Radio Echo Studies of the Moon" Physics and Astronomy of the Moon (Ed. Z. Kopal) Ch. 12, Academic Press, New York (1962).

2) V. S. Troitsky, "Radio Emission of the Moon, Its Physical State, and the Nature of Its Surface," The Moon, (Ed. Z. Kopal and Z. K. Mikhailov) p. 475-489, Academic Press, New York (1962).

3) N. S. Soboleva, Astron. J., USSR 39, 1124 (1962).

C. E. Heiles and F. D. Drake, Icarus 2, 281 (1963)

4) J. H. Piddington and H. C. Mennett, Aust. J. Sci. Res. 2A, 63 (1949).

V. S. Troitsky, M. R. Zelinskaya, L. N. Fedoseyev, Raderfizika 3 (1959).

P. G. Mezger, H. Strassl, Planetary Space Sci. 1, 213 (1959).

A. E. Salomonovich, "Thermal Radio Emission of the Moon and Certain Characteristics of Its Surface Layer," The Moon, (Ed. Z. Kopal and Z. K. Mikhailov), p. 491-495, Academic Press, New York (1962).

K. M. Strezhneva, V. S. Troitsky, "The Phase Dependence of Radio Emission of the Moon on 3.2 cm," p. 501-510, ibid.

A. G. Kislyakov, "The Radio Emission of the Moon of 4 mm," p. 511-518, ibid.

5) E. Pettit, Astrophys. J. 91, 408 (1940).

A. F. Wesselink, Bull. Astron. Inst. Netherlands 10 (1948).

J. C. Jaeger, Aute. J. Phys. 6, 10 (1953).

V. M. Sinton, "Temperature on the Lunar Surface," Physics and Astronomy of the Moon, (Ed. Z. Kopal) Ch. 11, Academic Press, New York (1962).

R. W. Shorthill, Conf. on Lunar Exploration, Virginia Polytech. Inst. (1962).

B. C. Murray and R. L. Wildey, J. Geophys. Res., p. 734 (1964).

6) W. E. Fensler, E. F. Knott, A. Olte, K. M. Siegle, "The Electromagnetic Parameters of Selected Terrestrial and Extra-terrestrial Rocks and Glasses," The Moon, (Ed. Z. Kopal and Z. K. Mikhailov, p. 545-565, Academic Press, New York (1962).

7) J. D. Halajian, "The Case for a Cohesive Lunar Surface Model," in "Geological Problems in Lunar Res.," Annals of the New York Acad. of Sci., V. 123, p. 671-710, (July 1965).

8) P. E. Glaser, A. E. Wechsler, A. E. Germeles, "Thermal Properties of Postulated Lunar Surface Materials," in "Geological Problems in Lunar Res.," Annals of New York Acad. of Sci., V. 123, p. 656-670, (July 1965).

9) L. D. Jaffe, The Lunar Surface Layer, (Ed. J. W. Salisbury and P. E. Glaser), p. 355, Academic Press, New York (1964).

10) B. Hopke, The Lunar Surface Layer, (Ed. J. W. Salisbury and P. E. Glaser), p. 323, Academic Press, New York (1964).

APPENDIX IX

THE EVIDENCE FOR A PARTICULATE MATTER IN SPACE AND
ITS POTENTIAL ACCRETION RATE BY THE MOON AND EARTH

"THIS APPENDIX IS ALSO ISSUED AS TG-10"

THE EVIDENCE FOR A PARTICULATE MATTER IN SPACE AND ITS POTENTIAL ACCRETION RATE BY THE MOON AND THE EARTH

By Edward P. Ney

August 1965

THE EVIDENCE FOR A PARTICULATE MATTER IN SPACE AND ITS POTENTIAL ACCRETION RATE BY THE MOON AND THE EARTH

ABSTRACT

16175

The sources of information about the interplanetary dust are examined. It is shown that the observations on the zodiacal light and the direct observation of particles near the Earth may be made compatible with the Earth collecting dust out of a volume of about 10^4 the volume traced out by the Earth. The infall of dust to the Earth corresponds to an increase in the Earth's radius of about 3 cm per million years. It is estimated that the corresponding figure for the Moon will not exceed about 30 Å per year and that to account for lunar erosion the incoming material would have to stir up more than 100 times its own mass of lunar surface.

TABLE OF CONTENTS

LIST OF ILLUSTRATIONS

THE EVIDENCE FOR A PARTICULATE MATTER IN SPACE AND ITS POTENTIAL ACCRETION RATE BY THE MOON AND THE EARTH

Edward P. Ney

Physics Department
University of Minnesota

I. Introduction

Our knowledge about the particulate component of the inter-planetary medium is derived from three types of observations. They are:

a) the F Corona of the Sun

b) the Zodiacal light

c) direct measurements on and near the Earth.

The purpose of this discussion will be to examine the evidence from these three sources of information and to see whether a consistent picture of the inter-planetary dust can emerge. This analysis will then lead to fluxes and sizes of particles incident on the Earth and the Moon within the limitations imposed by our knowledge of the three sources of information.

II. The Solar F Corona

During an eclipse of the Sun, the total intensity of the light from the Corona may be measured from the ground in the region of elongations between the limb of the Sun (one solar radius) and about three solar radii. At the outer elongation which is somewhat less than a degree from the center of the Sun the scattered light from the sky even during an eclipse precludes measurement of the Corona to greater distances. In this range of solar radii both the intensity and polarization of the solar Corona is now well known. Figures 1(a) and 1(b) give the approximate intensity and polarization of this Coronal light. The total Coronal illumination is known to consist of two parts--that contributed by the electrons trapped in the solar atmosphere, which is the true solar Corona, and another portion which is contributed by sunlight scattered by dust along the line of sight. The electron scattered light is called the K Corona and is representative of the solar atmosphere. The light scattered by the dust is called the F or Fraunhofer Corona because in this light the solar Fraunhofer lines may be seen. The thermal velocities of the electrons in the K Corona are so high that the Fraunhofer lines are eliminated by doppler shifts whereas the dust in inter-planetary space is relatively slow moving and displays the Fraunhofer lines. An even more striking evidence of the existence of the F Corona is apparent in the polarization as a function of elongation Figure 1(b). If all of the
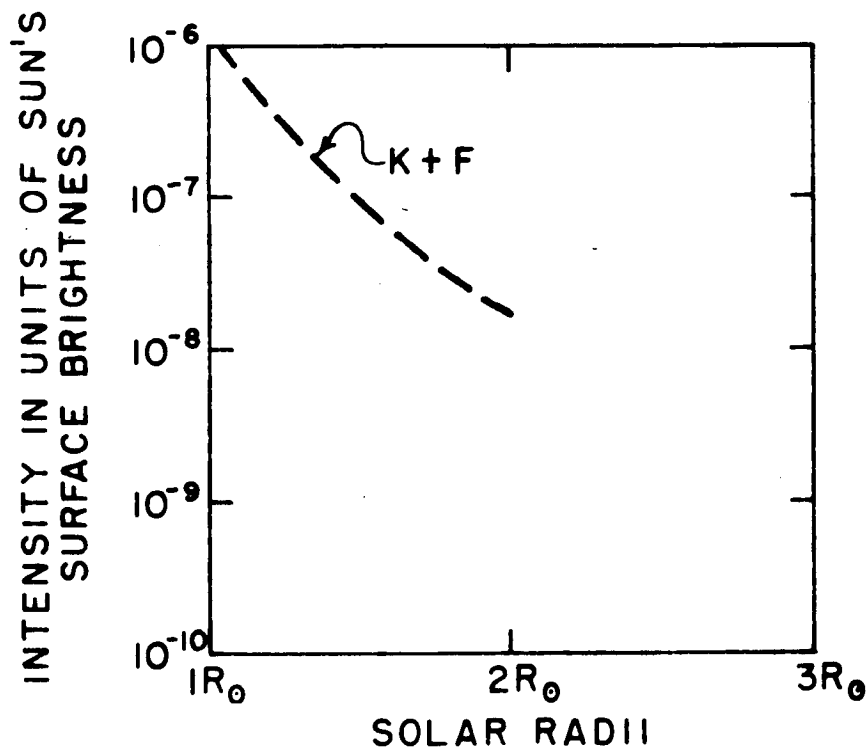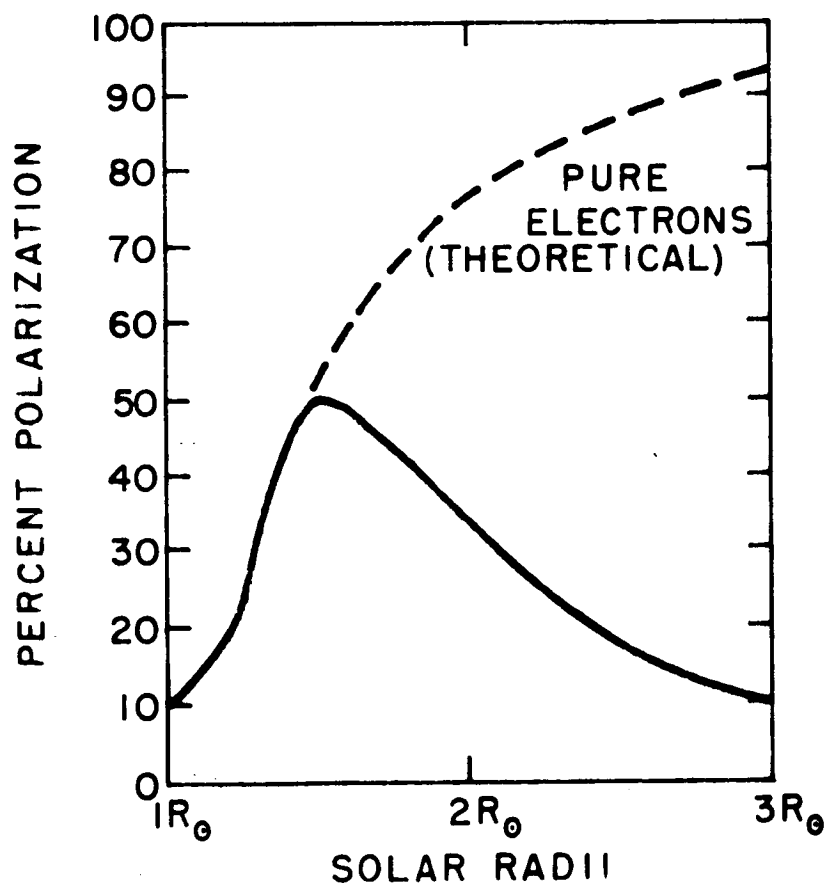
Fig. 1(a)

Fig. 1(b)

INTENSITY AND POLARIZATION OF THE CORONA

Figure 1

Coronal light arose from Thompson scattering by free electrons, the polarization of the Coronal light would be expected to follow the dotted curve indicated as theoretical. The reason that the K Coronal light is not 100% polarized at all elongations is that near the surface the Sun is not a proper point source; thus the polarization is approximately 15%. However, at a distance of approximately 3 or 4 solar radii the Sun is already a small enough source so that the polarization from pure electron scattering in the atmosphere would have risen to a very high value. In contrast to this, the observations show that a maximum polarization of about 50% is reached at 1.5 solar radii and at greater elongation this polarization drops reaching a value of about 15% at three solar radii. This is interpreted as resulting from the dilution of the Corona by the dust scattering along the line of sight of the observer and because of the preferentially forward and backward nature of this scattering the F Corona is quite unpolarized. The contributions of the F and K Coronas may be separated and from the separation one can derive a surface brightness of the F Corona or the light scattered by the dust which in turn leads to an estimate of the concentration of dust integrated along the line of sight passing close to the Sun's limb. The value derived from this experiment is essentially a total cross-section for scattering along the line of sight involved.

III. The Zodiacal Light

Figures 2(a) and 2(b) show the range of angles within which
the Zodiacal light, polarization and intensity may be measured.
The Zodiacal light is observed as a cone of illumination stretching
outward from the Sun along the ecliptic and is most visible when
the ecliptic is nearly vertical at Sun rise or Sun set and is
distinguishible after the twilight phenomena have disappeared.
The best measurements of the intensity and polarization of Zodiacal
light at solar elongation angles down to about 18°. In addition,
recent balloon experiments during total eclipses have filled in
the region between the inner Corona and the Zodiacal light shown
on Figure 2(a) and show that the F Corona of the Sun matches smoothly
to the outer Corona and to the Zodiacal light indicating strongly
that these are truly the same phenomena. The polarization of the
Zodiacal light can only be measured between 18° and about 100°
before the air glow contamination makes the measurement somewhat
uncertain. The measurement in this angular interval of the polari-
zation shows that the polarization is almost independent of angle
and is quite high; the values range from about 14% at 18° elongation
to about 18% polarization at 100° elongation. This polarization
as a function of angle gives the strongest evidence for the fact
that the Zodiacal cloud is circumsolar rather than circumterrestrial.
In order to get a flat polarization curve of this kind with as high
a value of polarization as 15% requires that the average scattering
angle always be approximately 90°. This condition is satisfied if
the particles that produce the Zodiacal cloud are in orbit about the
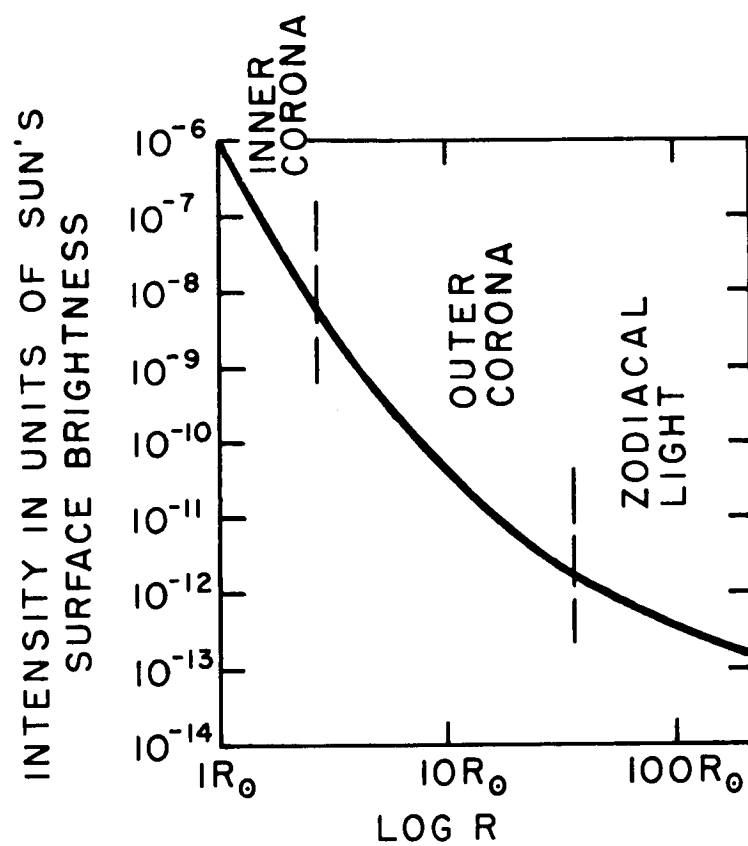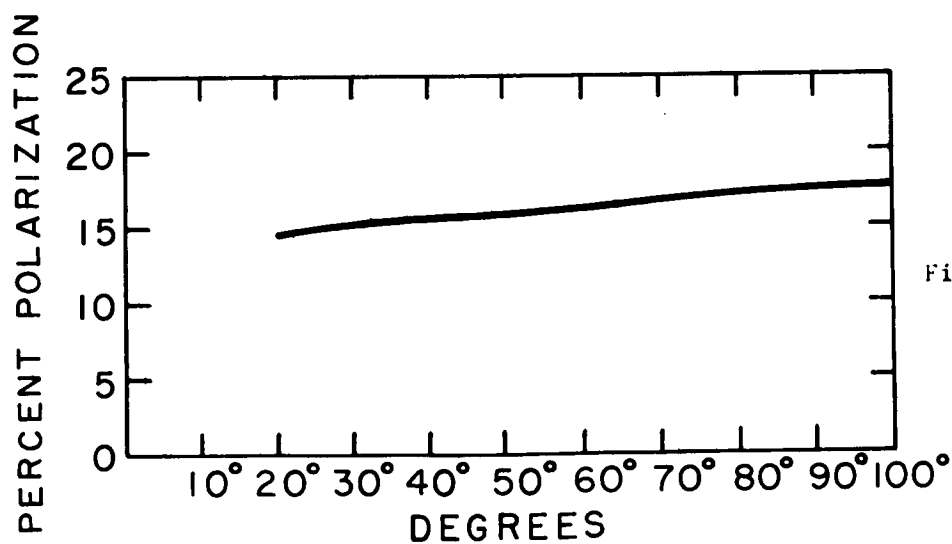
Fig. 2(a)

Fig. 2(b)

THE INTENSITY AND POLARIZATION OF THE ZODIACAL LIGHT

Figure 2

Sun and are more densely concentrated as one goes to smaller distances from the Sun. The Zodiacal light data and the F Corona data are best matched by a number density as a function of radius in which the number of particles per cm varies approximately $\frac{1}{R^{1.5}}$ where R is the distance measured from the Sun. The high polarization of the Zodiacal light was originally interpreted by Behr and Siedentopf as being due to Thompson scattering by electrons in the Zodiacal cloud. However, numerical calculations of the numbers of electrons involved led to the value of approximately 1000 electrons cm^{-3} at the orbit of Earth. Direct space measurements have shown that the number concentration of electrons is only about 10 cm^{-3} and therefore the high polarization of the Zodiacal light can definitely not be attributed to electron scattering. The high polarization is now interpreted instead as showing that the particles that scatter the Zodiacal light are predominately very small and of the order of one or several wavelengths of light in diameter.

Another important property of the Zodiacal light is that its color is essentially the same color as Sunlight. It, therefore, cannot be attributed to Rayleigh scattering which would make the light blue as it does the day-time sky. The high polarization and lack of color of the Zodiacal light are stringent limitations upon the kinds of particles which may be responsible for this illumination. We have made laboratory experiments with small dielectric and carbon spheres and find that in general with the dielectric spheres which are small enough to produce the required polarization one almost invariably gets too much bluing of the light

by Rayleigh scattering. However, it is possible with colloidal carbon particles approximately one micron in diameter to reproduce a polarization in excess of that measured in the Zodiacal light without producing appreciable color.

The model that we have described leads to the possibility of determining the density of particles in the Zodiacal cloud, i.e. the number of these particles per cubic centimeter of space. Figure 3 shows the scattering length, the cross-section per unit volume, and the cross section per gram of various assumed constituents of the Zodiacal cloud. It can be seen that the brightness of the Zodiacal light requires a value at orbit of Earth of approximately $10^{-20} cm^2/cm^3$. The high polarization of the Zodiacal light indicates that the radius of the particles is approximately one micron and this implies from Figure 1 that the mass density of the Zodiacal cloud at the orbit of Earth is approximately 10^{-24} grams per cm^3 and the scattering cross section per gram is approximately 10^4. For a reference also shown on this figure is the scattering expected from one electron per cm^3 in a plasma in which the electrons are diluted with an equal number of protons. A plasma with electron density of one $/cm^{-3}$ neutralized with protons, has a cross section of one cm^2 per gram, whereas the cross section per gram for scattering by dust grains of radius R is:

$$\frac{cross\ section}{gm} = \frac{\pi R^2}{4/3\ \pi R^3 \rho} \approx \frac{1}{R}$$
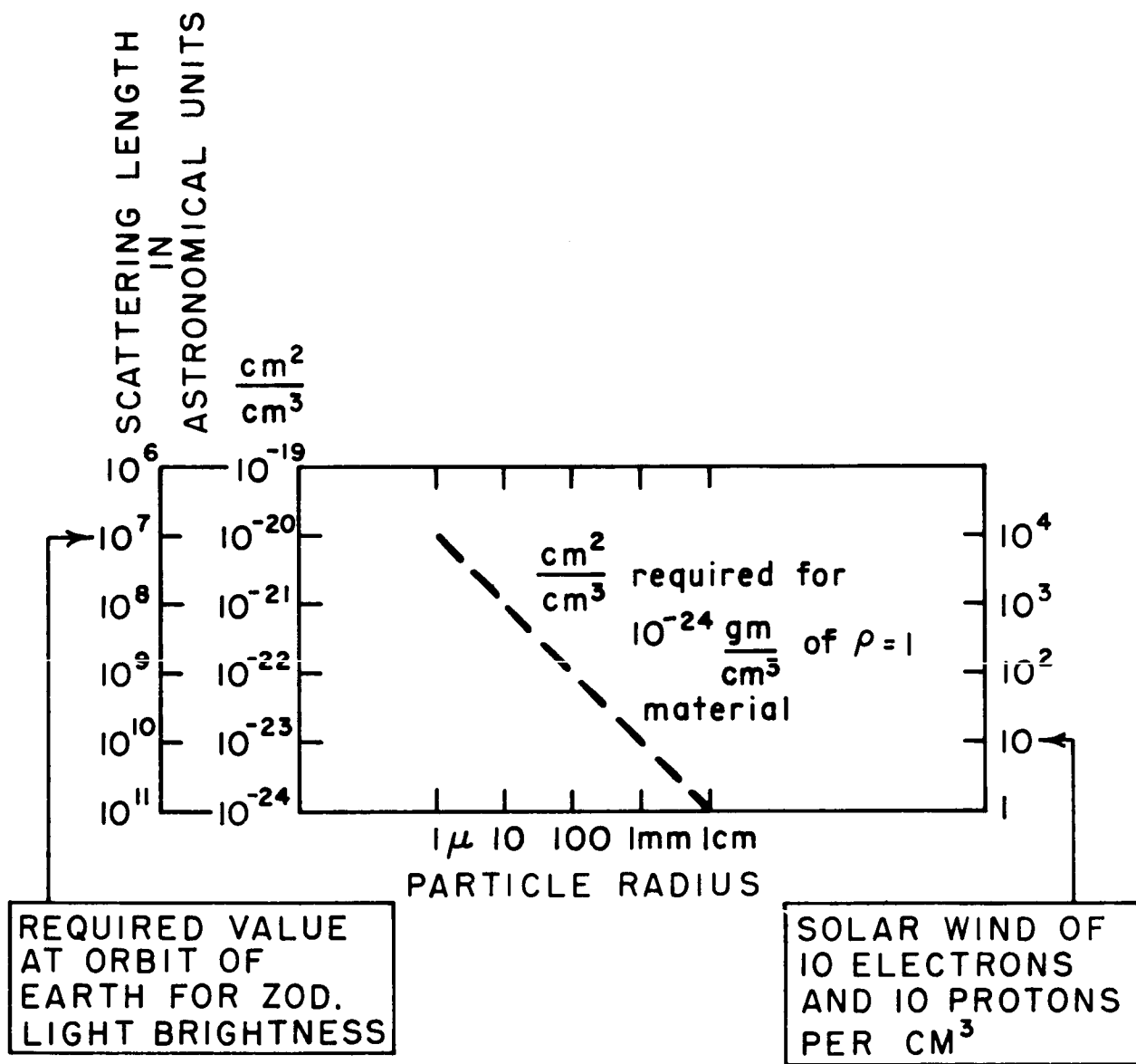
SCATTERING LENGTH AND CROSS SECTION FOR ZODIACAL LIGHT

Figure 3

Even though Thompson scattering has the highest individual particle scattering cross section, the one micron particles are 10^4 times as effective expressed in cm^2 per gram as are the electrons separately Thompson scattering. The reason for this apparent paradox is that the electrons in the dust grain may scatter coherently and therefore greatly exceed the sum of the individual Thompson scattering of the individual electrons from which the dust grain is made. Of course, for this to be true the dust grain must be the order of the wavelength of light for the coherence condition to be satisfied. The 10^4 cm^2 per gram for scattering particles and its consequent one micron radius also corresponds to the radiation pressure blow-out size for the solar system. One would therefore not expect to have particles smaller than this size and because of the rather steep size distribution, the larger particles contribute correspondingly less to the scattered light. An approximate model of the Zodiacal cloud would consist of a cloud of uniform particles of about one to two microns radius. The following simple argument shows that 10^4 cm^2 per gram corresponds to the radiation pressure blow-out size.

When radiation pressure exceeds gravity, it will do so throughout the solar system because both have the same $\frac{1}{\gamma^2}$ dependence on distance. We may, therefore, calculate the condition anywhere and choose to do it at the surface of the Sun. Condition for blow-out is: $F = mg = PA$ and,

$$\frac{A}{m} = \frac{cm^2}{gm} = \frac{g}{P}$$

The solar gravitational accelerations g is 3×10^4 $\frac{cm}{sec^2}$ and the radiation pressure at the Sun is $2 \frac{ergs}{cm^3}$ so the radiation blow-out condition is:

$$\frac{A}{m} = \frac{3 \times 10^4}{2} \sim 10^4 \frac{cm^2}{gm}$$

Although the Zodiacal light phenomena is quite a pronounced night time surface brightness illumination of the sky, the total mass of the material in the Zodiacal cloud is really rather small. If we considered that the mass density of particles at orbit of the Earth (10^{-24} grams cm^{-3}) existed all the way out to 10 astronomical units, the total mass of this cloud would only be 10^{19} grams, which is about the estimated mass of a comet and is about 10^{-9} of the mass of the Earth. In spite of this rather small mass in the Zodiacal cloud, there is a need for continual replenishment of the particles because of their removal by the Poynting-Robertson effect which causes all tiny particles to spiral inward toward the Sun. The physics of the Poynting-Robertson effect is that because the particles are in orbit around the Sun, the sunlight strikes the particles at approximately the angle beta where beta is the ratio of the orbital velocity of the speed of light. The direction in which the sunlight hits the particles is therefore always such as to remove momentum from them and to force them into smaller orbits. It can be shown that the time for a particle of radius α density ρ to spiral into the Sun from a distance R in astronomical units is given by $T = 10^7 \times 10^6 \alpha(\rho) R^2$, $T = 7 \times 10^6 \alpha\rho R^2$ years.

This shows that a particle of one-micron radius will spiral from the orbit of Earth into the Sun in the period of about 700 years. Because the particles are very probably charged by a photoelectric effect and are moving through the plasma of the solar wind, an additional energy loss mechanism is operative in addition to the Poynting-Robertson effect and our best estimates are that a one-micron particle would spiral into the Sun in a time between 100 and 1000 years. This means that the total mass of the Zodiacal cloud must be replenished in a period of this order. There seem to be two sources of the Zodiacal cloud each of which is adequately strong to replenish it. In the case of the cometary injection of the cloud, one would expect it to consist primarily of ices and in the case of the asteroidal contribution it would be expected to have a composition of normal meteors. It is impossible to say at this time which injection mechanism is stronger and very probably the Zodiacal cloud is a combination of both meteoritic debris from asteroids and ices and dust from comets. It is interesting to compare the net mass influx moving towards the Sun in the form of Zodiacal cloud with the mass flux outward from the solar wind. The mass flux inward from Zodiacal particles is between 10^4 and 10^6 times less than the mass flux outward in the solar wind. It can be seen then that the composition of the inter-planetary mediums is more determined by the solar wind than the Zodiacal cloud and the probable fate of the Zodiacal particle is to spiral inward toward the Sun until the melting region is reached at which point

it would become a part of the solar plasma and blow outward again as individual molecules or atoms in the solar wind. The diffuseness of the particles in the Zodiacal cloud may be emphasized by pointing out that with the average density of 10^{-24} grams per cm^3 at the orbit of Earth and a mass of approximately 10^{-12} grams per particle, that in the distance from Earth to Sun of 10^{13} cm there are only on the order of 1 to 10 particles in a cm^2 column stretching all the way from the Earth to the Sun.

In summary the observations on the F Corona and the Zodiacal light lead to a picture in which particles lie primarily in the plane of the ecliptic circle and Sun in Keplerian orbits, the main size of the particles being of the order of a micron radius. The density is of the order of $10^{-12}/cm^3$ at the orbit of Earth rising to approximately 10^{-11} particles per cm^3 at a tenth of an astronomical unit, the distance from the Sun at which they should become vaporized. If one were limited to the data so far described, one might estimate a mass influx to the Earth and (approximately the same) to the Moon of very small proportions. The particle density of 10^{-12} particles cm^{-3} at a collection velocity equal to the Earth's orbital velocity of 30 kilometers per second, leads to a flux of 3×10^{-6} particles per cm^2 per second. This value, however, is much too low as one might anticipate from the fact that the Earth collection radius for acquiring dust must be very much larger than its geometric radius and consequently the Earth or the Moon act as vacuum cleaners removing dust from a much larger volume of space than that cut out

by the geometric passage of the Earth or Moon through the solar system. We turn now, then, to the direct influx of particles to the Earth and will try to see whether this direct influx can be made to agree with the observations about the Zodiacal light.

IV. Direct Dust Measurements at and near the Earth

In recent years a number of measurements of particulate matter in space have been made from rockets and satellites and very recently a technique has been developed by J. Rosen at the University of Minnesota to measure in situ the amount of material falling into the Earth's atmosphere. We will describe this latter experiment in some detail because it leads to quantitative values averaged over some period of time for the influx of small particulate matter. The experiment of Rosen consists of pumping stratospheric air through a small scattering chamber during a balloon flight and observing the scattered light from individual tiny particles with two microscopes equipped with photomultipliers and operating in coincidence. It is possible with this equipment to detect particles down to 1/2 micron radius as determined in the laboratory with samples of standard size small dielectric and carbon particles. The measurement takes place in situ in the atmosphere and therefore does not involve the contamination problem of collecting samples and then bringing them back. It also has the advantage of being able to measure on a day-to-day or a year-to-year basis the particulate concentration of the atmosphere. Figure 4 shows the kind of record that Rosen's equipment gives. It is a plot of the number density of dust as a function of atmospheric pressure. The lower altitudes in the atmosphere below the tropopause are clearly meteorologically dominated. Most of Rosen's soundings show the void below the tropopause which we believe is due to rain out of the small particles. They also show very large concentrations of terrestrial

HEIGHT PRESSURE
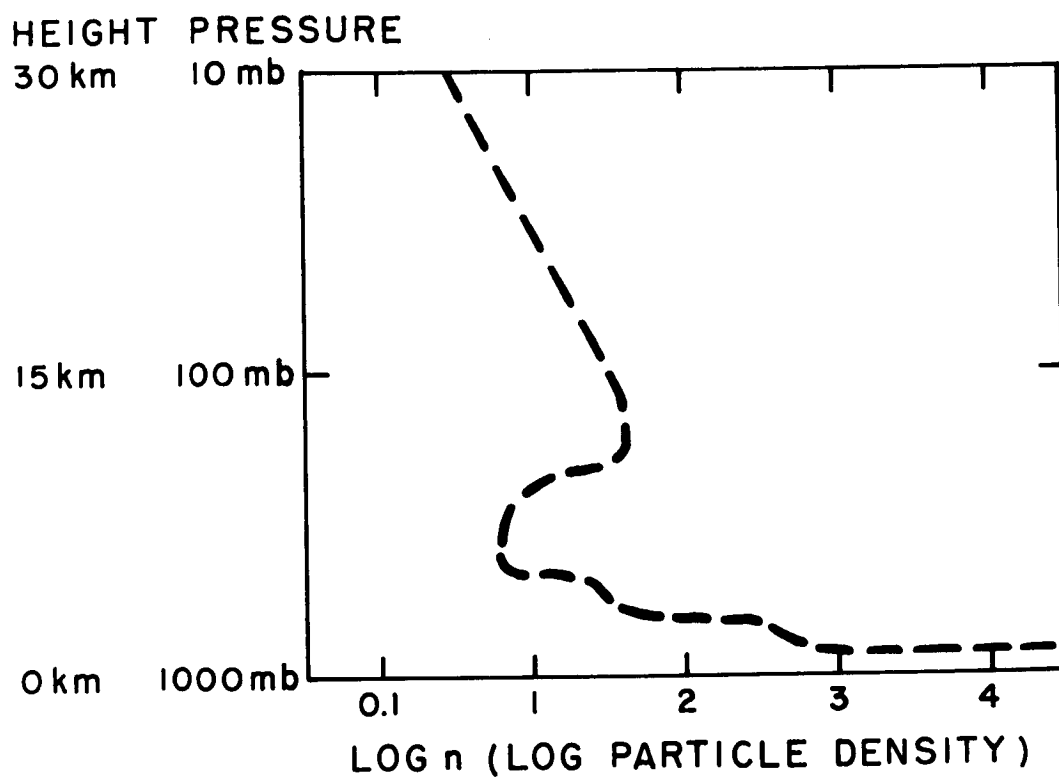
CONCENTRATION OF DUST PARTICLES' FUNCTION OF ALTITUDE IN THE EARTH'S ATMOSPHERE

Figure 4

dust near the ground. However, in the stratosphere where clouds

are rare, the typical Rosen sounding is one in which the number

density of particles is quite accurately proportional to the pressure.

The particles sampled are smaller than a molecular mean free path

in the atmosphere. As a consequence, one can show that their fall

velocity will be strictly inversely proportional to the atmospheric

pressure. If there is then a constant influx of particles at the

top of the atmosphere, this flux will be equal to the number

density of particles per cm^3 times their fall velocity. If the

fall velocity is inversely proportional to the pressure and the

influx is constant, the number density will strictly go as the

atmospheric pressure. Consequently, a measurement of particle

concentration at a given pressure and a calculation of the fall

velocity of the corresponding particles determines the flux. The

value determined by Rosen in this way averages to about approxi-

mately 1/30 of a particle cm^{-2} per second. The number density at

10 millibars pressure is 1/3 of a particle cm^{-3} and the corres-

ponding fall velocity approximately 1/10 of a cm per second. It

is important to point out that the particles have not fallen to this

altitude rapidly and their residence time in reaching an altitude

of 100,000 feet in the Earth's atmosphere is approximately 3 months.

In a sense, the Earth's atmosphere acts as a concentration mechanism

because of the decrease in fall velocity and it is somewhat amusing

that the highest number density of extra-terrestrial particles

occurs at an altitude of about 50,000 feet. At this altitude the

number density is approximately 3 particles cm^{-3}. The problem of

direct collection of the particles is quite difficult as can be seen
from the fact that in order to bring back a gram of particles one
would have to collect approximately 10^8 grams of air. It should
be pointed out that Rosen's measurements agree with the flux values
of the rocket and satellite measurements and probably represent
the actual flux of particles into the Earth. To compare Rosen's
measurements with the predictions on the basis of the Zodiacal
cloud one must remember that the particles observed in the atmosphere
are slowed down by atmospheric drag from the free fall velocity they
would acquire just outside the Earth's atmosphere. This free fall
velocity is 10 kilometers per second and the flux then of 1/30
of a particle cm^{-2} per second corresponds to a number density just
outside the atmosphere of 1/30 times 10^{-6} or of the order of 10^{-8}
particles cm^{-3}. This number is to be compared with the number
inferred from the Zodiacal light observations of 10^{-12} particles
cm^{-3} and can be seen to be 10^4 times larger than the particle
density in the undisturbed Zodiacal cloud. In order to attempt
to reconcile these two numbers, we must therefore examine in detail
the mechanism by which the Earth is able to collect material from
the Zodiacal cloud. In order to make the flux measurement at the
Earth compatible with the density of the Zodiacal cloud at the
orbit of the Earth it is necessary that the Earth be able to con-
centrate the dust by a factor of approximately 10^4. The model that
we adopt for estimating the volume swept out by the Earth is one in
which we assume the Zodiacal particles to be in Keplerian orbits in
the plane of the ecliptic like the Earth. The particles in orbit

at bigger radius than the Earth will be travelling with smaller velocities and those in smaller orbits will be travelling at higher velocities. Figure 5 shows the geometry of the Earth in the Zodiacal cloud and of the relative velocity of the Zodiacal cloud particles as viewed from the Earth. There will be some biggest distance shown as R_x at which the Earth is just able to collect particles from the Zodiacal cloud. The difference in velocity in the Keplerian orbits at a distance of R_x from the Earth is easily calculated and is shown to be:

$$\Delta v = 1/2 \left(\frac{GM_o}{R} \right)^{1/2} \frac{R_x}{R} \tag{1}$$

In order for the Earth to collect the particles from the Zodiacal cloud the conservation of angular momentum dictates that:

$$m\Delta v \, R_x = m \, v_{FF} \, R_E \qquad \text{where} \qquad v_{FF} = \sqrt{\frac{2G \, M_E}{R_E}} \tag{2}$$

Finally, simultaneous solution of Equation (1) and Equation (2) allows determination of the value of R_x and solution and insertion of the appropriate values shows that R_x is approximately 100 Earth radii. In this rather extreme model that we have assumed, it is therefore possible in the upper limit to collect particles from a volume of space 100^3 or 10^6 larger than the volume of the Earth. This somewhat more than resolves the factor of 10^4 required to reconcile the flux measurements at the Earth with the undisturbed Zodiacal cloud. There are, however, obvious shortcomings to this model. The most serious difficulty is that if the Zodiacal cloud

Velocity of Particles
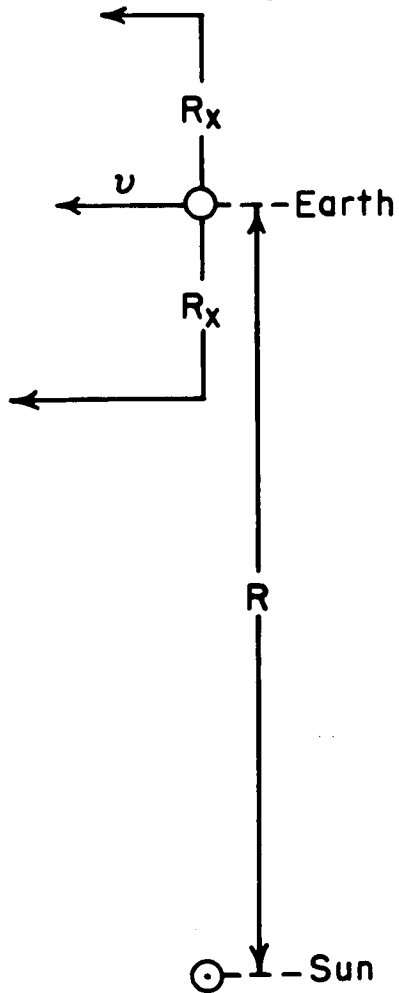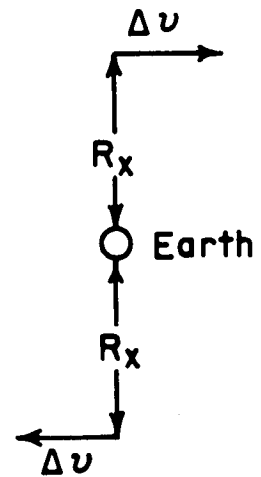
RELATIVE VELOCITY OF EARTH AND CLOUD PARTICLES

Figure 5

particles have orbits inclined with respect to the plane of the ecliptic, the collection volume for these off angle particles decreases rather rapidly and might even approach a collection volume which instead of being spherical with a radius of R_x is approximately pill box shaped with a radius of R_x and thickness equal to the radius of the Earth. In this case the collection volume would only be something on the order of 10,000 times the volume swept out by the Earth and just barely adequate to account for the discrepancy between the terrestrial number density in falling particles and the density in the undisturbed Zodiacal cloud. However, the fact that a collection volume of about this order of magnitude can be justified makes it worth calculating the influx of particles to the Earth implied by Rosen's measurement. If the density of the particles is one, the mass influx to the Earth is approximately 10^6 grams per year or about one ton per year for the whole Earth. The rate of growth of the Earth's radius due to the acquisition of these particles can be determined from the following equation:

$$\frac{dR}{dt} = \frac{nm}{\rho} \simeq 4\, n\, r^3 \qquad \text{where,} \quad n = \text{number density,}$$

$$m = \text{mass/particles, and}$$

$$r = \text{particle radius.}$$

It is seen that this equation leads to dR/dt of approximately 3 cm per million years of 300 Å per year. If we try to estimate the rate of acquisition of this material by the Moon, one must observe that the major collection of the Zodiacal cloud is

-21-

through the gravitational field of the Earth and that the orbits of the particles coming to the Earth take less time than the period in which the Moon revolves about the Earth. The Moon, therefore, sweeps out a doughnut of these particles which the Earth is collecting from the Zodiacal cloud. Various methods can be used to estimate the flux at the Moon compared to the flux on the Earth and our estimate is that the flux is of the order of a tenth of the terrestrial flux.

If we reduce the terrestrial flux by a factor of 10 for the moment, this would correspond to lunar acquisition rate Ω interplanetary material of 30 $\overset{o}{A}$ per year. It has been estimated by Gold that the lunar erosion requires the movement of approximately one micron a year of material from the highlands to the lowlands. Our figure for the input of 30 $\overset{o}{A}$ per year would imply that 300 times the material brought in from interplanetary space must be moved around on the Moon if the input of micrometeorites of the Zodiacal cloud is to be the stirring mechanism which is responsible for plowing the lunar surface.

V. Summary

In summary, the analysis of the data on the F Corona of the Sun, the Zodiacal light, and the direct measurement of fluxes of micro-particles of the Earth's surface, lead to the estimate of lunar acquisition of interplanetary particulate matter at the rate of about 30 Å per year. It is believed that this figure is probably reliable within a factor of 10, and certainly 100. If the figure is correct, it is necessary for the incoming particulate matter to stir up approximately 300 times its own mass of lunar material in order to account for the lunar erosion. It would seem in any event that the input of micrometeorites to the Moon is not in itself a serious source of lunar surface acquisition. If the present flux had existed throughout prehistoric times--a very tenuous assumption--in 10^9 years, the approximate life time of the Moon, a total of 300 cm of density "1" material would have been acquired from the interplanetary environment.

APPENDIX X

MECHANISM FOR LUNAR LUMINESCENCE

"THIS APPENDIX IS ALSO ISSUED AS TG-11"

MECHANISMS FOR LUNAR LUMINESCENCE

E.P. Ney, N.J. Woolf, and R.J. Collins

August 1965

MECHANISMS FOR LUNAR LUMINESCENCE

ABSTRACT

The visibility of luminescence on the Moon depends on the competing processes that illuminate the Moon and that provide energy for luminescence. It is shown that the most favorable times for seeing luminescence are at new Moon on the far side of the Moon, and during rare dark eclipses. The luminosity and color of these rare eclipses is explained.

Observations supposedly of luminescence during lunar day are criticized, and only the spectroscopic evidence is taken to support the reality of luminescence. Both direct and storage processes have been considered for converting energy to luminescence. Direct processes in lunar day cannot be energized by presently known sources of particles. If indirect processes occur they may give information about the dust particles at the extreme lunar surface.

TABLE OF CONTENTS

LIST OF ILLUSTRATIONS

TABLES

MECHANISMS FOR LUNAR LUMINESCENCE

E. P. Ney, N. J. Woolf, and R. J. Collins

August 1965

I. Introduction

For several years it has been claimed that the phenomenon of luminescence accounts for some observations of the Moon. The observations that have been interpreted this way include the fluctuating brightness of different lunar eclipses (Danjon 1921), the light pattern on the Moon during a lunar eclipse (Link 1962), filling in of solar spectral lines in the lunar reflection spectrum (Kozyrev 1956; Ring and Grainger 1962; Grainger 1963; Wildey 1964 and Spinrad 1965), the anomalous phase variation of the light reflected by certain craters (Van Diggelen 1965), and the anomalous brightness of one region in interference filter photographs (Kopal and Rackham 1963).

In all of these observations (except those of Wildey) luminescent intensities were supposedly observed that were sub-stantial fractions of normal moonlight, and thus would represent large amounts of energy. It is the purpose of this paper to examine possible mechanisms for lunar luminescence in the light of the energy requirements, and the presently known sources of excitation. Both direct conversion of the particle and photon flux on the lunar surface, and also storage of energy and rapid release will be considered.

II. Luminescence Observations

The reported observations relating to luminescence have been listed in the introduction. However, many of these phenomena have possible alternative explanations. The fluctuating brightness of eclipses correlates with solar activity, but also correlates with dust in the terrestrial atmosphere. It is not clear whether the responding element (if such exists) is the Moon, or the Earth.

The light pattern during lunar eclipses is seriously distorted by the extremely sharp backscatter peak of the lunar phase function (Van Diggelen 1965), and as Barbier has commented, this could be causing the phenomenon that Link has claimed to be luminescence.

The asymmetric phase variation for certain ray craters commented on by Van Diggelen are in compacted areas of the lunar crust, shown for example by enhanced radar reflectivities and thermal anomalies during eclipses. All these areas have their phase variation distorted so that the peak of the reflection is distorted towards specular reflection. In such areas, anomalous phase variation of this kind is not surprising, since the average slope of compacted formations will tend to be parallel to the lunar surface, and there seems to be no need to call on lunar luminescence.

The photography by Kopal and Rackham used interference filters, which are not always very uniform in transmission, and the region where luminescence was claimed was towards the edge of their plates.

From the published data it is not clear that all possible sources of systematic error have been eliminated, and so these results cannot yet be considered conclusive.

The most convincing data is perhaps that of Spinrad, who was surprised to find evidence of $\sim 17\%$ of luminescence on a lunar spectrum that he had merely taken for comparison purposes. The plate by Kozyrev on the 4th of October, 1955, showing about 16% luminescent intensity at H and K is likewise a good indicator. However, the photoelectric work has not yet produced consistent results. Grainger claims rather small amounts of luminescence that are time variable. Wildey, in a single night's observation could find no differential luminescence across the Moon, and one of us (NJW) in a similar, unpublished, observation found the same result.

III. The Brightness of the Moon

To observe luminescence on the Moon, the luminescent brightness must be comparable with the surface brightness of the Moon if the phenomenon is to be readily detectable. However, the lunar surface presents four regions of very different surface brightness. These are:

a) Lunar Day. The brightness of lunar day is well known (Harris 1961).

b) Lunar Night with Earthshine. This has been photometered by Danjon (1960).

c) Lunar Night without Earthshine. This can only occur on the far side of the Moon. The sky brightness will be similar to the darkest sky observed from Earth at night, and the lunar brightness will be this value multiplied by the lunar albedo.

d) Lunar Eclipses. The brightness of a lunar eclipse varies considerably and the range of values requires special consideration.

Fisher (1921) has correlated the variations in the brightness of lunar eclipses with the dustiness of the Earth's atmosphere. The dust in the atmosphere may be very much greater for example after a volcanic erruption. Barbier (1961) has pointed out that although the normal illumination during an eclipse is by refracted light, there is also a small component of illumination produced by scattered light. This sets a lower limit to the brightness of eclipses observed when the lower atmosphere is opaque to transverse traversal e.g. after a volcanic erruption. We have calculated the expected brightness in this case, noting that because of the aureole, the scale height of atmosphere that causes most of the illumination

will attain the surface brightness of a perfect diffusing screen
at the Earth's distance from the Sun. The calculated color of the
Moon for this case will be the normal color of the uneclipsed Moon,
and not the remarkably red color observed during normal, bright,
lunar eclipses. Such a dark eclipse was observed by Matsushima and
Zink (1964), and their observations are compared with our theoretical
predictions in Table 1. It is seen that the predicted intensity
and color are in excellent agreement with the observations.

Table 1

BRIGHTNESS AND COLOR OF A VERY DARK ECLIPSE WHERE THERE IS NO REFRACTED RAY:

Predicted:

$$\frac{\text{Brightness of full Moon}}{\text{Brightness of dark eclipse}} \simeq \frac{1/2 \times (\text{Lunar Distance})^2}{\text{Rad. of Earth} \times \text{Atm. Scale Hgt.}}$$

$$= 1.2 \times 10^6$$

BRIGHTNESS AT WAVELENGTHS NEAR 4500 Å (Blue):

$$\frac{\text{Brightness of full Moon}}{\text{Brightness of typical eclipse}} = 3 \times 10^4$$

Theoretical:

$$\frac{\text{Brightness of full Moon}}{\text{Brightness of dark eclipse}} \simeq 1.2 \times 10^6$$

Observed
Matsushima and Zink:

$$\frac{\text{Brightness of full Moon}}{\text{Brightness of dark eclipse}} = 3.2 \pm 0.9 \times 10^6$$

COLOR:

Observed:

$$\frac{\text{Ratio of yellow to blue intensity (typical eclipse)}}{\text{Ratio of yellow to blue intensity (full Moon)}} = 9$$

Theoretical:

$$\frac{\text{Ratio of yellow to blue intensity (dark eclipse)}}{\text{Ratio of yellow to blue intensity (full Moon)}} = 1$$

Observed
by Matsushima
and Zink:

$$\frac{\text{Ratio of yellow to blue intensity (dark eclipse)}}{\text{Ratio of yellow to blue intensity (full Moon)}}$$

$$= 0.9 \pm 0.1$$

Figure 1 shows all these surface brightnesses of the Moon, expressed in photons/cm^2 sec. for 1000 Å bandwidth centered at 5300 Å.
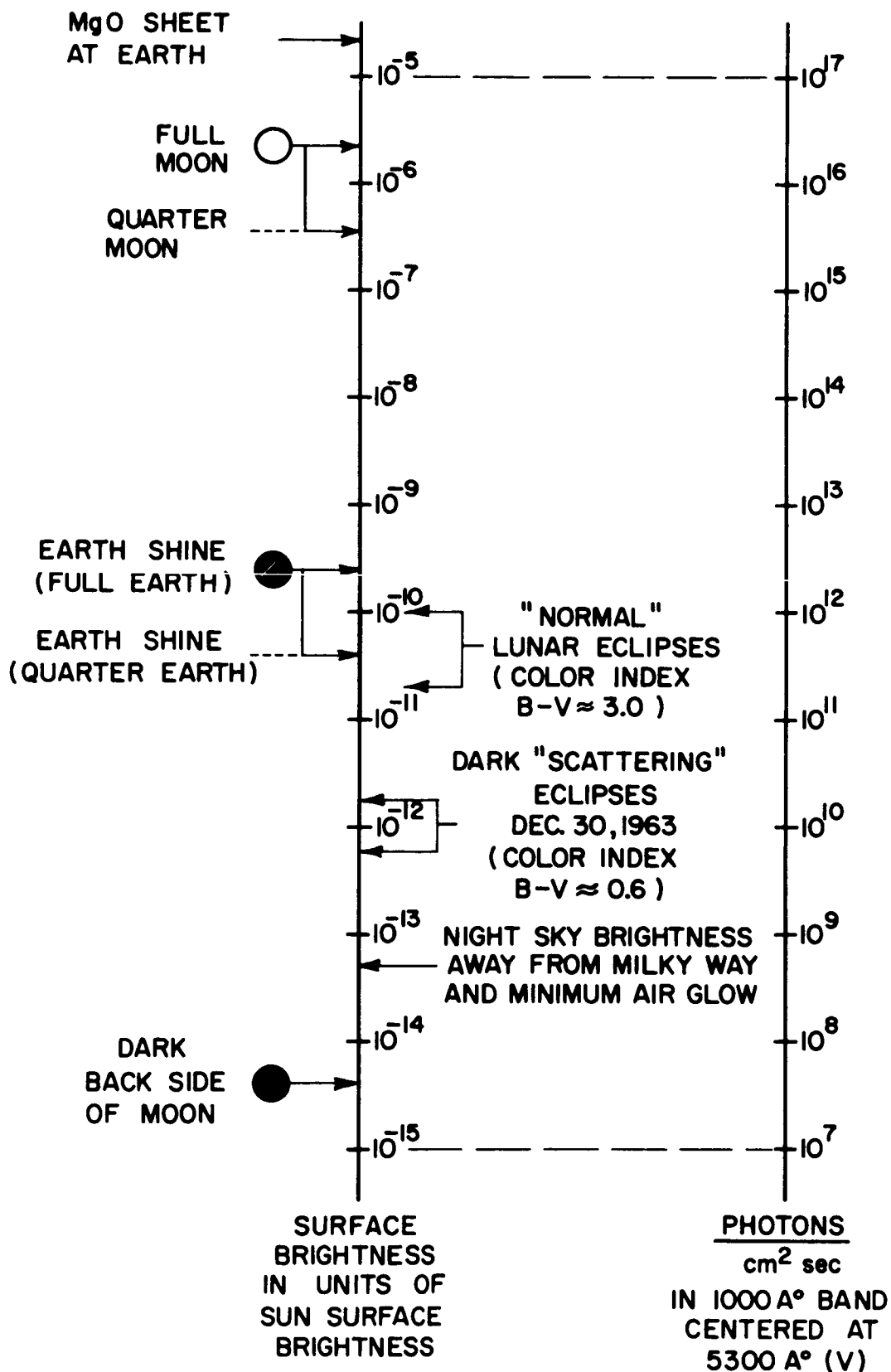
SURFACE BRIGHTNESS OF THE MOON

MgO SHEET
AT EARTH

FULL
MOON

QUARTER
MOON

EARTH SHINE
(FULL EARTH)

EARTH SHINE
(QUARTER EARTH)

DARK
BACK SIDE
OF MOON

10^{-5} — — — — — — — 10^{17}

10^{-6} — 10^{16}

10^{-7} — 10^{15}

10^{-8} — 10^{14}

10^{-9} — 10^{13}

10^{-10} — 10^{12}

10^{-11} — 10^{11}

10^{-12} — 10^{10}

10^{-13} — 10^{9}

10^{-14} — 10^{8}

10^{-15} — — — — — — — 10^{7}

"NORMAL"
LUNAR ECLIPSES
(COLOR INDEX
B-V ≈ 3.0)

DARK "SCATTERING"
ECLIPSES
DEC. 30, 1963
(COLOR INDEX
B-V ≈ 0.6)

NIGHT SKY BRIGHTNESS
AWAY FROM MILKY WAY
AND MINIMUM AIR GLOW

SURFACE
BRIGHTNESS
IN UNITS OF
SUN SURFACE
BRIGHTNESS

PHOTONS
$\overline{cm^2 \ sec}$
IN 1000 A° BAND
CENTERED AT
5300 A° (V)

Figure 1 Surface Brightness of the Moon

-7-

IV. Direct Excitation of Luminescence

The various fluxes of photons and particles incident upon the lunar surface have been estimated and are shown in Figure 2. The flux of photons has been given as a number, since in this energy range there is likely to be a preponderance of processes giving one observable photon per effective incident photon. On the other hand particle fluxes have been given in electron volts rather than by number. It is likely that one particle could give rise to many observable quanta, and since the observable photons have energies of a few e.v. the number of electron volts is an indication of the maximum number of photons that might be produced.

In Figure 2, the solar UV spectrum has been taken from Allen (1962). The soft and medium UV are constant; however, the hard UV will be time variable. The flux in the solar wind has been taken from the Mariner II measurements, Snyder and Nagabauer (1964). The energy has a peak to minimum variation of about a factor of 10. The flux of solar protons has been estimated from observations on large solar proton events during sunspot maximum (Freier and Webber 1963). The flux of solar protons is of course very time dependent during events as illustrated in this reference. The cosmic ray flux comes from McDonald (1959) and varies only by a factor of 2 with the sunspot cycle. The flux in the geomagnetic tail shown in Figure 2 requires some further discussion. The work of Ness and his collaborators has shown that the Earth has a geomagnetic wake in the anti-sun direction (Ness et al 1964). This wake has been
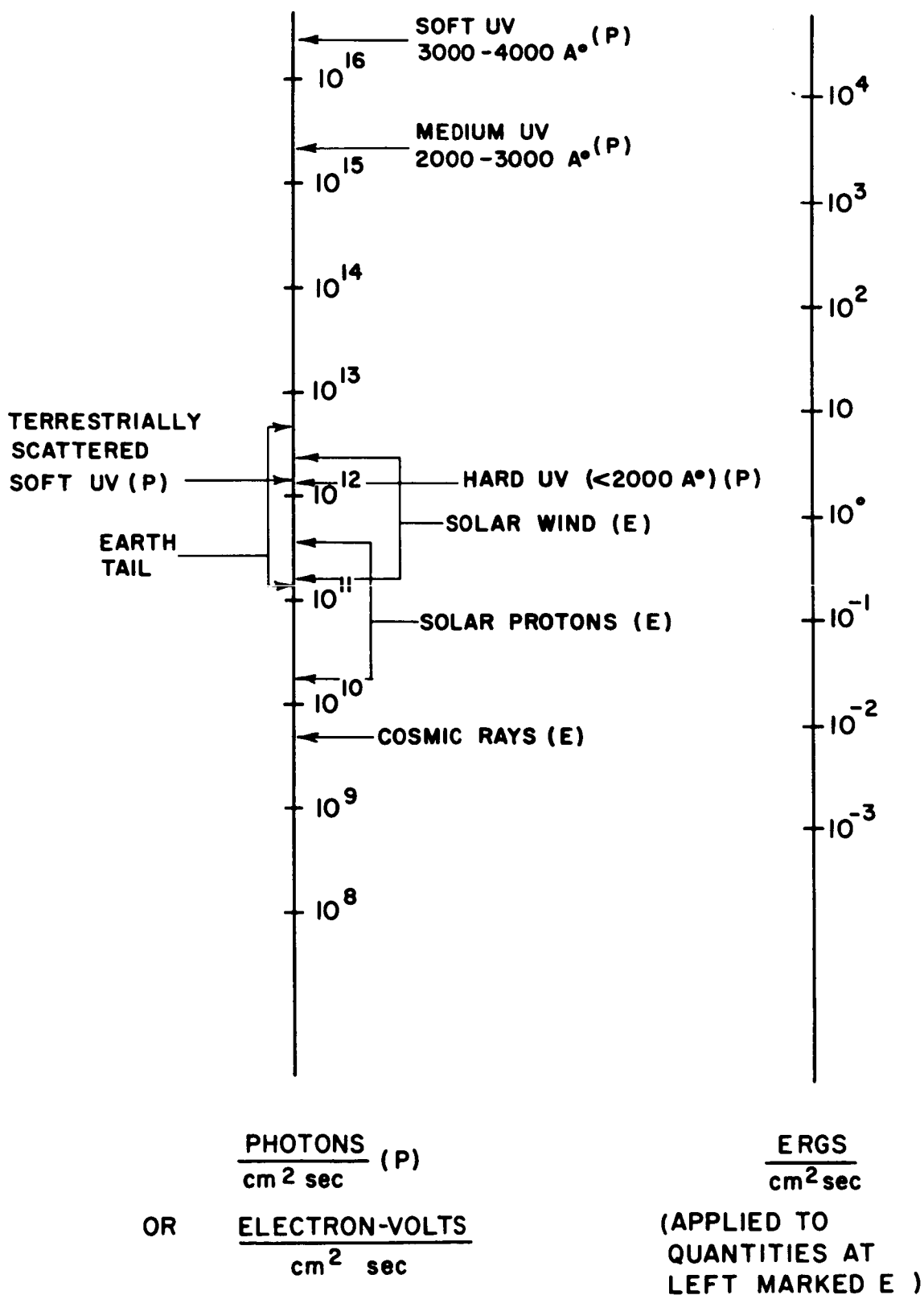
SOURCES OF IRRADIATION FOR MOON

Figure 2 Sources of Irradiation for Moon

observed experimentally to distances of 32 Earth radii which is over

half of the distance to the Moon and the experimental evidence

indicates that the geomagnetic wake of the Earth probably extends as

far as the Moon. Anderson (1965) has shown that the magnetic

fluctuations in the Earth's tail are associated with island fluxes

of energetic electrons. These island fluxes have geographic

extents larger than an Earth radius and presumably would at the

orbit of the Moon immerse the Moon in an energetic electron down-

pour. Anderson's measurements refer to particles of energy greater

than 50 KeV and, therefore, give only a lower limit to the energy

flux of particles expected in the geomagnetic tail. Sharp and his

collaborators (1965) and McDiarmid and his collaborators (1965)

have measured fluxes of electrons in low flying satellites over the

auroral zone and have shown that these electrons are similar in

intensity and energy with those observed by Anderson in the island

fluxes in the Earth's tail. In the case of Sharp's observations,

the energy spectrum of the particles was measured and it is there-

fore possible to make more realistic estimates of the total energy

involved in the high energy electrons. There is a strong indication

from the correlation of the island fluxes with changes in the

magnetic field that the total energy in the electrons is at least

in approximate equi-partition with the magnetic field which

changes, presumably during the acceleration of these particles.

Figure 3 shows a plot of the energy per square centimeter

per second according to the measurements of McDiarmid, Sharp and

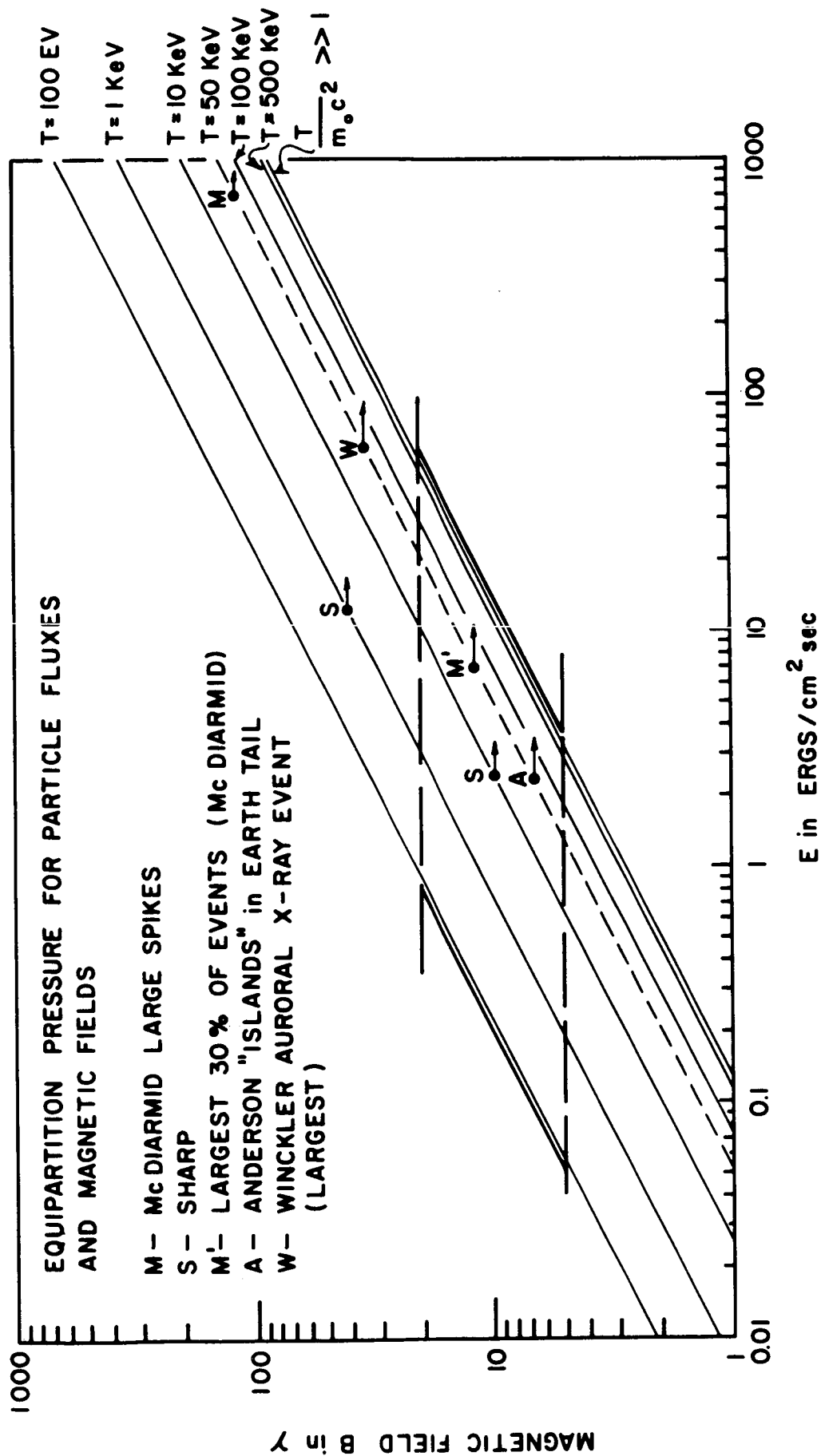Anderson. Also shown is a point from Winckler's observations of a

Figure 3 Equi-partition Pressure for Particle Fluxes and Magnetic Fields

very large auroral x-ray event which also leads to an estimate of the precipitating electrons in the auroral zone. In Figure 3 the magnetic field of energy equi-partition with these fluxes is shown as a function of the average energy of the electrons. It is clear that the energy fluxes are compatible with equi-partition with a field of approximately 10 gamma, the order of magnitude believed to be present in the Earth's tail at the vicinity of the Moon. Using the ideas presented in this discussion, then, we enter the value for the Earth's tail source of irradiation on the Moon as somewhere between 10^{11} and 5×10^{12} eV/cm^2 sec.

Also indicated as a source of radiation to the Moon is terrestrially scattered soft UV. It is interesting that within an order of magnitude, all of the sources of irradiation, hard UV, terrestrially scattered soft UV, the solar wind, the Earth's tail, solar protons are nearly the same. Cosmic rays give an order of magnitude less energy flux for irradiation. Figure 4 shows a combined plot of the ambient surface brightness of the Moon and the sources of irradiation which may produce luminescence in competition with this ambient radiation. On the left of this figure are the processes allowed by geometry and on the right are the direct processes which are allowed by geometry and energy conservation; that is, the energy fluxes must be greater than the ambient illumination in order for the luminescence to be detected. The cases in which the most pronounced luminescent effect are likely to show up are (i) the dark far side of the Moon when it is illuminated by the geomagnetic tail, solar protons and possibly even cosmic rays,
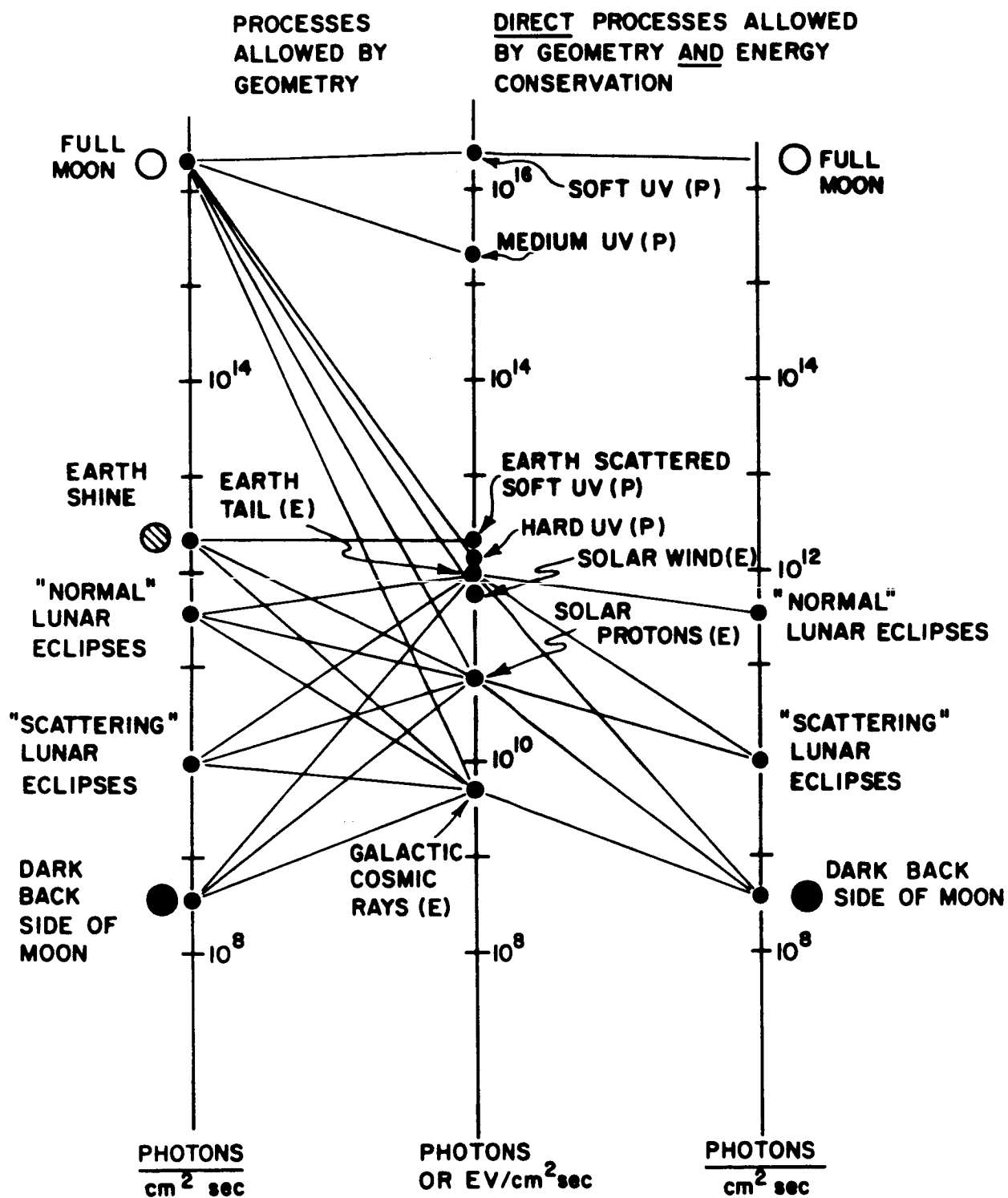
Figure 4   Direct Luminescent Processes

(ii) the very dark lunar eclipses under similar circumstances. Unfortunately, only one eclipse in about fifty is dark enough because of the low prevalence of large volcanic erruptions on Earth.

In looking at Figure 4, the luminescent efficiencies required in order to produce illumination equal to the ambient illumination are easily read off. The most spectacular, of course, is the Earth's tail illuminating the dark back side of the Moon. There it can be seen that a luminescent efficiency as small as 3×10^{-4} would be sufficient to produce a surface brightness as great as that believed to exist on the dark back side of the Moon due to illumination by star light and zodiacal light. Almost all transparent materials have luminescent efficiencies of the order 10^{-3} and some very much higher. It seems, therefore, extremely likely that a very important source of illumination of the dark back side of the Moon will be luminescence produced by the Earth's tail. It can be thought of as something like a lunar aurora except that the aurora is produced in the solid surface of the Moon and might be a distinctive feature of the surface which would allow one to determine something about the distribution of materials with high luminescent efficiencies. If there were any material present on the dark side of the Moon with a high luminescent efficiency like that of many phosphors, then the illumination would be expected to be a thousand times the ambient brightness of the dark side of the Moon. The processes just dis-cussed have ample energy available to compete with the background illumination. Next to these in ease of seeing would be luminescence

produced by soft UV radiation during lunar day. If this is the phenomena that has been observed spectroscopically, it might be time dependent because the efficiency of luminescent processes is temperature sensitive; however, the process should be repetitive from one lunation to the next.

V. Indirect Processes

To build up a store of energy on the surface of the Moon requires the development of a concentration of excited electrons in the surface. These electrons could be in excited states, traps, where there are energy barriers preventing recombination to the lower level. Alternatively, the electrons could be in metastable states. However, metastable states cannot provide a good storage mechanism in solids because of the short lifetimes of such states.

The energy stored in traps could either be released thermally, or by infrared stimulation. If infrared stimulation is effective, the release of energy would occur whenever sunlight was falling on the Moon, and since this would probably be the same time that the traps were being filled, luminescence would not be time dependent, and would appear as a direct process. On the other hand, if infrared stimulation is ineffective, thermal release could occur instead. The Moon heats up during lunar morning at a rate of 1° per 2000 seconds. The rate of thermal luminescence is so temperature sensitive that this could lead to sudden energy release.

Consider the total energy that could be stored. In a typical solid there are about 5×10^{22} atoms per cm^3 of material. On the Moon the depth of material to optical depth unity is about 0.01 cm (Hapke and van Horn 1963). (Traps lower down would be emitting photons that never reached the surface.) Thus, if a fraction n of atoms are associated with traps, there are $10^{20} n$ effective traps per cm^2 of lunar surface.

-16-

The bright luminescence observed by Kozyrev and Spinrad would demand a minimum total lunar emission of about 3×10^{16} photons per cm^2 and this number would have to be raised if either (a) luminescence lasted for more than 30 minutes or (b) more than a single 100 Å wide band of spectrum luminesces.

Thus, these observations demand that $n \geq 3 \times 10^{-3}$. Such high trap densities normally can only arise in highly irradiated material, but are perhaps not impossible in the small particles that make up the upper layer of the lunar surface.

For this reason we have constructed a model in which there are a number of traps of identical barrier exactly 1 ev in height, and determined the form that the energy release would take (see Appendix). This is shown in Figure 5. In this calculation it has been assumed that release takes place in the temperature rise before lunar noon. However, the rate of heating after a lunar eclipse is about 100 times greater, the phenomenon would be compressed into about 6 minutes, and the intensity produced could be correspondingly higher. Since in the lunar day, this mechanism would give a luminescence peak of 10 hours width, the fraction of traps needed to explain the observations would be at least 10^{-2}. Our previous comments on the likelihood of such high trap densities is still applicable.

With the storage mechanism of thermal luminescence, the time available for filling the traps would be the lunar afternoon and early morning. There would be a total of perhaps 10^6 seconds. We see that the traps might be filled by any incoming radiation providing
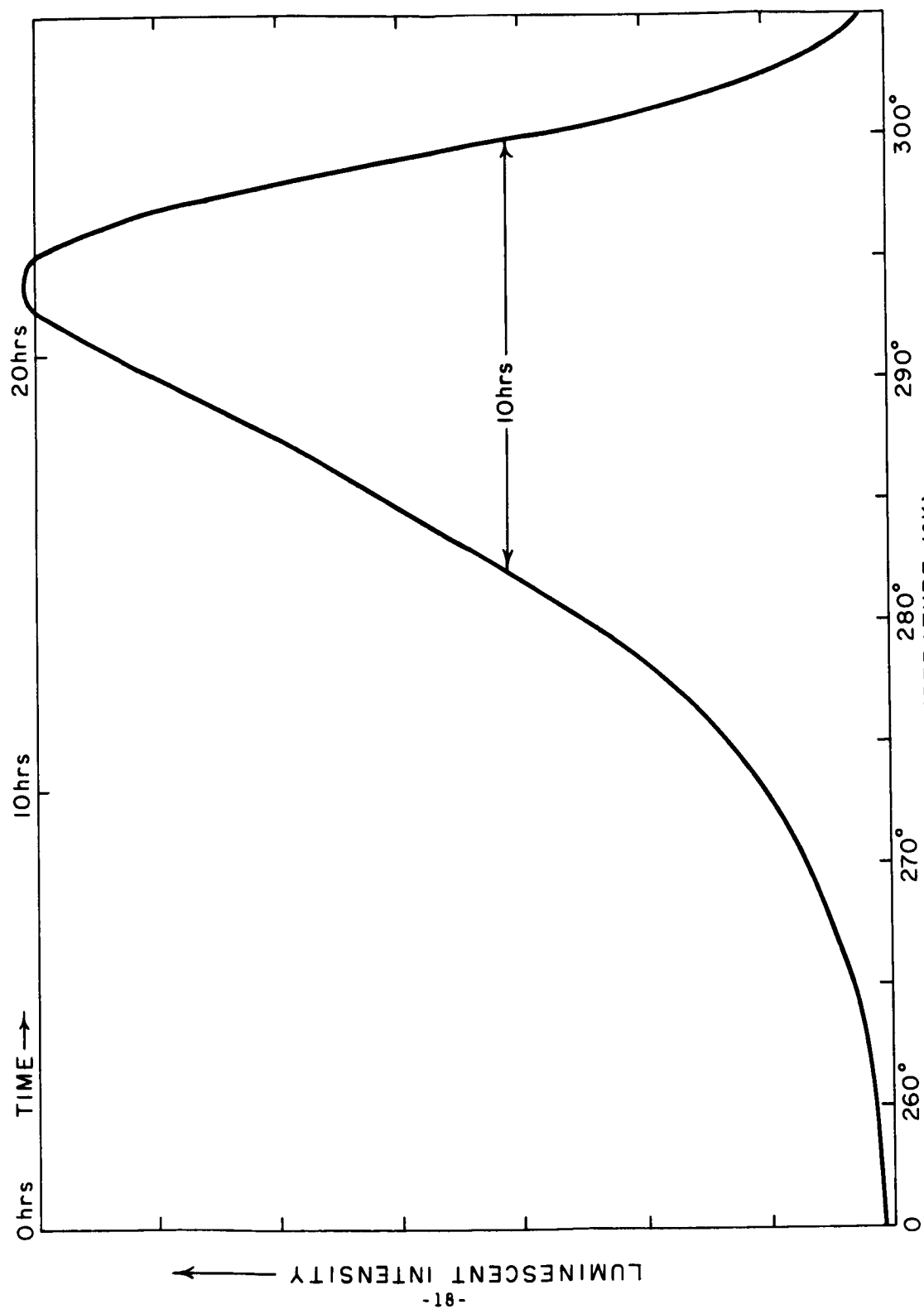
FIGURE 5   PREDICTED THERMAL LUMINESCENCE

more than 10^{12} photons or electron hole-pairs per second. The possible sources of energy then become the solar UV radiation, the solar wind, and less plausibly, the geomagnetic tail. Of these, the solar UV radiation seems adequate and most likely. If the mechanism operates, it could be detected by the form of its time variation, and the energizing source could be perhaps determined by seeing whether the amplitude of the luminescence is different in different lunar cycles (although the time at which the luminescence would occur would always be the same).

VI. Conclusions

There is relatively little energy available at the surface of the Moon to cause luminescence. The most marked luminescent events would be expected to be seen on the dark side of the Moon and at unusually dark lunar eclipses. If luminescence is visible during the light of the Moon, the only exciting radiation for direct processes must be solar ultra violet radiation. If storage processes are adequate, there could be thermal luminescence. Only in the case of the dark back side of the Moon immersed in the Earth's geomagnetic tail does it seem quite likely that the luminescence will be a dominant source of surface brightness, and in this case, the luminescent efficiency of the lunar material must be as large as about 0.1%.

BIBLIOGRAPHY

Allen, C. W., 1962, "Astrophysical Quantities," Second Edition.

Anderson, K. A., 1965, Phys. Rev. Letters 14, p. 888.

Anderson, K. A., Harris, H. K., and Paoli, R. J., 1965, J.G.R. 70, p. 1039.

Barbier, D., 1961, "The Solar System," III, ed. Kuiper, p. 249, University of Chicago Press.

Danjon, A., 1921, Comptes Rendus 173, p. 706.

Danjon, A., 1900, "The Solar System," II, ed. Kuiper, University of Chicago Press.

Diggelen, J. van, 1965, Planet. Space Sci. 13, p. 271.

Fisher, W. J.,1921, Harvard Coll. Obs. Reprints⊥No. 7.

Frier, P. and Webber, W. R., 1963, Science 142, p. 1587.

Grainger, J. F. and Ring, J., 1962, "Physics and Astronomy of the Moon," ed. Kopal, p. 385, Academic Press.

Grainger, J. F., 1962, Astr. Contr. U of Manchester, III, No. 104.

Hapke, B. and van Horn, H., 1963, J.G.R. 68, p. 4545.

Harris, D. L., 1961, "The Solar System" III, ed. Kuiper 272, University of Chicago Press.

Kopal Z., and Rackhma, T. W., 1963, Icarus 2, p. 481.

Kozyrev, N. A., 1956 Izvest. Krimsk. Astr. Obs. 16, p. 148.

Link, F., 1962, "Physics and Astronomy of the Moon," ed. Kopal, p. 161, Academic Press.

Maraushima, S. and Zink, J. R., 1964, A.J. 69, p. 481.

McDiarmid, I. B. and Burrows, J. R., 1965, J.G.R. 70, p. 3031.

McDonald, F. B., 1959, Phys. Rev. 116, p. 462.

Ness, N. F., Scearce, C. S., Seek, J. Bond Wilcox, J.M. Space Research VI, North Holland Publ. Co.

Ness, N. F., 1964, "The Earth's Magnetic Tail," GSFC Rept. X-612-64-392.

Ness, N. F., Scearce, C. S., and Seek, J. B., 1964, J.G.R. <u>69</u>, p. 3531.

Sharp, R. D., Reagan, J. B., Salisbury, S. R., and Smith, L. F., 1964, J.G.R. <u>70</u>, p. 2119.

Snyder C., and Neugebauer, M., 1964, Space Research IV North Holland Publ. Co.

Spinrad H., 1965, Icarus <u>3</u>, p. 500.

Wildey, R., 1964, P.A.S.P. <u>76</u>, p. 112.

APPENDIX

The Calculation of Thermal Luminescence.

If traps have an energy barrier of 1 ev, the probability of release per relaxation time will be approximately $e^{-11,606/T}$ where T is the surface temperature. In a solid we shall take the relaxation time to be 10^{-13} seconds. Thus if there are N filled traps, the rate of photon emission, which is the rate of release of traps will be $10^{13} N e^{-11,606/T}$. The lunar surface temperature T is given by the equation:

$$T = To + \frac{t}{2000} \quad ----- \quad (1)$$

where t is the time from an arbitrary zero (when $T = T_o$), and was taken as the time when the surface temperature was 250° K. If N_o traps were initially filled,

$$N_t = N_o - 10^{13} \int_{t=o}^{t=t} N_t \, e^{-\frac{11,606}{To + 0.0005t}} \, dt \quad (2)$$

and the rate of emission is dN/dt. These equations were solved by mechanical quadratures, and the results are given in Figure 3.

APPENDIX XI
STRUCTURE OF THE LUNAR DUST LAYER

"THIS APPENDIX IS ALSO ISSUED AS TG-12"

STRUCTURE OF THE LUNAR DUST LAYER

R. Smoluchowski

August 1965

STRUCTURE OF THE LUNAR DUST LAYER

ABSTRACT

) 6 17

Experiments show that corpuscular radiation such as solar wind can sinter fine dust by producing displaced atoms which diffuse towards the surface of the grain. The estimated rate of churning of the topmost layer of lunar dust excludes sintering through sputtering. It follows that the dust is probably not loose but is partly coherent (0.5 dyne per particle) which increases its mechanical strength and decreases its mobility. Lower layers of dust are compacted by meteoritic bombardment and a close packed density is reached probably at a depth of a meter or so. Loads which will not commence to sink in loose and in sintered dust are calculated.

Author

TABLE OF CONTENTS

LIST OF ILLUSTRATIONS

STRUCTURE OF THE LUNAR DUST LAYER

R. Smoluchowski

August 1965

I. Free Dust Model

Apart from the problems of the origin and of the quantity of dust on the lunar surface, it is of interest to inquire into the degree of its coherency. Considerations of various thermal and optical properties indicate that the required degree of porosity is of the order of 80% or more. If one assumes that each particle is reasonably spherical and that it rests on three other particles, then one cannot obtain a higher porosity than perhaps 30% without making very odd assumptions about the shape of the particles. It follows that either there are strong local bonds which permit a dust particle to rest on two or even only one particle or that the particles are indeed highly elongated and very irregular. The fact that dust adheres easily to various surfaces is well known, and the effect is usually explained in terms of electrostatic attraction or van der Waal's polarization forces. Experimental investigations in this field are exceedingly difficult, but it seems[1] that at least for quartz and for olivine the electrostatic forces play little role and that the polarization attraction is of the order of 10^{-2} dynes for one micron particle. Polarization attraction drops off so rapidly that it is negligible at a separation of about 10^{-8} cm which gives an energy of bonding less than 100 ev per particle. With a few tenths of an ev for each of van der Waal's bonds one obtains several hundred bonds across the area of contact which turns out to have a diameter of 50 to 100 Å. This is not unreasonable.

II. Meteoritic Bombardment

The local adhesive forces described above are quite sufficient to support a "fairy castle" structure to a depth of one meter or more if only the pressure caused by the upper layers is taken into consideration. This assumption neglects, however, the influence of meteorite and micrometeorite bombardment which will lead to a compaction of the deeper layers of the dust. Meteorites larger than the dust particles will be particularly effective in this respect while each micrometeorite comparable in size with the dust particles themselves will throw up perhaps 10^3 or more dust particles[2] which will fall back on the surface. Inasmuch as the rate of infall of meteorites drops rapidly with increasing size, one concludes that the density of particles of 1-10 micron size which are being thrown up is determined primarily by the flux of micrometeorites, which penetrate a few millimeters. If the total kinetic energy of an incident micrometeorite is converted into the kinetic energy of 10^3-10^4 dust grains, then the average flight time of each grain is of the order of 10 seconds. Combining this with the 5×10^{-3} per cm^2 per second flux of micrometeorites on the Moon's surface (see Ney's paper, Appendix IX), one obtains an instantaneous density of dust particles in flight, at all altitudes, of about 50 per cm^2. This calculation is based on the tacit assumption that the particles are so loosely bonded that upon impact of a micrometeorite they behave as if they were free. We shall see later that this assumption is questionable.

The micrometeorites larger than those considered above penetrate deeper and lead to a progressive compaction of the deeper layers of the dust. The product of the depth of penetration and the known infall rate gives the profile of compaction. If one assumes that the depth of penetration is proporational to the diameter of the meteorite, then only the upper few tens of cm of dust would be

compacted. A more realistic model is to consider the fact that upon impact individual dust particles acquire and transmit by collision velocities comparable with those of molecules at room temperature and that their mean free path is many times their diameter. This assumption leads to an apparent viscosity term which is proportional to velocity and then one obtains a fairly uniform compaction down to a depth of several meters. No experimental data for penetration of particulate target of sufficiently high porosity exist which would permit a verification of the possible theoretical models. Thus, it appears sensible to conclude that[2] the upper 1 cm or so of dust is continuously churned over at a rate of about once every 10^4 years (the upper 1 millimeter once every 100 years[3]) and has the porosity required by thermal and optical data while the lower layers are relatively unperturbed. These deeper layers are progressively more dense and reach a close packed arrangement of grains (porosity of 30%) at a depth of perhaps one meter. This agrees with conclusions reached by Shoemaker[3].

III. Sintering Caused by Sputtering

It has been long recognized that apart from the pulverizing influences of
the meteoritic bombardment (and the recently suggested chemical degradation[4])
there exist conditions on the Moon which tend to produce stronger bonds between
the dust particles than those caused by the ever present van der Waal's attraction.
This is not to say that the porosity of the dust layer decreases, but rather that
the local bonds at the points (areas) of contact change from the weak polari-
zation bonds to ionic, covalent or even metallic bonds, which are a factor of
ten or more stronger.

It was suggested that as a result of impacts some vaporization may occur
and that these gases may solidify at the intergranular contacts and strengthen
them. In the absence of any experimental data it is impossible to make a sensible
estimate of this effect although intuitively one is inclined to consider it
to be small. A much more important factor is the solar wind which produces
a flux of 10^8 protons per cm^2 per second of a velocity of about 600 km per second
including perhaps 15% alpha particles. Besides that, there are protons of much
higher energy but at such low fluxes that they can be ignored. As shown by
Wehner[5] these protons can produce a gradual sintering through sputtering.
Sputtering is the process in which a high speed ion or atom enters a solid and
produces a cascade of billiard ball collisions which result in the ejection of
one or more atoms from the solid. The most efficient sputtering occurs at
glancing angles which sends the sputtered atoms towards the next layer of dust.

The range of several kilovolt protons in a material like quartz can be
estimated by comparison with the known range in aluminum[6] and in certain
organic materials[7]. The result is that most of them will be stopped within

500 - 700 $\mathring{A}$. Thus, the sputtering effect is limited primarily to the outside layer of those particles which are on the surface of the dust layer. Some protons and some sputtered atoms will penetrate through the pores to a few deeper layers, but this is a small correction. Wehner observed sintering of powdered basalt at a total irradiation of 50 - 100 Coulombs per cm^2 which corresponds to an exposure to solar wind of the order of 10^5 years. In similar experiments Hapke[8] did not observe sintering, and the difference may be due to differences in experimental details such as voltage, rocking of the sample, continuous versus pulsed irradiation, quality of the vacuum, etc. Wehner's result has to be compared with the two estimates of churning rate quoted above. They give three to twenty years for the average lifetime of a 5 μ particle at the dust surface. Thus, it appears that under these conditions, sintering due to sputtering is quite improbable.

IV. Sintering Caused by Diffusion of Defects

The characteristic feature of the sputtering process is its dynamic character, i.e. it is a series of collision processes which is essentially temperature independent. Recently, it has been pointed out that solar wind not only produces sputtering with the rather low efficiency of one ejected atom per 20 - 50 incident protons, but that it also produces displaced atoms in the grains at the quite high rate of 5 - 10 displacements per one incident proton[9]. These displaced atoms occupy interstitial positions in the crystalline lattice and they either recombine with vacancies or reach the grain surface by a process of interstitial diffusion. All these defects are concentrated in the 500 - 700 $\overset{o}{A}$ thick layer at the surface of the irradiated grains.

Recent experiments done at the Brookhaven National Laboratory show that 80-micron diamond dust[10] sinters near $50°$ C when exposed to fast (about 1 Mev) neutrons of total flux of about 10^{20}. Similarly[11] 40 micron Al_2O_3 dust is sintered at approximately the same temperature after an irradiation of 6×10^{18} total flux. It is not known at what lower fluxes this effect begins to be observable. It is well established that neutron[12] and proton[13] irradiation can accelerate solid state reaction rates by factors of 10^6 or more by providing an excess of displaced atoms and vacancies. It is essential, however, that there be enough thermal agitation to provide the activation energy for motion of these defects. Experiments show that interstitials in various solids can move appreciably at temperatures as low as $10°K$. Inasmuch as the lunar surface temperature varies from about $400°K$ to $100°K$, one is quite sure that not only interstitials but even some vacancies will be mobile. The latter are usually more stable, and they lead to the formation of color centers, luminescence, etc.

The driving force which makes the defects diffuse towards the surface is a strain gradient and a concentration gradient caused by the fact that a free surface is a sink for all point defects.

In interpreting the BNL neutron irradiation data in terms of solar wind irradiation, one has to realize that, in contrast to protons, neutrons have very long mean free paths and produce defects throughout the volume of all the grains. Since Al_2O_3 is similar to SiO_2 in character of bonding and in Debye temperature, it is quite suitable for a semi-quantitative comparison. One also expects that in both solids the slowest moving interstitial will be oxygen.

Using the known formulae for defect formation by neutrons, one concludes that in the BNL experiments, the concentration of defects in the irradiation Al_2O_3 was between 10^{-4} and 10^{-3}. It seems reasonable to assume that in order to change a weak van der Waals' bond to a strong crystalline bond a few interstitials have to reach the grain surface per each atom on the surface. This means that during the BNL irradiation, defects from a layer of the order of a micron reached the surface. Putting appropriate numbers for vibration frequency and for interatomic distances, one obtains an activation energy for motion of interstitials of about 0.75 ev, which is not unreasonable.

Solar wind produces nearly 10^9 defects per cm^2 per second in the surface layer less than a micron thick. Thus, in the time of the order of a few months, there are enough defects produced to obtain sintering. The question remains, however, whether the temperature of the lunar surface is high enough for most of these defects to reach the surface of grains during this time.

Wesselink[14] calculated the variation of the subsurface temperature during the period of lunation assuming a uniform layer of an approximately low ($k\rho c$). From his results one obtains a gradient of 30 - 40° in the top 1 cm of the dust layer. The gradient is negative for full Moon and positive for new Moon. While Wesselink's model may be questioned in view of the undoubtedly higher values of ($k\rho c$) in deeper layers, the magnitude of the gradient will not be higher. Next, the effect of the periodic variation of the lunar surface temperature upon the diffusion process has to be taken into account. It appears that for reasonable values of the maximum and minimum temperature and for energies of motion of defects varying between 0.5 and 1 ev, the mean path of a diffusing interstitial is about one fifth of that obtained at the maximum temperature. This is illustrated in Figure 1. Using these results, one concludes that during the time of a few months, a defect can migrate about one micron and thus most of the defects produced in the top layer of a grain will indeed reach the surface and will make sintering possible.

It is essential to point out the basic difference between sintering caused by sputtering and that caused by diffusion of defects. As shown in Figure 2, sputtering occurs only during irradiation and thus only these points of contact could be sintered which can be reached by the sputtered atoms. On the other hand defects produced in the outside layer of surface grains stay in that layer for a considerable period of time after irradiation. Thus, even if churning occurs and irradiated particles are moved to lower layers of the dust, the diffusion and the sintering process still can take place because of the negligible difference in temperature. In fact, a certain amount of churning helps this kind of sintering because the highest concentration of defects is produced in that part of each surface grain which is normal to the direction of the solar wind and
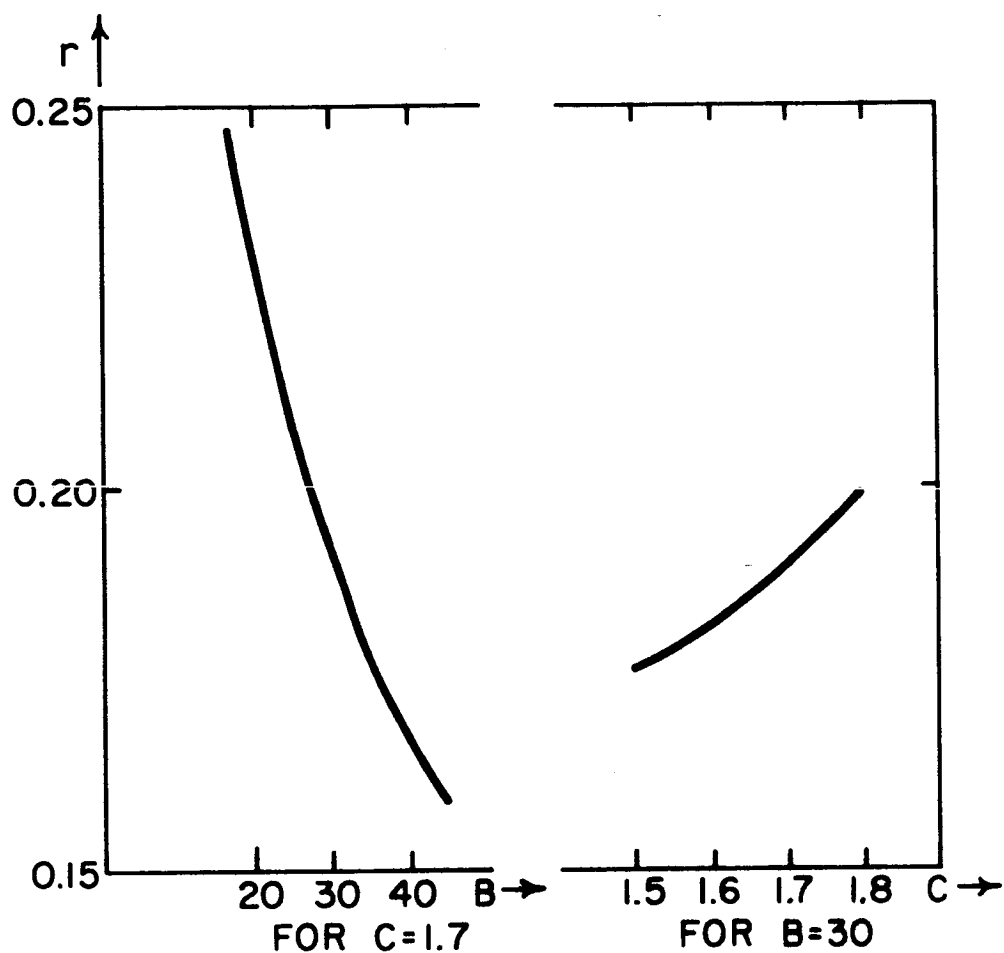
FIGURE 1 Ratio r of diffusion path averaged over the lunation period to diffusion path at the highest sub-solar temperature. $B = E/k(T_m - T_\ell)$ and $2C = (T_m + T_\ell)/(T_m - T_\ell)$ where E is activation energy, T_m is the highest and T_ℓ is the lowest temperature.
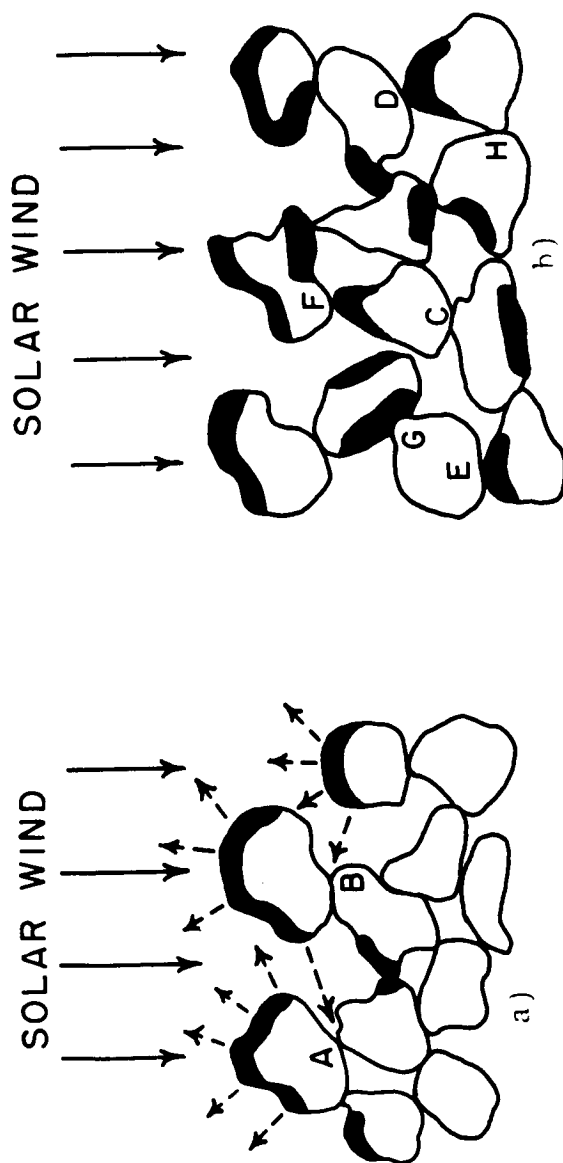
-9-

FIGURE 2 Comparison of sintering through sputtering and diffusion of defects.

a) Sintering through sputtering occurs only at A and B which can be reached directly by sputtered atoms. Dotted arrows indicate their typical directions.

b) Sintering through diffusion of defects after slight churning occurs within the dust layer at points D, E, F and G, but not at C and H.

Shaded regions indicate (on a greatly exaggerated scale) the heavily irradiated layers.

where there are no contact points. On the other hand, a churning period comparable to the diffusion time of a few months would prevent sintering. Admittedly, several quantitative aspects of this discussion of sintering through sputtering and through diffusion of defects are subject to considerable uncertainties. In particular a higher activation energy such as 2 ev for the migration of interstitials could increase the time of sintering from a few months to a few years. Nevertheless, the difference between a) 10^5 years of exposure to solar wind required for sintering through sputtering, b) several years of average lifetime of a particle on the lunar surface and 20 to 30 years of unperturbed position within the upper one centimeter, c) a few months of diffusion time necessary for sintering through migration of defects is so huge that it is doubtful that a more careful analysis would lead to totally different results.

V. Conclusions

a) It appears that lunar dust has a high degree of porosity in the upper 1 cm but at the same time it has considerable mechanical cohesion which results from lattice defects induced sintering. A large fraction of the grains will be attached to their neighbors by forces of the order of 0.5 dyne or more. It is quite likely that many grains form reasonably strong three-dimensional complexes which are not broken up by gentle churning but can be broken up by direct micrometeoritic impact.

b) A load will begin to sink in loose dust if the interparticle bonds are broken. This leads to a maximum value of 3 to 6 gr/cm^2 (or 6 to 12 lbs/ft^2) for micron size dust bonded with polarization forces and to a value ten times higher for stronger (sintered) bonds. These values are in reasonable agreement with experimental values.[15,16]

c) The compaction of dust alters the depth to which micrometeorites and small meteorites can penetrate. It does not seem possible to suggest at this time a reliable model which would permit calculation of the gradient of compaction and of the loss of porosity with increasing depth. There seems to be little doubt, however, that such a gradient exists and that close packing is reached at a depth of perhaps a meter or so.

d) Existence of strong bonds between a few grains of dust may lead in effect to the formation of highly irregular and perhaps elongated quasi particles and agglomerates. This, in turn, helps to understand the stability of the observed very low porosity.

e) The coherency of grains will lower by a factor of 5 or more the number of individual dust particles of a few microns size which are thrown up by micrometeoritic impact. As a result, the churning rate of the top layer of dust will be considerably slower than the estimates based on free dust would indicate. This will enhance diffusion but it is doubtful whether even under such circumstances sintering through sputtering could take place.

REFERENCES

1) P. E. Glaser, Final Report AFCRL-64-970 (II) N65-22451, November 1964.

2) E. J. Öpik, "Progress in Astronaut. Sciences," Vol. I., p. 219, 1962.

3) E. M. Shoemaker, JPL Technical Report No. 32-700, February 10, 1965.

4) J. J. Naughton, I. L. Barnes and D. A. Hammond, Science 149, 630, 1965.

5) G. K. Wehner, D. L. Rosenberg and C. E. KenKnight, Fourth Quarterly Status Report, NASA CR 56292, N 64-24023, April 1964.

6) J. R. Young, J. Appl. Phy. 27, 1, 1956.

7) S. Person, F. Hutchinson and D. Marvin, Rad. Res. 18, 397, 1963.

8) B. Hapke, Ann. N. Y. Acad. Sciences, 123, 711, 1965.

9) R. Smoluchowski, Science (in print).

10) D. Keating, private communication.

11) P. Levy, private communication.

12) G. J. Dienes and A. C. Damask, J. Appl. Phy. 29, 1713, 1958.

13) A. Spilners and R. Smoluchowski, "Symp. on Reactivity of Solids," Amsterdam, 1960.

14) A. J. Wesselink, Bull. Astr. Inst. Netherlands 10, 351, 1948.

15) L. D. Jaffe in "The Lunar Surface Layer" ed. by J. W. Salisbury and P. E. Glaser, Academic Press, New York (1964)

16) J. D. Halajian, Ann. New York Acad. of Science 123, 671, 1965.

APPENDIX XII

SOME CONSIDERATIONS CONCERNING RADAR RETURNS FROM THE LUNAR LIMB

"THIS APPENDIX IS ALSO ISSUED AS TG-13"

SOME CONSIDERATIONS CONCERNING

RADAR RETURNS FROM THE LUNAR LIMB

H. Suhl

August 1965

SOME CONSIDERATIONS CONCERNING RADAR RETURNS FROM THE LUNAR LIMB

ABSTRACT

16178

Some problems involving the radar backscatter of small objects on a dielectric or conducting plane are treated. These results are used to discuss the wavelength, polarization, and angular (delay) dependence of the radar reflection of the Moon. The sign of the limb polarization is the same in this model as in Hagfors' model.

Author

TABLE OF CONTENTS

LIST OF ILLUSTRATIONS

SOME CONSIDERATIONS CONCERNING RADAR RETURNS FROM THE LUNAR LIMB

H. Suhl

August 1965

I. Background

The purpose of this note is to comment on those aspects of J. V. Evans'

contribution "Radar Studies of the Moon," July 1965, that deal with radar echo

power versus delay in the limb region. Chapters III and IV of that paper indicate

that an annulus of angular orientation ϕ (see Figure 1) and fixed area "$2\pi act$"

(a = radius of Moon, c = velocity of light, and t = pulse length) gives a back-

scattered power which varies as cos ϕ for $\frac{\pi}{2}$ $>\phi>\phi_{min}$ (λ), where ϕ_{min} (λ) is a

certain wavelength dependent minimum angle. From Evans' report, henceforth

referred to as E, we see that:

$$\phi_{min} \text{ (68 cms)} = 78^{o}$$

$$\phi_{min} \text{ (3.6 cms)} = 60^{o}$$

$$\phi_{min} \text{ (.8 cms)} = 40^{o}$$

We will assume throughout that the <u>peak</u> reflected power (from the highly specular

leading edge of the Moon) is always a fixed fraction of the incident power, at

all these wavelengths. At 68 cms and 3.6 cms this seems to be a good assumption

since the leading edge gives an overwhelmingly strong return and since the total

reflectivity does not change between these two wavelengths. At .8 cms this is

more questionable. Unfortunately, no direct data are given in E concerning

$P(\phi)/P_{inc}$, the ratio of power returned for the annulus near ϕ, to the incident
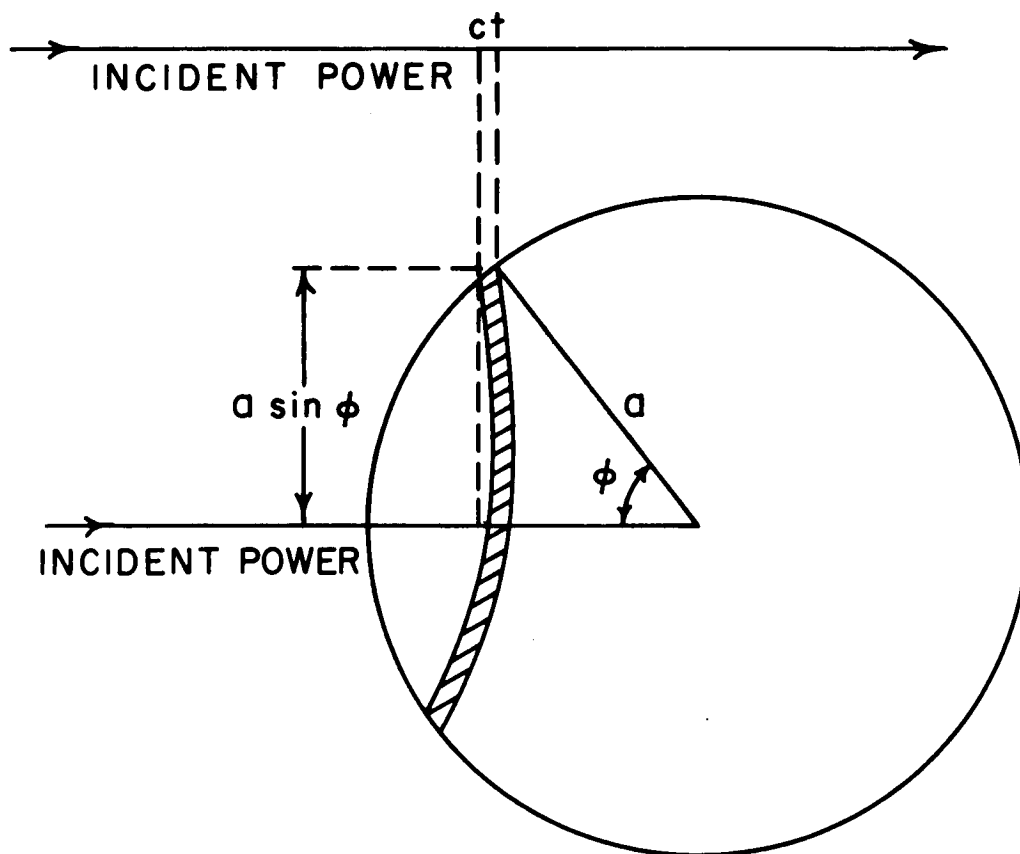
FIGURE 1 BACKSCATTER FROM AN ANNULUS AT LATITUDE ϕ.

power*. With this assumption, it then follows that the curves of relative echo

power versus delay (or ϕ) are a direct measure of the backscattering cross section

versus ϕ. In figure 2 we have plotted $- \log P(\phi)/P(o)$ versus $\log \lambda$, for $\phi = 60^{\circ}$

using Figures 11, 14 and 15 of E. It is noted from the data that any other

choice of ϕ (within the cos ϕ-law range) will merely translate the entries

vertically, without changing the relative positions. We note that the two

points d = .8 cms and d = 3.6 cms quite accurately fit a law $P(\phi) \sim \lambda^{-2}$,

whereas the average law for all three wavelengths is nearer $P(\phi) \sim \lambda^{-1.5}$.

*Evans feels that little significance should be attached to the apparent changes
in reflectivity between 3.6 and .86 cms, because of inadequate allowance for the
diffuse component in interpretation of the .86 cm data (See E, Page 63).
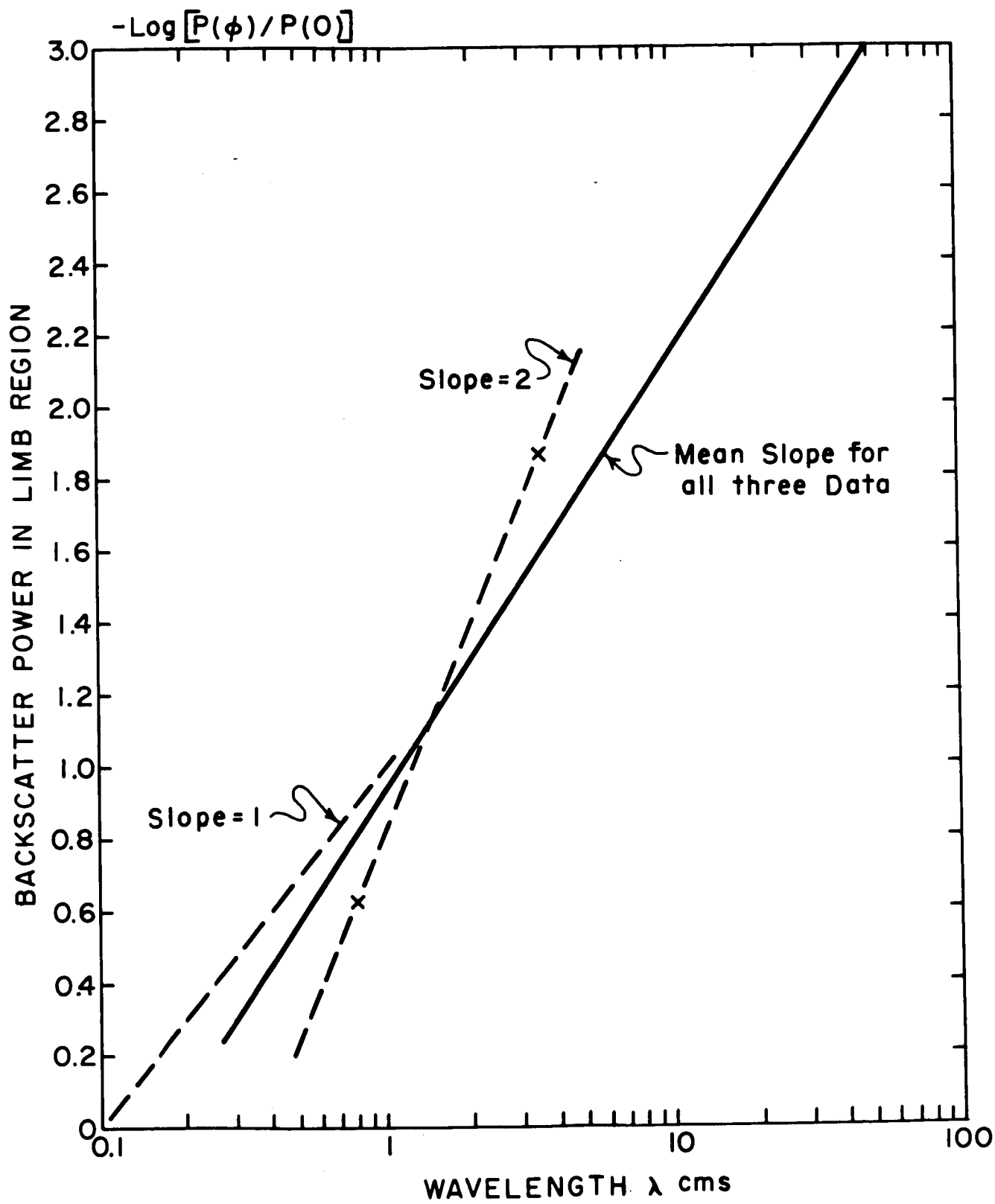
FIGURE 2   BACKSCATTER POWER IN LIMB REGION VS. WAVELENGTH

-4.-

II. Theory

Let us now consider a model of a lunar surface, consisting of a dense dielectric sphere covered rather loosely with dielectric rubble. It is then immediately clear that a substantial fraction of the rubble must consist of sizes less than the smallest of the three wavelengths; otherwise no marked frequency dependence of the grazing-angle-backscatter would be found. Our problem is to determine the backscatter of this surface at low angles of incidence. The only serious attempt to treat a model of this kind appears to have been made by Twersky[1]. Twersky discusses scatterers covering a <u>perfectly</u> <u>conducting</u> surface, but his general reasoning applies to dielectric surfaces also. His work is distinguished from the more usual procedures in that the more important aspects of multiple scattering are properly taken into account.

We begin by stating his results for the case of hemispherical objects small compared with a wavelength. For non-grazing incidence, he finds, aside from the specular component a differential cross section varying as λ^{-4} as in Rayleigh scattering. For grazing incidence, he notes that multiple scattering effects must become much more important than for normal incidence, since the radiation in order to reach in individual scatter must skim over all the scatters between it and the source, exciting them in the process. Their secondary radiation stands in definite phase relation to the source, and the field at the individual scatter is therefore changed. The resulting correction to the "single body" differential scattering cross section takes the form of a multiplicative factor:

$$M(\phi) = \left| 1 - \frac{\pi \rho \, \vec{f}(\vec{k}_r, \vec{k}_i) \cdot \vec{e}}{k^2 \cos \phi} \right|^{-2} \tag{1}$$

(evidently an "optical model" effect) where ρ is density of objects p.u. area, $k = 2\pi/\lambda$, ϕ the angle of incidence, $\vec{f}(\vec{k}_r, \vec{k}_i)$ the vector scattering amplitude due

to one object in the specular direction (k_i and k_r are unit vectors in the direction of the incident and reflected waves respectively.) Twersky (contrary to common usage) defines $\vec{f}$ to be dimensionless, i.e. his scattered wave in a general direction $\vec{q}$ is defined as:

$$\vec{f}(\vec{q},\vec{k}_i) \frac{e^{ikR}}{kR} \qquad \text{with } \vec{q} = \vec{R}/R$$

$\vec{e}$ is a unit vector normal to the plane of incidence; $\vec{f}$ is meant to be the scattered E-field for E polarized normal to the plane of incidence and the scattered H-field when E is polarized in the place of incidence. For obvious reasons f is very small in the former case if the objects are small compared with the wavelength (in fact, if they are small compared with $\lambda/\cos\phi$) and if the surface has a moderately high dielectric constant or is conducting.) Hence, we restrict the discussion to the case of "vertical" polarization (E in the plane of incidence). Finally we note that for small $\rho(\vec{f}\cdot\vec{e})/k^2$ the multiple scattering factor (i) may be replaced by unity, unless ϕ is close to grazing. The formula for the differential scattering cross section per unit area is:

$$\sigma(\vec{q},\vec{k}_i) = \frac{\rho}{k^2} \left| \vec{f}(\vec{q},\vec{k}_i) \right|^2 M(\phi) \qquad (2)$$

Close to the grazing incidence, i.e. for $\cos\phi < \rho (\vec{f}\vec{e})/k^2$, this formula becomes in the backscatter direction:

$$\sigma(-k_i,k_i) = \frac{k^2}{\pi^2\rho} \frac{\left| \vec{f}(-k_i,k_i) \right|^2}{\left| \vec{f}(k_i,k_i)\cdot\vec{e} \right|^2} \cos^2\phi \qquad (3)$$

In the case of hemispherical bosses of radius (a) distributed on a conducting place, Twersky finds for vertical polarization and (a) $<\lambda$.

$$\vec{f}(q,k_i) = i(ka)^3 \left[\vec{e}_\theta (\sin\theta - 2\sin\phi\sin\chi) - \vec{e}_\chi 2\cos\theta\sin\chi \right] + 0(ka)^6$$

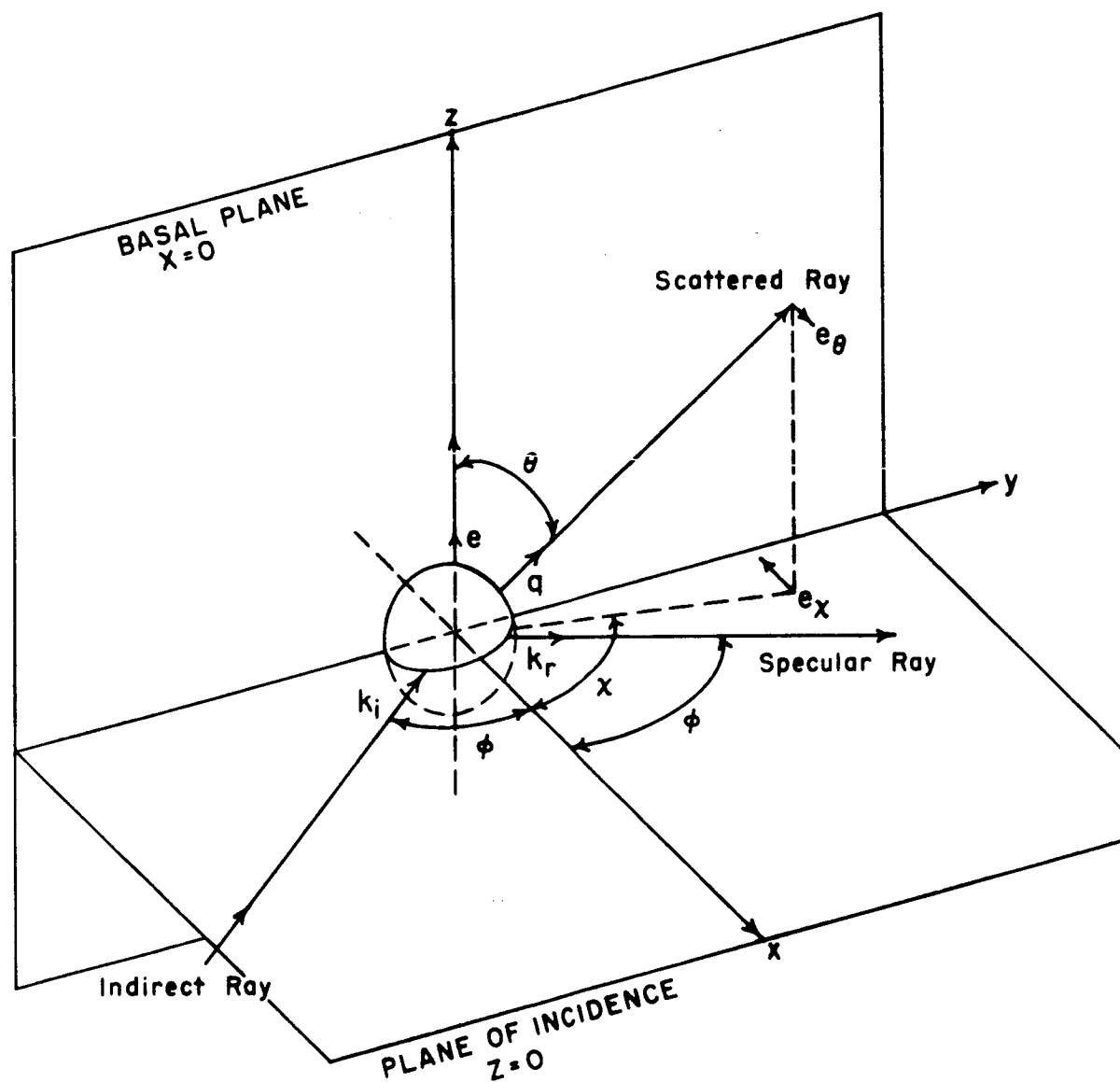The geometry is shown in Figure 3. The individual boss is located at the origin

FIGURE 3   Scattering Geometry for Hemispherical Boss on a Conducting Ground (X=0).

of the conducting plane, (the plane X = 0). The plane of incidence is taken to be Z = 0, θ, χ are the usual spherical polar coordinates giving the direction of $\vec{q}$, ϕ is the angle of incidence, $\vec{e}_\theta$, $\vec{e}_\chi$ are unit vectors in the direction of θ and χ increasing. Evidentally $q = -k_i$ means:

$$\theta = \frac{\pi}{2}, \quad \chi = -\phi, \text{ and so}$$

$$f(-k_i, k_i) = i(ka)^3 \, \vec{e}_\theta \, (1 + 2 \sin^2 \phi); \quad (e_\theta \text{ along } -Z)$$

Similarly:

$$\vec{f}(k_i, k_i) = i(ka)^3 \, \vec{e}_\theta \, (1 - 2 \sin^2 \phi); \quad (e_\theta \text{ along } -Z)$$

Hence, to lowest order in $\cos \phi$ we get from (3):

$$\sigma(-k_i, k_i) = \frac{9k^2}{\pi^2 \rho} \cos^2 \phi \tag{4}$$

i.e. backscattering is inversely proportional to the square of the wave-length, and proportional to the square of the grazing angle. The range of validity of this result is:

$$\cos \phi \ll ka^3 \pi \rho$$

Let ξ be the fraction of area covered with objects; clearly,

$$\xi = \pi a^2 \rho$$

Hence, the range of validity of (4) is:

$$\cos \phi \ll \frac{2\pi a}{\lambda}$$

On the other hand, the assumption was $\lambda / a \gg 1$, hence eq. (4) is restricted to very near grazing incidence. Nevertheless, we shall assume these results to hold when λ is only a few times (a).

III. Application to Dielectric Surfaces and a Model of the Lunar Surface

The multiple scattering argument of course carries over without modification. On the other hand, f must be recalculated (Twersky used the Rayleigh method of images applicable only when the bare surface is perfectly conducting.) So long as the objects are smaller than λ this is not difficult. The polarization of the object can then be calculated as though it were in an electrostatic field equal in magnitude to the electric field at the plane surface, which is taken to be uniform (see appendix). The object is then allowed to radiate as an electric dipole (plus if need be, a quadrupole, etc.) above a dielectric ground. For this purpose, the polarization of the E field (and hence of the induced dipole moment) may be regarded as normal to the ground since we are concerned mainly with low incident horizon angles. For spherical objects above a ground of sufficiently high dielectric constant

$$\sigma \ (-k_i, k_i) = \frac{Ck^2}{\pi^2 \rho} \ \cos^2 \phi \tag{5}$$

where C is a certain number depending on the dielectric constant of the object and on the Fresnel coefficient of the basal plane.

We now describe the lunar surface as it might appear to electromagnetic radiation at wavelength λ. Objects of size $>\lambda$ tend to appear like solid, continuous ground serving as undulating base-surface for object of size $<\lambda$, to which formula (5) is assumed to apply. Reflections from different slopes of the base surface will be in random phase relation to each other, and so a formula like (5) must be averaged over base plane orientations. (Before this is done it is necessary to derive $\sigma_{av}(-k_i, k_i)$, the mean cross section for objects $<\lambda$, properly evaluated to take into account multiple scattering.) As the result

-9-

of the averaging over base orientations, the dominant part of (5) will go as $\cos \phi$, provided slopes of magnitude $\geq \frac{\pi}{2} - \phi$ exist among the object of size $> \lambda$, and that $\frac{\pi}{2} - \phi$ is not so large as to preclude a covering layer of objects of size $< \lambda$.

We first calculate $\sigma_{av}(-k_i, k_i)$. For a distribution of objects of size $< \lambda$, we have in place of (1)

$$M(\phi) = \left| 1 - \frac{\pi}{k^2 \cos \phi} \int_0^{\lambda^3} \rho(v) \left(\vec{e}_f \cdot \vec{f}(v, k_r k_i) \right) dv \right|^2$$

where $\rho(v)dv$ is the number of objects per unit area, with volume between v and $v + dv$. The actual variation of σ with wavelength is thus critically dependent on the size distribution.

From meteoritic data one might be inclined to infer a law of the form

$$\rho = Av^{-\mu}; \qquad\qquad v > v_o$$
$$\quad = 0; \qquad\qquad\quad v < v_o$$

where v_o is of the order of a few millimeters (lunar dust is disregarded here) and where $\mu > 2$. If n_o is the total number of objects per unit area, then

$$n_o = A \int_{v_o}^{\infty} v^{-\mu} \, dv$$

and so

$$A = v_o^{\mu-1} (\mu-1) n_o$$

Thus,

$$\rho(v) = \frac{n_o}{v_o} \left(\frac{v}{v_o} \right)^{-\mu}$$

On the other hand, for $\phi \sim \frac{\pi}{2}$, and sufficiently large dielectric constant,

$$\vec{e} \cdot \vec{f} = B(ka)^3 = B\, k^3\, v$$

where B is a constant of order one (see appendix). Hence,

$$\int_0^{\lambda^3} \rho(v)\; e \cdot f\; dv = \frac{n_o}{v_o}\; B\, k^3 \int_{v_o}^{\lambda^3} v \left(\frac{v}{v_o}\right)^{-\mu} dv$$

$$= \frac{n_o v_o B}{\mu - 2} \left(\frac{2\pi}{\lambda}\right)^3$$

if $v_o \ll \lambda^3$,

Provided $\cos\phi < n_o v_o \dfrac{2\pi}{\lambda}$ \hfill (6)

we then have:

$$\sigma(v)\; dv = \frac{C'k^2 \rho(v)\, v^2 (\mu-2)^2}{n_o^2\, v_o^2}\; \cos^2\phi\; dv$$

where C' is again a constant, $\sigma(v)\,dv$ is the scattering cross section, per unit area, from objects between volume v and $V + dv$. The total cross section from objects up to size λ is now:

$$\sigma = \frac{C'k^2}{n_o^2\, v_o^2}\; (\mu-2)^2\; \cos^2\phi\; \frac{n_o}{v_o} \int_{v_o}^{\lambda^3} \left(\frac{v}{v_o}\right)^{-\mu} v^2\; dv \hfill (7)$$

There are now two cases to be discussed:

1) if $\mu > 3$, the upper limit on the integral is again unimportant, and $\sigma \sim 1/\lambda^2$.

2) if $\mu < 3$, the upper limit dominates.

Let us suppose that $\mu = 2.4$, corresponding to known meteorite size distributions. Then,

$$\sigma = C'\; \frac{k^2 (\mu-2)^2\, \lambda^{3(3-\mu)}}{n_o v_o^{\,3-\mu}(3-\mu)}\; \cos^2\phi \hfill (8)$$

-11-

For $\mu = 2.4$, this gives

$$\sigma \propto 1/\lambda^{0.2}$$

i.e. a very slow dependence on wavelength. On the other hand, $\mu = 2.7$ would

give:

$$\sigma \propto 1/\lambda^{1.1}$$

in closer accord with the data. Finally, formula (8) must be averaged over

the slope distribution of the substratum. We had already noted that a distri-

bution of local slopes extending to angles $\frac{\pi}{2} - \phi$ or greater will cause the

leading term of (8) to go like $\cos \phi$ rather than $\cos^2 \phi$. If we regard as

substratum all features of size $> \lambda$, it is evident that at the shortest wave-

lengths, 3.6 cm and .8cms, the substratum will certainly contain slopes many

times those indicated by the quasi-specular analysis in the center region of

the Moon. At 68 cms, this is perhaps debatable; on the other hand a substratum

slope fluctuation of only 12° is needed in this case in accord with the quasi-

specular results.

The above results are applicable only for angles for which condition (6)

is satisfied. If we simply assume $n_o = v_o^{-2/3}$ (owing to the preponderance

of small objects), condition (6) requires:

$$\cos \phi < 2\pi \frac{v_o^{1/3}}{\lambda} = 2\pi \frac{r_o}{\lambda}$$

where v_o is the radius of the smallest objects. No value of v_o fits all three

wavelengths.

The reasons may well lie in a number of oversimplifications of the present

theory; among them are the following:

If the objects are distributed throughout a layer of certain thickness,

perhaps graded in size (or packing fraction) from small (or dilute) at the

surface to large (or dense) towards the interior, Twersky's M-factor must be recalculated. It is evident that the dependence of M (ϕ) on cos ϕ will be weakened (since for an infinite medium the "optical model" effect must obviously be independent of propagation direction). Since the <u>effective</u> dielectric constant of the Moon is estimated at 2.6 from the total cross section, whereas the bulk density of the Moon suggests a dielectric constant of 5 at the very least, it seems quite probable that a graded layer several wavelengths deep does, in fact, exist on the surface.

IV. Polarization Results

In conclusion we point out that the interpretation of the Hagfors polarization data presented in E (Pages 58 et. seq.) may not be unique (as suggested by T. Gold during the Summer Study Group session). If $\cos \phi < \sqrt{\epsilon - 1}$ where ϵ is the dielectric constant; the total electric field (incident plus reflected) when E is polarized perpendicular to the plane of incidence is only a fraction

$$\frac{2 \cos \phi}{\sqrt{\epsilon - 1}}$$

of the incident field, while for parallel polarization it is a fraction

$$\frac{2\epsilon \cos \phi}{\sqrt{\epsilon - 1}}$$

for $\cos \phi < \dfrac{\epsilon - 1}{\epsilon^2 - 1}$ and even larger otherwise.

Hence, parallel polarization induces at least ϵ times as large a dipole moment in objects on the ground as does normal polarization. Assuming (without much justification) that dipoles parallel to the ground re-radiate only $\frac{1}{\epsilon}$ as effectively as dipoles perpendicular to ground, we see that there is a factor ϵ^2 between the backscattering for parallel and normal polarizations. A more refined theory, (including detailed differences in the re-radiation of the two directions), might thus provide further information on ϵ.

-14-

REFERENCES

1) V. Twersky. On the Scattering and Reflection of Electromagnetic Waves by
    Rough Surfaces. Trans. I.R.E. AP-5, 81-90. (1957a)

2) J. A. Stratton. Electromagnetic Theory, McGraw-Hill Book Co., Inc.
    pp. 586-587 (1941)

APPENDIX

Radiation From Small Dielectric Spheres on a Dielectric Plane

If the radii of the spheres are appreciably smaller than the wavelength, the dipole moment induced in them may be computed from electrostatics. If E_i, E_r, E_t are the incident reflected and transmitted fields calculated for the smooth dielectric surface, the problem reduces to solving Laplace's equation for a dielectric sphere placed in contact with the plane $y = 0$, into a field $E_i + E_r$; $z > 0$; and E_t; $z < 0$; these being evaluated at the surface and considered uniform in their respective half-spaces. This is still a difficult problem in electrostatics. For qualitative purposes it is sufficient to consider the sphere to be in the field $E_i + E_r$, and to neglect the changes in the induced polarization due to the presence of the dielectric slab. Then the polarization is uniform and equal to $3 \frac{\varepsilon-1}{\varepsilon+2}$ $(E_i + E_r)$ and the dipole moment is $p = 3v \frac{\varepsilon-1}{\varepsilon+2}$ $(E_i + E_r)$.

We have from standard formulae,

$$E_i + E_r = \frac{2 \cos \phi}{\cos \phi + \sqrt{\varepsilon - \sin^2 \phi}} \, E_i$$

For E polarization normal to the incidence plane, and

$$H_i + H_r = \frac{2\varepsilon \cos \phi}{\varepsilon \cos \phi + \sqrt{\varepsilon - \sin^2 \phi}} \, H_i$$

for E polarization parallel to the incidence plane; the E-field components in this case are:

$$E_{\text{normal to surface}} = \frac{2\varepsilon \sin \phi \cos \phi \, E_i}{\varepsilon \cos + \sqrt{\varepsilon - \sin^2 \phi}}$$

$$E_{\text{tangent to surface}} = \frac{2 \sqrt{\varepsilon - \sin^2 \phi} \cos \phi \, E_i}{\varepsilon \cos \phi + \sqrt{\varepsilon - \sin^2 \phi}}$$

The total field re-radiated in the incidence direction by the induced polarization (see Stratton[2]) is not very greatly different from what may be expected from a free dipole. The Hertz vector of the dipole moment p is

$$\pi = \frac{e^{ikr}}{r} \, p$$

The backscatter field from which (disregarding $E_{\text{tangential}}$ to obtain an order of magnitude result) is approximately

$$E_{\text{Back}} = \frac{2\pi}{\lambda}^3 \frac{e^{ikr}}{kr} \, p$$

Hence,

$$\frac{e^{ikr}}{kr} \, f = \frac{E_{\text{Back}}}{E_i + E_r}$$

or,

$$f = \frac{2\pi}{\lambda}^3 \frac{\varepsilon - 1}{\varepsilon + 2} \frac{2 \cos \phi}{\cos \phi + \sqrt{\varepsilon - \sin^2 \phi}} \qquad (\perp \text{Pol.})$$

$$\doteq \left(\frac{2\pi}{\lambda}\right)^3 \frac{\varepsilon - 1}{\varepsilon + 2} \frac{2\varepsilon \cos \phi \sin \phi}{\varepsilon \cos \phi + \sqrt{\varepsilon - \sin^2 \phi}} \qquad (\parallel \text{Pol.})$$

Two cases are now to be distinguished.

I. If $\varepsilon \cos \phi \ll \sqrt{\varepsilon - \sin^2 \phi}$ or, $\cos \phi \ll \dfrac{\varepsilon - 1}{\varepsilon^2 - 1}$

then f goes like $\cos \phi$ both for $\parallel$ and $\perp$ polarization. In that case H is independent of ϕ, and multiple scattering is readily seen to be negligible. The backscatter cross-section then goes as $\lambda^{5-3\mu}$ when averaged over the power law for particle sizes. For $\mu = 2.4$, this gives $\lambda^{-2.2}$, a too rapid variation with wavelength.

II.   If $\cos \phi > \dfrac{\epsilon - 1}{\epsilon^2 - 1}$, then a more pronounced difference in $f_{\perp}$ and $f_{\parallel}$

results, and if ϵ is sufficiently large for given ϕ, then the results become

essentially the same as those for a conducting substrate, and the power law

for λ is substantially that indicated in the main text. In the case of the

data at 68 cm, this would require $\epsilon \sim 8$, the shorter wavelength measurements,

carried to 80° only, would be consistent with $\epsilon = 4$. On the basis of a graded-

layer theory in which small (effectively dilute) material overlies larger

(effectively denser) material it is not unreasonable to expect such a

variation in effective dielectric constant.